

# **Multiscale geoarchaeological investigation of rockshelter deposits using the example of Sodicho, Ethiopian Highlands**

Inaugural-Dissertation

zur

Erlangung des Doktorgrades

der Mathematisch-Naturwissenschaftlichen Fakultät

der Universität zu Köln

vorgelegt von

Elena Amelie Hensel

aus Neustadt an der Weinstraße

Köln, 2023

Berichtersteller:  
(Gutachter)

Prof. Dr. Olaf Bubenzer

Prof. Dr. Frank Schäbitz

Tag der mündlichen Prüfung: 21.10.2022

## Abstract

The potential of the new and promising archaeological site Sodicho Rockshelter to provide a geoarchaeological context, for prehistoric human-environment interaction and palaeoenvironmental shifts in its surroundings, has been investigated with a multidisciplinary and multimethodological approach. The results now promote the site as a new key site for geoarchaeological research in tropical regions. Located in the southwestern Ethiopian Highlands, the site is part of a region that is renowned for the study of human origins, evolution, and the dispersal of our ancestors across the African continent and beyond its borders. Significant human fossil finds from sites such as Omo/Kibish or Herto highlight the importance of this region. In Ethiopia, the dispersal of the anatomically modern humans (AMH) can be seen as a movement to another region or a migration into another continent, but also as an upward movement to elevated regions.

Hypotheses that the topographical and climatic diversity of Ethiopia favored the development of environmental, and ecological refugia in the highlands, raises several research questions, such as the climatic impact that forced the humans to adapt or retreat, and the identification of push and pull factors for their dispersal. Furthermore, questions emerged as to why humans repeatedly chose to disperse into the mountains, and how they coped with the harsher conditions in higher altitudes (e.g., higher ultraviolet radiation, lower oxygen levels) that are challenging for the human body. However, comprehensive terrestrial palaeoenvironmental archives and continuous archaeological records are still very scarce in Ethiopia. Chronostratigraphic gaps, discordances, and the influence of erosion create common uncertainties about the forcing factors for regional environmental and climatic variability. Moreover, it remains unclear what impact the mentioned changes had on the landscape, flora, fauna, and of course our human ancestors.

In this doctoral thesis, a multiproxy, geoarchaeological approach is chosen to address research hypotheses on prehistoric human-environment interaction and palaeoclimatic driven dispersal theories in the tropical highlands during the Late Pleistocene and the following Holocene. This study is integrated into the multi- and interdisciplinary approach of the Collaborative Research Centre 806 "Our Way to Europe - Culture-Environment Interaction and Human Mobility in the Late Quaternary" (CRC 806), which focuses on the climatic, environmental and cultural context to understand the migration of anatomically modern humans from the African continent into Central Europe as one of the "sinks".

By approaching the study area and addressing the research questions, using different spatial and temporal scales, it has been shown that the Sodicho Rockshelter is a unique site that contains evidence on repeated high-altitude occupation during the last 27 ka cal BP. It is the first site in southwestern Ethiopia that holds dated occupation phases during the Last Glacial Maximum (LGM,  $\sim 21 \pm 2$  ka), and thus contributes to the research debate on an environmental refugia.

This study presents the geoarchaeological results of micromorphological investigations various sedimentological, and geochemical analyses, radiocarbon dating, and the evidence from collaborating disciplines of archaeology, and archaeobotany, in relation to the local archaeological record and regional paleoenvironmental changes. Based on the results, processes such as site formation, post-depositional disturbances and the identification of the geogenic, biogenic und anthropogenic depositional agents were determined. The archaeological evidence and sedimentary stratigraphy provide insights into human behavior such as stone tool manufacturing, fire activity, site maintenance, and dumping activities. In addition, a more detailed examination at the microstratigraphic record enabled the identification of shifting moisture conditions during the African Humid Period (AHP,  $\sim 15 \pm 5$  ka). By identifying specific palaeoenvironmental signals in the sediment sequences, a comparison with supraregional palaeoclimatic records was possible. This highlights the potential of multiscale research in the volcanic rockshelter and the possibility to be correlated to other archaeological and palaeoenvironmental sites at the Horn of Africa and beyond.

## Kurzzusammenfassung

Das Potenzial der neuen und vielversprechenden archäologischen Fundstelle Sodicho Rockshelter, um den geoarchäologischen Kontext für prähistorische Mensch-Umwelt-Interaktionen und Paläoumweltveränderungen in der Umgebung zu liefern, wurde mit einem multidisziplinären und multimethodischen Ansatz untersucht. Die Ergebnisse verdeutlichen nun, dass die Fundstelle als neuer wichtiger Standort für die geoarchäologische Forschung in tropischen Regionen betrachtet werden kann. Die Stätte liegt im südwestlichen Hochland von Äthiopien und ist somit Teil einer Region, die für die Erforschung des menschlichen Ursprungs, der Evolution und der Ausbreitung unserer Vorfahren innerhalb des afrikanischen Kontinents und über dessen Grenzen hinaus bekannt ist. Bedeutende menschliche Fossilfunde, die aus Fundstellen wie Omo/Kibish oder Herto stammen, unterstreichen die Bedeutung dieser Region. In Äthiopien kann die Ausbreitung des anatomisch modernen Menschen nicht nur als ein Auszug in eine andere Region oder Migration in einen anderen Kontinent betrachtet werden, sondern auch als eine Bewegung nach oben in höher gelegene Regionen.

Die Hypothese, dass die topografische und klimatische Vielfalt Äthiopiens die Entwicklung ökologischer Refugien im Hochland begünstigt hat, wirft mehrere Forschungsfragen auf, z. B. nach den klimatischen Auswirkungen, die Menschen zur Anpassung oder zum Rückzug zwangen, und nach der Identifizierung von Push- und Pull-Faktoren die verantwortlich waren für ihre Ausbreitung. Außerdem stellt sich die Frage, warum sich die Menschen immer wieder für eine Migration in die Berge entschieden und wie sie mit den für den menschlichen Körper belastenden Bedingungen (wie höhere UV Strahlung, geringer Sauerstoffgehalt) in höher gelegenen Regionen zurechtkamen.

Umfassende terrestrische Paläoumweltarchive und kontinuierliche archäologische Aufzeichnungen sind in Äthiopien jedoch noch sehr rar. Chronostratigraphische Lücken, Diskordanzen und der Einfluss von Erosion schaffen generell Unsicherheiten über die treibenden Faktoren für die regionale Umwelt- und Klimavariabilität. Sowie die Auswirkungen, die diese Veränderungen auf die Landschaft, die Flora, die Fauna und natürlich unsere menschlichen Vorfahren hatten.

In dieser Doktorarbeit wird ein geoarchäologischer Multiproxy-Ansatz gewählt, um Forschungshypothesen zur prähistorischen Mensch-Umwelt-Interaktion und zu paläoklimatisch bedingten Ausbreitungstheorien im tropischen Hochland während des späten Pleistozäns und des folgenden Holozäns zu untersuchen. Diese Studie ist in den multi- und interdisziplinären Ansatz des Sonderforschungsbereichs 806 "Our Way to Europe - Culture-Environment Interaction and Human Mobility in the Late Quaternary"

(SFB 806) integriert, der sich auf den klimatischen, ökologischen und kulturellen Kontext konzentriert, um die Migration des anatomisch modernen Menschen (AMH) vom afrikanischen Kontinent nach Mitteleuropa, als eine der "Senken", zu verstehen.

Durch die Annäherung an das Untersuchungsgebiet und die Auseinandersetzung mit den Forschungsfragen, auf verschiedenen räumlichen und zeitlichen Ebenen, konnte gezeigt werden, dass das Sodicho Rockshelter eine einzigartige Fundstelle ist, die Beweise für eine wiederholte Besiedlung vom Hochland während der letzten 27 ka cal BP erhalten hat. Es ist die erste Fundstelle im Südwesten Äthiopiens, die datierte Besiedlungsphasen während des Letzten Glazialen Maximums (LGM,  $\sim 21 \pm 2$  ka) aufweist und somit einen Beitrag zur Forschungsdebatte um ein Umweltrefugium leistet. In dieser Studie werden die geoarchäologischen Ergebnisse mikromorphologischer Untersuchungen, verschiedener sedimentologischer und geochemischer Analysen, Radiokohlenstoffdatierungen und die Hinweise aus den kooperierenden Disziplinen der Archäologie und Archäobotanik, in Bezug auf die lokalen archäologischen Befunde und regionalen Paläoumweltveränderungen präsentiert. Auf der Grundlage der Ergebnisse wurden die Entstehungsprozesse der Fundstellen, sedimentäre Ablagerungsprozesse und postsedimentäre Störungen und die Identifizierung der geogenen, biogenen und anthropogenen Ablagerungsfaktoren identifiziert. Die archäologischen Befunde und die Sedimentstratigraphie geben Aufschluss über menschliches Verhalten, wie beispielsweise die Herstellung von Steinwerkzeugen, Feueraktivitäten, die Instandhaltung des Standortes und Entsorgungsaktivitäten. Darüber hinaus ermöglicht die detailliertere Betrachtung des mikrostratigraphischen Sedimentarchivs die Identifizierung variabler Feuchtigkeitsbedingungen während der Afrikanischen Feuchtperiode (AHP,  $\sim 15 \pm 5$  ka). Durch die Identifizierung spezifischer Paläoumweltsignale in den Sedimentabfolgen war ein Vergleich mit überregionalen paläoklimatischen Aufzeichnungen möglich. Dies unterstreicht das Potenzial der multiskaligen Forschung in vulkanischen Abris (Felsüberhänge) und die Möglichkeit, diese mit anderen archäologischen und paläoökologischen Fundstellen am Horn von Afrika und darüber hinaus in Beziehung zu setzen.

## Acknowledgements

First of all, I want to express my gratefulness to my supervisor, Prof. Dr. Olaf Bubenzer, for the opportunity to work within Project A1 of the CRC 806. He already supported and motivated me during my Master's thesis, and this continued through the entire phase of the PhD. He encouraged me to believe in my strengths, to take my own scientific and methodological path and to reach out to the scientific community, by presenting my work at national and international conferences. Although a large part of the communication had to take place remotely due to a variety of circumstances, he was always available, even on short notice, when a deadline was right around the corner. I sincerely thank him for his patience and the trust he had in me, even when plans changed quickly or family commitments took precedence.

Further I would like to thank my second advisor PD Dr. Martin Kehl, for his scientific advice and the inspiring discussions about my methodological approaches. He not only introduced me to micromorphology, he guided me through the methodology and its obstacles and also conveyed the importance of microscopic evidence in our research field. I am grateful for his intensive review of my presentations and manuscripts and for his constructive criticism to improve their quality.

I would like to thank my third doctoral committee member Dr. Oliver Bödeker for the exchange of scientific ideas as well as personal support. I had always been able to talk to him about difficulties when it came to staying motivated during lockdown. He also motivated me to use the time during the PhD to further develop hard and soft skills.

I thank Prof. Dr. Frank Schäbitz who agreed to being a member of the thesis defense committee and review my thesis. As director of the IRTG, I got to know him as an approachable supervisor who promoted the development of all doctoral students with care. Moreover, I would like to express my gratitude to Prof. Dr. Martin Melles for being a part of the commission as chair of the thesis defense committee.

A very special thank goes to Dr. Ralf Vogelsang, who not only contributed to my scientific development as a reliable co-author, but also through his support and constructive exchange during the fieldwork in Ethiopia. He guided the excavations at Sodicho Rockshelter with effortlessness and humor, while maintaining the scientific focus. In the same breath, I would like to thank all the colleagues and collaborators from the A1 project, scientific staff from University of Cologne, the student assistants, and of course all the helping hands at the excavations in Ethiopia. Their joint effort laid the foundation

for my work at Sodicho Rockshelter. In particular during the excavations I participated, these include Thomas Albert, Trhas Hadush, Tom Noack, Christian Schepers, and especially Dr. Minassie Girma Tekelemariam, who was also a friendly office neighbor.

At this point, I would like to thank Dr. Isabell Schmidt, who has been supporting me since my master's thesis in her project. She encouraged me to teach together with her, and she has shown me how important it is for women in science to stand up for our own views.

Not to be left unmentioned are also colleagues who became good friends through the shared journey to the doctorate. Even though we come from different disciplines, we are all the same when it comes to accomplishing this challenge.

I want to thank the coauthors of the published manuscripts that are part of my PhD research for their support, the integration of their own research, and for stimulating discussions, that have helped me to develop a better understanding of the significance across the various disciplines. I also want to thank the reviewer for their careful reading of the manuscripts and very constructive comments, that improved our manuscripts.

I thank the German Research Foundation for funding this research project (DFG; Grant-No.: 57444011—SFB 806). Furthermore, I thank the Graduate School of Geosciences (GSGS), and especially Dr. Karin Boessenkool, for providing a start-up honours grants, which gave me the opportunity to prepare my PhD research, and a travel grant in order to attend an international conference. A joint thanks also goes to the GSGS and the Integrated Research Training Group (IRTG) for the opportunity to participate in various training programs.

Ευχαριστώ τον Δημοσθένη και τον Shaun για την υποστήριξη και την αγάπη σας τους τελευταίους μήνες. Μου δείξατε ότι μπορώ να πιστέψω στον εαυτό μου και στις ικανότητές μου.

Finally, I would like to thank my family and especially my parents, my sister and her lovely family for their support and affection. The conditions over the last few years have not been ideal, but just one short phone call with one of you has made me smile and strengthened me to keep going. The love and humor that we share in our family is inspiring, but keeps me grounded at the same time. Daher widme ich diese Arbeit Euch, meiner geliebten Familie.

---

## List of Abbreviations

AHP	African Humid Period
AMH	anatomically modern human
AO	Ammonium oxalate
BC	black carbon
BP	years before present (refers to calibrated radiocarbon ages)
BPCAs	benzene polycarboxylic acids
CAB	Congo Air Boundary/Belt
cal BP	calibrated years before present (refers to radiocarbon ages)
CIA	Chemical Index of Alteration
CRC	collaborative research centre
depth b.s.	depth below surface
DEM	Digital Elevation Model
ENSO	El Niño Southern Oscillation
H (1)	Heinrich event 1
ka	kilo annum – 1000 years
ITCZ	Intertropical Convergence Zone
LGM	Last Glacial Maximum
LSA	Late Stone Age
Ma	million years ago
MIS	marine isotope stage
MS	magnetic susceptibility
MSA	Middle Stone Age
OC	organic carbon
OIL	oblique incident light
PPL	plane-polarized light
ppm	parts per million
RI	redness index
SRTM	Shuttle Radar Topography Mission (remote sensing data)
TBR	Tropical Rain Belt
TC	total carbon
TIC	total inorganic carbon
TN	total nitrogen
TOC	total organic carbon
WC	Walker circulation
XPL	cross-polarized light

XRD	x-ray diffraction
XRF	x-ray fluorescence
YD	Younger Dryas

## Table of Contents

Abstract .....	I
Kurzzusammenfassung .....	III
Acknowledgements.....	V
List of Abbreviations .....	VII
Table of Contents .....	IX
List of Tables .....	X
List of Figures .....	XI
1. Introduction .....	1
1.1 Geoarchaeological approach.....	1
1.2 Sodicho Rockshelter as a potential human-environment archive.....	3
1.3 The Collaborative Research Centre 806 .....	7
1.3.1 Research by project A1 in Southwestern Ethiopia.....	8
1.4 Aims and objectives of this thesis.....	9
1.5 Research design and applied methodology.....	14
1.5.1 Fieldwork .....	14
1.5.2 Previous fieldwork of the CRC 806.....	16
1.5.3 GIS-Methods.....	16
1.5.4 Laboratory investigations .....	17
1.5.5 Chronology - Age depth model.....	22
1.5.6 Supportive investigations .....	22
1.6 Thesis structure.....	24
1.7 Setting of the study area .....	25
1.7.1 Present geological and geomorphological setting.....	25
1.7.2 Research site description .....	27
1.7.3 Past geological processes.....	31
1.7.4 Climatic setting.....	32
1.7.5 Vegetation.....	34
2. Combining geomorphological–hydrological analyses and the location of settlement and raw material sites – a case study on understanding prehistoric human settlement activity in the southwestern Ethiopian Highlands .....	36
2.1 Supplement material .....	50

3. Stratigraphy and Chronology of Sodicho Rockshelter – A New Sedimentological Record of Past Environmental Changes and Human Settlement Phases in Southwestern Ethiopia .....	52
3.1 Supplement material .....	73
4. A Multi-Method Approach for Deciphering Rockshelter Microstratigraphies — The Role of the Sodicho Rockshelter (SW Ethiopia) as a Geoarchaeological Archive .....	81
4.1 Supplement material .....	118
5. Synoptic Discussion .....	127
5.1 Local scale: Understanding site formation and human impact.....	128
5.2 Regional scale: Reconstructing past environmental signals, and regional settlement activity .....	133
5.3 Supraregional Scale: Implications for settlement history and adaptation to the environmental shifts.....	136
5.4 Applicability of the multiscale study .....	138
5.5 Implementation of results into the context of the CRC 806 .....	140
5.6 Critical review of this research: Limitations and future perspectives .....	141
6. Conclusion .....	145
7. References.....	148
Appendix A.....	CLXV
Appendix B.....	CLXXI
Appendix C .....	CLXXXII
Chapter Contribution .....	CLXXXIII
Curriculum vitae .....	CLXXXIV
Erklärung.....	CLXXXVI

## List of Tables

Table A 1: Summary of applied laboratory methods on the bulk sediment samples from profile F35 SW. Samples that were measured and included in the results of this doctoral thesis are marked with an X. .... CLXVI

Table A 2: Summary of applied laboratory methods on the bulk sediment samples from profile F35 SW; continuation of table A 1. Samples that were measured and included in the results of this doctoral thesis are marked with an X. .... CLXVII

Table A 3: Summary of applied laboratory methods on the bulk sediment samples from profile F35 SW; continuation of table A 1. Samples that were measured and included in the results of this doctoral thesis are marked with an X. ....	CLXVIII
Table A 4: Summary of applied laboratory methods on the bulk sediment samples from profile G35 SE. Samples that were measured and included in the results of this doctoral thesis are marked with an X. ....	CLXIX
Table A 5: Summary of applied laboratory methods on the bulk sediment samples from profile G35 SW; continuation of table A 4. Samples that were measured and included in the results of this doctoral thesis are marked with an X. ....	CLXX

## List of Figures

Figure 1.1 Idealized geoarchaeological research design in order to merge an archaeological record with past landscape processes (modified after F. Sulas and C. French (French 2015)). ....	3
Figure 1.2 Illustration of several dependencies (push and pull factors) that influenced prehistoric humans to occupy a particular region, in this case the highlands. ....	6
Figure 1.3 Structure of the CRC 806, during the third funding phase. Project A1 is part of research group “R” = Regional Models, marked in red (mod. after Richter et al. 2017). ....	7
Figure 1.4 Research design of this doctoral research, highlighting major methods, research aims and supportive investigations (own design). ....	15
Figure 1.5 Strategy used to collect the micromorphological samples at the Sodicho Rockshelter. (A) Sample blocks SOD_2 to SOD_5 (from the top) at profile F35, SOD_5 was lost during the sampling process; (B) Sample block SOD_1 at profile J29; (C) Sample block SOD_II at profile F35, supported in gypsum (Photos by R. Vogelsang, 2016 (A-B); E. Hensel, 2018 (C)). ....	18
Figure 1.6 Location of the study area (red square) within the Southwestern Ethiopian Highlands (Raster map data by Natural Earth). ....	26
Figure 1.7 Map of the study area with locations of research sites discussed in the following chapters (DEM data by ASTER GDEM and Natural Earth raster map data). ....	27
Figure 1.8 Photos of the surrounding area of Mt. Sodicho. (A) View of the entrance area of Sodicho Rockshelter within the outcropping trachytic bedrock; (B) The surroundings of Mt. Sodicho are characterized by permanent and episodic streams; (C) Mt. Sodicho is part of a series of silicic domes, as seen on the photo; (D) Clearing at the slopes and movement of livestock promotes degradation and runoff; (E) View from the northern	

summit of Mount Sodicho, towards the flanks of the Wagebeta calderas; (F) Round huts and flat-roofed huts are found on the mountain slopes which are used for cultivation (Photos by E. Hensel, 2017).....	29
Figure 1.9 Panoramic view into the Sodicho Rockshelter. Dark staining of the rock surface is caused by the exposure to moist conditions (Photo by C. Schepers, 2018; mod. after Hensel et al. 2021). .....	29
Figure 1.10 Photos in the close surroundings of Mt. Damota. (A) View to the summit of Mt. Damota, taken from the streets of Sodo (Photo by E. Hensel). (B) Most of the natural vegetation cover had been replaced by cultivated land along the flanks of Mt. Damota (Photo by S. Meyer). .....	30
Figure 1.11 Photos of significant features at the Bisare River catchment. (A) Degraded areas have been formed by gully erosion and extensive badland formation. (B) Swampy area in the western part of the upper Bisare catchment (Photos by O. Bubenzer, mod. after Hensel et al. 2019). .....	31
Figure 1.12 Climate chart of Maisai, at Mt. Sodicho (A), and Sodo, at Mt. Damota (B), showing monthly mean temperature ([°C]) and average monthly precipitation (based on an observation period from 1990-2019). The charts are based on the interpolated datasets of the Climatic Research Unit (CRU) Time-Series (TS) Version 4.04 and were derived from ClimateCharts.net (Zepner et al. 2021). .....	33
Figure 1.13 Map of potential vegetation for the study area (A). Map of pot. vegetation covering Ethiopia and northern Kenya (data from Friis et al. 2010; raster data and tools from //vegetationmap4africa.org (van Breugel et al. 2015)). .....	35
Figure 5.1 Flow chart showing the different spatial scales of applied geoarchaeological methods and the major scientific outcome of this research.....	128
Figure 5.2 (A) Road construction work along the steep mountainside exposed the obsidian raw material deposit of Fulasa. (B) Scattered obsidian, and obsidian gravels show signs for transport/ reworking (Photos by E. Hensel).....	135
Figure 5.3 Map of the Horn of Africa showing the location of the main study site and important archaeological sites, situated in Ethiopia (DEM data by ASTER GDEM and Natural Earth raster map data) (modified from Hensel et al. 2021). .....	144
Figure A. 1 Schematic illustration of the excavation profiles F35 west and north, G35 south and J29 south. Blue blocks refer to micromorphological sample blocks and thin sections are indicated as whitish squares (mod. from Hensel et al. 2022). .....	CLXXI
Figure A. 2 Schematic illustration of the micromorphological sample block SOD_01, and the position of the thin sections (mod. from Hensel et al. 2022).....	CLXXII

---

Figure A. 3 Schematic illustration of the micromorphological sample block SOD_02, and the position of the thin sections (mod. from Hensel et al. 2022).....	CLXXIII
Figure A. 4 Schematic illustration of the micromorphological sample block SOD_03, and the position of the thin sections (mod. from Hensel et al. 2022).....	CLXXIV
Figure A. 5 Schematic illustration of the micromorphological sample block SOD_04, and the position of the thin sections (mod. from Hensel et al. 2022).....	CLXXV
Figure A. 6 Schematic illustration of the micromorphological sample block SOD_I-1, and the position of the thin sections (mod. from Hensel et al. 2022).....	CLXXVI
Figure A. 7 Schematic illustration of the micromorphological sample block SOD_I-4, and the position of the thin sections (mod. from Hensel et al. 2022).....	CLXXVII
Figure A. 8 Schematic illustration of the micromorphological sample block SOD_II-3, and the position of the thin sections (mod. from Hensel et al. 2022).....	CLXXVIII
Figure A. 9 Schematic illustration of the micromorphological sample block SOD_7, and the position of the thin sections (mod. from Hensel et al. 2022).....	CLXXIX
Figure A. 10 Schematic illustration of the micromorphological sample block SOD_6, and the position of the thin sections (mod. from Hensel et al. 2022).....	CLXXX
Figure A. 11 Schematic illustration of the micromorphological sample blocks SOD_III and SOD_IV, and the position of the thin sections (mod. from Hensel et al. 2022). ...	CLXXXI

## Chapter I

### 1. Introduction

#### 1.1 Geoarchaeological approach

**Where do we come from?** This question does not only regard to the fundamental issue about the African cradle of our human ancestors. Furthermore, it connects the research topics of past human migration, adaptation, and the external natural factors that influenced the expansion across the globe and the preference for certain regions. The reconstruction of past geomorphological, climatological, and environmental conditions in research areas and archaeological significant sites can help to narrow down palaeoenvironmental factors that were responsible for pushing and pulling past human dispersal in the past. Geoarchaeological multiscale investigations offer an interdisciplinary approach and a broad spectrum of research methods to link earth sciences with archaeological research, in order to tackle the above-mentioned research topics (Gilbert et al. 2017). In general, the focus lies in the investigation of human-environment interaction, such as geomorphological, climatic, and human induced landscape changes, as well as the reconstruction of palaeoenvironmental conditions, and past human activity (Goldberg and Macphail 2006, French 2015, Siart et al. 2018). With regard to research on the subject of human dispersal in eastern Africa, Ethiopia in particular (White et al. 2003, Aubert et al. 2012, Schaebitz et al. 2021) is still seen as one of the key regions for the multi-regional development of anatomically modern humans within the African continent and the expansion beyond its borders (Hublin et al. 2017, comp. Scerri et al. 2019).

At the current state of research, the oldest fossils that show features of the early stages of anatomically modern humans date back to 300 ka and originate from the site Jebel Irhoud, western Morocco (Hublin et al. 2017). The oldest fossils from Ethiopia, where found within the Kibish formation at the Omo River (Omo/Kibish, ~ 190 ka) (McDougall et al. 2005, Fleagle et al. 2008, Aubert et al. 2012) in southern Ethiopia and at Herto, Middle Awash (~ 160 ka) (White et al. 2003). Several Ethiopian cave and rockshelter sites, as well as open air sites, hold evidence for human occupation since the Late Pleistocene (Tribolo et al. 2017, Blinkhorn et al. 2022). However, archaeological records are often fragmented and incomplete, and the fossil evidence is sparse. Past and also present environmental changes, disturbances and erosion events, are the most probable causes for the interruption of past occupation phases, leaving the cultural and environmental records incomplete. Nevertheless, palaeoenvironmental research allows

to study the relationship between migrational response of humans and past climate change (Foerster et al. 2012, Foerster et al. 2015, Schaebitz et al. 2021). The refugial hypothesis suggests that East Africa provides suitable conditions due to its diverse ecology, topographic complexity and therefore habitat heterogeneity (Basell 2008, Brandt et al. 2012, Mirazón Lahr 2013, Mirazón Lahr and Foley 2016).

Within this doctoral research, a variety of geoarchaeological methods are integrated to address research topics about past human-environment interaction in the prehistoric southwestern Ethiopian Highlands, at different spatial and temporal scales. The main research area is the new promising site Sodicho Rockshelter and its surroundings. For the first time at this site, a multi-method approach is used to reconstruct site formation, (post-) depositional processes and the impact of prehistoric hunter-gatherers.

Geoarchaeological research is a continuously changing discipline, as new methods are introduced or developed within the associated interdisciplinary fields. Such is the case with the concept of digital geoarchaeology, where the research fields of geosciences overlap with those of humanities and computer sciences (Siart et al. 2018). With help of the geoscientific field and laboratory methods, and digital tools different spatial and temporal scales are considered. This allows the study of entire geographical regions by expanding the spatial resolution to a macro scale or the investigation of a local scale, such as around an archaeological site (Siart et al. 2018). By focusing at a micro scale, individual thin sediment deposits within an archaeological stratigraphy can be examined (French 2015). At this point, it should be mentioned that the classifications of the scales are not clearly defined within the scientific community. Thus, the terms often differ for scales that describe the same characteristics (comp. Goldberg and Macphail 2006, French 2015, Garrison 2016, Siart et al. 2018, Cordova 2018). This means that the applied scales for this study are specifically determined.

As already stated in publications on geoarchaeology (a.o. Goldberg and Macphail 2006, French 2015, Siart et al. 2018, Stolz and Miller 2022), the strength of this research field lies in its integrative approach and the ability to be merged with research concepts from other disciplines. According to several geoarchaeological research designs that have already been developed (French 2015, Siart et al. 2018, Stolz and Miller 2022), the different types of data obtained by the diverse disciplines can be used to generate a wide range of information (Fig. 1.1). This includes the natural science data from geo-archives and bio-archives, along with data from the humanities, archaeological, historical and ethnographic research, as well as information obtained from various dating methods. The data obtained provide information about local sedimentary deposits, soil development, erosion, vegetation change or chronostratigraphic periods of human settlement activity, among other variables. At a higher level, the interpretation of the

collected data can provide information about the influence of short and long-term sub-regional climatic events, on the environment and humans (French 2015).

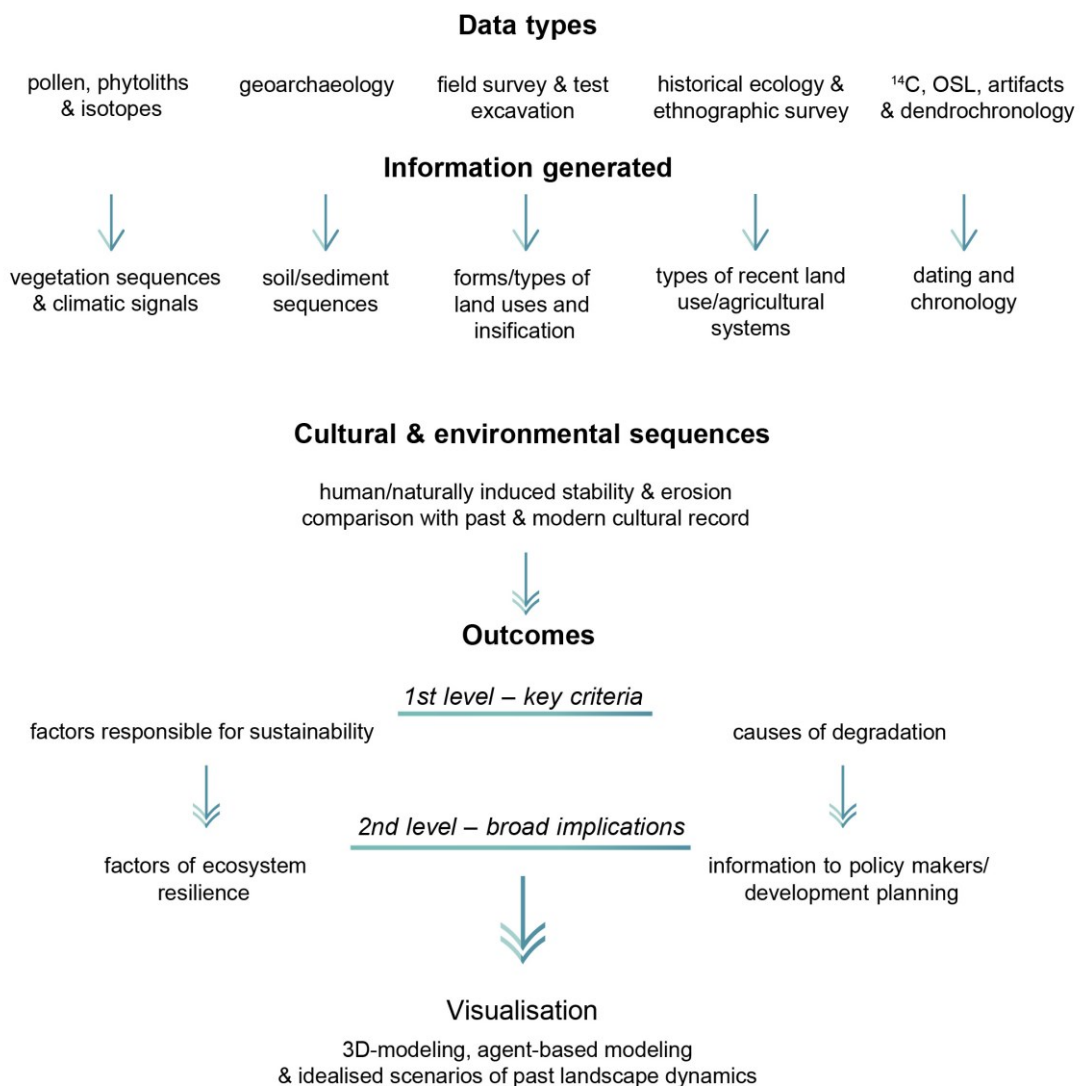


Figure 1.1 Idealized geoarchaeological research design in order to merge an archaeological record with past landscape processes (modified after F. Sulas and C. French (French 2015)).

## 1.2 Sodicho Rockshelter as a potential human-environment archive

For a reconstruction of human and palaeoenvironmental influences at a certain site, a complete preservation of the archaeological material as well as of the sedimentary deposits are crucial. Caves and rockshelters, such as the Sodicho Rockshelter provide excellent study conditions for geoarchaeological research, as they function as sediment traps that allow the investigation of different depositional conditions. This means that

multiple sources of deposits, such as autochthonous geogenic, allochthonous geogenic, anthropogenic and biogenic sediments entered cave and rockshelters, depending on the variability and intensity of external environmental factors (Goldberg and Sherwood 2006, Mentzer et al. 2017). This is especially true for rockshelters, which are often described as cavities that are wider than they are deep, and that are usually filled by direct and indirect sunlight (Birndorfer et al. 2022). Consequently, there is often a greater impact on the sedimentological, archaeological and zooarchaeological record from changing external environmental conditions within rockshelters. Thus, a reconstruction of the external circumstances could be reflected more precisely.

With this information in mind, the sediment stratigraphy at Sodicho Rockshelter can be used as a record of local climatic and environmental variability. By identifying single depositional processes, and the comparison with climatic records from lacustrine sediments or calculated models, the research scale can be expanded to a supraregional scale, while at the same time it demonstrates the potential for using existing research and methodological approaches in order to investigate rockshelter stratigraphies. The last mentioned must be considered, since countless factors may be responsible for failing a preservation of key indicators in a rockshelter stratigraphy, which could relate to the past environment. These include post-sedimentary influences of organisms, but also facts such as the climatic circumstances at the site. For instance, sites in tropical regions, e.g. parts of Ethiopia, are often characterized by warm and humid tropical climates, which are associated with a high intensity of weathering. Climatic fluctuations, in some cases very rapidly shifting, may also have affected sedimentary deposits in the past. Studies in southeastern Ethiopia and northern Kenya, identified rapid climatic changes that had an impact on the landscape, flora, and fauna, especially during the Late Pleistocene and the following Holocene (e.g., Junginger and Trauth 2013, Foerster et al. 2015, Gebru Kassa 2015, Trauth et al. 2019, Schaebitz et al. 2021, comp. Schaebitz et al. 2021b). Changes from cold dry, with a reduction of about 15–20 % moisture availability as during the Last Glacial Maximum (LGM,  $\sim 21 \pm 2$  ka), to extremely humid conditions during the African Humid Period (AHP,  $\sim 15$ –5 ka), with a calculated increase of 25–40 % moisture availability did affect the environment and especially the vegetation cover significantly. It also forced humans to adapt to the circumstances and abandon certain regions (Basell 2008, Fischer et al. 2021). In the context of this study presented here the migration does not only refer to the lateral movement into another preferred region or as far as another continent, it could also refer to a vertical movement into high-altitude landscapes with more favorable resources (Basell 2008, Brandt et al. 2012). In terms of geoarchaeological research, summarized by Röpke et al. in the subchapter on high mountain ranges (Birndorfer et al. 2022) mountainous landscapes are of

geoarchaeological interest as they exhibit increased geomorphological dynamics, with an increase in erosion and accumulation processes. With increasing height, the mean temperatures fall, and physical weathering increases, unlike decreasing chemical weathering (Cordova 2019). The complex orographic effect, especially in tropical highlands plays a crucial role in the variability of rainfall intensity (Fazzini et al. 2015, Van den Hende et al. 2021). In addition, the physical strain on humans increase at higher altitude, not least by increased UV radiation and decreasing oxygen content (Aldenderfer 2006). Thus, the vertical landscape structure and the dynamic geomorphodynamic of highlands, such as the study area in the southwestern highlands of Ethiopia, offer an attractive landscape for studying prehistoric settlement phases, as they hold a variety of suitable and therefore potentially preferred environments. Studies on prehistoric high-altitude settlement and vertical use patterns of the mountain areas can also be found, to name but a few, in the regions of the Peruvian Andes (occupation in height ~ 4500 m a.s.l.) and the Tibetan Plateau (occupation in height 3280 m a.s.l.) (Rademaker et al. 2014, Chen et al. 2019). Fincha Habera in the Bale Mountains, at an altitude of 3469 m above sea level, is the oldest dated archaeological site of a mountain region in Africa with an age of 47 to 31 ka BP (Ossendorf et al. 2019). While in the Bale Mountains the groups of hunter-gatherers are likely to have moved along the ice-free edges of glaciers in search of suitable raw material, there is evidence of the exploitation of different tropical ecozones along the mountain slopes in the highlands at other sites of Ethiopia. These include sites, such as the small rockshelter (DEN12-A01) and several other finds around the crater lake of Dendi, with an altitude of 3000 m a.s.l. (Vogelsang et al. 2018, Schepers et al. 2020). Moving closer to the main Sodicho Rockshelter site, Mochena Borago is located on Mount Damota at 40 km in immediate vicinity, and again, studies of settlement patterns suggest similar use of the different altitudinal zones in the highlands (Vogelsang and Wendt 2018). This pattern in mind, the tropical ecozones offered a variation in vegetation, provided protection and food for a wide range of animals. It is hypothesized that prehistoric foragers were thus able to exploit an abundance of vital resources within the different ecozones of the highlands (Vogelsang and Wendt 2018, Schepers et al. 2020).

According to the Mountain Refugium Hypothesis, mountainous locations like the Ethiopian Highlands were a possible environmental refugium for prehistoric groups coping with cold and hyper arid conditions in the surrounding lowlands (Basell 2008, Stewart and Stringer 2012, Brandt et al. 2012 and 2017). Based on the study of Blinkhorn et al. (2022), a research on the evaluation of refugia in Africa, the basic concept of a refugium is a region that enables a given group of organisms, in this case humans, to cope with conditions of increased climatic and environmental stress and to adapt to new

conditions. The data review in Basell 2008 pointed to the formation of forest refugia in the highlands of Ethiopia and Kenya during MIS 6 and 4, phases that were longer, colder and comparably dryer to the LGM. Clear evidence for these circumstances and the human response for MIS 6 and 4 is still scarce in eastern Africa and even more limited for MIS 2 (Basell 2008). In the Horn of Africa discontinuous archaeological stratifications are quite common. Studies at sites such as Goda Buticha, the Ziway-Shala basin and Mochena Borago observed a chronological gap, that has been dated to a timeframe that correlates to the MIS 2 (Tribolo et al. 2017). Archaeologically, this phase is of interest as it marks the progression from the lithic typologies, defined as the Middle Stone Age (MSA) to the Late Stone Age (LSA). The transition between these important technological innovations is still not clearly defined and remains poorly understood in the Horn of Africa (Basell 2013, Tribolo et al. 2017, Leplongeon et al. 2021). It should be noted that up to this point in research it cannot be determined how great the influence of precise habitat preferences of prehistoric humans was (Basell 2013) and which role factors such as cultural innovations, traditions or individual adaptation played (Fig. 1.2). The present study therefore does not address this issue, but rather relies on the new geoarchaeological results to discuss push and pull factors, including vital resources and environmental drivers, to address the question regarding the migration of prehistoric humans to regions such as the southwestern highlands of Ethiopia.

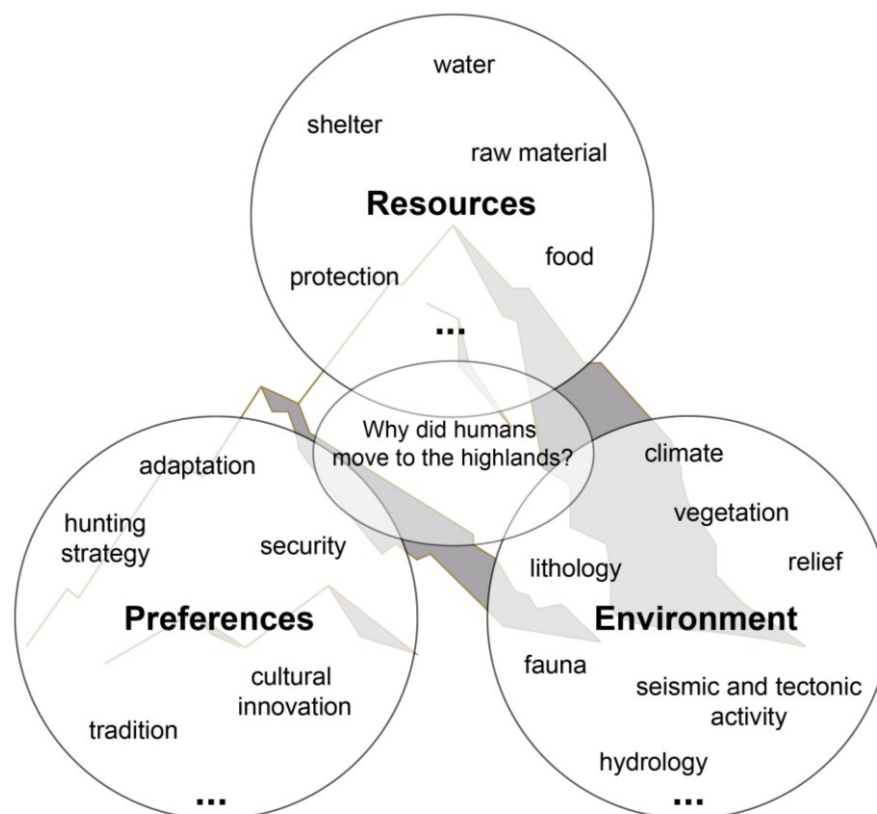


Figure 1.2 Illustration of several dependencies (push and pull factors) that influenced prehistoric humans to occupy a particular region, in this case the highlands.

### 1.3 The Collaborative Research Centre 806

This PhD dissertation is embedded in the Collaborative Research Centre 806 “Our Way to Europe – Culture-Environment Interaction and Human Mobility in the Late Quaternary”, funded by the German Research Foundation (Deutsche Forschungsgemeinschaft, DFG). Since its beginning in 2009 the CRC 806 established a research focus during the past two funding phases that concentrated on cultural-environmental context and palaeoclimatic conditions that lead to dispersal processes of anatomically modern humans (AMH) from Northeastern Africa to Western Eurasia. This involves the study of push and pull factors within different temporal scales, starting with the Marine Isotope Stage MIS 6 (about 190,000 years ago) to the MIS1 on a regional and continental scale.

The collaborating institutions comprise of various university departments, institutes, and non-university institutions within the fields of geosciences, archaeology (prehistoric archaeology), meteorology and philosophy from the University of Cologne, the University of Bonn and the RWTH Aachen University. In this case, the CRC 806 benefits from the diversity of scientific disciplines and research methods in order to address interdisciplinary research questions. The research structure of the third and final funding phase (2017-2021) has a circular form (Fig. 1.3).

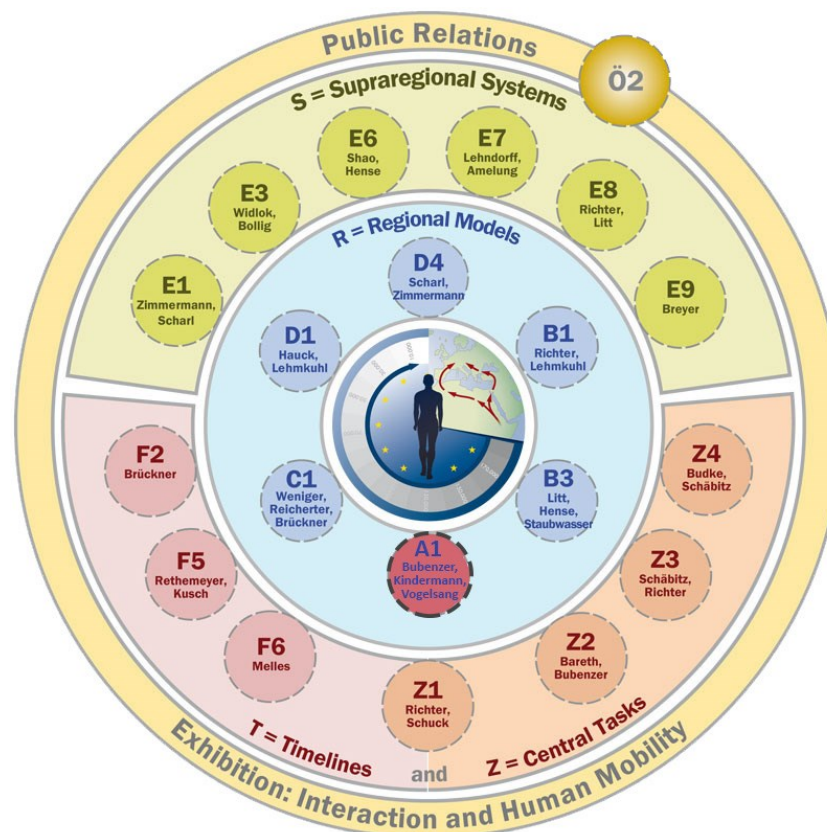


Figure 1.3 Structure of the CRC 806, during the third funding phase. Project A1 is part of research group “R” = Regional Models, marked in red (mod. after Richter et al. 2017).

The Regional Modal Groups (A1, B1, B3, C1, D1 and D4) in the center are symbolizing the investigations and interpretations concerning important key sites in northeast Africa, Levant, Eastern and Western Mediterranean, Balkan Peninsula, Near East and Central Europe. The outer circle is divided into three parts, representing the cooperating Supra-regional System (S) Group, the Timelines (T) Group, and the Z-Group concerning data management and administrative tasks.

The projects of S Group (E1, E3, E6, E7, E8, E9) will provide further datasets through the use of an additional methodological spectrum. These include modelling of population dynamics and regional climatic conditions on the basis of already available data, investigation of faunal assemblages, but also a philosophical reflection addressing concepts such as materiality and agency in archaeology and anthropology. The timeline group (F2, F5 and F6) covers the chronological framework of the CRC and supports the hypotheses and research aims of the CRC with dating methods such as  $^{14}\text{C}$ , optically stimulated luminescence dating and palaeomagnetic dating.

### **1.3.1 Research by project A1 in Southwestern Ethiopia**

Project A1 “Out of Africa – Late Pleistocene Rock Shelter Stratigraphies and Palaeoenvironments in Northeast Africa” covers study areas in the Eastern Egyptian Desert and in Ethiopia. Under the direction of the principal investigators Prof. Dr. Olaf Bubbenzer, Dr. Karin Kindermann and Dr. Ralf Vogelsang the following major research objectives were set for both research areas:

- 1) investigation of key stratigraphies at rockshelters and their surroundings to establish a chronological framework,
- 2) reconstructing different Pleistocene landscape settings in the research areas with help of archaeological sediments, which offer the possibility for a reconstruction of the environmental and cultural history,
- 3) identification of implications on the dispersal/migration of Homo sapiens.

Archaeological and geomorphological research in Egypt focused on archaeological layers from Sodmein Cave, with oldest layers of about 130 ka, and on Sodmein Playa basin, comprise of surface concentrations of Middle Stone Age (MSA) artifacts associated with Pleistocene lacustrine deposits (Kindermann et al. 2013, Kindermann et al. 2018, Henselowsky et al. 2022).

Since the first funding phase of the SFB 806 in 2009, the stratigraphies at the Mochena Borago Rockshelter on Mount Damota in the southwestern Ethiopian Highlands has

been a main focus. Through a cooperation with the Southwest Ethiopia Archaeological Project, under the direction of Steven Brandt (University of Florida), with Elisabeth Hildebrand (Stony Brook University, New York) and their team, 2 m of stratified Late Pleistocene and Holocene sediment deposits and cultural remains were investigated (Gutherz et al. 2002, Fisher 2010, Brandt et al. 2012). Stone artifact assemblages comprise of obsidian MSA and LSA artifacts.

The depositional processes that developed a very complex and inhomogeneous stratigraphy in Mochena Borago occurred in multiple phases and composed of geogenic and anthropogenic deposits. The cultural remains in the main trench were dated to the Late Pleistocene with an age of 36 and > 50 ka and the Holocene occupational layer are dated back a calibrated age of ~ 8 ka cal BP (Brandt et al. 2017). A chronostratigraphic hiatus of ~ 30 ka between the two epochs, which is also identified at other sites in Ethiopia (see chapter 1.2), leaves unanswered questions about the settlement history and environmental changes in the area. Multiple episodes of water saturation which lead to major erosion processes have been suggested in the development of the gap, that encompasses the hyper-arid period of the LGM (Brandt et al. 2012, Brandt et al. 2017). So far cultural occupation at Mochena Borago has only been recorded during periods with intermediate humid conditions, which means that this site does not provide robust evidence for the use of the region as a refugium during extremely dry periods, such as during MIS 2. First test excavations in 2015 at the new site Sodicho Rockshelter, revealed parts of a stratigraphy that has the potential to preserve a comparable multi-layered deposit with cultural remains of hunter-gatherer communities.

#### **1.4 Aims and objectives of this thesis**

The main aims of this doctoral thesis are an understanding of prehistoric human-environment interactions in the southwestern Ethiopian Highlands during the Late Pleistocene and Holocene. Furthermore, this study attempts to close chronological gaps and to verify and challenge the current state of research for the mentioned time periods. For this purpose, a variety of geoscientific methods are applied at different spatial and temporal scales. The addressed main aims include objectives that are proposed by Project A1 - Late Pleistocene Rock Shelter Stratigraphies and Palaeoenvironments in Northeast Africa, of the CRC 806, concerning the establishment of a geo- and archaeo-chronological framework in the study area.

## **1. Recent relations of the hydrological system are also applicable for the past**

The actual hydrological system and the location of archaeological sites provide suitable insights into ancient morphodynamics, and their influence on prehistoric human mobility, as well as the accessibility of past obsidian raw material sources in the southwestern Ethiopian Highlands.

### *Objective 1.1.: Investigation of the current hydrological system and geomorphological processes that relate to erosion and the human influence*

Complex relief and mountainous formations, given in the Ethiopian Highlands, are driven by tectonic and climatological processes as well as morphodynamic changes. Excessive erosion processes, like gully erosion and badland formation are very common phenomena (Billi and Dramis 2003, Mukai 2017). Human impact and the intensification of agriculture and cattle farming which is often connected to the removal of the natural vegetation cover, are further causes on today's soil erosion and morphodynamic transformations (Fryirs and Brierley 2012, Castillo and Gómez 2016). For this study high resolution satellite imagery and digital elevation models (DEM) were used to investigate the current landscape dynamics and the actual hydrological system. In this context the three following research areas are being focused on: the volcanic mountains Damota and Sodicho, and the banks of the Bisare River, a tributary of the Bilate River. Hydrological data such as the catchment area and the stream networks are reconstructed with the modelling tool ArcHydro in ArcMap. The temporal classification is based on radiocarbon dating of selected drilling cores from the swampy, upper Bisare catchment.

### *Objective 1.2.: Implications for prehistoric settlement activity by combining GIS based mapping with systematic survey of archaeological open-air sites and obsidian raw material exposure*

Well-preserved archaeological and terrestrial palaeoenvironmental archives that allow an understanding of the interaction between prehistoric settlement activity and palaeoenvironmental conditions are still rare. So far, within the study area, prehistoric settlement activities are documented by cultural finds within the Mochena Borago Rockshelter on Mount Damota, including oldest MSA artifacts dating > 50 ka (Brandt et al. 2012, Brandt et al. 2017). Most of the obsidian raw material used for stone tool production came from the outcrops of the Baantu area, located about 20 km from the site (Brandt et al. 2017). Furthermore, MSA and LSA surface artifacts occurrences are found on the flanks of Mount Damota (Vogelsang and Wendt 2018). According to studies by Benito-Calvo et al. (2007) surface finds of archaeological artifacts and the occurrence

of obsidian raw material qualify the region around the Bisare River as suitable for geoarchaeological investigations. For the area at Mount Sodicho, no comparable observations have yet been made so far.

To investigate the interplay between past hydrological conditions, prehistoric settlement activity and raw material availability, geomorphological–hydrological datasets are combined with mapped locations of archaeological sites, and raw material outcrops. This method aims to understand the effect of the hydrological system on present accessibility of obsidian raw material sources and the visibility and preservation of archaeological sites, in general.

## **2. The sediment stratigraphy of Sodicho Rockshelter holds crucial information about site formation processes in a volcanic rockshelter and prehistoric human activity**

The Ethiopian Highlands hold important archaeological records in caves and rockshelter covering human occupation phases of the Late Pleistocene and Holocene (Brandt et al. 2012, Tribolo et al. 2017). The well-studied key stratigraphy of the Mochena Borago offers insights into complex site formation processes within a tropical rockshelter and into the past of prehistoric hunter-gatherer during > 50 ka to ~ 36 ka (Brandt et al. 2017). Nevertheless, a major chronostratigraphic gap of about 30 ka within the sediment records leave unanswered questions. The Sodicho Rockshelter has the potential to be a further important site in this area. Comparable sediment accumulation processes could give information about regional palaeoenvironmental shifts and human settlement phases.

### **Objective 2.1.: Understanding site formation processes in volcanic rockshelters in the tropical highlands**

The development of archaeological stratigraphies within caves and rockshelter depends on dynamic depositional processes, environmental changes and the conditions within the shelter (Goldberg and Sherwood 2006, Mentzer et al. 2017). In tropical regions, humidity and the influence of changing moisture conditions have a major effect on deposits. At the Sodicho Rockshelter, the human impact is an additional factor, which influences site formation and post-depositional processes. A variety of geoarchaeological methods will be used to determine the complex sediment composition, to distinguish geogenic, biogenic and anthropogenic sediment deposition and alteration processes, and to determine the pace of shifting conditions.

*Objective 2.2.: Identifying the human context and human behavior at the site*

At prehistoric archaeological sites evidence of human behavior is often limited to the discovery of lithic artifacts (Cornelissen 2013). In the Horn of Africa further findings that represent human presence are given, but the archaeological sequences are often short and discontinuous (Tribolo et al. 2017), which leads to missing information about the transition between African prehistory, such as the Middle Stone Age (MSA) and Later Stone Age (LSA) (Leplongeon et al. 2021). The determination of the sediment composition in Sodicho is followed by an in-depth study of the human impact on the deposits, considering microstratigraphic changes. Attention will also be given to the micromorphological investigations on human behavior, with emphasis on the reconstruction of human fire activity and indication for site maintenance.

*Objective 2.3.: Establishing a comprehensive radiocarbon chronology*

Several archaeological sites in Ethiopia that have preserved prehistoric cultural material share a major chronostratigraphic gap of roughly 17.5 to 33 ka, thus spanning certain parts of the MIS 2 (Tribolo et al. 2017). This includes for instance Mochena Borago with a hiatus from ~ 38 to ~ 7,6 ka (Brandt et al. 2012, 2017), and Goda Buticha from ~ 25 to ~ 7.5 ka (Pleurdeau et al. 2014, Tribolo et al. 2017). First test excavations at Sodicho yielded sediment deposits that have the potential to be comparable in thickness and age to Mochena Borago. Radiocarbon dating and a first calculated age-depth model will be used to get chronological control of the stratigraphy and to diminish the major chronological gap that is known for the Horn of Africa.

### **3. The geoarchaeological research contributes to the Mountain Refugium Hypothesis**

There is still an ongoing discussion on the effect of short and long termed climatic events that had a major impact on past African environment and therefore on prehistoric humans (Foerster et al. 2015, Trauth et al. 2019). In many studies, the adaptation of the prehistoric hunter-gatherer to harsh environmental conditions is linked to a retreat into an environmental refugia (Basell 2008, Stewart and Stringer 2012). The Ethiopian Highlands are proposed as one such potential environmental refugium during cold and hyper-arid phases, such as during the MIS 4 and MIS 2, when smaller groups were forced to abandon the lowlands and moved up into higher mountain ranges (Brandt et al. 2017).

Objective 3.1.: Identifying regional palaeoenvironmental signals within the sedimentological record at Sodicho

In course of this study, the results on sediment deposition and alteration processes will be linked to local and supraregional environmental signals (e.g., shifting moisture conditions, volcanic eruptions, natural bush fire) to identify possible differences in the deposits, that could mirror long-term climatic trends or even short-term events. The determination of possible proxies for the degree of weathering - changes in moisture and dryness - will be investigated using sedimentological, geochemical and micromorphological investigations.

Objective 3.2.: Implications for prehistoric human occupation and cultural adaptation to a changing environment

Evidence of prehistoric human settlement in the Ethiopian Highlands can be found in archaeological open-air sites or within rockshelter stratigraphies. The Mochena Borago Rockshelter is the only well studied and securely radiocarbon dated site (Brandt et al. 2012, Brandt et al. 2017) within close vicinity of the Sodicho Rockshelter. In order to identify the environmental circumstances driving human migration (testing the Mountain Refugium Hypothesis), the detected depositional processes of Sodicho are compared with information on regional settlement history and past climate events.

**4. The geoarchaeological research results are applicable to other archaeological research sites at tropical caves and rockshelters**

Rockshelters and caves often provide a record of repeated human occupation and a geo-archive of past environmental and climatic changes (Woodward and Goldberg 2001). Differences in depositional conditions are based on parent rock, climatic and environmental conditions, and biogenic impact. It is particularly evident in a tropical regime, where sediment and soils are often exposed to highly fluctuating moisture conditions, which can alter the deposits.

Objective 4.1.: Linking and highlighting the results in comparison to other important geoarchaeological research sites

The Sodicho Rockshelter is a promising site, that persevered archaeological information about prehistoric hunter-gatherer occupation and the past environment. Due to discontinuous, short stratigraphies, as well as major chronostratigraphic gaps, there is a lack of comprehensive evidence on the way of life of East African hunter-gatherers and the environment in which they moved. The new geoarchaeological research results shall

be linked to other rockshelter sites, in order to highlight the importance of the data and to identify the extent spatial and temporal transferability. Sodicho could act as a new potential key site for geoarchaeological research at difficult archaeological stratigraphies, and at the same time be a prime example of research approaches and methodological practices in tropical rockshelters. Thereby, it can be determined which combination of methods shall be applied for the different scale levels.

## **1.5 Research design and applied methodology**

The research design of this doctoral research comprises of an interdisciplinary geoarchaeological approach that is based on the initial research questions formulated by Project A1 from the CRC 806 (see chapter 1.3). It addresses the former mentioned hypotheses and formulated objectives of this thesis. This combines a variety of geoscientific field and laboratory investigations, computer methods and the cultural-historical context, which is clarified by archaeological investigations. The following design represents a workflow with important steps and applied methodology based on the understanding of different scales of geoarchaeological investigation (Fig. 1.4). While the regional landscape scale focuses on the investigation of the research area from a distance, with help of satellite-derived GIS analysis, further sedimentological and geochemical methods zoom into the sediment stratigraphy at the Sodicho Rockshelter. Supporting studies and external palaeoenvironmental records are consulted for the verification of the results and the correlation of the data. The main aim of this study will be the reconstruction of the human environment-interaction, palaeoenvironmental changes and the impact of prehistoric human occupation in the southwestern Ethiopian Highlands.

### **1.5.1 Fieldwork**

As part of the third phase of the CRC 806, two final fieldwork and excavation campaigns were conducted at the Sodicho Rockshelter during 2017 and 2018. A first geoarchaeological survey took place in November 2017 within the Sodicho Rockshelter itself and the close surroundings by a geomorphological mapping the location of raw material outcrops and scatter finds at Mt. Sodicho. Rock samples were examined and described in the field to investigate the mineralogical composition of the rockshelter bedrock and lithological changes at Mt. Sodicho.

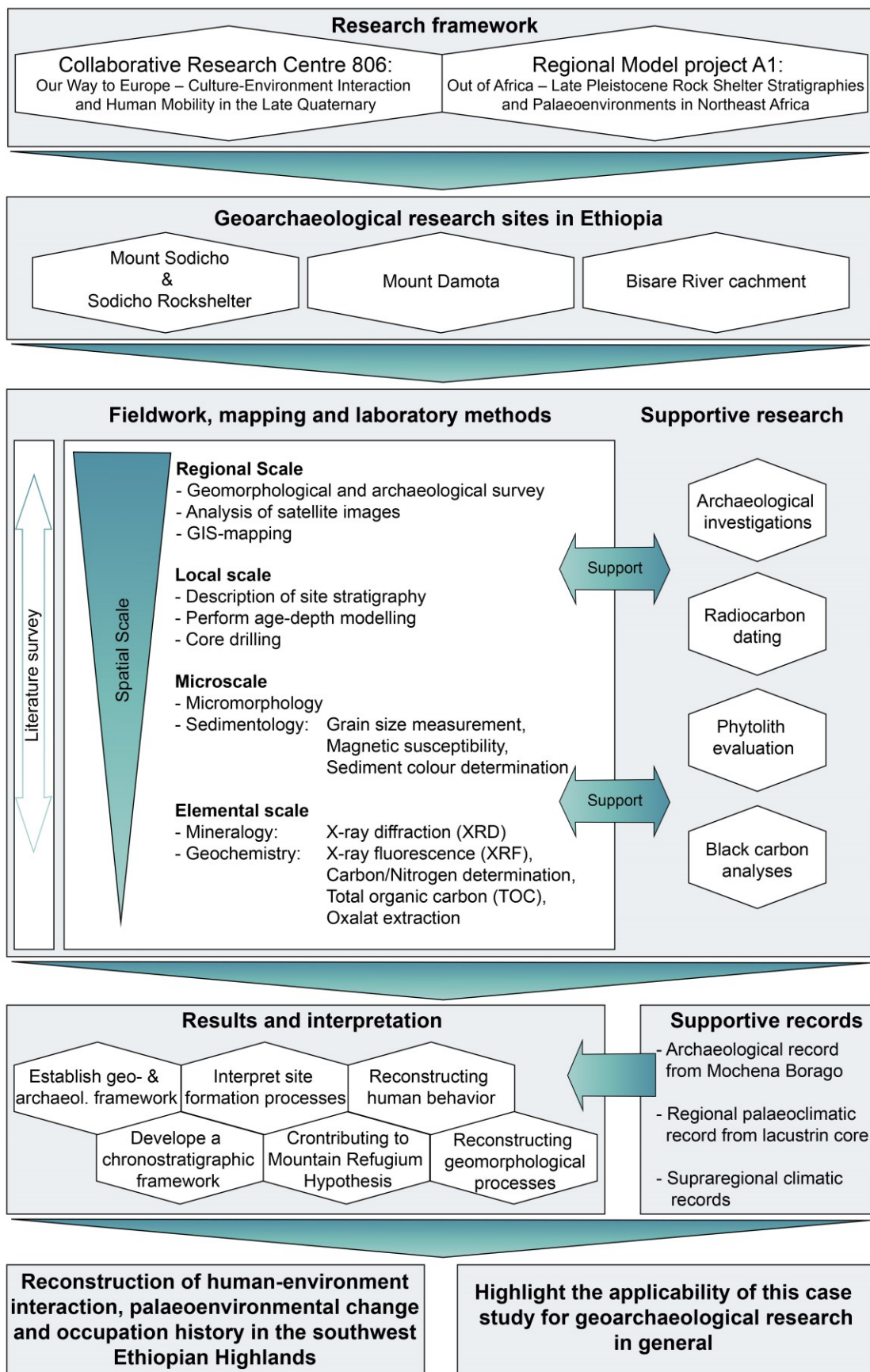


Figure 1.4 Research design of this doctoral research, highlighting major methods, research aims and supportive investigations (own design).

Stratigraphic description of the sediment layers at the excavation site was done according to the description of sediment texture, sediment color (Munsell Soil Color Charts©) and special characteristics. Bulk sediment samples, in a two 2 cm resolution, were taken from two excavation profiles for sedimentological and geochemical analyses, and phytolith investigations. During a second, shorter field stay in November 2018, further bulk sediment samples were taken from the lowest excavated stratigraphic layers. In addition, micromorphological monoliths were extracted and 20 bulk sediment samples were taken from each sediment unit within two excavated profiles for black carbon analyses. After the completion of the excavation, a short raw material survey was undertaken to the area of Fulasa and Chebe, east of the Wagebeta Caldera complex.

### **1.5.2 Previous fieldwork of the CRC 806**

Previous to this study, geoarchaeological research trips to the study area took place in context of the CRC 806 studies from 2012 onwards and sample material was collected, that was incorporated into this study. Percussion drilling cores were obtained in the basin of the Bisare River area during the field campaigns of 2014 and 2015 (see chapter 1.5.6). At Sodicho Rockshelter, the main site itself, the excavated archaeological material (especially the lithic artifacts) has been documented since the first excavations in 2015. Charcoal and seed samples have been taken from the excavation site, for radiocarbon analysis (see chapter 1.5.6). In addition, 6 of the 10 micromorphological monoliths were already sampled in 2016 (see chapter 1.5.4).

### **1.5.3 GIS-Methods**

Geographical Information Systems (GIS methods) were used for geomorphological and hydrological mapping of the study area in the southwestern Ethiopian Highlands, and to incorporate information from field survey data, such as mapped geomorphological information or archaeological findings. The base “maps” for all analyses were extracted digital elevation models (DEM) covering the different study areas. The DEM was generated using high-resolution panchromatic satellite images of Pléiades 1A satellites (by Astrium Services/Spot Image, Airbus Defence and Space) with a 2 m resolution. ASTER GDEM data (by METI and NASA), with a resolution of 30 m was used to fill the gaps between the study areas of choice. Within the image analysis software ENVI (5.3 by Harris Geospatial Solutions) two satellite images of one area were manually fitted together, by setting tie points, in order to create a panchromatic image. The geomorphological surface data (terrestrial analyses) were determined by the GIS-

software ArcGIS 10.6 by ESRI. In order to reconstruct the hydrological system, the modelling tool set of ArcHydro (ESRI) was used. Again, the DEM functioned as a base map and features such as flow directions, flow accumulation, surface runoff, and catchment areas were calculated. In order to create visual maps, such as those used in introductions, additional Natural Earth raster map data was used to produce illustrative geomorphological maps. The raster data for introductory maps featuring lithological properties of the surface geology were provided by USGS.

#### **1.5.4 Laboratory investigations**

Bulk sediment samples were determined with a 2 cm resolution at two columns at two excavation profiles. Exceptions were difficult areas around bigger rocks, increasing the sample thickness to 4 cm. All samples were analyzed at the Institute of Geography at the University of Cologne, Germany. Pre-treatments include drying all samples at 40 °C in the drying chamber and sieving to less than 2 mm. A part of the material was grinded and homogenized for geochemical analysis with a zircon ball mill. A simple overview of the methods applied to individual sediment samples is provided in the tables A1 to A5 in Appendix A.

##### *a) Micromorphology*

Micromorphology is a method to analyze unconsolidated sediment and soil samples (Stoops 2021). The sampling of undisturbed sediment blocks was conducted at four excavation squares (F35 North, F35 West, G35 South, J29 South), during the excavations in 2016 and 2018 (Fig. 1.3). The micromorphological monoliths were taken from all sediment layers, also covering the layer boundary, to enable a gapless sampling. The removed sample were secured with commercially gypsum bandages. Thin sections preparation was performed at the thin section laboratory of Mr. Dipl. -Ing. Beckmann, Schwülper-Lagesbüttel. The impregnation of the sediment monoliths in a vacuum as well as the preparation of the < 30 µm thick, uncovered thin sections followed the instructions of Beckmann (1997). The observation and description of the thin sections followed the guidelines and terminology of Stoops (2021). A first microscopic examination was carried out with a polarizing microscope BH-2 (Olympus, Hamburg, Germany). For further detailed observations, the polarizing microscope Axiolab (Zeiss, Oberkochen, Germany) was used in polarized light (PPL), between crossed polarizers (XPL), and under oblique incident light (OIL). During the microscopic analyses the thin sections were covered with oil to enhance the feature contrast. Digital images were performed by using the digital image capture software Axiovision (Zeiss, Oberkochen, Germany). In order to document

the overall composition, the thin sections were flatbed scanned with help of a CanoScan 9000F (Canon) (Arpin et al. 2002), under PPL and XPL, and using black and red backgrounds. Additional information about each thin section and its position in the stratigraphy can be found in Appendix B.



Figure 1.5 Strategy used to collect the micromorphological samples at the Sodicho Rockshelter. (A) Sample blocks SOD\_2 to SOD\_5 (from the top) at profile F35, SOD\_5 was lost during the sampling process; (B) Sample block SOD\_1 at profile J29; (C) Sample block SOD\_II at profile F35, supported in gypsum (Photos by R. Vogelsang, 2016 (A-B); E. Hensel, 2018 (C)).

#### b) Granulometry

The grain size distribution was determined with a Laser Diffraction Particle Size Analyser (Beckmann Coulter LS13 320, Beckmann Coulter, Inc.) in which a suspension is laser scanned. The sediment particles refract the light waves and the resulting scattering provides information about the diameter. All ungrounded samples were pre-treated with hydrogen peroxide ( $\text{H}_2\text{O}_2$ , 15 %) to remove organic opal and washed with demineralized water, after the reaction has subsided. In order to prevent an aggregate formation coagulation sodium pyro-phosphate ( $\text{Na}_4\text{P}_2\text{O}_7$ , 46 g/l) was added and the samples placed in a horizontal shaker for 12 hours before the measurement. In a second run, focusing on the silicate composition of the sediment, a selection of samples (comp. appendix A) were additionally treated with HCl (10 %) following the dissolution of the organic material in order to dissolve carbonates from the sediment. In this step, the

carbonates are dissolved from the sediment. Subsequently, these samples were also washed and dispersed with  $\text{Na}_4\text{P}_2\text{O}_7$ . The Fraunhofer optical mode was chosen during the measurement and the calculation of grain size parameters are based on Folk and Ward (1957). The results were statistically evaluated with the GRADISTAT software version 8 (Blott and Pye 2001).

#### c) *Sediment color*

Since the sediment color is an important soil and sediment characteristic for composition, soil forming processes and past conditions, a spectral analysis was chosen, besides a soil characterization with the Munsell Soil Color Chart in the field. The measurement was performed with a bench-top spectrophotometer CM-5 from (Konica Minolta, Inc., Japan), in the laboratories of the Geological Institute at the University of Aachen. The sample material is placed into a quartz glass petri dish and measured without any further preparation (Eckmeier and Gerlach 2012). The wavelength of the reflected light of the sediment particles are measured in the visible range (VIS) from 360 to 740 nm. The results are given in an Excel file provided by the SpectraMagic ® NX CM-S100w color management software. The analysis provides wavelength, the Munsell color values (Hue, Chroma, Value) and color coordinates of the visible light. This includes the CIE Lab (International Commission on Illumination - $L^*a^*b^*$ ). The value is pronounced with the  $L^*$ , and the color dimensions with  $a^*$  (green to red) and  $b^*$  (blue to yellow) (Markl 2008, Eckmeier and Gerlach 2012).

The Redness Index (RI), which reflects iron oxides or pedogenetic induced haematite, are calculated with the help of the CIElab values according to Barrón and Torrent (1986), using the following formula:

$$RI = \frac{a^*(a^{*2}+b^{*2})^{\frac{1}{2}}10^{10}}{b^*L^{*6}}$$

#### d) *Magnetic susceptibility (MS)*

The mass specific magnetic susceptibility (MS) describes magnetizability iron-bearing minerals in rock, sediment, and soil when exposed to a magnetic field (Dearing 1999, Fassbinder 2007). The measurement provides information pedogenic processes (e.g. palaeosoils), heat induces sediment transformations or the development of magnetite ( $\text{Fe}_3\text{O}_4$ ), by iron-reducing soil bacteria. In the best case, it enables a reconstruction of transport, deposition and formation processes within sedimentary sequences (Dearing 1999, Goldberg and Macphail 2006). In an archaeological context, enhanced magnetic

susceptibility vales allow an assumption of heated resp. burned sediment (French 2015). The double determination of the samples was performed with a Bartington MS2 Magnetic Susceptibility System with a MS2k sensor and measured twice under laboratory conditions. The sieved sample material is weight into a plastic vessel ( $10\text{m}^3$ ) provided by Bartington, slightly compacted, and afterwards measured with a low frequency (0.46 Hz) followed by high frequency (4.6 Hz) (Dearing 1999, Bartington Instruments Ltd. 2015). A calibrations sample ( $\text{Si} = 3.104 \times 10^{-5}$ , at  $22\text{ }^\circ\text{C}$ ) prevents deviations.

#### *e) Carbon content*

In order to estimate the organic content in the sediment and the C/N ratio samples were homogenized and measured with a Vario EL Cube (Elementar Analysensysteme GmbH, Hanau, Germany). For the determination of total carbon content (TC) and the total nitrogen content (N) 20 mg of the homogenized sample material were weighed into tin boats and measured with blanks, and equipment/ laboratory standards. In a second procedure, that focuses on the total organically bounded carbon (TOC), only a selection of the samples was weight into silver boats. The samples were then dried on a hot plate ( $120\text{-}140\text{ }^\circ\text{C}$ ) and the substrate pipetted with hydrochloride acid (HCl, 10 %) at regular intervals, on the day of the measurement. As soon as the substrate no longer reacts, the boats can be folded in tin foil and placed in the elemental analyzer. The two measurement procedures are carried out in the "CN operation mode" with helium (He) as carrier gas. The results are exported into Excel and given as percentage.

#### *f) Major and trace element composition*

The elemental concentration and composition within the sediment samples was estimated with a portable X-ray fluorescence (pXRF) analyzer (Niton™ XL3t, Thermo Scientific™) under laboratory conditions, i.e dried and homogenized sediment is pressed into small pellets and measured three times in a custom-fit transportable test stand. For the measurement, the samples were placed on a  $4\text{ }\mu\text{m}$  thin barium foil, and analyzed in the Mineral mode with four filters (Main= 50 kV, Low = 15 to 20 kV, High = 50 kV, Light = 8 kV) for 40 sec each. Each measurement must be stopped manually for 160 sec. The measurement results are downloaded from the device via the NTD software, converted into Excel and given in the unit CPS/ua.

Using a handheld is very time efficient, but nevertheless not all elements, such as phosphorus, can be measured accurately (Hunt and Speakman, 2015). Therefore, a selection of the samples (tab. A1–A5) was measured at the Institute of Physical Geography and Geoecology at the RWTH Aachen. Here the homogenizes samples were pressed to tablets and measured twice with a SPECTRO XEPOS energy dispersive X-

ray fluorescence (ED-XRF, SPECTRO Analytical Instruments GmbH). In addition to the element composition (%), the contained oxides (%) were also recorded during the measurement and exported into an Excel file. From this information, further indices could be calculated, such as the chemical index of alteration (CIA), calculated according to Nesbitt and Young (1982):

$$CIA = \frac{Al_2O_3}{Al_2O_3 + NA_2O + K_2O + CaO}$$

*g) Ammonium oxalate extractable Fe, Mn, Al, and Si*

The determination of amorphous pedogenic oxides such as Iron (Fe), Manganese (Mn), Aluminum (Al), and Silicon (Si) was performed by using acidified ammonium oxalate, a moderate acidic reaction, following the instructions of Tamm (1932) and Schwertmann (1969). For the analysis 20 reference samples (comp. appendix A) were selected from all sediment units. For each sample, 0.5 g of dry fine sediment (< 2 mm) was mixed with 50 ml of extraction solution, consisting of 28.42 g of NH<sub>4</sub>-oxalate (2C<sub>2</sub>O<sub>4</sub> x H<sub>2</sub>O) and 18.01 g of the anhydrous oxalic acid (H<sub>2</sub>C<sub>2</sub>O<sub>4</sub>), admixed with 1 l of ultrapure water. In the following the samples were shaken for two hours, under completely dark conditions, then centrifuged (5 min, 4000 rotations/per min), and afterwards filtered with qualitative filters. While opal and crystalline iron oxides are not dissolved, active non-crystalline oxides, organically bonded oxides and Fe, Al and Si from allophane and allophane-like components are dissolved and can be determined in the extract (Rennert 2019). The extracts were measured in an Inductively Coupled Plasma Optical Emission Spectrometry (ICP-OES) (Thermo XSeries 2, Accela Pump). The results are given in mg metal/kg of sediment based on the sample weight:

$$Fe_o = \frac{a * b}{c}$$

a = content of iron in the extract in mg/l

b = dilution in ml (usually 100 ml)

c = soil weight in g (usually 0.5 - 1 g)

### 1.5.5 Chronology - Age depth model

A classical model to estimate the calendar ages of deposits in a certain depth is a reliable and well used tool in the study of drilling cores. The age-depth model for Sodicho Rockshelter was established by using the clam2.3.5 package in the RStudio software (Version 1.3.959) according to the code by Blaauw (2010). For this semi-automatically process the uncalibrated  $^{14}\text{C}$  ages (section 1.5.6 b), with their first standard deviation errors distributions were included and modelled with a linear interpolation. The developed model will be used to provide an overview of changes in sediment accumulation rates. In an initial attempt, sedimentological and geochemical results will be plotted against the ages to illustrate climatic and environmental changes over time.

### 1.5.6 Supportive investigations

Intensive interaction with cooperating research in the disciplines of archaeology, archaeobotany, geology and mineralogy made it possible to expand insights in the context of cultural remains, the palaeoenvironment, and the creation of a chronology.

#### *a) Analysis of artifact typology*

The durability of lithic raw material makes knapped lithic artifacts one of the most important archaeological finds regarding prehistoric human behavior. At Sodicho, all archaeological finds (e.g., lithic artifacts, charcoal, seeds) were single plotted using a Leica TS02 total station during the excavations, individually bagged, and assigned a unique identification number. The analyses of these artifacts include the observation and description of tools, flakes (debitage), and residual, the identification of chosen raw material, as well as the reconstruction of manufacturing and typo-technological development.

#### *b) Radiometric dating*

To establish a reliable chronology (chapter III) via radiocarbon dating, several samples were collected during the excavations 2015-2018 at the Sodicho Rockshelter. A total of 28 samples of seeds and charcoal were analyzed at the radiocarbon AMS lab Beta Analytics Limited, Florida, USA. Additionally, two charcoal and one soot sample were measured at the Center of Accelerator Mass Spectrometry (AMS) of the University of Cologne, Germany. At both laboratories the inorganic carbon and humid acids were removed with an acid and alkali (AAA) pre-treatment. The conventional radiocarbon ages

where calibrated with Calib8.10, by applying the most recent calibration curve IntCal20.<sup>14</sup>C (Reimer et al. 2020).

In order to obtain a chronological orientation/ framework within a fluvial sequence in the basin of the Bisare River swamps, two out of eleven percussion drilling cores were sampled and tested for radiocarbon dating. A plant sample and a sediment sample were taken and analyzed at the Radiocarbon AMS laboratory of the University of Cologne. The radiocarbon samples were then calibrated with OxCal v.4.2.3 by applying the calibration curve IntCal13 (Ramsey et al. 2013, Reimer et al. 2013).

*c) Black Carbon content and quality*

For the chemical analyses of fire residue within the sediment deposits of Sodicho, the black carbon (BC) content and composition were determined by oxidation of BC to benzene polycarboxylic acids (BPCA). 20 samples were taken from two squares F35 and G35, dried (40° C), sieved (> 2 mm), milled and then prepared according to the instructions of Glaser et al. (1998) and Brodowski et al. (2005). The samples were measured with a gas chromatograph equipped with a flame ionization detector (FID; Packard 6890 gas chromatograph, Hewlett Packard GmbH, Waldbronn, Germany), and an HP-5 capillary column (30 m x 0.32 mm i.d., 0.25 mm film thickness, Macherey-Nagel, Düren, Germany). For each sample a threshold of 5 mg organic carbon was maintained and the ratio of B5CA/B6CA was used as a proxy for changes in combustion temperatures (Schneider et al. 2010, Wolf et al. 2013).

*d) Phytolith ratio*

Opal phytoliths are inorganic silicate bodies, that develop in plant cells and tissue. Plant roots take up monociliate acid ( $H_4SiO_4$ ) through polymerization. For this preliminary qualitative analysis, 15–20 g bulk sediment of 15 samples were chosen. In each sample, 300 phytoliths with the morphotypes elongate (ELO\_ENT), blocky (BLO) and acute bulbosus (ACU\_BUL) were counted. The ratio of burned (clear, transparent) to unburned (brownish, black core) phytoliths were noted. This ratio is suggested to be a further indication for possible fire intensity/ combustions temperature. In this research, detailed quantitative analysis of the phytolith morphotypes was not included, since a comparison with recent phytoliths from the Southwest Ethiopian Highlands are needed.

## 1.6 Thesis structure

This thesis includes three peer-review publications concerning geoarchaeological research at the Sodicho Rockshelter and in the surrounding area, in different spatial and chronological scales. With each chapter an attempt is made to narrow down the spatial scale of research, according to the research design (Fig. 1.4), beginning with the analysis of regional satellite images, proceeding with the formation processes of the site's stratigraphy, and reaching the finest microscopic changes within the sedimentary layers. The order of the included publications is arranged by the date of publication and submission, respectively. The following short overviews describe the primary focus of each chapter.

The first **chapter I** of this doctoral thesis introduces the research aims, the design of this dissertation, and the different scales that are used in this geoarchaeological research. In addition, an introduction to the research area, and its geological, geomorphological and climatological setting is presented. Furthermore, the state of the geoarchaeological, archaeological and palaeoclimatological research in southwestern Ethiopia is described. **Chapter II** focuses on the research about the distribution of mapped archaeological sites and obsidian raw material outcrops and its relations with the hydrological systems within the catchment around Mt. Sodicho, Mt. Damota, and of the Bisare River catchment. The publication gives a first introduction into the broader study area and presents the results of geomorphological–hydrological analyses and structured field survey with help of GIS-mapping. In addition, three radiocarbon dates built the chronological framework.

In **chapter III** the spatial scale is narrowed down to the excavated stratigraphy at the Sodicho Rockshelter. It is focusing on site formation processes, palaeoenvironmental changes and settlement phases of Late Pleistocene and Holocene hunter-gatherers during the last 27 ka years. This chapter presents the first results of sedimentological, geochemical analyses, a preliminary chronological frame via radiocarbon dating, and the first insights into the analyses of archaeological finds. With the help a classical age-depth model anthropogenic and environmental proxies were established that provide an insight into occupation phases that were interrupted by local environmental changes that correspond to lacustrine records of southwestern Ethiopia and supraregional climatic shifts.

Based on the knowledge about site formation processes, the radiocarbon chronology and the initial palaeoenvironmental implications, further results of the geoarchaeological research at the Sodicho Rockshelter are presented and discussed in **chapter IV**. Within this study micromorphological observations were used to verify the information about sediment deposition and post-depositional alteration and to quantify microscopic signs

for human behavior. By comparing the observations with black carbon analysis and a qualitative ratio of burnt and unburnt phytoliths, behavioral patterns such as human fire activity can be determined. For a deeper insight into the weathering state of the sediment an acidic ammonium oxalate extraction was used. These results contribute to an understanding of the influence of changing moisture conditions on a rockshelter stratigraphy and the preservation of information.

**Chapter V** discusses the key findings and interpretations of the previous chapters by relating to the working hypothesis of this thesis. It also highlights the significance of the new results in the context of the geoarchaeological research field.

This final **chapter VI** concludes this doctoral research by highlighting the significance of the geoarchaeological results. The agenda for further research at the Sodicho Rockshelter and other possible sites in the research area is discussed in a subchapter.

## **1.7 Setting of the study area**

### **1.7.1 Present geological and geomorphological setting**

Ethiopia is a country of many different landscapes and offers the contrast between high elevated plateaus, a rift fault system and extensive depressions. The research area is located in the southwestern Ethiopian Highlands, an elevated region in the Southern Ethiopian Plateau (SEP), close to the border of the western central and southern Main Ethiopian Rift (MER) (Fig. 1.6). Here the mountain ranges can reach heights of ~ 2000–3000 m above sea level (a.s.l.). Today, tectonic and residual landforms characterize the study area; extinct volcanic cones alternate with caldera complexes, steep slopes, gorges, prominent fault systems, and natural basins. A prominent feature in the north of the study area is the Wagebeta Caldera complex, a series of three almost circular depressions with steep slopes, that date back to 3.6 to 4.2 Ma. They are the origin of Pliocene volcanic activity that is connected to tectonic stress of the late development of the MER system (WoldeGabriel et al. 1992). The calderas are aligned above the Goba-Bonga lineament, a west-east transverse depression, that crosses the western central and southern Main Ethiopian Rift (MER) (WoldeGabriel et al. 1990, Abbate et al. 2015). To the south of these formations several volcanic domes and lavas characterize the landscape. They consist predominantly of fine-grained basalt, light colored rhyolite and trachyte, ignimbrite, and welded tuff (Chernet 2011, Abbate et al. 2015).

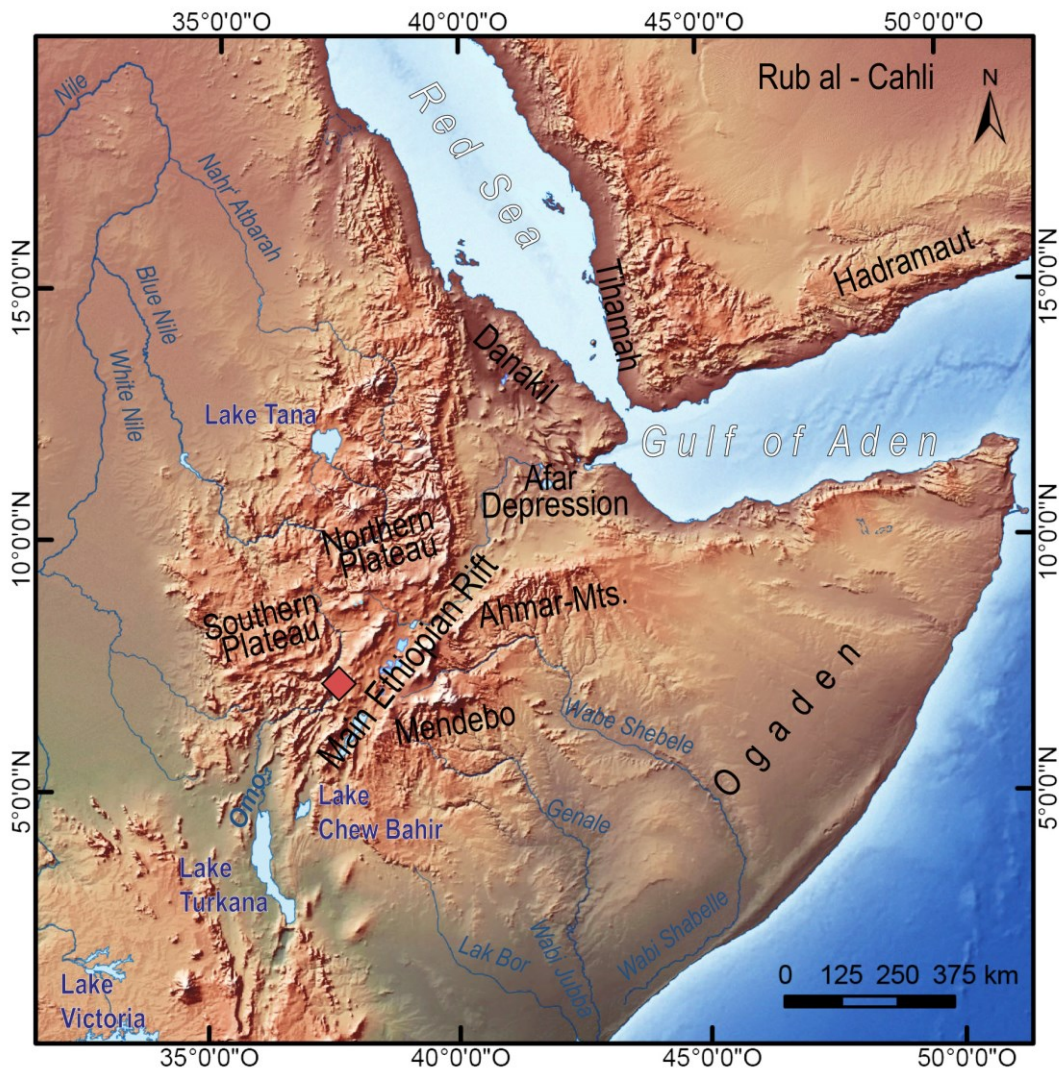


Figure 1.6 Location of the study area (red square) within the Southwestern Ethiopian Highlands (Raster map data by Natural Earth).

Most of Ethiopia's lakes are centered along the NW-SW trending Ethiopian Rift System, which are fed by rivers draining in from the highlands (Ayenew and GebreEgziabher 2015). Within the study area the western permanent streams flow into the Omo basin, of the north-south running Omo River, which flows into Lake Turkana (WoldeGabriel et al. 1992). River systems to the east flow directly in Lake Abaya or join the Bilate River, a major river, which is a tributary river to Lake Abaya itself (Corti et al. 2013). In general, the soil development on the southwestern Plateau is influenced by rising topography, increasing rainfall and dropping temperatures. Although the formation of deep soils is favored in the hilly terrain, these are often only moderately fertile (Yeshitela and Bekele 2002). Soil erosion, river erosion and gully formation are very common degradation processes in the study area, that expose bedrock and common soil types, such as

Chromic Luvisols (LVcr) [clay rich, nutrient-holding capacity, with red faint], Umbric Nitisol (NTum) [mixture of clay and iron coatings, phosphate-fixing capacity], Haplic Vertisols (VRha) [clayey soils, common shrink and swell processes, because of montmorillonite] (IUSS Working Group WRB, 2014). Where the top soil has been removed by erosion or gully incising has been advanced, badland-type morphology develops (Billi 2015).

### 1.7.2 Research site description

This study focuses on a study region in the southwestern Ethiopian Highlands, around 320 km from the capital Addis Ababa, and in particular on an area that belongs to the administrative zone of Kembata Tembaro and Wolayita, which are part of the southern situated regional state Southern Nations, Nationalities, and Peoples' Region (SNNPR).

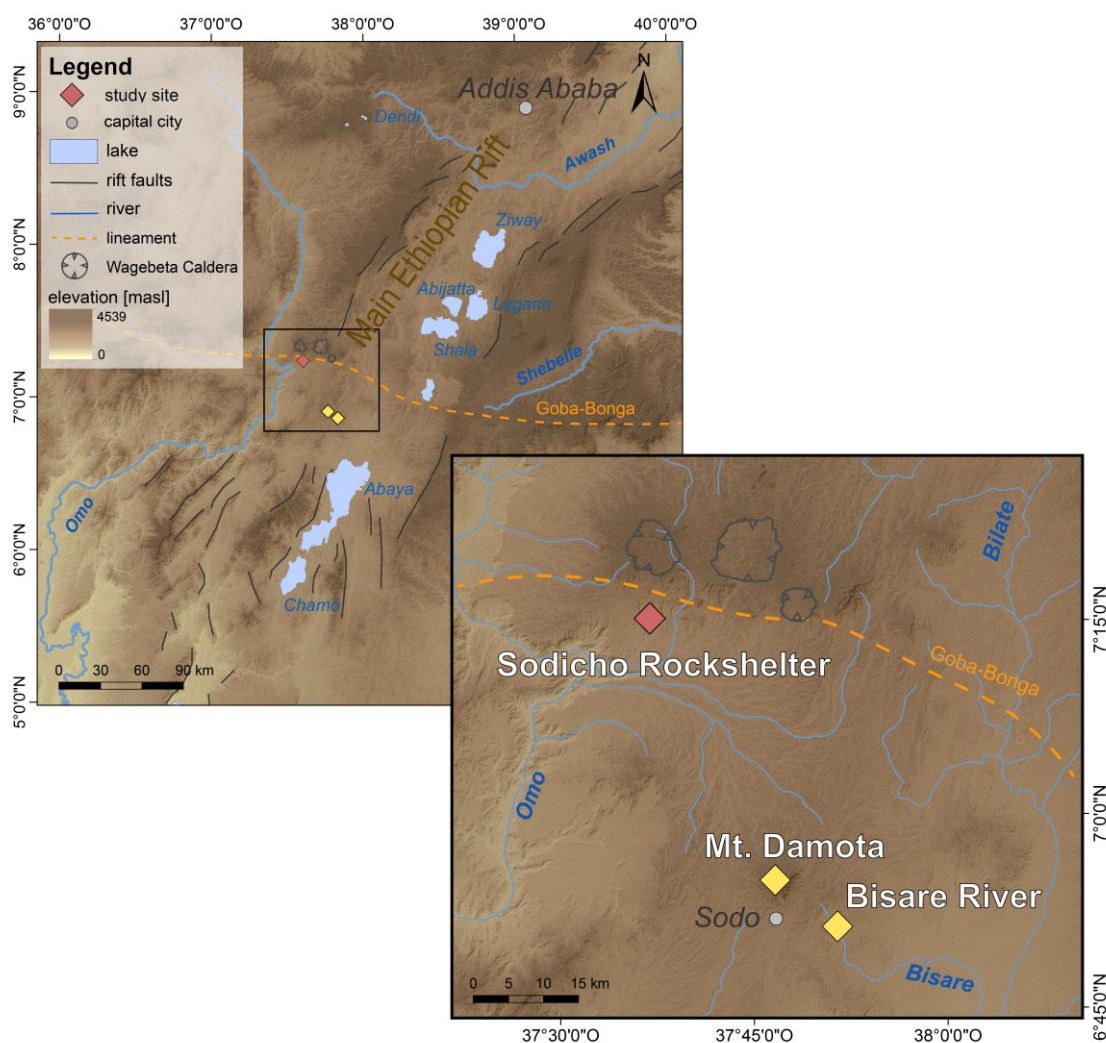


Figure 1.7 Map of the study area with locations of research sites discussed in the following chapters (DEM data by ASTER GDEM and Natural Earth raster map data).

### Sodicho Rockshelter on Mount Sodicho

The Sodicho Rockshelter, the main archaeological site of this doctoral research, lies on the southwestern flanks of the trachytic Mount Sodicho (Fig. 1.7). The mountain itself has an irregular dome structure with greyish to yellowish trachyte cropping out. At the western mountain flank rhyolite lava and welded tuff are common, and basaltic material was exposed only at the western foot of Mt. Sodicho. A hydrological system with episodic and permanent streams did incise into the mountain (Fig. 1.8 B). From the flat and wide summit of the mountain, with a height of about 2100 m a.s.l., the basin of the Omo River can be seen to the southwest, the edges of the Wagebeta Caldera complex to the north, and a series of further volcanic formations in close distance (Fig. 1.8 C). The prominent features of the summit of Mount Damota rise in about 40 km to the southeast. Housing units and agriculturally utilized areas are situated on the perimeter of the mountain (Fig. 1.8 F). The majority of the vegetation has been cleared for the cultivation of food crops, and what is left of presumed natural forests is only present in patches on steeper slopes or has been replaced by eucalyptus trees. One consequence of the deforestation is erosion along the slopes and the resulting increase in soil degradation.

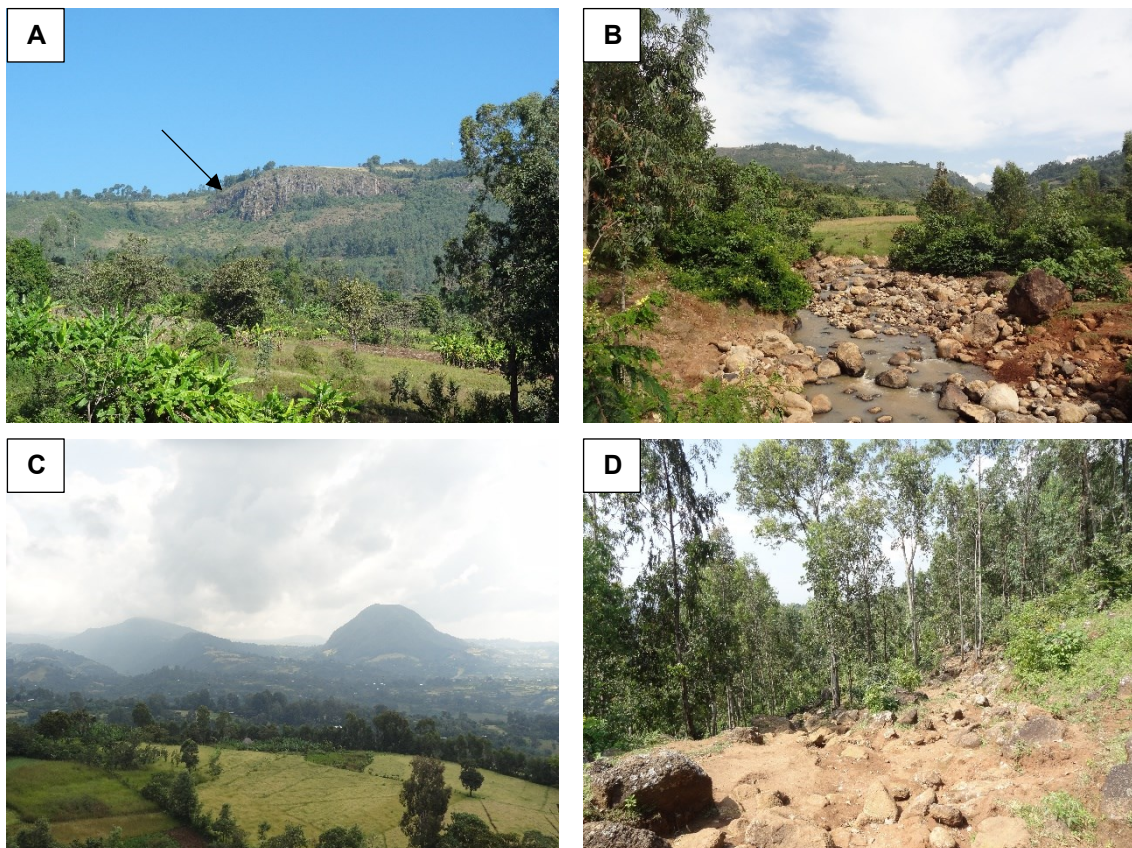


Figure 1.8 Continue on next page.



*Figure 1.8 Photos of the surrounding area of Mt. Sodicho. (A) View of the entrance area of Sodicho Rockshelter within the outcropping trachytic bedrock; (B) The surroundings of Mt. Sodicho are characterized by permanent and episodic streams; (C) Mt. Sodicho is part of a series of silicic domes, as seen on the photo; (D) Clearing at the slopes and movement of livestock promotes degradation and runoff; (E) View from the northern summit of Mount Sodicho, towards the flanks of the Wagebeta calderas; (F) Round huts and flat-roofed huts are found on the mountain slopes which are used for cultivation (Photos by E. Hensel, 2017).*

The Sodicho Rockshelter is situated at an elevation of about 1930 m a.s.l., below steep rock walls and its opening is facing the south (1.8. A). Looking into the landscape from a narrow ridge directly in front of the rockshelter entrance, the Omo River basin and the outline of Mt. Damota can be identified. Inside, the rockshelter walls show signs for a heavy influence of moisture (Fig. 1.9), such as dark staining along the walls and cracks in the ceiling, drip holes and shallow water pools.



*Figure 1.9 Panoramic view into the Sodicho Rockshelter. Dark staining of the rock surface is caused by the exposure to moist conditions (Photo by C. Schepers, 2018; mod. after Hensel et al. 2021).*

## Mount Damota

The Mount Damota, dormant igneous volcanic mountain, is situated northern of the city Sodo (Fig. 1.10 A). With a summit in 2908 m a.s.l., several prominent landscape features are visible, such as the lower relief topography of the Main Ethiopian Rift to the east, with several rift valley lakes in the north and the Lake Abaya to the south (Brandt et al. 2012). Visible rivers are the Bilate River, and Omo River basin. Lithological, Mt. Damota can be classified as a greenish grey trachyte that overlies rhyolitic to trachytic lava and ignimbrites of the pyroclastic Nazret Group (Chernet 2011, Brandt et al. 2012, Corti et al. 2013). Furthermore, the mountain is characterized by rocky outcrops, deep gorges, and steep slopes (Abbate et al. 2015). Often, natural vegetation can only be found in the topographic features just mentioned, because agriculture, cattle farming and extensive erosion in the recent past had a major influence (Fig. 1.10 B). Nevertheless, this study area offers variation in vegetation and faunal habitats within the vertical ecozones (Vogelsang and Wendt 2018). The mouth of the archaeological key site Mochena Borago is located on the southwest flank of the mountain below a seasonally active waterfall (Brandt et al. 2012).



*Figure 1.10 Photos in the close surroundings of Mt. Damota. (A) View to the summit of Mt. Damota, taken from the streets of Sodo (Photo by E. Hensel). (B) Most of the natural vegetation cover had been replaced by cultivated land along the flanks of Mt. Damota (Photo by S. Meyer).*

## Bisare River

The third study area is located at the upper catchment of the Bisare River. The river basin lies at the margins of the Ethiopian Rift valley, about 10 km east of Mt. Damota and 35 km northwest of Lake Abaya. The catchment is situated in the Hobitcha caldera, a south-east facing horseshoe, which is associated with Quaternary rhyolitic volcanism. Rhyolitic lava flow and pyroclastic products are outcropping at the edges of the caldera (Corti et al. 2013). Alluvial sediment, glaciais and valley fills including interbedded volcanic rocks are common, and are incised by gullies and gorges (Fig. 1.11 A). Moreover, the

extensive gully erosion and the formation of badlands is a common phenomenon in depressions (Benito-Calvo et al. 2007). Bisare is a western tributary of the Bilate River, a north south running stream, that flows into the northern part of Lake Abaya. Swampy areas are located in the upper part of the catchment (Fig. 1.11 B).

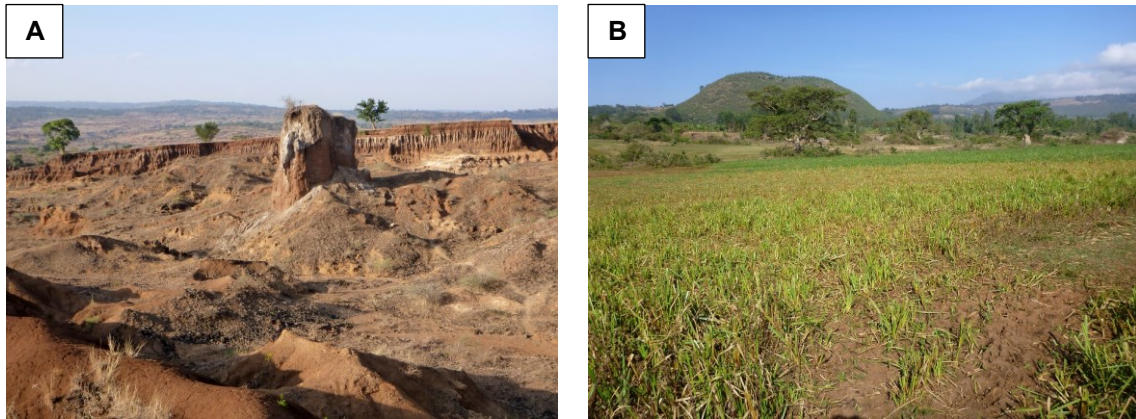


*Figure 1.11 Photos of significant features at the Bisare River catchment. (A) Degraded areas have been formed by gully erosion and extensive badland formation. (B) Swampy area in the western part of the upper Bisare catchment (Photos by O. Bubbenzer, mod. after Hensel et al. 2019).*

### 1.7.3 Past geological processes

Today, Ethiopia's characteristic landscape with the prominent Rift Valley and countless relics of past volcanic activity and faulting processes speaks for a complex geological and geomorphological development. The geological development of Ethiopia already dates back to mantle plum action during the Proterozoic (comp. Abbate et al. 2015). For a detailed review of the literature dealing with East African passive margin processes and the formation of the Main Ethiopian Rift, the reader is referred to Abbate et al. (2015). The Southern Ethiopian Plateau is connected to the formation processes of the Main Ethiopian Rift, which can be divided into the Northern MER, Central MER and Southern MER, according to temporal differences of rifting and faulting processes (WoldeGabriel et al. 1990, Corti et al. 2013).

The study area lies marginal in a transition zone between the Central MER and the Southern MER. Findings of Plateau Flood Basalts, with the oldest ages of about 45 to 35 Ma, suggesting a pre-rift, initial volcanism since the Late Eocene (Chernet 2011, Abbate et al. 2015). With the onset of the main rifting processes, extensive volcanic activity and uplift in the Mio-Pliocene (~ 9–2 Ma) promoted the eruption of acidic pyroclastic rocks (ignimbrites) known as the Nazret Group (Chernet 2011, Corti et al. 2013). During the late phase of the main rifting the transverse Goba-Bonga lineament developed, crossing the MER from east to west into the Somali Plateau. This was

associated with further volcanism on both sides of the MER. The huge complex of the Bale Mountains, with elevations of about 4300 m, are a probable sign for this volcanism on the Somali Plateau (Abbate et al. 2015). As for the Southern Ethiopian Plateau and the study area, the Wagebeta Caldera complex and silicic domes are associated with volcanic activity from 4.2 to 3.6 Ma (WoldeGabriel et al. 1990). Late Pliocene (~ 2.9 Ma) trachytic lava flows formed Mount Damota, and are suggested to have continued into the Quaternary (WoldeGabriel et al. 1990, Chernet 2011, Corti et al. 2013). Although this has not been investigated by geological surveys, it can be assumed that the trachytic Mount Sodicho was also formed in the same time range of the late development of the rift system. Except for the prominent silicic domes, the lower elevated structure is covered by Pleistocene alluvial and occasional lacustrine sediments (Corti et al. 2013). Interbedded within these lacustrine deposits are basalt flows and pyroclastic material derived from volcanic centers, such as the Hobitcha (or Obitcha) caldera. This horseshoe-shaped caldera is situated southeast of Mount Damota and a rhyolitic flow within the caldera provided an estimated age of ~ 1.57 Ma, corresponding to Quaternary volcanic activity (Chernet 2011, Corti et al. 2013).

#### **1.7.4 Climatic setting**

Ethiopia's landscape, with its diverse topography, causes a variability in temperatures and precipitation within the country's borders (Fazzini et al. 2015). This means that there are extremely dry and hot areas, such as in the Danakil Desert with temperatures that can reach 50 °C, and tropical mountain regions like the Bale Mountains with temperatures that fall below 7 °C (Gasse 2000, Nyssen et al. 2015). Due to its close proximity to the equator, the African Tropical Rain Belt (TRB = Intertropical Convergence Zone ITCZ), which shifts annually, has a major influence (Fazzini et al. 2015, Nicholson 2018). The movement is connected to the sun zenith position, resulting in a maximum solar heating (=insolation) (Gasse 2000). In addition, moisture availability in eastern Africa is connected the atmospheric walker circulation and changes in sea surface temperatures of the Indian Ocean (Griffith 1972, Tierney et al. 2008, Segele et al. 2009, Viste and Sorteberg 2013). In this case convective systems form, which are influenced by the summer monsoon that interacts with the dry northeastern "Harmattan" wind system (Viste and Sorteberg 2013, Nicholson 2018). Further studies document that changes in SST of the Indian Ocean and Atlantic Ocean are correlating with variations in the walker circulations (WC), which are also believed to be associated with the occurrence of the El Niño Southern Oscillation phenomenon (Nicholson 2018). Consequently, Ethiopia experiences a bimodal precipitation pattern per year. In total, an

amount of more than 2000 mm of annual rainfall can be reached in the highlands, which is a high average in precipitation in the Horn of Africa. The mean annual rainfall is significantly higher at sites in the highlands due to orographic effects (Griffith 1972, Gasse 2000, Viste and Sorteberg 2013). Generally, the months June/July to September are the boreal summer rainy season, called “Kiremt” (also known as Kirmet, or Kermit), which brings 55–95 % of annual rainfall to parts of Ethiopia (Segele and Lamb 2005, Berhanu et al. 2013, Belay et al. 2021). During the beginning of this phase the TRB is in its most northern position (16°N to 20°N) and low-level convergences cause increased precipitation (Nyssen et al. 2015, Nicholson 2018). Studies by Segele and Lamb (2005) showed that a delayed Kiremt is connected to warm SSTs of the Indian Ocean and also the Arabic Sea. On the other hand, an early onset of the heavy rainy season is connected to warm SSTs of the equatorial central and eastern Pacific Ocean. The second weaker, less voluminous rainy season “Belg” (‘little rains’) with ~ 32 % of mean annual rainfall, follows a dry season which spans the months November to February (Nyssen et al. 2015, Belay et al. 2021). During a dry season, the region can experience an average of less than 50 mm of rainfall per month (Brandt et al. 2012, Nyssen et al. 2015, Hildebrand et al. 2019).

Within the study area, temperatures are consistent on average throughout the year (Fig. 1.12). A difference between the two wet phases is not clearly indicated because of the high intensity of rainfall. After all the tropical Highlands are called “water towers” of Ethiopia (Griffith 1972, Viste and Sorteberg 2013).

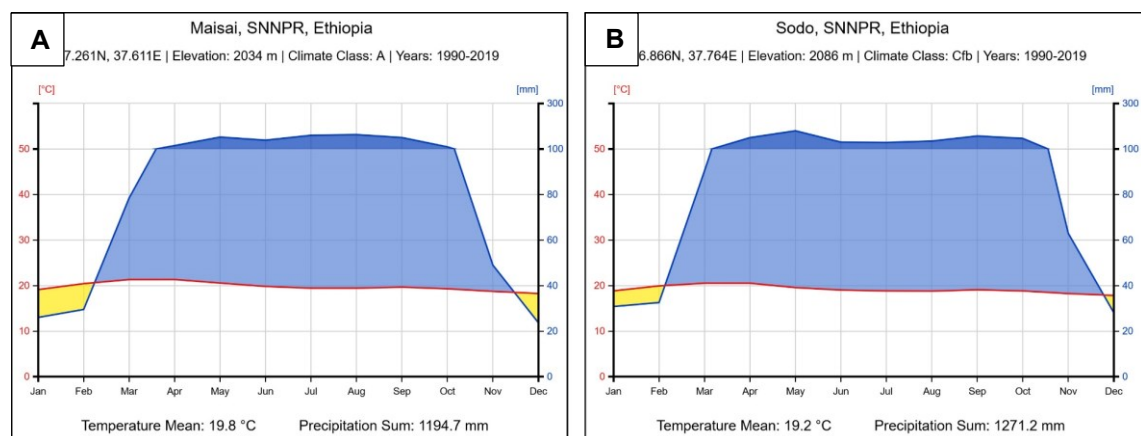


Figure 1.12 Climate chart of Maisai, at Mt. Sodicho (A), and Sodo, at Mt. Damota (B), showing monthly mean temperature (°C) and average monthly precipitation (based on an observation period from 1990-2019). The charts are based on the interpolated datasets of the Climatic Research Unit (CRU) Time-Series (TS) Version 4.04 and were derived from ClimateCharts.net (Zepner et al. 2021).

During the Quaternary the climate of southwestern Ethiopia was characterized by fluctuating wet and dry conditions (Gasse 2000, Foerster et al. 2012, Trauth et al. 2019, Schaebitz et al. 2021). According to the studies by Kaboth-Bahr et al. (2021) about the synthesis of terrestrial and marine proxy records, there is also the influence of the Walker Circulation (WC). The results pronounce the tight link between the WC and the phenomenon of the palaeo-ENSO (El Niño-Southern Oscillation) variability during the last ~ 620 ka. This process created a pronounced east-west dipole with differences in surface and tropospheric temperatures, resulting in humid conditions on one side of the continent and arid conditions on the other side (Kaboth-Bahr et al. 2021). These circumstances are still applicable for today's climate.

Combined study results on geochemical proxies (such as K/Zr record) from the Chew Bahir sediment record, that cover the last ~ 200 ka, verified that the humid/arid alternations were paced in a 20 ka rhythm, and that this is influenced by shifts in orbital-controlled insolation intensity in the tropics. The last mentioned is further influenced by variations of the orbital force's eccentricity and precession. The study also revealed that the climate fluctuations increased the frequency since ~ 60 ka, with a trend to drier conditions (Schaebitz et al. 2021). Still a rather moist phase from 45 to 35 ka BP, was detected within the sediment record, followed by cold and arid conditions of Marine Isotope Stage 2 (MIS 2, ~ 29–12 ka BP). A desiccation of the former palaeolake Chew Bahir verified extreme arid conditions during the Last Glacial Maximum (LGM, ~ 21 ± 2 ka) (Foerster et al. 2012, Foerster et al. 2015, Trauth et al. 2019). With the onset of the Early Holocene African Humid Period (AHP, ~ 15 to 5 ka) the humid conditions increased again. However, arid phases, such as Older Dryas stadial (OD, ~ 14 ka) and the Younger Dryas event (YD, 12.8–11.6 ka) could be detected with further shorter dry spells (~ 10.5, ~ 9.5, 8.15–7.8 and ~ 7 ka) during the transition from the Late Pleistocene to the Holocene. Apart from short humid events ~ 3, ~ 2.2, and 1.3 ka, that are indicated in the sediment record, the Holocene progressed with an increase in arid conditions (Foerster et al. 2012, Foerster et al. 2015).

### 1.7.5 Vegetation

Ethiopia's natural vegetation is very heterogeneous due to its topographical and climatic diversity (Billi 2015). Also, the natural forest cover has been declining, connected to the severe influence of human cultivation and deforestation, still various endemic and indigenous plants can be found (Yeshitela and Bekele 2002). The present vegetation of the study area consists of patchy forests that alternate with open forest areas, bush lands

and grasslands. Following the descriptions of potential vegetation of Friis et al. (2010), the study sites fall mainly into the mid altitude zone (*woyna dega*) and the lowland zone (*kola*), while the summit of Mt. Damota reaches up into the highland zone (*dega*) (Brandt et al. 2012, Vogelsang and Wendt 2018).

The potential vegetation type of the higher regions, surrounding Mt. Damota and Mt. Sodicho is represented by dry evergreen Afromontane forest and grassland complex (type DAF), where extensive grassland, shrubs, and small to large size trees are to be found (Fig. 1.13). The potential vegetation types south of Mt. Sodicho and the riverine vegetation along the Omo River, can be identified as small to moderate sized woodland and wooded grassland, characterized by the common species of the genera *Combretum* and *Terminalia* (Combretaceae) (type CTW). The third common potential vegetation type can be found in lower altitude regions, such as around the study area at the Bisare River basin. This vegetation type (type ACB) is very diverse, and includes mainly different subtypes of woodland, grassland and scrubland, which are well adapted to slightly drier conditions (Friis et al. 2010).

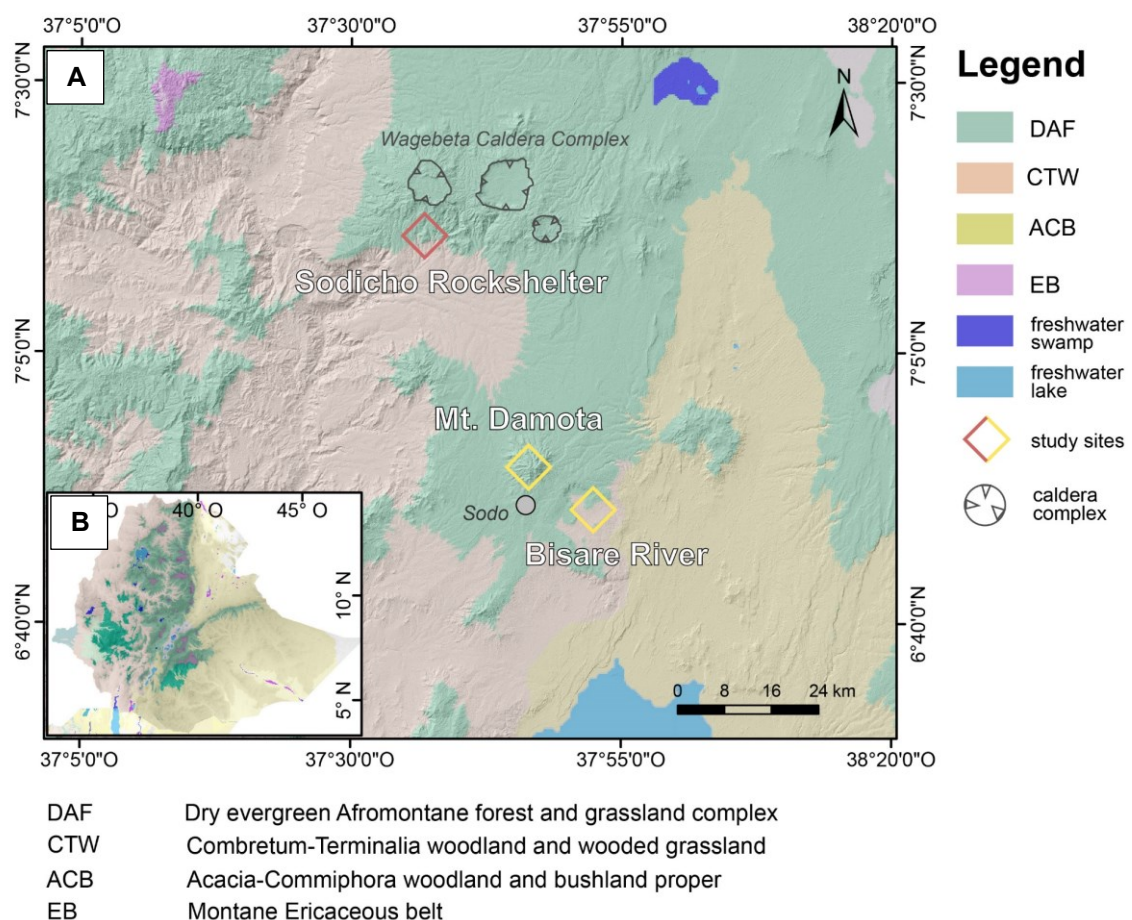


Figure 1.13 Map of potential vegetation for the study area (A). Map of pot. vegetation covering Ethiopia and northern Kenya (data from Friis et al. 2010; raster data and tools from //vegetationmap4africa.org (van Breugel et al. 2015)).

## Chapter II

### **2. Combining geomorphological–hydrological analyses and the location of settlement and raw material sites – a case study on understanding prehistoric human settlement activity in the southwestern Ethiopian Highlands**

Elena A. Hensel<sup>1</sup>, Oliver Bödeker<sup>2</sup>, Olaf Bubenzer<sup>3</sup>, Ralf Vogelsang<sup>4</sup>

1 Institute of Geography, University of Cologne, Cologne, 50923, Germany

2 Department of Geoscience, University of Cologne, Cologne, 50923, Germany

3 Institute of Geography & Heidelberg Center for the Environment (HCE), Heidelberg University, Heidelberg, 69120, Germany

4 Institute of Prehistoric Archaeology, University of Cologne, Cologne, 50923, Germany

Published at the *E&G Quaternary Science Journal* 68, 201–2013, 2019

doi: <https://doi.org/10.5194/egqsj-68-201-2019>

Special Issue: *Geoarchaeology and past human–environment interactions*

Note: The following pages originate from the original peer-reviewed article published at E&G Quaternary Science Journal.

E&G Quaternary Sci. J., 68, 201–213, 2019  
<https://doi.org/10.5194/egqsj-68-201-2019>  
 © Author(s) 2019. This work is distributed under  
 the Creative Commons Attribution 4.0 License.



Open Access  
**E&G** Quaternary  
 Science  
 Journal

Research article

## Combining geomorphological–hydrological analyses and the location of settlement and raw material sites – a case study on understanding prehistoric human settlement activity in the southwestern Ethiopian Highlands

Elena A. Hensel<sup>1</sup>, Oliver Bödeker<sup>2</sup>, Olaf Bubbenzer<sup>3</sup>, and Ralf Vogelsang<sup>4</sup>

<sup>1</sup>Institute of Geography, University of Cologne, Cologne, 50923, Germany

<sup>2</sup>Department of Geoscience, University of Cologne, Cologne, 50923, Germany

<sup>3</sup>Institute of Geography & Heidelberg Center for the Environment (HCE), Heidelberg University, Heidelberg, 69120, Germany

<sup>4</sup>Institute of Prehistoric Archaeology, University of Cologne, Cologne, 50923, Germany

**Correspondence:** Elena A. Hensel ([elena.hensel@uni-koeln.de](mailto:elena.hensel@uni-koeln.de))

**Relevant dates:** Received: 8 January 2019 – Revised: 26 August 2019 – Accepted: 29 August 2019 – Published: 17 October 2019

**How to cite:** Hensel, E. A., Bödeker, O., Bubbenzer, O., and Vogelsang, R.: Combining geomorphological–hydrological analyses and the location of settlement and raw material sites – a case study on understanding prehistoric human settlement activity in the southwestern Ethiopian Highlands, *E&G Quaternary Sci. J.*, 68, 201–213, <https://doi.org/10.5194/egqsj-68-201-2019>, 2019.

**Abstract:** During this study, the recent relations between the hydrological systems and the distribution of archaeological sites and obsidian raw material outcrops within the catchment of the Bisare River, around Mt Damota, and around Mt Sodicho in the southwestern Ethiopian Highlands were investigated. To do so, we combined geomorphological–hydrological analyses with field surveys and GIS mapping. The aim was to try to transfer these recent interrelations into the past to better understand the factors that influenced prehistoric human settlement activity. The natural geomorphodynamics in landscapes such as the southwestern Ethiopian Highlands were and still are characterized by the interplay between endogenous processes (tectonics, volcanism) and climatic fluctuations and, during the recent past, also by human activity. In the considered region, protective and potentially habitable rock shelters are found at the volcanic slopes of Mt Damota and Mt Sodicho at high elevations. In addition, in some areas recent morphodynamic processes make obsidian raw material available near the surface. However, archaeological and terrestrial paleoenvironmental archives that allow an understanding of the interplay between prehistoric settlement activity and paleoenvironmental conditions are still rare. Therefore, the surroundings of formerly occupied rock shelters were investigated to illustrate the effect of the recent fluvial morphodynamics (erosion and accumulation) on surface visibility and preservation of archaeological obsidian raw material. This recent information can be used to make assumptions about the former hydrological system and to thereby get answers to research questions such as those about the past accessibility of obsidian raw material for prehistoric humans. The results suggest that the study area is currently affected by a highly dynamic hydrological system, which is indicated by phenomena such as the formation of swamps due to sedimentation in natural depressions. In addition, wide areas

of the Bisare River catchment are affected by gully erosion, which leads to land degradation but also to the exposure of the above-mentioned lithic raw material outcrops. Human influence strongly increased during the Holocene until today, especially on the mountain flanks. This in turn increased soil loss and erosion of archaeological sites, which complicates the transfer of the current morphodynamics into the past. Although it cannot be finally confirmed that prehistoric hunters and gatherers systematically used fluvially exposed raw material, based on our results it can be assumed that humans frequented this area, due to the local availability of such kind of material.

### Kurzfassung:

Im Rahmen dieser Studie wurden die aktuellen Zusammenhänge zwischen hydrologischen Systemen, sowie der Verbreitung archäologischer Fundplätze und von Obsidian-Rohmateriallagerstätten im Einzugsgebiet des Bisareflusses, um Mount Damota sowie um Mount Sodicho im südwestlichen äthiopischen Hochland untersucht. Hierfür wurden geomorphologisch-hydrologische Analysen mit Geländesurveys und Gis-Kartierungen kombiniert. Das Ziel war der Versuch, die aktuelle Situation in die Vergangenheit zu übertragen, um die prähistorische menschliche Siedlungsaktivität besser zu verstehen. Das natürliche geomorphologische Prozessgeschehen in Landschaften wie dem südwestlichen äthiopischen Hochland wurde und wird durch das Zusammenspiel von endogenen Prozessen (Tektonik, Vulkanismus) sowie Klimaschwankungen und in jüngster Zeit auch durch menschliche Aktivitäten geprägt. In der betrachteten Region finden sich höher gelegene, schützende und potentiell bewohnbare Felsüberhänge (Rockshelter) an den Vulkanhängen des Mt. Damota und des Mt. Sodicho. Außerdem wird durch aktuelle morphodynamische Prozesse in einigen Bereichen Obsidian als Rohmaterial oberflächennah verfügbar. Archäologische und terrestrische Paläoumweltarchive, die es ermöglichen, das Zusammenspiel zwischen prähistorischer Besiedlung und Umweltbedingungen zu verdeutlichen, sind jedoch noch selten. Daher wurde die Umgebung der ehemals bewohnten Rockshelter untersucht, um die Auswirkungen der rezenten fluvialen Morphodynamik (Abtragung und Akkumulation) auf die oberflächennahe Sichtbarkeit und Erhaltung archäologischer Rohmaterial-Fundstellen zu verdeutlichen. Die gewonnenen Informationen können dafür verwendet werden, Annahmen über das ehemalige hydrologische System zu treffen und somit Antworten auf Forschungsfragen wie jener nach der ehemaligen Zugänglichkeit von Obsidian-Lagerstätten für den prähistorischen Menschen zu erhalten. Die Ergebnisse legen nahe, dass das Untersuchungsgebiet derzeit von einem hochdynamischen hydrologischen System geprägt wird, was sich beispielsweise durch Phänomene wie der Ausbildung von Sümpfen aufgrund von Sedimentation in natürlichen Depressionen zeigt. Darüber hinaus stehen weite Bereiche des Einzugsgebiets des Bisareflusses unter dem Einfluss von Gullyerosion (Grabenerosion), welche zu Bodendegradierung und zur Freilegung der oben genannten lithischen Rohmaterialien führt. Insbesondere an den Bergflanken nahm der anthropogene Einfluss während des Holozäns stark zu. Dies wiederum verstärkte den Bodenabtrag und die Erosion archäologischer Fundstellen, was den Transfer der aktuellen Morphodynamik auf die Vergangenheit erschwert. Obwohl nicht eindeutig nachgewiesen werden kann, dass prähistorische Jäger und Sammler fluvial freigelegtes Rohmaterial gezielt nutzten, kann basierend auf unseren Ergebnissen davon ausgegangen werden, dass die lokale Rohmaterialverfügbarkeit zu einer verstärkten Frequentierung der Region durch prähistorische Menschen führte.

## 1 Introduction

The landscape of the southwestern Ethiopian Highlands was created by tectonic stresses and Late Pleistocene–Holocene eruptive activity, as well as by the increasing influence of human activity in recent times. The development of topographic barriers and natural basins that were induced by tectonic uplift or faulting created a complex relief with ridges and ravines (De La Torre et al., 2007; Benito-Calvo et al., 2007). Large areas of today's surface are influenced by erosional processes, for example, by widespread gully erosion

and badlands formation that are common causes of morphological transformations in Ethiopia today (Billi and Dramis, 2003). In many cases, this development is linked to human influence and the intensification of agriculture (Castillo and Gómez, 2016). Up to now, there are only a few terrestrial geoarchives in East Africa with reconstructions of Pleistocene and Holocene precipitation or temperature changes (Tierney et al., 2008; Tierney et al., 2011; Foerster et al., 2012, 2015). Due to the rare paleoclimatic data but also due to the lack of valuable archaeological information, there is

still an ongoing discussion on how short- and long-term climatic events and trends affected prehistoric humans living on the Horn of Africa. Available paleoclimatic records from lake sediments from Ethiopia and Kenya document wet–dry transitions that likely affected prehistoric humans and their adaptation to the changing environment. In this context, one proposed hypothesis is the retreat of human groups into highland regions with higher precipitation rates during dry periods (Basell, 2008; Foerster et al., 2015; Junginger and Trauth, 2013).

Our study discusses the following research questions. (1) How does the actual hydrological system of the study area look like? (2) What role does this system play in present accessibility of obsidian raw material sources and the visibility and preservation of archaeological sites? (3) Which geomorphological features related to erosion are present? (4) Can we make assumptions about the ancient hydrological system and landscape dynamics and, on their influence, on the accessibility of past obsidian raw material sources? For our studies we selected three research areas in the southwestern Ethiopian Highlands, ca. 250 km southwest of Addis Ababa, that are located within a radius of 40 km of one another (Fig. 2). (1) Mt Damota is a volcanic mountain that became of archaeological interest because of its key site, the Mochena Borago Rockshelter, which is one of the most important Late Pleistocene and Holocene sites in eastern Africa (Brandt et al., 2012). (2) Mt Sodicho is located ca. 40 km to the northwest of Mt Damota and marks the second research area. The archaeological site Sodicho Rockshelter is located on the southern flanks of this volcanic mountain. (3) The banks of the Bisare River, a tributary of the Bilate River, are located southeast of Mt Damota (Fig. 2a).

Archaeological records within the rock shelter sediments of, e.g. Mt Damota or Mt Sodicho, provide information about ancient human–environment interactions. Additionally, numerous open-air sites at the slopes of Mt Damota provide a complementary record of former human settlement (Brandt et al., 2012; Vogelsang and Wendt, 2018). The main trench at Mochena Borago yielded three major lithostratigraphic units with archaeological material classified as Middle Stone Age (MSA), dating to ages between 36 and >50 ka (Brandt et al., 2017). However, a sedimentological hiatus in the stratigraphy from ~36 to ~8 ka leaves unanswered questions about deposition processes and the occupation at that site until the Holocene (Brandt et al., 2012, 2017). Vogelsang and Wendt (2018) examined multiple archaeological surface localities classified as MSA and Late Stone Age (LSA) sites on the western flank of Mt Damota to reconstruct prehistoric settlement patterns. They recognized intensification of settlement activities from the MSA to the LSA, as well as a different organization of the site clusters along the mountain slopes. Whereas the reconstructed MSA settlement areas show a linear, vertical orientation and include different altitudinal belts, the LSA sites form one large cluster with interconnected smaller sub-groups. The former is interpreted as a

land use model that offered short access to various eco-zones in different elevations, a strategy that might have been advantageous during times of environmental stress. Following our first results for the Sodicho Rockshelter, archaeological settlement layers with preserved and recently dated lithic material fill the Late Pleistocene and Holocene occupational gap (~36 to ~8 ka) from Mochena Borago. Generally, the volcanic rocks of Mt Damota and Mt Sodicho do not contain any naturally occurring obsidian, although this is the most common raw material used for the production of stone artefacts at all archaeological sites in the region (Brandt et al., 2012, 2017). The third study area at the permanent Bisare River site shows a high potential for geoarchaeological investigation (Benito-Calvo et al., 2007), since obsidian raw material was exposed by gully erosion and archaeological artefacts from all stone age periods are scattered within the catchment area. The main causes of gully formation and further development are still not clear, although several factors are potentially relevant for the development of this incision. These often include, e.g. higher precipitation after arid phases, loose topsoil material, and sparse vegetation due to intense land use (Billi and Dramis, 2003; Fryirs and Brierley, 2013; Mukai, 2017). By studying swamp formation in the upper Bisare catchment, the influence of alternating wet and dry phases on the regional landscape dynamics could exemplarily be investigated for the last several years (for long-term climatic fluctuations, please compare Trauth et al., 2019). These alternations lead to changes in erosion and deposition. Generally, our analysis of the landscape archive at the Bisare River sheds light on site preservation and raw material availability.

In order to understand ancient human–environment interactions, understanding the past morphodynamics is crucial. We followed a diachronous approach and tried to transfer today's knowledge about the local fluvial dynamics that affect archaeological assemblages and raw material outcrops by degradation into the past. In the framework of this study we applied geomorphological and hydrological analyses via remote sensing and field surveys. In doing so, we mapped the current flow directions and stream networks and compared these with signs of former human occupation.

## 2 General settings of the study area

### 2.1 Geological and geomorphological setting

The study area is located in the southwestern Ethiopian Highlands north of Lake Abaya, between the north–south-running Omo River in the west and the Bilate River in the east, at the border of the western central and southern Main Ethiopian Rift and the southern Ethiopian Plateau (Fig. 1b). On average, the mountain ranges rise to 2000–3000 m above sea level (a.s.l.). Plio–Pleistocene volcanic activity and Late Pleistocene to Holocene tectonic stress formed characteristic natural basins, steep slopes, and gorges. Silicic volcanic material, including the trachytic solid rocks of Mt Damota and

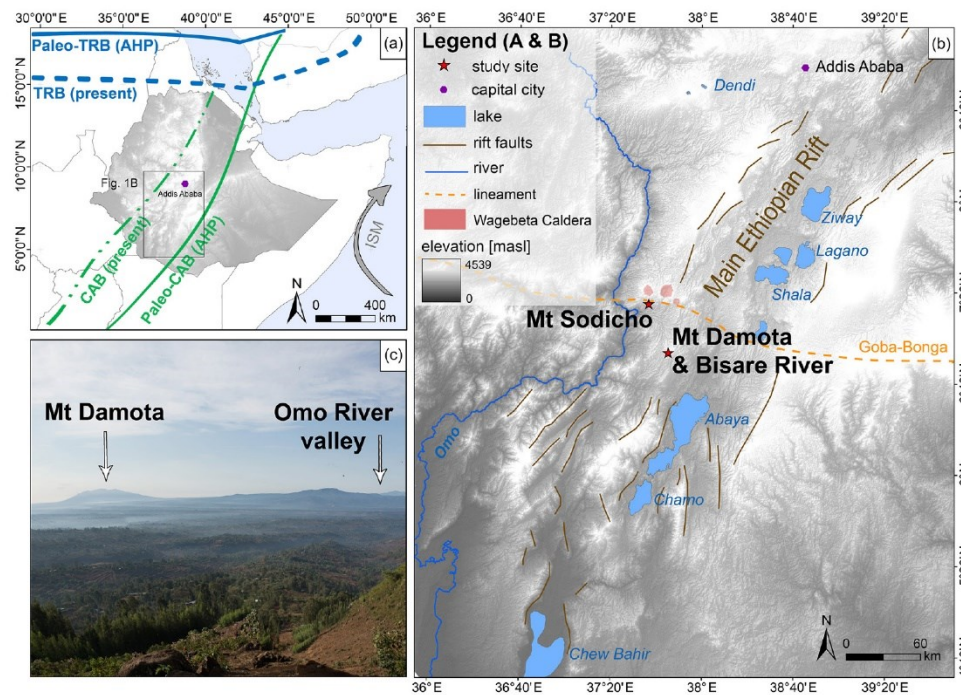


**Figure 1.** (a) Map showing the flow of the Indian Summer Monsoon (ISM) and the current northernmost position of the tropical rain belt (TRB) during August (TRB, present) and its shifted northernmost position for August during the African humid period (Paleo-TRB, AHP, ~ 15 ka BP to ~ 5 ka BP). The map also refers to the present position of the Congo Air Boundary (CAB) and its shift during the AHP (modified from Junginger and Trauth 2013). (b) Research area at the rift margins in the southwestern Ethiopian Highlands, showing the major geological fault system of the Main Ethiopian Rift, the big lake systems, the Wagebeta Caldera Complex, and the Goba-Bonga lineament. The study sites are marked by red stars (DEM data by ASTER GDEM; illustration by Elena Hensel). (c) Photo taken from the southern flank of Mt Sodicho, showing the silhouette of Mt Damota and the Omo River valley (viewing direction south-southwest) (Photo by Christian Schepers, illustration by Elena Hensel).

Mt Sodicho, is part of the rift shoulder trachytic volcanism, which developed in the Pliocene during the late stages of the formation of the Ethiopian Rift (Chernet, 2011; Corti et al., 2013; Abbate et al., 2015).

Mt Damota is a dormant igneous volcanic mountain with a height of 2908 m a.s.l., which is primarily composed of greenish grey trachyte (Brandt et al., 2012). It is part of a larger silicic complex and overlies a pyroclastic rock formation of rhyolitic to trachytic lava and ignimbrites that are associated with the Nazret Group (Chernet, 2011; Corti et al., 2013). Woldegabriel et al. (1990) assumed a formation of the trachytic flows of the volcano during the Late Pliocene (~ 2.9 Ma). Mt Sodicho, with an elevation of about 2100 m a.s.l., belongs to the Wagebeta Caldera Complex (Fig. 1b). The mountain lies directly on the Goba-Bonga lineament, a transversal east–west depression with transversal structures that crosses the Main Ethiopian Rift (Bonini et al., 2005; Corti, 2009; Corti et al., 2013). The Bisare River catchment is situated southwest of Mt Damota within the Hobitcha Caldera structure (Fig. 2c). The river is a western tributary of the Bilate River that flows into the northern part of Lake

Abaya. This lake is located in a quasi-endorheic basin (Schütt et al., 2005). The Bisare River is associated with glacial and valley fills including interbedded volcanic rocks. The latter are not older than 200 ka and developed from the Middle to Upper Pleistocene up to the Holocene (De La Torre et al., 2007). Archaeological finds in the area of the Bisare River catchment comprise open-air artefact scatters and widespread raw material locations, which are currently exposed as a result of river incision (Benito-Calvo et al., 2007; De La Torre et al., 2007; Abbate et al., 2015; Vogelsang, unpublished observation, 2011, 2012).

## 2.2 Climatic setting

The Ethiopian Highlands receive more than 2000 mm of annual rainfall, which is the highest average amount at the Horn of Africa (Griffith, 1972; Viste and Sorteberg, 2013). Annual climatic variations in Ethiopia are related to moisture brought by the summer monsoon that interacts with the dry northeastern “Harmattan” wind system and to changes in the north–south directed pressure gradient (Viste and Sorteberg,

2013; Nicholson, 2018). A further influence is changes in sea surface temperatures of the adjacent Indian Ocean (Griffith, 1972; Tierney et al., 2008; Segele et al., 2009; Viste et al., 2013). Inter-annual changes in precipitation are linked to the shifting of the tropical rain belt (TRB), low-level convergences, and the role of the accentuated topography (Nicholson, 2018) (Fig. 1a). The Congo Air Boundary (CAB) is an additional but less relevant source for moisture variability in Ethiopia (Junginger and Trauth, 2013). Most of the annual precipitation (50%–90%) falls during boreal summer from June to September, called “Kirmet” in this area. Regions with the highest precipitation receive up to 350 mm of rainfall per month (Berhanu et al., 2013). The vegetation of the study area around Mt Damota and Mt Sodicho encompasses two classification types according to Friis et al. (2010): grasslands and mountainous woodland between 1600 and 3300 m a.s.l. belong to the “dry evergreen montane forest and grassland complex” classification and evergreen trees between 1500 and 2600 m a.s.l. to the “moist evergreen montane forest” classification. The mountain flanks of Mt Damota and Mt Sodicho were reshaped by human deforestation, intensive subsistence farming, and subsequent partly severe soil erosion during the last few decades (Fig. 1c). The paleoclimate of southwestern Ethiopia of the last 45 ka was characterized by fluctuations of moister and drier conditions (Foerster et al., 2012; Trauth et al., 2019). According to the paleoclimate record of the Chew Bahir drill cores, arid conditions during the Last Glacial Maximum (LGM, ~ 24–18 ka) led to a desiccation of the former paleolake (Foerster et al., 2012, 2015; Trauth et al., 2019) (Fig. 1b). Subsequently, an abrupt change is visible after ~ 15 ka with a transition from extreme arid to humid conditions, marking the starting point of the African humid period (AHP, ~ 15 to 5 ka). This was a period with a generally higher and stable availability of moisture but was, however, interrupted by several dry spells. Exemplary arid phases were the Older Dryas stadial (OD, ~ 14 ka) and the Younger Dryas event (YD, 12.8–11.6 ka), followed by shorter dry events (~ 10.5, ~ 9.5, 8.15–7.8 and ~ 7 ka). The end of the AHP was marked by an increase in aridity that persists to this day. Exceptions were short humid events at ~ 3, ~ 2.2, and 1.3 ka (Foerster et al., 2012, 2015).

### 3 Material and methods

#### 3.1 Mapping and survey

The research areas around Mt Damota and Mt Sodicho were mapped during field surveys from 2015 to 2018 that were supported by high-resolution satellite imagery. Geomorphological mapping in the field included the description of rock outcrops, surface exposures, geomorphological features, and signs of the influence of extensive modern human occupation in the area. Afterwards, topographical features such as reliefs and slopes, as well as drainage ways and further geomorphological properties, were extracted from a high-resolution dig-

ital elevation model (DEM) (Sect. 3.2). Archaeological surveys in the surrounding area of Mt Damota were conducted from 2010 to 2014, resulting in the discovery of 63 open-air sites. The surveys included different landforms of the tropical highlands in various altitudes, following “stratified random sampling” (Shafer, 2016; Vogelsang and Wendt, 2018). Systematic archaeological and geomorphological surveys of the western Bisare River and Bilate River were undertaken in 2006 by the research group around De la Torre et al. (2007) and in 2011, 2012, and 2014 by the research team of the Collaborative Research Centre 806 (CRC806) “Our way to Europe”. The excavations at Sodicho Rockshelter on Mt Sodicho started in 2015.

#### 3.2 GIS-based analyses

The image analysis software ENVI (5.3 by Harris Geospatial Solutions) was used to extract high-resolution digital elevation models (DEM) using panchromatic images of Pléiades 1A (by Astrium Services/Spot Image, Airbus Defence and Space) satellites, with a 2 m resolution, and ASTER GDEM data (by METI and NASA), with a resolution of 30 m. For this, identical tie points on both satellite images were manually fitted together to create panchromatic images. The high-resolution DEMs generated from the Pléiades satellite scenes cover areas spanning Mt Sodicho, Mt Damota, and the Bisare River catchment, and singular ASTER scenes were used to fill gaps.

Surface and hydrological data were determined by a Geographical Information System (ArcGIS 10.6 by ESRI) using the beforehand-created DEMs functioning as base “maps”. The modelling tools of Arc Hydro (ESRI) were used for the extraction of the hydrological features, such as flow direction and accumulation, surface runoff, and catchment areas. The calculated GIS data sets can be requested from the CRC 806 Database via <https://doi.org/10.5880/SFB806.49>. These parameters allowed a quantitative raster- and vector-based calculation of the actual drainage systems (Bolten et al., 2006). Freely available satellite images of the Google Earth Timelapse NASA Landsat programme from 2009 to 2017 were used to identify annual landscape transformations, i.e. swamp formation and reduction (Fig. 3). In addition, viewshed analyses from both mountaintops (Mt Damota and Mt Sodicho) were conducted with ArcGIS 10.6 (ESRI) to test the significance of the archaeological rock shelters at high evaluations and their importance for prehistoric hunter-gatherers. To do so, a body height of 1.60 m was defined.

#### 3.3 Radiocarbon dating

Several percussion drilling cores were obtained from 11 drilling locations in the basin of the Bisare River swamps in 2014 and 2015. The drilling locations were placed over the entire swamp area. Drilling locations in the surrounding area were not considered, since the surroundings are dominated

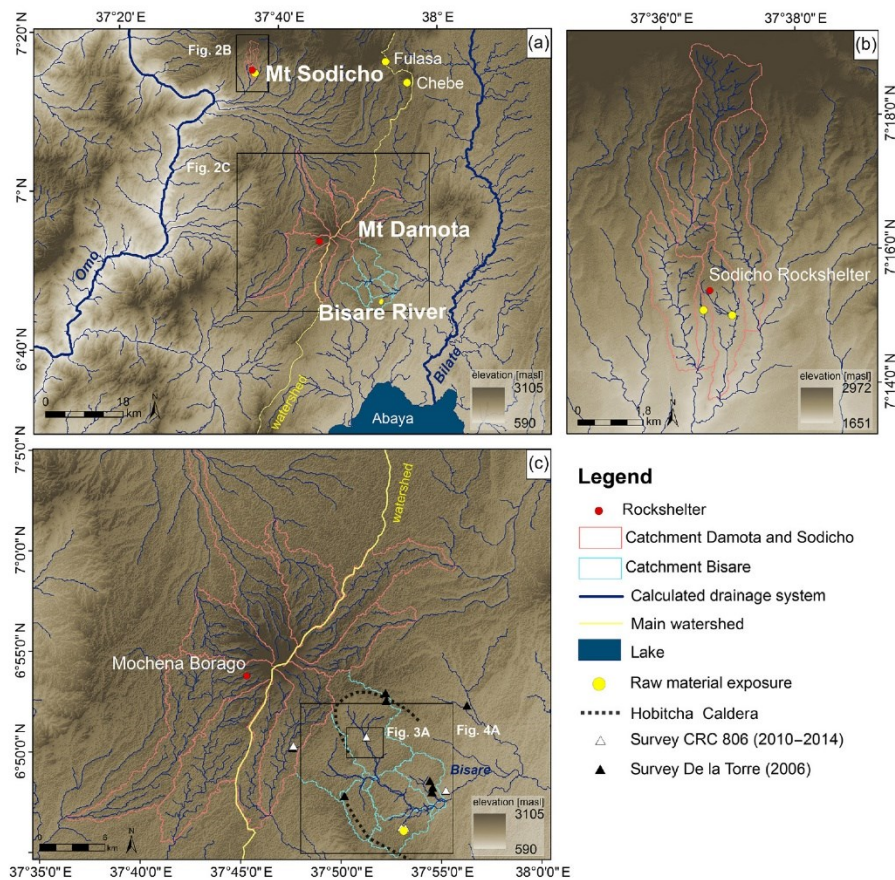


**Figure 2.** (a) Map showing the calculated drainage networks in the study area for the three study sites: Mt Damota, the Bisare River catchment, and Mt Sodicho. Primary drainage systems mainly support the two major south running rivers: Omo and Bilate. (b) Drainage network at the southern flank of Mt Sodicho. (c) Drainage network of Mt Damota and the Bisare River. The triangles illustrate archaeological evidence mapped by De la Torre (2006) and by the CRC 806 (2010–2014) (DEM data from Mochena and Bisare by ASTER GDEM; DEM data from Sodicho by Astrium's Pléiades; illustration by Elena Hensel).

**Table 1.** Radiocarbon ages for the samples from the BIS03 and BIS07 drilling cores.

Sample label	Sample ID	Material	Depth b.s.l. (cm)	Age (years BP)	±	Age (years CE)	$\delta^{13}\text{C}$ (‰)
COL2819.1.1	BIS03-RC1	plant	118	–325	34	n/a	–28.6
COL3300.1.1	BIS07-C1_W	plant	280	> modern	–	1957–1998	–11.2
COL3301.1.1	BIS07-C1_S	sediment	280	25	35	1694–1919	–21.2

n/a: not applicable.

by modern agriculture and therefore excessively influenced by human activity. In this study, we present three samples from cores BIS03 and BIS07 of the uppermost part of swamp I, which were tested for radiocarbon dating (Table 1). Both cores were drilled in fluvial sequences located on the edges of the swamp (Fig. 3a). The three radiocarbon samples, from either plant (BIS03-PC1 and BIS07\_W) or sediment mate-

rial (BIS07-C1\_S), were extracted from silty to sandy sediments in the upper 3 m of the drilling cores. The radiocarbon AMS lab of the University of Cologne analysed the samples with acid and alkali (AAA) pre-treatment to remove inorganic carbon and humic acids. The conventional radiocarbon ages were calibrated with OxCal v. 4.2.3, applying the cal-

ibration curve IntCal13 (Ramsey et al., 2013; Reimer et al., 2013).

## 4 Results

### 4.1 GIS-based analyses

The geomorphological and hydrological analyses of the two mountains and the Bisare River catchments were based on high-resolution DEMs that were calculated based on remote sensing data. With the help of the catchment analysis, recent large-scale drainage lines of the study area around Mt Damota and Mt Sodicho were defined (Fig. 2a). In combination with a geomorphological field survey, small-scale and large-scale gully erosion could be identified.

1. Mt Damota has a typical radial drainage system, which is crossed by a main watershed (Fig. 2c). This watershed is running north–south through the entire study area, separating the runoff into a western and an eastern direction. The western streams drain into the Omo River basin, whereas the eastern streams drain towards Lake Abaya but without an inflow into the Bisare River catchment. This is caused by the horseshoe-shaped Hobitcha Caldera that functions as a barrier between the eastern streams and the Bisare River catchment.
2. Mt Sodicho's stream network and drainage lines mainly flow into the Omo River basin. According to the hydrological analyses and the field observations from 2017, Mt Sodicho has a radial drainage network, which gave the mountain its characteristic irregular form (Fig. 2b). Permanent streams and seasonal creeks (only flowing during the rainy season) flow down the mountain flanks into a larger south-running dendritic drainage network that belongs to the drainage network of the Wagebeta Caldera Complex. Nowadays, the surface morphology on Mt Sodicho is influenced by intensive agriculture. Small-scale surface erosion (10–20 m in width) was mapped on the upper slopes (Fig. 1c). In the past, the vegetation was probably removed to create cultivation areas, which are now jeopardized by increasing erosion. These active gullies are currently used as pathways for the local population and their cattle, which further enhances degradation and runoff. Raw material provenance of lithic artefacts that were found at Mt Sodicho is still not proven. So far, obsidian raw material with distinct signs of transport could be observed as fluviially transported boulders or debris along the surrounding drainage systems and river banks. In Fig. 2b, these raw material findings are illustrated as yellow dots. Additionally, two obsidian outcrops were discovered to the east of Mt Sodicho during the latest survey in November 2018. Within a distance of 30–36 km from Sodicho Rockshelter, the two outcrops named Chebe and Fulasa

were still in the range of movement of the Late Pleistocene hunter-gatherers (Fig. 2a).

3. The Bisare River flows into the Bilate River. The latter is the main tributary of the 15 000 km<sup>2</sup> large catchment of Lake Abaya (Chernet, 2011). Based on the hydrological and geomorphological analyses, different geomorphic features could be observed (Fig. 2c): the research area lies within a dynamic hydrological system, showing a high to moderate runoff of surface water (Berhaun et al., 2013). With the help of a longitudinal profile, starting at the Bisare River catchment and following the Bilate River into Lake Abaya, a sudden change in the slope (knickpoint) could be identified. This knickpoint is situated ~ 15 km along the profile, where the river flows out from the Hobitcha Caldera (Fig. 5). The study of knickpoints can be used to identify potential areas for sedimentation. Three connected swamps of different sizes and altitudes formed in low-energy parts of the river valley in the upper part of the catchment (Fig. 3). They were documented during geomorphological field mapping in 2014. A highly exaggerated longitudinal profile, running transversely through the lakes, illustrates the local stair-like morphology. Unlike swamp 3, the two upper basins of swamps 1 and 2 are situated in an area with highly dynamic permanent and episodic streams. Via satellite imagery (Google Earth Timelapse NASA Landsat programme), we observed that the two upper swamps are supplied by episodic tributaries during wet seasons (Fig. 3b–d). Gully erosion and sheet-wash erosion are widespread phenomena particularly in the lower part of the Bisare catchment (Fig. 4a). Here, surface runoff and erosion-outcropped artefact assemblages are predominantly from the Middle Stone Age (De La Torre et al., 2007). These assemblages were preserved in Pleistocene alluvial soils at the flanks of the river basin. Also, outcrops of in situ obsidian raw material and scattered lithic surface finds were found by De La Torre et al. (2007) and our research team in the southern degraded areas. Formerly buried material was exposed to the surface, and the lithics had been partly transported due to constant erosion and extensive badlands formation, mainly at the lower part of the river catchment. Erosion and badlands formation initiated from the edge of the rift valley and spread upstream of the Bisare (Fig. 4c–e). Figure 4d and e visualize subsurface material cropping out in this degraded area, which varies between reddish-brown regolith and greyish ignimbrite.

According to the viewshed analyses from the mountain-tops of Mt Damota and Mt Sodicho, all-round views over the landscape are possible. The views reach from the lakes of the central Main Ethiopian Rift Valley in the distant north, over the Bilate River in the east, Lake Abaya to the south, the Gibe and Omo river valleys to the southwest, and up the Wolayta–

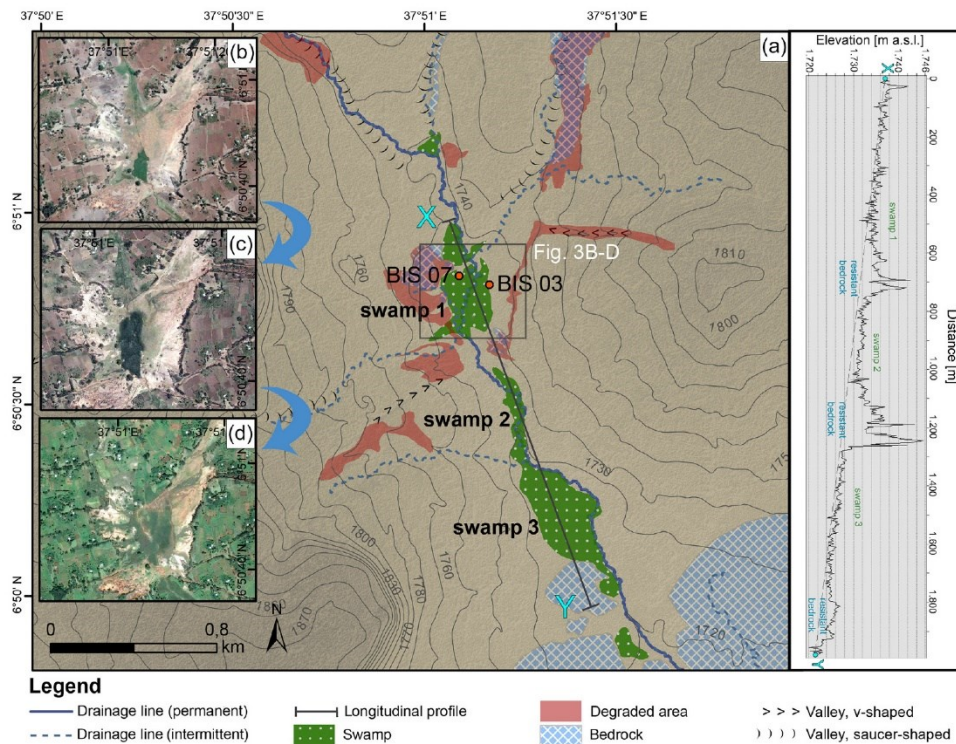


**Figure 3.** (a) Map showing the dimension of the three swamps on the Bisare River. The positions of the two drillings in swamp 1 are marked with red dots (DEM data by ASTER GDEM). The sequence of images (b)–(d) illustrates the changes of swamp 1 during different wet and dry phases: (b) following a dry season (21 March 2009), (c) following a wet season (15 November 2009), and (d) during a wet season (17 October 2014) (swamp data set by Svenja Meyer; Satellite images by ©Google Earth Timelapse NASA Landsat programme). The super-elevated longitudinal profile X–Y illustrates the geomorphological position of the swamps in the Bisare River basin, leading to a step-like topography, extracted from the DEM based on Pléiades 1A satellite imagery (DEM data by ASTER GDEM; illustration by Elena Hensel).

Hadiya Highlands to the west. During clear weather conditions, the opening area of the Sodicho Rockshelter offers a complete view to Mt Damota and the Omo River basin in the west (Fig. 1c). The view directly from Mochena Borago is limited to the southeast and east, and therefore Mt Sodicho is out of sight. These results verify a locational advantage of both rock shelters, i.e. Mochena Borago on Mt Damota and Sodicho Rockshelter on Mt Sodicho, for watching game in the surrounding lowlands.

#### 4.2 Radiocarbon dating

The modern radiocarbon ages of two botanical samples (BIS03-PC1 and BIS07\_W) and one sediment sample (BIS07-C1\_S), originating from two drilling cores taken in a depth of up to 2 m below the surface level in the uppermost part of swamp 1, revealed that the upper 3 m of the sedimentary basin fill are of modern age (Table 1). This demonstrates a high sedimentation rate at least in this swamp.

#### 5 Discussion

Several processes of degradation, such as gully or river erosion, led to the exposure of obsidian raw material localities and open-air sites with scatters of stone artefacts (Fig. 4a–d). This is particularly true in the Bisare River basin with its areas of different stream energy where the swamps form sediment traps for the eroded material today. One main question was why these step-like swamps formed and if their formation process can be used to obtain paleoenvironmental information. We propose that during wetter phases stronger gully erosion is activated, and resulting sediment slugs are able to hold up further sediment flux. This can be described as a cut-and-fill process with sediment accumulation in times with relatively intensive erosion and active gully, and channel incision in periods of less active gully, e.g. less intensive erosion (Nanson and Croke, 1992; Brierley and Fryirs, 1999; Fryirs and Brierley, 2013; Orti et al., 2019). The consequence is swamp development due to damming of the stream and sediment trapping. Therefore, this area can be assumed to

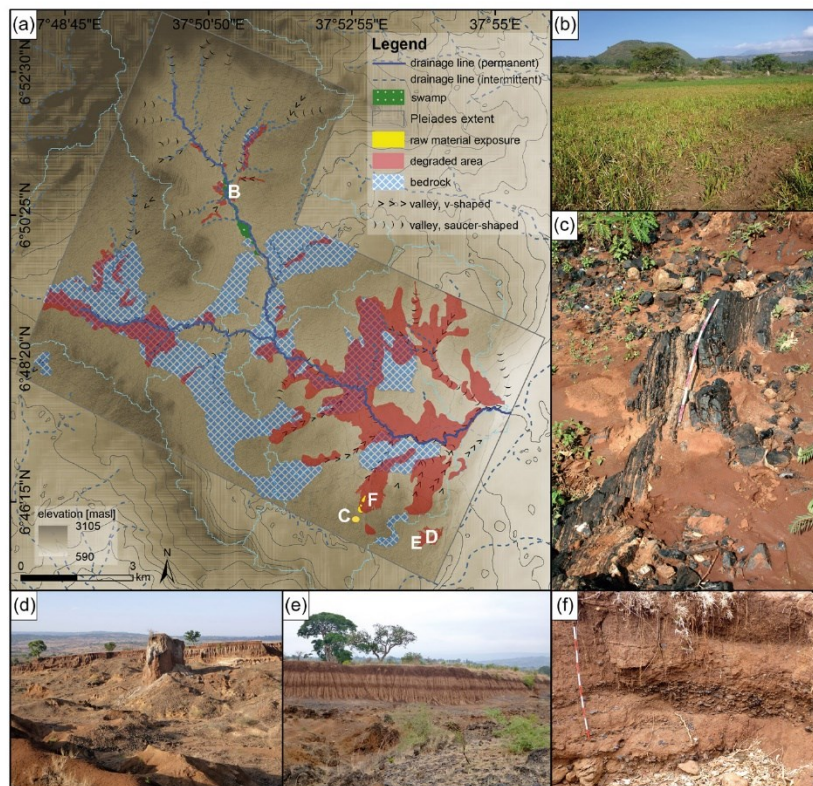


**Figure 4.** (a) Map showing the Bisare River catchment. Degraded areas are mainly characterized by gully erosion. (b) Image of the wet, swampy area in the upper part of the catchment (swamp 1). (c) Obsidian raw material outcrop. (d) Badlands formation and gully erosion is a common phenomenon in the depressions of the catchment. (e) Gully-erosion-exposed paleosols alternating with volcanic ash. (f) Relocated obsidian flakes exposed in a gully of a degraded area (swamp data set by Svenja Meyer; photography by Olaf Bubenzer; illustration by Elena Hensel).

be very sensitive towards external changes and disturbances, e.g. a change in sediment flux rate. The southernmost part of swamp 3 has the widest dimension, which is most probably the result of a change of bedrock (Fig. 3). A more resistant rock type must have created a natural “bottleneck”, which caused natural damming that was intensified by additional damming by sediment slugs during certain periods. As a consequence, the slow-moving water got dammed up, leading to sedimentation and preventing erosion of these accumulated sediments (Machado, 2015). Generally, changes of sediment supply from tributaries into the Bisare and then into the Bilate River must have had a significant geomorphological effect on the main hydrological system in the form of the incision and subsequent aggradation of transported material. In summary, we view this as a geogenic sediment cascade system, where relatively young sediments should have been transported into the lower basin only after the higher basins were filled up (Fig. 3a) (Fryirs and Brierley, 2013; Fryirs, 2016). However, the radiocarbon samples (BIS07-C1) of the sediment in the uppermost basin yielded modern ages, al-

though they are assumed to contain the oldest sediments (Table 1). With a possible sediment cascade and our radiocarbon dates in mind, we state that the development of the swamps must be a relatively recent phenomenon that is linked with the current high erosion and accumulation rates in the area of the Bisare River. Therefore, we suggest that the surficial Pleistocene deposits that are currently largely being exposed by badlands formation in the region must have been completely removed by fluvial erosion, leading to formation of the basins. Afterwards, the basins were refilled by the recent fine-grained sediment that we dated with radiocarbon (Table 1).

With respect to the present-day lithic raw material accessibility and preservation, our geomorphological field observations from 2014 and 2015 coincide with the published observations by Vogelsang and Wendt (2018) on obsidian outcrops in the Humbo area of the Bisare River catchment (Fig. 2c). These authors state that the predominance of obsidian for the production of stone artefacts is not surprising, considering the proximity of the rich sources in the Humbo area to known

archaeological sites (Vogelsang and Wendt, 2018). Furthermore, the glassy structure of the obsidian allows a very precise production of lithic tools (Rapp, 2009). Together, this could explain the extreme dominance of obsidian in all lithic assemblages. However, the question arises whether the activity of the hydrological system and erosion processes at Bisare had a comparable intensity during Late Pleistocene and early Holocene to mid-Holocene, leading to the exposure of a similar amount of raw material. If this was not the case, hunter-gatherers were not able to focus only on the local obsidian deposit in the Humbo area but had to select alternative sources. In this context, also the effects of today's vegetation have to be considered. Today's intensive farming and deforestation, e.g. at the flanks of Mt Sodicho, strongly changed the actual surface runoff but might also directly destroy archaeological deposits. The current destruction and relocation of raw material is visible in the form of scattered obsidian debris and large boulders found along the streams at Mt Sodicho (Fig. 2b). At the moment, we cannot verify if prehistoric hunter-gatherers were able to use such kinds of displaced raw material, but this would be an interesting question for future research. Generally, we think that understanding the hydrological system is fundamental for the evaluation of obsidian raw material availability in this area. However, we still do not know the rate and the start of gully erosion and badlands formation in our study area that are known as inhomogeneous processes – in intensity as well as in duration (Castillo and Gómez, 2016). If the Late Pleistocene hydrological system was as highly dynamic as it is today, gully erosion might have already been initiated by natural processes during that period. We only expect this for certain climatic phases in which the paleoenvironmental conditions promoted such a dynamic system due to higher precipitation. Accordingly, several studies demonstrated variable climatic conditions at the Horn of Africa during the Late Pleistocene and Holocene. Transitions from humid to arid conditions and vice versa led to rise and shrinkage of lake levels and also affected the connecting drainage networks (Sagri et al., 2008; Carnicelli et al., 2009; Foerster et al., 2012; Junginger and Trauth, 2013; Foerster et al., 2015; Trauth et al., 2019). We propose that the connected drainage systems in our research area, such as the Bisare River, might have reacted to these transitions with changes in their depositional and erosional behaviour. Furthermore, considering the location of our research areas within a region that have been tectonically active since the Plio–Pleistocene, we can assume that the aforementioned extensive surface processes most likely started already during the Late Pleistocene (Fig. 5). However, we propose that due to today's intensified human impact in the form of clearance of the vegetation cover and cropland expansion, leading to higher runoff, obsidian raw material comes more frequently and in higher amounts up to the surface than during prehistoric times.

Archaeological evidence from Mt Damota and Sodicho Rockshelter shows that groups of prehistoric humans seem

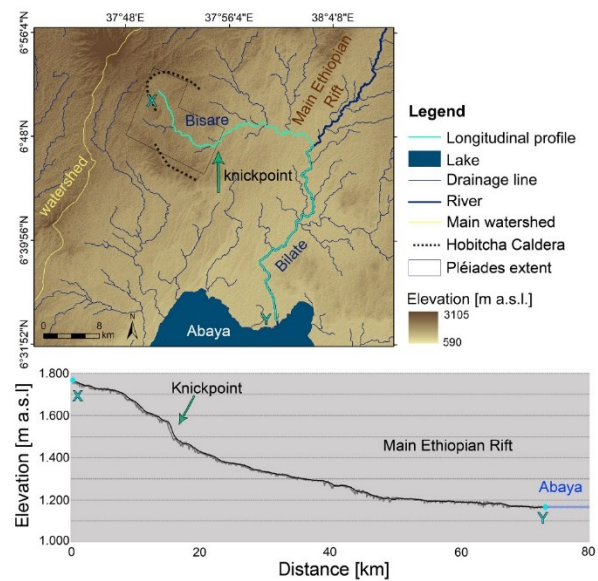


**Figure 5.** Map showing the calculated drainage networks southeast of the Bisare River catchment that flow into Lake Abaya. Following the longitudinal profile of the Bisare River (green line and graph), a sudden change in slope (knickpoint) at the outflow from the Hobitcha Caldera stands out (DEM data by ASTER GDEM; illustration by Elena Hensel).

to have adapted to former climatic and hydrological changes, leading to different environmental conditions, with repeated occupation of the rock shelters at higher elevations under different environmental conditions (Brandt et al., 2012, 2017; Vogelsang and Wendt, 2018). During such periods these groups were probably exploiting these higher elevated areas with the awareness of their sufficient water and food resources, shelter, and the access to obsidian raw material (cf. Vogelsang et al., 2018). Although it is not yet clear which specific obsidian outcrops were used by the prehistoric humans, first results of obsidian microprobe analysis point to the exploitation of raw material from outcrops in the Bisare area by the inhabitants of both rock shelters (Vogelsang, unpublished information, 2019).

## 6 Conclusions

This study gives an insight into the potential of a combination of hydrological and geomorphological analyses by applying field surveys, remote sensing, geographical information systems, and radiocarbon dating, as well as investigations of the archaeological site distribution, to reconstruct the interplay between past hydrological conditions and Paleolithic settlement activity in a mountainous area of the southwestern Ethiopian Highlands. With our results, we were able to describe the current landscape dynamics and the actual

state of known rock shelters and open-air sites, as well as raw material preservation in the study areas. The preserved evidence for repeated human occupation during the Late Pleistocene and Holocene at Sodicho Rockshelter (Vogelsang, unpublished information, 2015 to 2018) hints that the highlands could have provided a refugium during arid phases such as the Last Glacial Maximum (LGM,  $\sim 21 \pm 2$  ka) (Mark and Osmaton, 2008). At Mochena Borago, settlement activities reach back  $> 50$  ka. During such periods, the exploitation of different, elevation-bound ecosystems allowed access to a heterogeneous spectrum of faunal and lithic resources for prehistoric humans (Vogelsang and Wendt, 2018). Humid–arid transitions in the past must have led to pronounced erosion and badlands formation. We suggest that there is a relationship between widespread gully erosion, badlands formation, and raw material availability. Currently, the study area is a region with strong recent sediment erosion and simultaneous accumulation in a cascading system. Looking into the future, given strongly increased human impact during the last few decades acting together with the currently very active hydrological system, intensified soil loss will lead to further degradation of the archaeological material. However, the transfer of today’s circumstances into prehistoric times is complicated, as we cannot prove that currently active processes, e.g. swamp formation, were also active during the Pleistocene. Furthermore, the research sites are situated in an area close to the Main Ethiopian Rift, i.e. a region with pronounced tectonic activity that also has a significant impact on the regional geomorphodynamics. Therefore, at this stage the results do not allow any distinct statement about the transfer of the modern morphodynamics to ancient times, as we have identified only recent phenomena. This means that the calculated drainage lines show the current state in a very active hydrological system that is influenced by both natural effects and intensive human activity. Nevertheless, in the context of further interdisciplinary research that combines well-resolved archaeological and alluvial chronostratigraphies it will be possible to obtain a better general understanding of the interplay between former settlement activity and paleoenvironmental conditions in the Ethiopian Highlands during the Pleistocene.

**Data availability.** GIS data sets can be requested from the CRC 806 Database via <https://doi.org/10.5880/SFB806.49> (Hensel et al., 2019).

**Author contributions.** The geomorphological field mapping and drilling were carried out by OBU and OBo. Archaeological survey was conducted by RV. EAH performed GIS-based mapping, geomorphological–hydrological analyses, and preparation of the paper. All co-authors contributed to, read, and approved the paper.

**Competing interests.** The authors declare that they have no conflict of interest.

**Special issue statement.** This article is part of the special issue “Geoarchaeology and past human–environment interactions”. It is not associated with a conference.

**Acknowledgements.** We kindly thank the Authority for Research and Conservation of Cultural Heritage (ARCC) of Ethiopia for their permission and general support, and the Ministry of Mines and Energy for the approval of our export permits. This study was conducted as a part of project A1 “Out of Africa – Late Pleistocene Rock Shelter Stratigraphies and Palaeoenvironments in Northeast Africa” in the framework of the Collaborative Research Centre 806 (CRC 806) “Our way to Europe”. We thank Janet Rethemeyer and colleagues from the radiocarbon AMS lab of the University of Cologne for radiocarbon dating the Bisare samples. We are very grateful to Svenja Meyer for her great effort for project A1 and for her participation during various field seasons in Ethiopia especially. Special thanks also go to Taylor Otto for the English proofreading, as well as to Minassie Tekelemariam and Bahru Zinaye for their support in the field. We thank Andrea Zerboni, an anonymous referee, and the editors for constructive and insightful comments, which significantly helped to improve this paper.

**Financial support.** This research has been supported by the Deutsche Forschungsgemeinschaft (DFG, German Research Foundation) (grant no. 57444011 – SFB 806).

## References

- Abbate, E., Bruni, P., and Sagri, M.: Geology of Ethiopia: a review and geomorphological perspectives, in: *Landscapes and Landforms of Ethiopia*, edited by: Billi, P., Springer, Dordrecht, the Netherlands, 33–64, [https://doi.org/10.1007/978-94-017-8026-1\\_2](https://doi.org/10.1007/978-94-017-8026-1_2), 2015.
- Basell, L. S.: Middle Stone Age (MSA) site distributions in eastern Africa and their relationship to Quaternary environmental change, refugia and the evolution of *Homo sapiens*, *Quaternary Sci. Rev.*, 27, 2484–2498, <https://doi.org/10.1016/j.quascirev.2008.09.010>, 2008.
- Benito-Calvo, A., De la Torre, I., Mora, R., Tibebe, D., Morán, N., and Martínez-Moreno, J.: Geoarchaeological potential of the western bank of the Bilate River (Ethiopia), *Analele Universității din Oradea, Seria Geographie*, XVII, 99–104, 2007.
- Berhanu, B., Melesse, A. M., and Seleshi, Y.: GIS-based hydrological zones and soil geo-database of Ethiopia, *CATENA*, 104, 21–31, <https://doi.org/10.1016/j.catena.2012.12.007>, 2013.
- Billi, P. and Dramis, F.: Geomorphological investigations on gully erosion in the Rift Valley and the northern highlands of Ethiopia, *CATENA*, 50, 353–368, [https://doi.org/10.1016/S0341-8162\(02\)00131-5](https://doi.org/10.1016/S0341-8162(02)00131-5), 2003.
- Bolten, A., Bubenzer, O., and Darius, F.: A digital elevation model as a base for the reconstruction of Holocene land-

- use potential in arid regions, *Geoarchaeology*, 21, 751–762, <https://doi.org/10.1002/gea.20137>, 2006.
- Bonini, M., Corti, G., Innocenti, F., Manetti, P., Mazzarini, F., Abebe, T., and Pecskey, Z.: Evolution of the Main Ethiopian Rift in the frame of Afar and Kenya rifts propagation, *Tectonics*, 24, 1–21, <https://doi.org/10.1029/2004TC001680>, 2005.
- Brandt, S., Hildebrand, E., Vogelsang, R., Wolfhagen, J., and Wang, H.: A new MIS 3 radiocarbon chronology for Mochena Borogo Rockshelter, SW Ethiopia: Implications for the interpretation of Late Pleistocene chronostratigraphy and human behavior, *J. Archaeol. Sci. Reports*, 11, 352–369, <https://doi.org/10.1016/j.jasrep.2016.09.013>, 2017.
- Brandt, S. A., Fisher, E. C., Hildebrand, E. A., Vogelsang, R., Ambrose, S. H., Lesur, J., and Wang, H.: Early MIS 3 occupation of Mochena Borogo Rockshelter, Southwest Ethiopian Highlands: implications for Late Pleistocene archaeology, paleoenvironments and modern human dispersals, *Quatern. Int.*, 274, 38–54, <https://doi.org/10.1016/j.quaint.2012.03.047>, 2012.
- Brierley, G. J. and Fryirs, K.: Tributary–trunk stream relations in a cut-and-fill landscape: a case study from Wolumla catchment, New South Wales, Australia, *Geomorphology*, 28, 61–73, [https://doi.org/10.1016/S0169-555X\(98\)00103-2](https://doi.org/10.1016/S0169-555X(98)00103-2), 1999.
- Carnicelli, S., Benvenuti, M., Ferrari, G., and Sagri, M.: Dynamics and driving factors of late Holocene gullying in the Main Ethiopian Rift (MER), *Geomorphology*, 103, 541–554, <https://doi.org/10.1016/j.geomorph.2008.07.019>, 2009.
- Castillo, C. and Gómez, J. A.: A century of gully erosion research: Urgency, complexity and study approaches, *Earth Sci. Rev.* 160, 300–319, <https://doi.org/10.1016/j.earscirev.2016.07.009>, 2016.
- Chernet, T.: Geology and hydrothermal resources in the northern Lake Abaya area (Ethiopia), *J. Afr. Earth. Sci.*, 61, 129–141, <https://doi.org/10.1016/j.jafrearsci.2011.05.006>, 2011.
- Corti, G.: Continental rift evolution: from rift initiation to incipient break-up in the Main Ethiopian Rift, East Africa, *Earth. Sci. Rev.*, 96, 1–53, <https://doi.org/10.1016/j.earscirev.2009.06.005>, 2009.
- Corti, G., Sani, F., Philippon, M., Sokoutis, D., Willingshofer, E., and Molin, P.: Quaternary volcano-tectonic activity in the Soddò region, western margin of the Southern Main Ethiopian Rift, *Tectonics*, 32, 861–879, <https://doi.org/10.1002/tect.20052>, 2013.
- De La Torre, I., Benito-Calvo, A., Mora, R., Martínez-Moreno, J., Morán, N., and Tibebe, D.: Stone Age occurrences in the western bank of the Bilate River (Southern Ethiopia) – Some preliminary results, *Nyame Akuma*, 67, 14–25, 2007.
- Foerster, V., Junginger, A., Langkamp, O., Gebru, T., Asrat, A., Umer, M., Lamb, H.F., Wennrich, V., Rethemeyer, J., Nowaczyk, N., Trauth, M. H., and Schaebitz, F.: Climatic change recorded in the sediments of the Chew Bahir basin, southern Ethiopia, during the last 45,000 years, *Quaternary Int.*, 274, 25–37, <https://doi.org/10.1016/j.quaint.2012.06.028>, 2012.
- Foerster, V., Vogelsang, R., Junginger, A., Asrat, A., Lamb, H. F., Schaebitz, F., and Trauth, M. H.: Environmental change and human occupation of southern Ethiopia and northern Kenya during the last 20,000 years, *Quaternary Sci. Rev.*, 129, 333–340, <https://doi.org/10.1016/j.quascirev.2015.10.026>, 2015.
- Friis, I., Sebsebe, D., and Breugel, P.: Atlas of the potential vegetation of Ethiopia, Det Kongelige Danske Videnskabernes Selskab, Copenhagen, 2010.
- Fryirs, K. A.: River sensitivity: a lost foundation concept in fluvial geomorphology, *Earth Surf. Proc. Land.*, 42, 55–70, <https://doi.org/10.1002/esp.3940>, 2016.
- Fryirs, K. A. and Brierley, G. J.: *Geomorphology analysis of river systems: an approach to reading the landscape*, John Wiley & Sons, Chichester, West Sussex, England, 2013.
- Griffiths, J.: Ethiopian highlands, *World survey of climatology*, 10, 369–381, 1972.
- Hensel, E. A., Bödeker, O., Bubenzer, O., and Vogelsang, R.: Combining geomorphological–hydrological analyses and the location of settlement and raw material sites – a case study on understanding prehistoric human settlement activity in the southwestern Ethiopian Highlands, *E&G Quaternary Sci. J.*, 69, 1–14, <https://doi.org/10.5194/egqsj-69-1-2019>, 2019.
- Junginger, A. and Trauth, M. H.: Hydrological constraints of paleo-Lake Suguta in the Northern Kenya Rift during the African humid period (15–5 ka BP), *Global Planet. Change*, 111, 174–188, <https://doi.org/10.1016/j.gloplacha.2013.09.005>, 2013.
- Junginger, A., Vonhof, H., and Foerster, V. E.: AGU Fall Meeting Abstracts, How wet is wet? Strontium isotopes as paleo-lake level indicators in the Chew Bahir basin (S-Ethiopia), American Geophysical Union, Fall Meeting 2016, (abstract no. PP23A-2310), 2016.
- Machado, M. J.: Geomorphology of the Adwa District, in: *Landscapes and Landforms of Ethiopia*, edited by: Billi, P., Springer, Dordrecht, Netherlands, 163–178, <https://doi.org/10.1007/978-94-017-8026-1>, 2015.
- Mark, B. G. and Osmaton, H. A.: Quaternary glaciation in Africa: Key chronologies and climatic implications, *J. Quaternary Sci.*, 23, 589–608, <https://doi.org/10.1002/jqs.1222>, 2008.
- Mukai, S.: Gully erosion rates and the analysis of determining factors: A case study from the semi-arid Main Ethiopian Rift Valley, *Land Degrad. Dev.*, 28, 607–615, <https://doi.org/10.1002/ldr.2532>, 2017.
- Nanson, G. C. and Croke, J. C.: A genetic classification of floodplains, *Geomorphology*, 4, 459–486, [https://doi.org/10.1016/0169-555X\(92\)90039-Q](https://doi.org/10.1016/0169-555X(92)90039-Q), 1992.
- Nicholson, S. E.: The ITCZ and the seasonal cycle over equatorial Africa, *B. Am. Meteorol. Soc.*, 99, 337–348, <https://doi.org/10.1175/BAMS-D-16-0287.1>, 2018.
- Orti, M. V., Negussie, K., Corral-Pazos-De-Provens, E., Höfle, B., and Bubenzer, O.: Comparison of Three Algorithms for the Evaluation of TanDEM-X Data for Gully Detection in Krumhuk Farm (Namibia), *Remote Sensing*, 11, 1327, <https://doi.org/10.3390/rs11111327>, 2019.
- Ramsey, C., Scott, E., and Van der Plicht, J.: Calibration for Archaeological and Environmental Terrestrial Samples in the Time Range 26–50 ka cal BP, *Radiocarbon*, 55, 2021–2027, [https://doi.org/10.2458/azu\\_js\\_rc.55.16935](https://doi.org/10.2458/azu_js_rc.55.16935), 2013.
- Rapp, G.: Lithic Materials, in: *Archaeomineralogy, Natural Science in Archaeology*, edited by: Rapp, G., Springer, Berlin, Heidelberg, Germany, 60–90, [https://doi.org/10.1007/978-3-540-78594-1\\_4](https://doi.org/10.1007/978-3-540-78594-1_4), 2009.
- Reimer, P. J., Bard, E., Bayliss, A., Beck, J. W., Blackwell, P. G., Ramsey, C. B., Buck, C. E., Cheng, H., Edwards, R. L., Friedrich, M., Grootes, P. M., Guilderson, T. P., Hafflidason, H., Hajdas, I., Hatté, C., Heaton, T. J., Hoffmann, D. L., Hogg, A. G., Hughen, K. A., Kaiser, K. F., Kromer, B., Manning, S. W., Niu, M., Reimer, R. W., Richards, D. A., Scott, E. M.,

- Southon, J. R., Staff, R. A., Turney, C. S. M., and van der Plicht, J.: IntCal13 and Marine13 Radiocarbon Age Calibration Curves 0–50,000 Years cal BP, *Radiocarbon*, 55, 1869–1887, [https://doi.org/10.2458/azu\\_js\\_rc.55.16947](https://doi.org/10.2458/azu_js_rc.55.16947), 2013.
- Sagri, M., Bartolini, C., Billi, P., Ferrari, G., Benvenuti, M., Carnicelli, S., and Barbano, F.: Latest Pleistocene and Holocene river network evolution in the Ethiopian Lakes Region, *Geomorphology*, 94, 79–97, <https://doi.org/10.1016/j.geomorph.2007.05.010>, 2008.
- Schütt, B.: Deposition of modern fluvio-lacustrine sediments in Lake Abaya, South Ethiopia – A case study from the delta areas of Bilate River and Gidabo River, northern basin, *Z. Geomorph. N. F.*, 138, 131–151, 2005.
- Segele, Z. T., Lamb, P. J., and Leslie, L. M.: Large-scale atmospheric circulation and global sea surface temperature associations with Horn of Africa June–September rainfall, *Int. J. Climatol.*, 29, 1075–1100, <https://doi.org/10.1002/joc.1751>, 2009.
- Shafer, H. J.: Research design and sampling techniques, in: *Field Methods in Archaeology*, edited by: Hester, T. R., Shafer, H. J., and Feder, K. I., Routledge, Oxford, England, 2016.
- Tierney, J. E., Russell, J. M., Huang, Y., Damsté, J. S. S., Hopmans, E. C., and Cohen, A. S.: Northern Hemisphere Controls on Tropical Southeast African Climate During the Past 60,000 Years, *Science*, 322, 252–255, <https://doi.org/10.1126/science.1160485>, 2008.
- Tierney, J. E., Lewis, S. C., Cook, B. I., LeGrande, A. N., and Schmidt, G., A.: Model, proxy and isotopic perspectives on the East African Humid Period, *Earth Planet. Sc. Lett.*, 307, 103–112, <https://doi.org/10.1016/j.epsl.2011.04.038>, 2011.
- Trauth, M. H., Asrat, A., Duesing, W., Foerster, V., Kraemer, K. H., Marwan, N., Maslin, M. A., and Schaebitz, F.: Classifying past climate change in the Chew Bahir basin, southern Ethiopia, using recurrence quantification analysis, *Clim. Dynam.*, 53, 1–16, <https://doi.org/10.1007/s00382-019-04641-3>, 2019.
- Viste, E. and Sorteberg A.: Moisture transport into the Ethiopian highlands, *Int. J. Climatol.*, 33, 249–263, <https://doi.org/10.1002/joc.3409>, 2013.
- Vogelsang, R. and Wendt, K. P.: Reconstructing prehistoric settlement models and land use patterns on Mt. Damota/SW Ethiopia, *Quatern. Int.*, 485, 140–149, <https://doi.org/10.1016/j.quaint.2017.06.061>, 2018.
- Vogelsang, R., Bubbenzer, O., Kehl, M., Meyer, S., Richter, J., and Zinaye, B.: When Hominins Conquered Highlands – an Acheulean Site at 3000 m a.s.l. on Mount Dendi/Ethiopia, *Journal of Paleolithic Archaeology*, 1, 302–3013, <https://doi.org/10.1007/s41982-018-0015-9>, 2018.
- Woldegabriel, G., James, L. A., and Robert, C. W.: Geology, geochronology, and rift basin development in the central sector of the Main Ethiopian Rift, *Geol. Soc. Am. B.*, 102, 439–485, [https://doi.org/10.1130/0016-7606\(1990\)102<0439:GGARBD>2.3.CO;2](https://doi.org/10.1130/0016-7606(1990)102<0439:GGARBD>2.3.CO;2), 1990.

## 2.1 Supplement material

This supplementary material is available at the CRC 806-Database under the DOI: 10.5880/SFB806.49. The original data table below contains an overview of GIS datasets corresponding to the following open access publication:

Hensel, E. A., Bödeker, O., Bubenzer, O., and Vogelsang, R. (2019). Combining geomorphological–hydrological analyses and the location of settlement and raw material sites – a case study on understanding prehistoric human settlement activity in the southwestern Ethiopia Highlands. *E&G Quaternary Science Journal* 68, 201–213, doi: <https://doi.org/10.5194/egqsj-68-201-2019>.

---

**Supplementary data of Hensel et al. 2019, E&G Quaternary Sci. J.**


---

This data corresponds to the article and shall be quoted as such using the provided DOI: Hensel, E. A., Bödeker, O., Bubenzer, O., and Vogelsang, R. (2019). Combining geomorphological–hydrological analyses and the location of settlement and raw material sites – a case study on understanding prehistoric human settlement activity in the southwestern Ethiopia Highlands. *E&G Quaternary Science Journal* 68, 201–213, doi: <https://doi.org/10.5194/egqsj-68-201-2019>.

CRC806-Database, DOI: 10.5880/SFB806.49

<b>GIS file</b>	<b>Description</b>
<i>Bisare_cat</i>	Calculated catchment grid of the Bisare River; derived from generated digital elevation models.
<i>Bisare_gul</i>	Mapped areas with degraded areas (mainly gully erosion) at the Bisare River.
<i>Bisare_orm</i>	Mapped obsidian raw material outcrop in the catchment area of the Bisare River.
<i>Bisare_swa</i>	Mapped dimension of swamp on the Bisare River.
<i>Chebe_orm</i>	Mapped obsidian raw material outcrop.
<i>FulusaKebele_orm</i>	Mapped obsidian raw material outcrop.
<i>MtDamota_cat</i>	Calculated catchment grid of Mount Damota; derived from generated digital elevation models.
<i>MtDamota_cat_dr</i>	Calculated drainage network within the catchment of Mount Damota.
<i>MtSodicho_cat</i>	Calculated catchment grid of Mount Sodicho; derived from generated digital elevation models.
<i>MtSodicho_cat_dr</i>	Calculated drainage network within the catchment of Mount Sodicho.
<i>MtSodicho_ormA</i>	Mapped obsidian raw material (fluvially transported).
<i>MtSodicho_ormB</i>	Mapped obsidian raw material (fluvially transported).

## Chapter III

### **3. Stratigraphy and Chronology of Sodicho Rockshelter – A New Sedimentological Record of Past Environmental Changes and Human Settlement Phases in Southwestern Ethiopia**

Elena A. Hensel<sup>1</sup>, Ralf Vogelsang<sup>2</sup>, Tom Noack<sup>3</sup>, Olaf Bubenzer<sup>4</sup>

1 Institute of Geography, University of Cologne, Cologne, 50923, Germany

2 Institute of Prehistoric Archaeology, University of Cologne, Cologne 50923, Germany

3 Institute of Geography & Heidelberg Center for the Environment (HCE), Heidelberg University, Heidelberg 69120, Germany

Published in *Frontiers in Earth Science* 8(640), 1–20, 2021

doi: <https://doi.org/10.3389/feart.2020.611700>

Special Issue: *Integrating Paleoclimate, Stratigraphy, Sedimentology & Paleontology in Human Evolution and Dispersal Studies - from Early Hominins to the Holocene*

Keywords: geoarchaeology, radiocarbon, stratigraphy, sedimentology, geochemistry, Late Pleistocene, Holocene, African Humid Period.

Note: The following pages originate from the original peer-reviewed article published at *Frontiers Earth Science*.



# Stratigraphy and Chronology of Sodicho Rockshelter – A New Sedimentological Record of Past Environmental Changes and Human Settlement Phases in Southwestern Ethiopia

Elena A. Hensel<sup>1\*</sup>, Ralf Vogelsang<sup>2</sup>, Tom Noack<sup>2</sup> and Olaf Bubenzer<sup>3</sup>

<sup>1</sup>Institute of Geography, University of Cologne, Cologne, Germany, <sup>2</sup>Institute of Prehistoric Archaeology, University of Cologne, Cologne, Germany, <sup>3</sup>Institute of Geography and Heidelberg Center for the Environment (HCE), Heidelberg University, Heidelberg, Germany

## OPEN ACCESS

### Edited by:

Christian Zeeden,  
Leibniz Institute for Applied  
Geophysics (LIAG), Germany

### Reviewed by:

Alvise Barbieri,  
University of Algarve, Portugal  
Andrea Zerboni,  
University of Milan, Italy

### \*Correspondence:

Elena A. Hensel  
elena.hensel@uni-koeln.de

### Specialty section:

This article was submitted to  
Quaternary Science, Geomorphology  
and Paleoenvironment,  
a section of the journal  
Frontiers in Earth Science

**Received:** 29 September 2020

**Accepted:** 19 November 2020

**Published:** 14 January 2021

### Citation:

Hensel EA, Vogelsang R, Noack T and  
Bubenzer O (2021) Stratigraphy and  
Chronology of Sodicho Rockshelter –  
A New Sedimentological Record of  
Past Environmental Changes and  
Human Settlement Phases in  
Southwestern Ethiopia.  
*Front. Earth Sci.* 8:611700.  
doi: 10.3389/feart.2020.611700

The preservation of archaeological remains and environmental information in a sediment accumulation can vary in caves and rockshelters, depending on external climatic conditions, and the circumstances within the shelter. Several sediment stratigraphies in the Horn of Africa are characterized by erosion layers, discordances and chronological gaps, that create uncertainties about the impact of climatic and environmental shifts on human settlements. Archaeological sites in Ethiopia that preserve information about human occupation during the Upper Pleistocene and Holocene often deal with major gaps during a period corresponding to MIS 2. In this study we present the first results of sedimentological, geochemical analyses and radiocarbon dating at Sodicho Rockshelter (1930 m above sea level) that provide evidence on high altitude settlement during this mentioned chronostratigraphic gap and subsequent time slices. This new archaeological site in the southwestern Ethiopian Highlands hosts a 2-m-long sediment record. So far, a stratigraphy has been excavated that dates back to ~27 ka, including several settlement phases of Late Pleistocene and Holocene hunter-gatherers and providing information on environmental changes. A multiproxy approach was chosen to establish a first general stratigraphy of the site and to disentangle the sediment composition as well as site formation processes. The results suggest a variation of allochthonous and autochthonous geogenic deposits, and anthropogenic accumulation processes. With the help of radiocarbon dating, anthropogenic layers were dated covering the arid Last Glacial Maximum (LGM, ~21 ± 2 ka). The occupation phases were interrupted in cause of environmental changes. The most prominent is the accumulation of reddish, archaeological sterile deposits that can be chronologically associated with the African Humid Period (AHP, ~15–5 ka BP). Geochemical records point to dry spells within this humid phase, suggesting correlations with regional climate signals of lacustrine sediments. These sediment accumulations of past wet conditions are covered by alternating layers of Holocene volcanic fallout and sediments with preserved cultural material. Our study

provides a preliminary impression of still poorly understood time periods of human occupation in the southwestern Ethiopian Highlands. The data obtained from Sodicho Rockshelter could validate the current state of knowledge and partially reduce the chronostratigraphic gap.

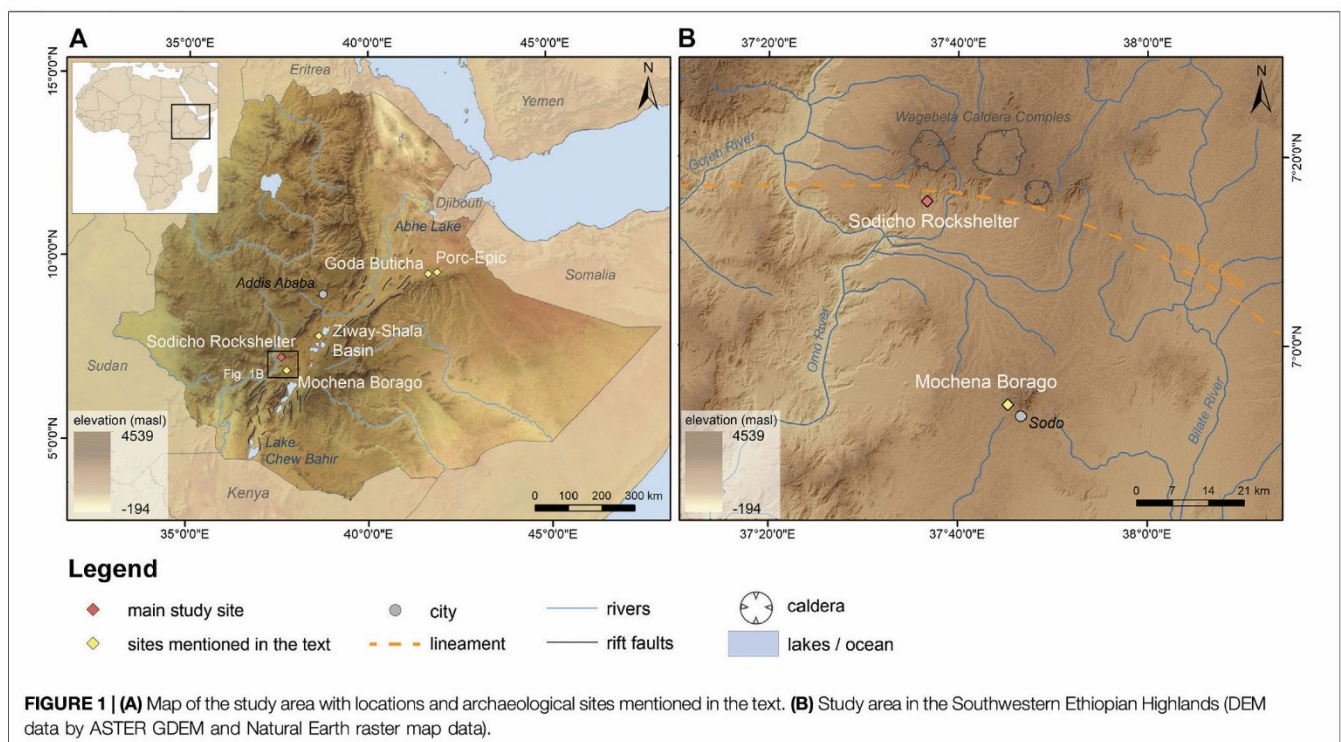
**Keywords:** geoarchaeology, stratigraphy, sedimentology, geochemistry, late pleistocene, holocene, african humid period, radiocarbon dating

## INTRODUCTION

The development of a sediment stratigraphy within a rockshelter setting is driven by diverse sediment origins and changing conditions of the regional environment, including human agency. The different sediment sources, e.g., geogenic (autochthonous and allochthonous), anthropogenic, and biogenic often result in a diverse, intermitted deposition. Like caves, rockshelters function as a sediment trap, however, they are often partly or completely exposed to weather conditions, which in turn explains the variability in deposition. The prehistoric humans used these places as natural shelters (Mentzer, 2017). The use of caves and rockshelters by prehistoric humans has been part of geoarchaeological research in several regions, such as southern and northern Africa, Europe or the Levant (Goldberg and Bar-Yosef, 1998; Goldberg et al., 2009; Marean et al., 2010; Miller et al., 2013; Kehl et al., 2014; Klasen et al., 2018; Inglis et al., 2018). The studies investigated the natural forces contributing to deposition of sediment and the active modification of sediment structures by human activities (e.g., fireplaces, trampling and bedding) (Goldberg et al., 2009; Miller et al.,

2013). Deposits can be altered, masked or even erased from the sedimentary record by post-depositional processes, resulting in gaps of knowledge and uncertainties leading to rather short and discontinuous archaeological sequences (Kuehn and Dickson, 1999). In the Horn of Africa, especially in Ethiopia, these gaps in stratification are quite common. In most cases, they correlate with the transition from the Middle Stone Age (MSA) to the Late Stone Age (LSA) during the period of the MIS 2 (Tribolo et al., 2017). Several studies at sites such as Goda Buticha, the Ziway-Shala basin and Mochena Borago identified a stratigraphical and a chronological gap, spanning from ~38 ka and reaching into the Holocene (Figure 1A) (Tribolo et al., 2017).

Although terrestrial paleoenvironmental records are very scarce in Ethiopia, they provide a useful source for the reconstruction of past varying environmental conditions. Lacustrine sediments from Ethiopian and Kenyan lakes refer to hyper arid conditions during the Heinrich Events (H) and the Late Glacial Maximum (LGM, ~21 ± 2 ka), followed by overall moist conditions of the African Humid Period with intermediate dry spells (Mark and Osmaton, 2008; Junginger and Trauth, 2013; Foerster et al., 2015). Higher



moisture availability in the highlands could have permitted the survival of vegetation, animals and humans during the arid phases. In this case, rockshelters in high altitude regions might have attracted hunter-gatherers, despite the challenging conditions for human physiology (Foerster et al., 2015; Vogelsang and Wendt, 2018).

Sodicho Rockshelter is located about 40 km NW from the aforementioned Mochena Borago Rockshelter site, which is one of the archaeological key-sites in northeastern Africa and shares a comparable well-structured sedimentological and archeological sequence (Brandt et al., 2017; Hensel et al., 2019). With this study we introduce preliminary results of geoarchaeological and archaeological investigations of Sodicho Rockshelter and relate the results to regional climatic records. We attempt to reconstruct geogenic and biogenic site formation processes and to compare them to the cultural induced processes. The aim of this study is 1) to determine the sediment composition, 2) to reconstruct the site formation processes in the shelter, 3) to develop a first  $^{14}\text{C}$  chronology and 4) put the human occupation in the context of the geoarchaeological results.

## BACKGROUNDS

### Geoarchaeological Research

Until now, the most important rockshelter in the southwestern Ethiopian Highlands is Mochena Borago on Mount Damota. Since 1998, several research teams investigated almost 2 m of stratified Holocene and Late Pleistocene deposits. The latter preserved cultural remains dating between 36 and >50 ka (Gutherz et al., 2002; Fisher, 2010; Brandt et al., 2012; Brandt et al., 2017). In 2009 the Collaborative Research Center 806 (CRC 806, <http://www.sfb806.uni-koeln.de>) joint the investigations of Steven Brandt (Southwest Ethiopia Archaeological Project) at Mochena Borago. Geoarchaeological research at Mochena Borago aimed to reconstruct site formation processes with the help of geomorphological investigations and micromorphological observations (Brandt et al., 2017). During archaeological and geomorphological surveys in the surroundings, Sodicho Rockshelter was first visited in 2012 (Brandt et al., 2017; Vogelsang and Wendt, 2018; Hensel et al., 2019). Further research in the area focused on the exposure of archaeological records along the valleys of the Bilate River and its tributary the Bisare River, southwest of Mt. Damota. According to the studies, abundant archaeological material occurs in sediments, that are exposed by badland formation. These badlands are not older than 200 ka and hold mostly MSA and LSA obsidian artifacts. However, some sites also hold artifacts that show characteristics of the late Early Stone Age (ESA) (Benito-Calvo et al., 2007; De la Torre et al., 2007). Geomorphological-hydrological analyses around Mt. Damota and Mt. Sodicho revealed that the region is influenced by a very dynamic system of permanent and episodic river networks. The resulting soil erosion and the exposure and destruction of archaeological open-air sites and raw material outcrops emphasizes the importance of protected rockshelter

stratigraphies and their potential to preserve archaeological deposits and environmental information (Hensel et al., 2019).

### Geology, Geography, Climate and Vegetation of Study Area

Sodicho Rockshelter is located E 37°36'44 and N 7°15'21 in the southwestern Ethiopian Highlands. The cavity opens to the south and is situated at the slopes of Mount Sodicho at an elevation of about 1930 m above sea level (Hensel et al., 2019). The complex tectonic and volcanic structures of the Main Ethiopian Rift are situated to the west. To the east lies the deep canyon of the Omo River (Figure 1B). The mountain itself consists of a greyish to yellowish trachyte, and is part of a series of silicic domes, lavas and tephra that lie ~8 km south of the three circular Wagebeta Calderas. The past volcanic formations date back 3.6 to 4.2 Ma into the Pliocene and during the late phase of the rift system development in Ethiopia (WoldeGabriel et al., 1990; WoldeGabriel et al., 1992; Chernet, 2011; Hensel et al., 2019). The volcanic formations are aligned along the transverse east-west Goba-Bonga lineament, a depression that crosses the center of the Main Ethiopian Rift (Bonini et al., 2005; Corti, 2009; Corti et al., 2013). The present appearance of the area is shaped by Late Pleistocene to Holocene tectonic stress, climatic, and geomorphological changes (Benito-Calvo et al., 2007). A network of episodic and permanent streams drains down the slopes of Mt. Sodicho toward the Omo River, creating the mountain's characteristic irregular shape. The increased human influence during the last decades is visible by cleared slopes for cultivation and cattle farming (Hensel et al., 2019). The major soil type is the kaolinite rich, red colored Humic Nitisol, a fertile soil type, common in the humid tropics (Berhanu et al., 2013; IUSS Working Group WRB, 2014). The modern climate in the southwestern Ethiopian Highlands is a complex and variable system that is characterized by two rainy seasons with an average precipitation of about 2,000 mm per year. Over 50% of the annual rain in the SW Ethiopian Highlands falls in course of the "Kirmet", the main rainy season during the boreal summer (June to September). During the months November to February the region experiences the dry period with an average <50 mm per month, followed by a second weaker rainy season, the "Belg" (Fisher, 2010; Brandt et al., 2012; Hildebrand et al., 2019). These annual and inter-annual precipitation changes are connected to the interaction of the moist summer monsoon and the dry northeastern "Harmattan" wind system, resulting in changes of the north-south directed pressure gradient (Viste and Sorteberg, 2013; Nicholson, 2018). Further influences on the annual precipitation are associated with changes in sea surface temperature (SST) of the Indian Ocean, the northern shifting tropical rain belt, low-level convergences, and the Congo Air Boundary in lesser relevance (Griffiths, 1972; Segele et al., 2009; Tierney et al., 2011; Junginger and Trauth, 2013; Viste and Sorteberg, 2013; Nicholson, 2018).

Up to now, only the last 45 ka are analyzed from a drilling core in the Chew Bahir basin, which is situated ~300 km from Mount Sodicho. Its catchment area runs through the SW Highlands, which means that Chew Bahir was also affected by climatic

conditions prevailing in the highlands. According to sedimentological and geochemical investigations of these lake sediments, the past climate in the southwestern highlands has undergone arid and humid phases. A rather moist phase from 45 to 35 ka BP was followed by arid conditions (Foerster et al., 2012). During the cold and arid Marine Isotope Stage 2 (MIS 2, ~29–12 ka BP), lake levels and river catchments changed, which influenced the surrounding habitat of flora and fauna (Foerster et al., 2012; Foerster et al., 2015; Stewart and Jones, 2016). The aridity ended after 15 ka with an increase in humidity. This indicated the beginning of the Early Holocene African Humid Period, which stretched out until 5 ka and was interrupted by shorter dryer periods (Foerster et al., 2012; Foerster et al., 2015; Hildebrand et al., 2019; Trauth et al., 2019).

## MATERIALS AND METHODS

### Fieldwork and Archaeological Excavation

The excavations at Sodicho Rockshelter were conducted annually from 2015 to 2018. Of two 50 × 50 cm test pits in 2015, one was extended to an excavation trench with an area of four square meters, each split into 50 × 50 cm quadrants that were excavated individually (Figure 2C, F34/35 and G34/35). Big boulders stopped the extension of the second test pit (Figure 2C, E41), which was located in one of the cavities at the rear wall of the shelter. Both trenches are situated in backward areas that seem to be well protected from humidity, in terms of dripping water and trickle. Archaeological excavations followed natural stratigraphic boundaries, subdivided vertically into arbitrary spits with a maximum thickness of 5 cm. Spits never transversed natural stratigraphic boundaries, i.e. a spit definitely ended when visible sediment changes were observed during excavation. Specific archaeological features, such as hearths or pits, were excavated in the same way but separately from the surrounding matrix. No total station was available during the first fieldwork in 2015. Therefore, the grid system of the test pits was set up with measuring tapes and leveling taken with a surveyor's level. Archaeological finds of the test pits were recovered via dry sieving in three stages, using mesh widths of 10, 5, and 2.5 mm. The closest spatial allocation of these finds is to one of the artificial spits. During the subsequent excavations all archaeological finds >5 mm were single plotted using a Leica TS02 total station and provenience information such as grid unit, depth, level and stratum, as well as material type (e.g., stone, bone, charcoal) were recorded. Each find was then bagged individually and assigned a unique identification number. The excavated sediments were dry sieved to recover smaller finds using 10-, 5-, and 2.5-mm mesh size. The total station was also employed to map each stratum, feature or natural disturbance as it was exposed, and forms recorded information on sedimentology, spatial and vertical configurations and other relevant data. In addition, plan views of each excavation spit and stratigraphic profiles were mapped on grid paper and recorded with digital photographs. The geoarchaeological fieldwork included on-site observation with an analysis of the sediment deposits (Supplementary Table S1) and a classification of the common

lithological composition of the bedrock in the rockshelter itself. Furthermore, several half-day surveys along the mountain flanks of Mt. Sodicho were undertaken to identify lithological changes of bedrock and geomorphological conditions of the area.

### Multiproxy Sediment Analyses

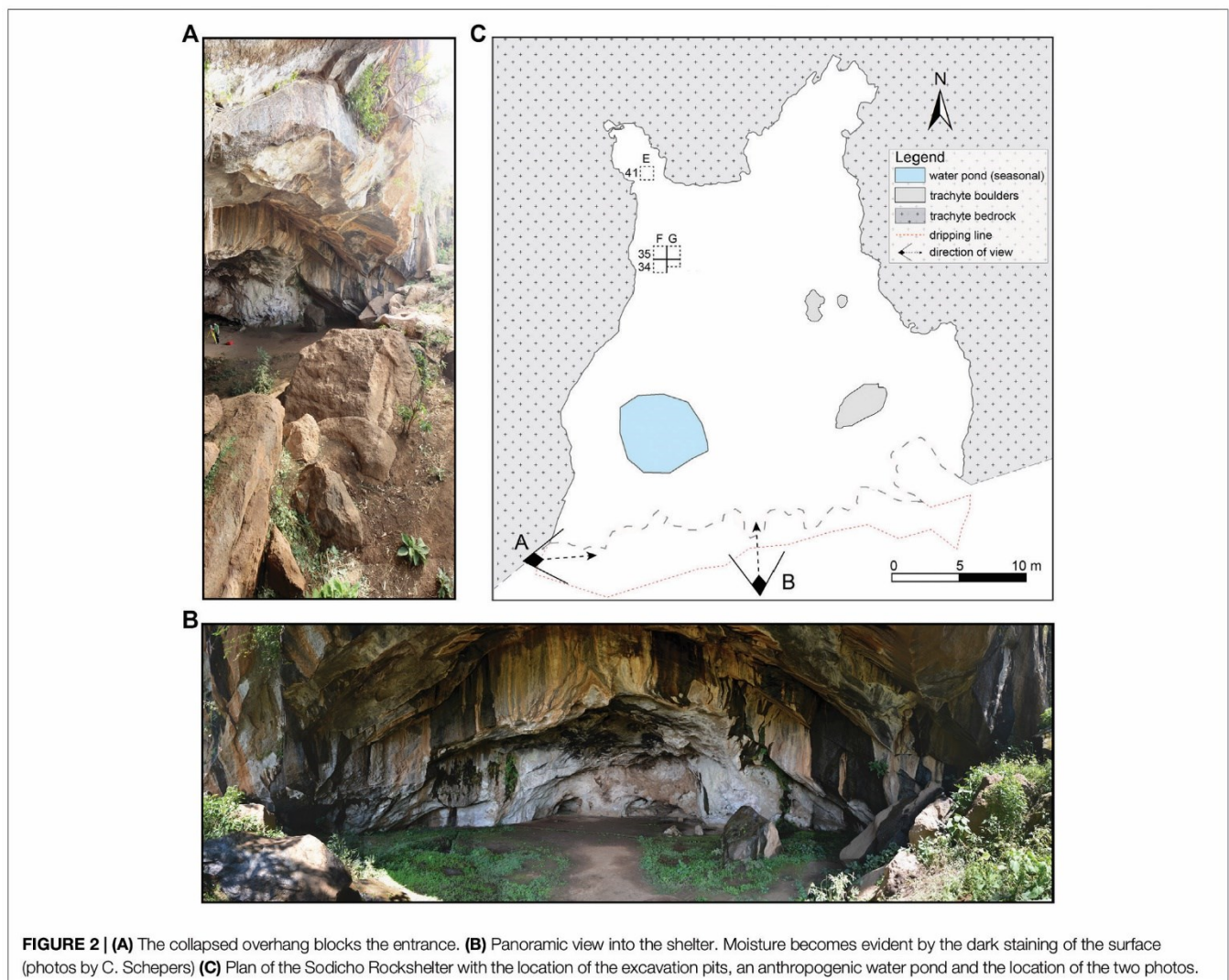
Bulk sediment samples were determined with a 2 cm resolution at the west facing profile from square F35 and the south facing profile from square G35 (Figure 3). Lower sediment samples were taken from square G35 because collapsed blocks in F35 hindered further sampling in this square. Both sample columns overlap by approximately 30 cm. The sample thickness was increased to 4 cm in layers of difficult access, e.g., around bigger rocks. As a pre-treatment the samples were dried at 40°C in a drying chamber and sieved to remove material >2 mm.

The granulometry was determined with a Laser Diffraction Particle Size Analyzer (Beckmann Coulter LS13 320, Beckmann Coulter, Inc.) and pretreated with hydrogen peroxide (H<sub>2</sub>O<sub>2</sub> 15%) to remove organic opal. In addition, several reference samples were treated with hydrochloric acid (HCl 10%) to remove organic and inorganic carbon. Prior to the measurements, Na<sub>2</sub>PO<sub>5</sub> (46 g/L) was applied to all samples to avoid coagulation. The results were evaluated and statistically measured with the GRADISTAT software version 8 (Blott and Pye, 2001) and the parameters are based on Folk and Ward (1957).

Sediment color was measured with a VIS spectrophotometer (Konica Minolta CM-5) to determine the reflected wavelength from the sample in a visible range of 360–740 nm and converted into L\*a\*b\* values (Eckmeier and Gerlach, 2012). The L\*a\*b\* values express the extinction of light in the spectra from absolute black (L\*0) to absolute white (L\*100) and the color ranges from green to red (a\* to +a\*) as well as from blue to yellow (b\* to -b\*). The redness index (RI) was calculated applying the L\*a\*b\* variables according to Barrón and Torrent (1986)  $RI = \frac{a^* (a^{*2} + b^{*2})^{1/2}}{b^* L^{*0}}$ .

The mass specific magnetic susceptibility was determined by using a Bartington MS2 Magnetic Susceptibility System with a MS2k sensor and measured twice under laboratory conditions on the sieved and weighed in samples. For further geochemical investigations a part of the material was grinded with a vibrating zircon ball mill (Mixer Mill MM 400, Retsch). The total carbon content (TC) was measured with a vario EL cube (Elementar Analysensysteme GmbH). In addition, the total organic carbon (TOC) content was measured on a few reference samples after a pretreatment of HCl (10%).

For the determination of the major and trace elemental composition two methods using X-ray fluorescence (XRF) were applied. First, all grinded samples were measured with a handheld Niton™ XL3t XRF Analyzer (Thermo Scientific™) under laboratory conditions, viz. samples were pressed in pellets and measured twice in a test stand. This method has the advantage that many samples can be measured relatively quickly and easily after a relatively complex preparation. However, studies with a portable XRF devices (pXRF) have shown that the spectrometer cannot properly measure elements like phosphorous (Hunt and Speakman, 2015).



Therefore, to verify the results of the pXRF analyzer, and to derive geochemical indicators for alteration and weathering a selection of the samples were measured at the Institute of Physical Geography and Geoecology at the RWTH Aachen. Here the grinded samples were also pressed to tablets and measured twice with the SPECTRO XEPOS energy dispersive X-ray fluorescence spectrometer (Spectro). The resulting elements and oxides were then chosen as representing indicators for depositional changes. A chemical index of alteration (CIA) was calculated according to the calculations of Nesbitt and Young (1982):  $CIA = \left[ \frac{Al_2O_3}{Al_2O_3 + Na_2O + K_2O + CaO} \right] \times 100$ .

### Age Determination

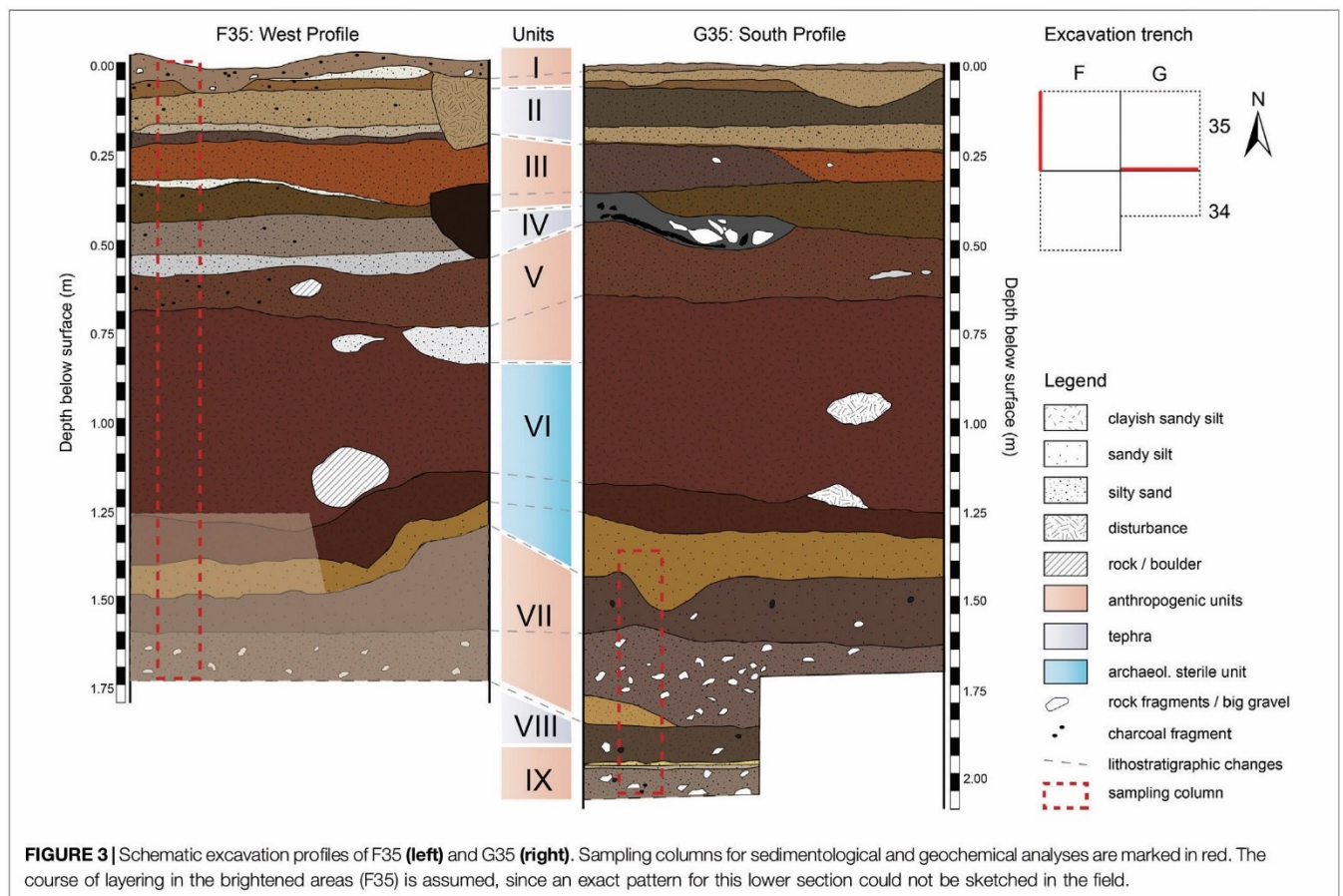
A total of 31 samples were collected in the squares F34, F35, and G35 during the excavations in 2015 to 2018 (Figure 2). The radiocarbon AMS lab Beta Analytics Limited analyzed 28 samples of seeds and charcoal. Additionally, two charcoal and one soot sample, the latter scratched from the besmoked outer face of a cooking pot sherd, were measured at the AMS laboratory of the University of Cologne. The results were calibrated with Calib8.10.

using the IntCal20.<sup>14</sup>C curve (Reimer et al., 2020). A classic age depth model was established with the clam2.3.5 package in RStudio according to Blaauw (2010). In the model the radiocarbon ages were calibrated with the northern hemisphere terrestrial calibration curve IntCal20.<sup>14</sup>C.

## RESULTS

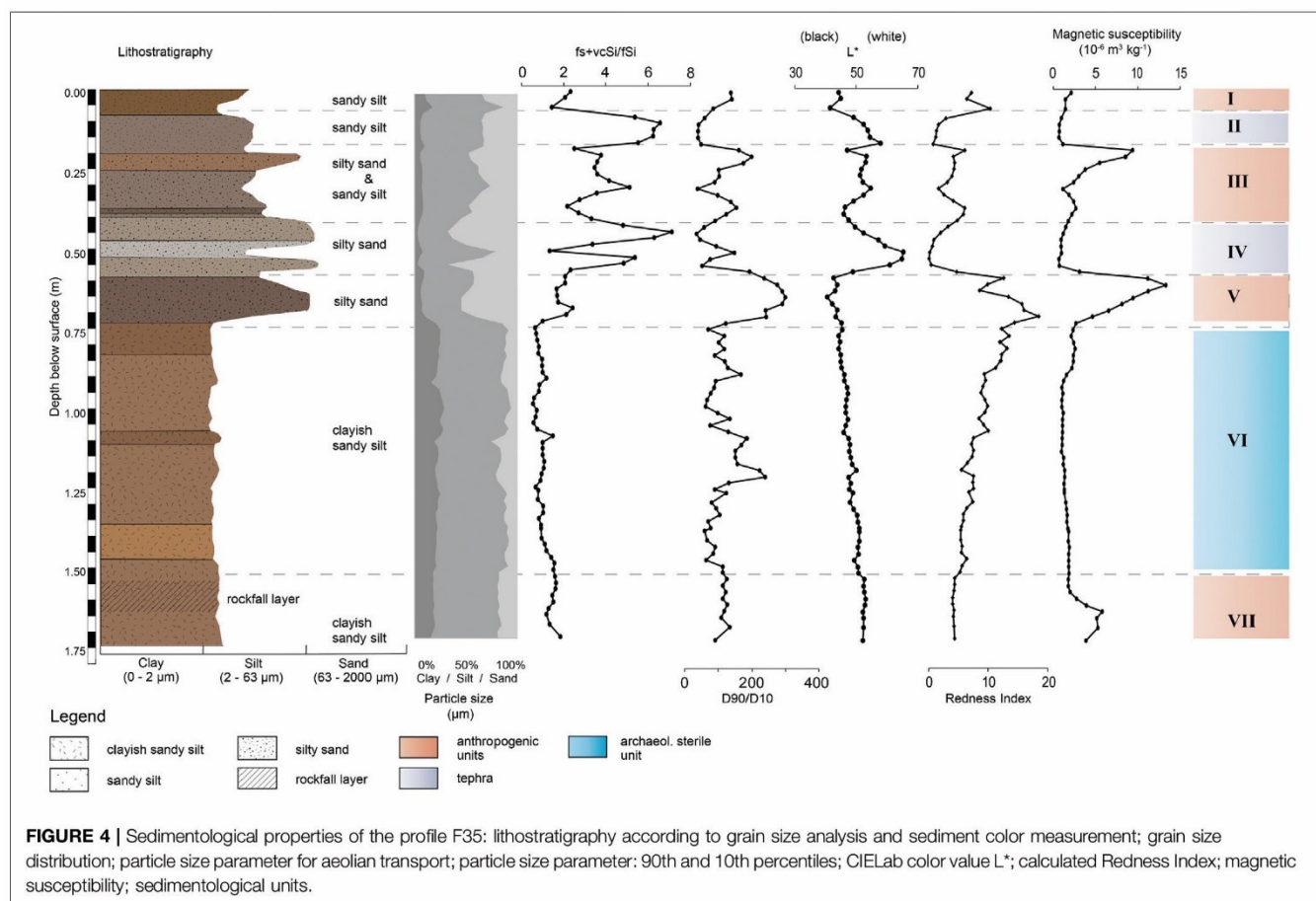
### Field Observations at the Sodicho Rockshelter

The south facing opening of the rock shelter is almost completely protected by big trachytic boulders (2 diam.) that originate from the partial collapse of the originally larger front overhang (Figure 2A). This hinders the direct influence of precipitation and fluvial weathering into the flat shelter. However, the blocking rocks cause a slight downward slope into the shelter. The sediment accumulation therefore differs spatially, which in turn can influence the characteristics of certain sediment layers, like deposit thickness. The interior



of Sodicho Rockshelter is characterized by the effects of moisture, which seeps through cracks in the ceiling and the walls, generating dark staining on the rock surface, and creating shallow pools and drip holes with stagnant water during wet seasons (Figure 2). A larger water pond in the western entrance area was dug by the local population living there. Big boulders and blocks in the south eastern corner are rounded by water dripping down the roof. Low growing plants and shrubs cover certain parts of the floor and grow along fissures at the rock shelter walls. During dry season the rock shelter can dry up almost completely. Apart from the dark staining at the walls and ceiling the trachyte differs in color, crystallization and softness within the shelter. The western wall is characterized by a pale gray trachyte with a rather crumbly matrix due to granular disintegration. Distinct alveolar weathering (honeycomb weathering) is common and parts of the walls show flaking of the rock surface and uneven exfoliation of the rock surface, which creates curved surfaced boulders. The color of the trachyte changes toward the eastern wall to a mustard yellow with well-crystallized and colorless potassium feldspar minerals. Several overhangs along the rock shelter walls are darkened by soot caused by human-induced burning. A low and narrow cavity in the north eastern back is extremely stained by fire activity. The lower ceiling has obtained a shiny, greasy surface due to the close fire exposure.

First observations during excavation revealed a complex stratigraphy with distinguishable sediment units and prominent boundaries. Some of the sediment units (Unit I, III, V, VII and IX) correspond to archaeological layers, that contain cultural material, such as obsidian artifacts and charcoal, and human-made structures, such as pits and hearth. A 60 cm thick sterile sediment deposit roughly divides the deposits and associated human occupation phases into two parts. In the upper part of the stratigraphy, the anthropogenic units alternate with lighter-colored geogenic units identified as tephra. The boundaries between these units are not uniform. Whereas the boundary between a cultural layer and an overlying tephra is sharp (e.g., between Units V and VI or between III and II), the transition between a cultural layer to a subjacent tephra seems gradual (e.g., between Units IV and III or between Units II and I). The tephra layers are exclusively of geogenic origin and therefore cultural remains are absent. Intermixing only occurs when the volcanic deposits have been relocated or disturbed by subsequent construction of pits or hearths. The lower part of the stratigraphy, below the thick sterile unit, is characterized by a large rockfall deposit, followed by anthropogenic deposits and geogenic deposits. The different layers in the lower section of the stratigraphy are difficult to distinguish, due to gradual or unclear layer boundaries and even mixing of the layers. Bioturbation can be recognized sporadically as insect or rodent



borrows in all units. There is no macroscopic evidence of rooting by plants in the excavated stratigraphy. A detailed description of each unit, with its most important components can be found in the **Supplementary Table S1**.

### Multiproxy Sediment Analyses

Macroscopic investigations of the 2 m stratigraphy revealed a complex interplay of cultural layers with light colored tephra and a 60 cm thick sterile sediment deposit. With the help of sedimentological and geochemical analysis nine sedimentological units (I–X) can be systematically differentiated.

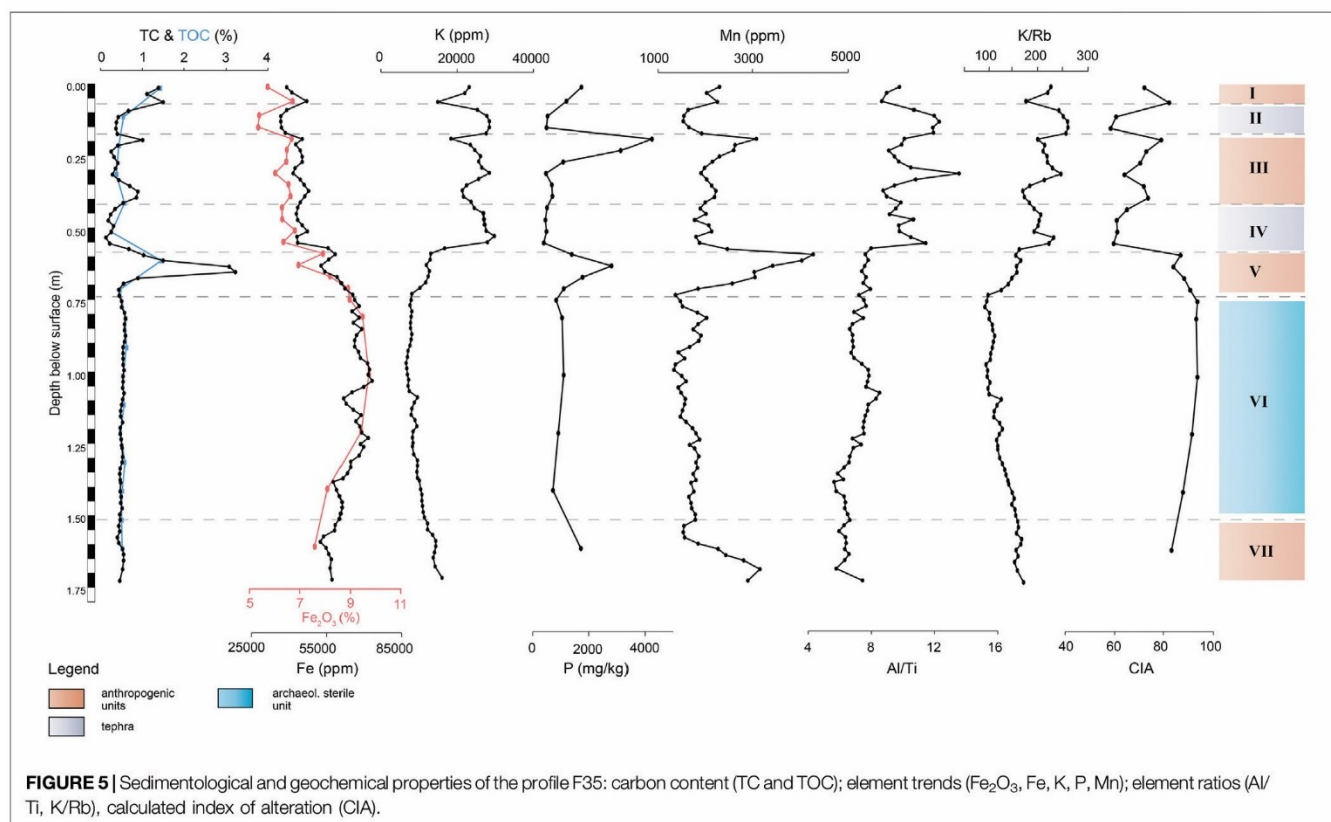
#### Profile F35

We measured all sediment samples with a grain-size analyses to investigate changes in particle size distribution through the whole stratigraphy. It turns out that (sandy) medium to coarse silt is the omnipresent mean fraction, although the (silty) fine sand content is increased in several layers of the upper (0.00–0.73 m) profile section. The grain size peaks in Unit IV and V. The graph in **Figure 4** shows that the clay content increases suddenly within the sterile layer of Unit VI. According to the statistical analyses, the sample curves show a bi- and polymodal distribution and overall very poor sorting. The amount of the grain size fractions that corresponds to aeolian transport, e.g., fine sand and very coarse silt (40–125  $\mu\text{m}$ ), ranges from 9 to 41% with peaks in Unit

II and IV. Within these layers the ratios of 90th to 10th percentiles are low, resulting in a better sorting (Kehl et al., 2014).

Comparing these results of the granulometric analyses with the samples in which the carbonate was previously destroyed (by means of HCl 10%), little change in the particle size distribution can be detected (**Supplementary Figure S1**). The peak within Unit V is also verified. Only the samples within the sterile Unit VI show a slightly different behavior to the samples which were exclusively sampled with  $\text{H}_2\text{O}_2$ . Nevertheless, the main grain size fraction remains sandy medium silt to sandy coarse silt.

Using VIS spectrophotometer to analyze the color of the dried and powdered sediment, significant color changes in the upper part of the sediment column are obvious. Shades of dark brown alternate with lighter gray colors and more intense red-brown colors. In **Figure 4** the lighter shades of Units II and IV are particularly prominent, which are accompanied by an increase in the  $L^*$  values and a decrease in the  $a^*$  and  $b^*$  values (**Supplementary Figure S1**). The  $a^*$  value peaks in Unit V and in the upper part of Unit III, which could also be observed in the field. Especially this part of Unit III appeared brick-red under the prevailing lighting conditions inside the excavation trench. The values of the redness index (RI) corresponds to the  $a^*$  values and the iron content within the sedimentary sequence. It also illustrates the decrease of iron oxides within Unit VI.



Magnetic susceptibility (MS) was measured in order to identify signals of human induced burning. The peak values are found in Unit III, V and VII, where archaeological finds are concentrated. Also, the darker color of the sediment, e.g., decreased values of the  $L^*$  curve, correspond to higher magnetic susceptibility. The minimum values are found in Unit II, IV, VI and the lower part of Unit III.

The carbonate content in the samples varies strongly in the upper part of the profile and peaks within Units I, III and especially in Unit V. Within the lower section of the profile the amount remains relatively constant at around 0.5%. The measured TOC content shows minor deviations from the TC curve, thus it can be expected that little or no carbonate was precipitated after sedimentation (Figure 5).

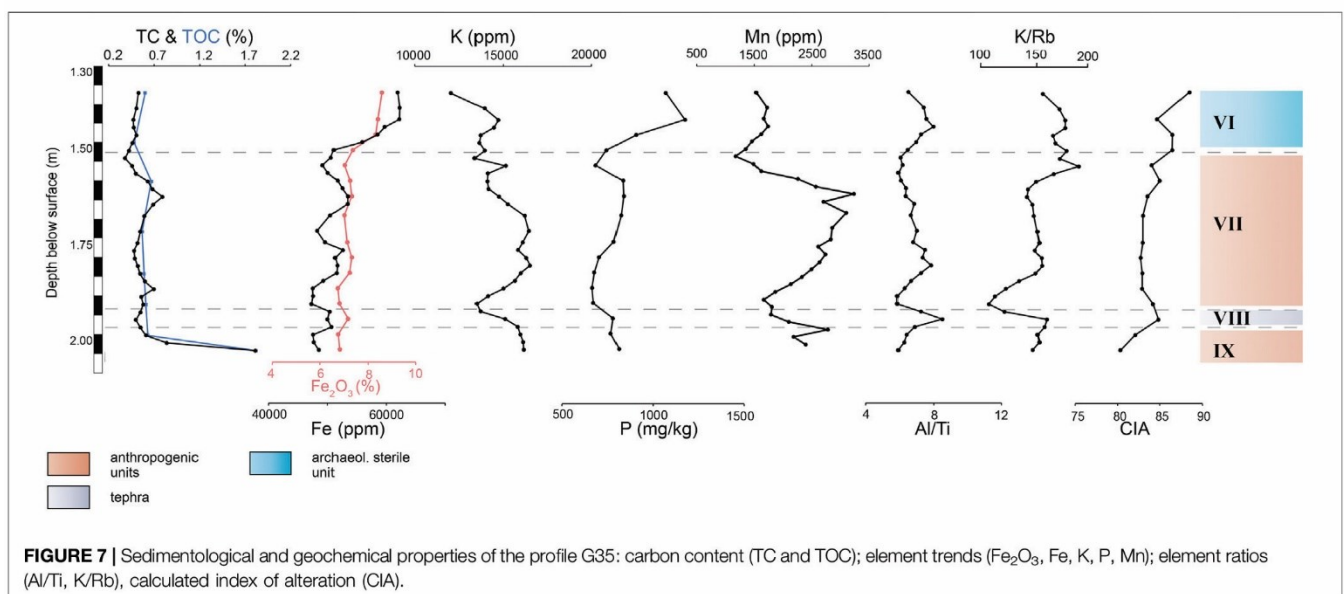
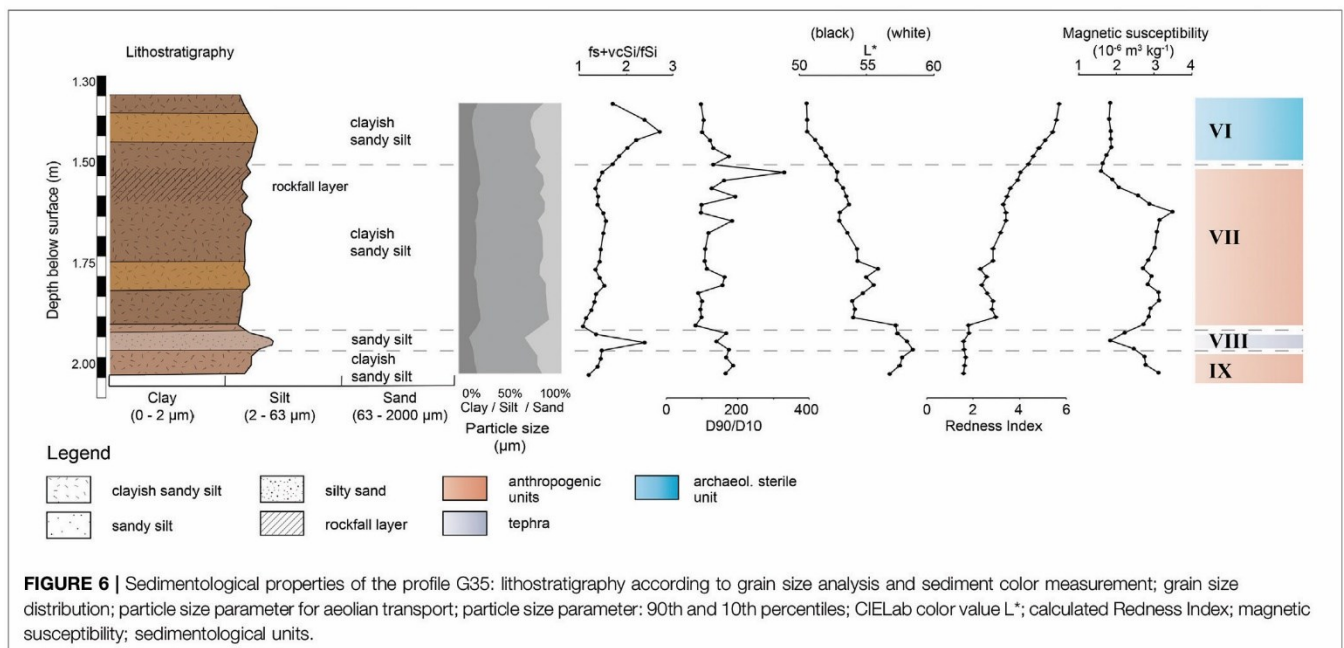
An XRF analysis allows the detection of several counted elements present in the samples, but only a selection of the results is considered in this study. Figure 5 illustrates that Iron (Fe), one of the most common trace elements on earth, shows relatively low values in the upper profile part. With the beginning of the Unit VI the Fe counts and the Iron (III) oxide ( $\text{Fe}_2\text{O}_3$ ) percentage amount rise. The elements aluminum (Al) and titanium (Ti), often used as indicators for stronger weathering, show a similar course with enrichment in the sterile clayish Unit VI (Supplementary Figure S1). Diametrical to this are the curves of mobile alkali metal potassium (K), rubidium (Rb) and halogen chlorine (Cl), which are abruptly depleted in Unit VI. Peak values are found

in Units II, IV and in the middle part of Unit III. The light element Silica (Si) is enriched within the same units in the upper part of the profile. The values of calcium (Ca), strontium (Sr), phosphorus (P) and manganese (Mn) are elevated in the Units III, V and VII which represent anthropogenic layers (Figure 5).

Selected element ratios, as Al/Ti and Fe/Al indicate major changes in the source areas of the deposits. Following the graphs in Figure 5 and Supplementary Figure S3 the Units II, IV and the middle of Unit III that can be characterized as volcanic ash with higher ratios of Al/Ti and Fe/Al. In contrast, Unit VI differs by very low values. According to the ratios of mobile to less mobile elements, e.g., between K/Ti and K/Rb, the lower section of the profile reflects changes into a regime with increased weathering (Brown, 2011; Arnaud et al., 2012; Kehl et al., 2014; Kehl et al., 2016). The calculated chemical index of alteration (CIA) peaks in the lower Unit VI of the profile. The resulting graph of the Mn/Fe ratio in Supplementary Figure S3 shows an increase in the anthropogenic Units I, III and V.

### Profile G35

The lower examined section in square G35 consists of the sedimentological Units VI to IX. The granulometric analyses and statistical analyses points to a tri- and polymodal grain size distribution as well as a very poor sorting throughout all the samples. (Sandy) medium silt is the dominant mean fraction within the whole sample column with variations of very fine sandy medium silt to medium and coarse silt. The exception



are two peaks within Unit VI and Unit VIII where the grain size is slightly higher. In addition, there is an increased proportion of the grain sizes fine sand and coarse silt (40–125  $\mu\text{m}$ ) which can be associated to an aeolian origin (Figure 6) (Kehl et al., 2014). The samples with this specific grain size range also show low ratios of the 90th and 10th percentiles and therefore a higher sorting.

The analyses of the sediment color show insignificant changes from brown to light brown. With increasing depth, the luminance ( $L^*$ ) increases and the red tones ( $a^*$ ) decrease (Supplementary

Figure S2). During the field work the lower sediment sequences were described as reddish due to the limited daylight inside the shelter and the high moisture of the sediment. Actually, the calculated redness index in Figure 6 illustrates a slow decrease of the values with increasing depth, which are synchronous to the Fe and  $\text{Fe}_2\text{O}_3$  values.

The magnetic susceptibility shows increased values in the upper part of Unit VII and in the lower most Unit IX that is an anthropogenic layer. The values peak in the settlement layers, but generally less pronounced as in the profile F35.

**TABLE 1** | Radiocarbon ages for samples from Sodicho Rockshelter, arranged by archaeological excavation units.

Lab code	Excavation unit (square-quarter-level)	Specimen	S.Unit	Conventional <sup>14</sup> C-date [BP]	Calibrated <sup>14</sup> C age range (2σ) [cal BP] IntCal20.14c	Prob. (%)	δ <sup>13</sup> (‰)	Sample depth [cm b.s.]
Beta-449167	F34-SW-02	Charcoal	I	250 ± 30	<b>270–322</b>	56	–27.9	8
Beta-449166	F34-NW-02	Charcoal	I (pit)	350 ± 30	<b>315–411</b>	59	–24.8	11
COL3149.1.1	F35-SW-06	Soot	III	1944 ± 46	<b>1,741–1,948</b>	93	–26.1	excl.
COL3150.1.1	F35-SW-07	Charcoal	III	1806 ± 42	<b>1,685–1,824</b>	59	–24.1	excl.
Beta-449168	F34-NW-10	Charcoal	III (pit)	2,130 ± 30	<b>1,999–2,153</b>	88	–25.7	48
Beta-486041	G34-NW-11	Charcoal	V (hearth)	3,860 ± 30	<b>4,227–4,407</b>	84	–25.0	44
Beta-449169	G35-NE-15	Charcoal	V	3,920 ± 30	<b>4,242–4,424</b>	99	–26.4	56
COL3153.1.1	F35-SW-14	Charcoal	V	4,054 ± 45	<b>4,418–4,647</b>	88	–27.2	excl.
Beta-449170	G35-NE-18	Charcoal	V	4,060 ± 30	<b>4,422–4,621</b>	92	–24.9	69
Beta-450067	F34-NE-18	Seed	V	4,190 ± 30	<b>4,617–4,765</b>	74	–21.7	69
Beta-449171	G35-NE-19	Seed	V	4,130 ± 30	<b>4,567–4,729</b>	64	–23.3	77
Beta-449175	G35-NE-20	Seed	V	4,160 ± 30	<b>4,610–4,828</b>	94	–24.6	84
Beta-434190	G35-NE-23		VI	4,130 ± 30	<b>4,567–4,729</b>	64	–25.9	excl.
Beta-449172	G35		VI	9,540 ± 40	<b>10,695–10,897</b>	51	–22.3	150
Beta-449173	G35-NE-23	Charcoal	VII	11,620 ± 40	<b>13,401–13,521</b>	75	–22.1	excl.
Beta-481344	G35-SE-24	Charcoal	VII	12,560 ± 40	<b>14,812–15,122</b>	85	–25.1	159
Beta-523129	G35-NE-27	Org. Mat	VII	5,640 ± 30	<b>6,390–6,490</b>	78	–25.2	160
Beta-434191	G35-NE-28	Charcoal	VII	13,970 ± 50	<b>16,738–17,121</b>	100	–21.7	158
Beta-434192	G35-NE-28	Charcoal	VII	13,930 ± 50	<b>16,718–17,072</b>	100	–24.0	156
Beta-449174	G35-NE-28	Charcoal	VII	13,870 ± 50	<b>16,644–17,025</b>	100	–22.2	156
Beta-521542	F35-SE-26 B	Charcoal	VII	13,970 ± 50	<b>16,738–17,121</b>	100	–25.6	165
Beta-521541	F35-SE-26 a	Charcoal	VII	4,010 ± 30	<b>4,415–4,530</b>	99	–25.3	163
Beta-521539	F35-SE-27 a	Charcoal	VII	13,870 ± 40	<b>16,664–17,016</b>	100	–25.8	170
Beta-521540	F35-SE-27 B	Charcoal	VII	13,860 ± 50	<b>16,631–17,016</b>	100	–25.9	170
Beta-481345	G35-SE-31	Charcoal	VII	14,910 ± 50	<b>18,134–18,293</b>	100	–25.4	178
Beta-481347	G35-SE-37	Charcoal	IX	17,800 ± 60	<b>21,392–21,867</b>	100	–24.5	199
Beta-487731	G35-SE-37d	Sediment	IX	21,210 ± 70	<b>25,292–25,749</b>	100	–24.3	203
Beta-486039	G35-SE-37C	Charcoal	IX	22,360 ± 80	<b>26,396–26,960</b>	100	–24.7	203
Beta-521544	G35-SE-38 a	Charcoal	IX	22,350 ± 80	<b>26,392–26,953</b>	100	–24.2	204
Beta-521545	G35-SE-38 B	Charcoal	IX	22,510 ± 80	<b>26,452–27,107</b>	100	–26.2	206
Beta-521547	G35-SE-39 B	Charcoal	IX	22,450 ± 70	<b>26,433–27,029</b>	100	–25.5	206

Roman numbers indicate sedimentological unit. The bold numbers represent the calibrated <sup>14</sup>C age range (2σ) in cal BP. Samples Beta-434190 and Beta-449172 were taken from the archaeologically sterile layer. Red numbering indicates sample depth that were defined by the excavation unit, "excl." illustrates samples that were excluded from the depth model.

The measured carbonate content in the samples also represents the TOC content as in the samples of profile F35, since the pretreatment with HCl (10%) did not show any significant changes in the values. Thus, the carbonate content of the samples can be addressed as organic carbon. A post-depositional formation of inorganic carbon, such as gypsum or carbonates is therefore insignificant. The carbonate content is expressed in three extreme peaks within the Units VII and IX.

The resulting curves of Si and Ti show similarities especially in the increased values within the anthropogenic Units VII and IX. The lowest values are found in the Units VI and VIII (Supplementary Figure S2). Ca and Mn are increased in Unit VII and IX, that is comparable with the peak values of magnetic susceptibility within the cultural layers. Especially Mn is marked by higher values in Unit VII (Figure 7). Rb and strontium also share the same minimum as Ti within Unit VII, although the resulting curve differs in Unit IX with slightly increasing values. The values of K on the other hand show a different pattern with minimum values in Unit VIII. In contrast the P, Cl values peak in Unit IV and IX, following the increasing grain size. The graph of Al does not show as pronounced

changes as in profile F35 but it displays a rising gradient of the values within the units with a higher mean grain size.

The ratios of Al/Ti and Fe/Al, that are often used to indicate changes in the source area of sediments during deposition (Kehl et al., 2014), show only slight variations within profile G35. In Figure 7 and Supplementary Figure S4 the low values of the ratios of K/Ti and K/Rb indicate a slightly increased influence of weathering on the deposits in Unit VII (Brown, 2011; Arnaud et al., 2012; Kehl et al., 2014; Kehl et al., 2016). These rather small changes can also be observed in the calculated CIA. As already observed in the profile F35, the Mn/Fe ratio is increased in the anthropogenic influenced layers VII and IX (Supplementary Figure S4).

## Radiocarbon Chronology

According to the analyses, the stratigraphy can be roughly divided in five settlement phases, including the uppermost dated phase of recent times (Table 1). This proves repeated occupation by humans since more than 20 thousand years. The radiocarbon samples originate predominantly from anthropogenically

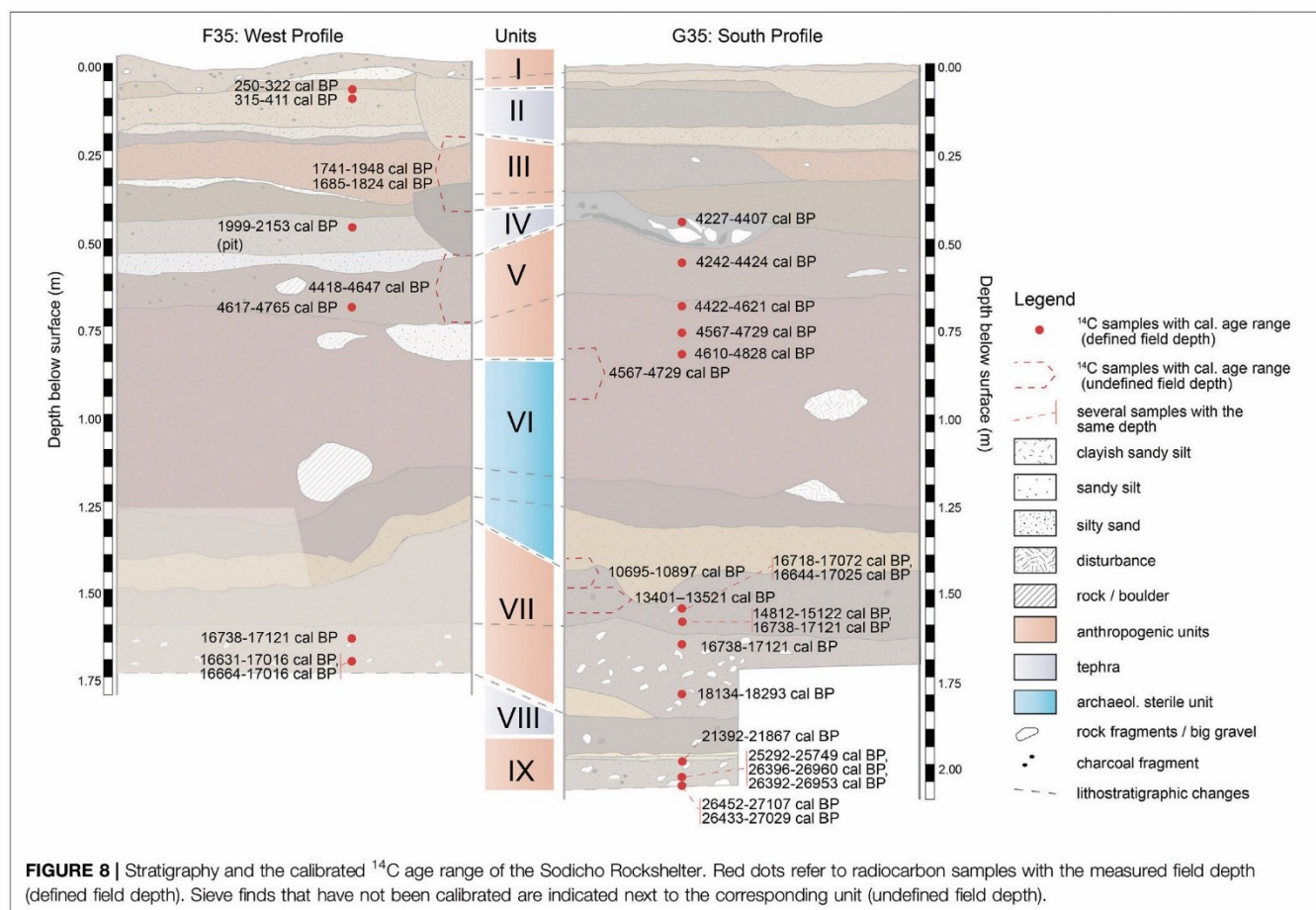


**FIGURE 8 |** Stratigraphy and the calibrated  $^{14}\text{C}$  age range of the Sodicho Rockshelter. Red dots refer to radiocarbon samples with the measured field depth (defined field depth). Sieve finds that have not been calibrated are indicated next to the corresponding unit (undefined field depth).

influenced layers (Figure 8), with the exception of samples Beta-434190, Beta-449172 and Beta-481345, which originate from archaeologically sterile layers. The samples Beta-523129 and Beta-521541 show comparably younger radiocarbon ages to the samples of the same depth, which probably indicates post-depositional displacement or inconsistencies in the sampling procedure.

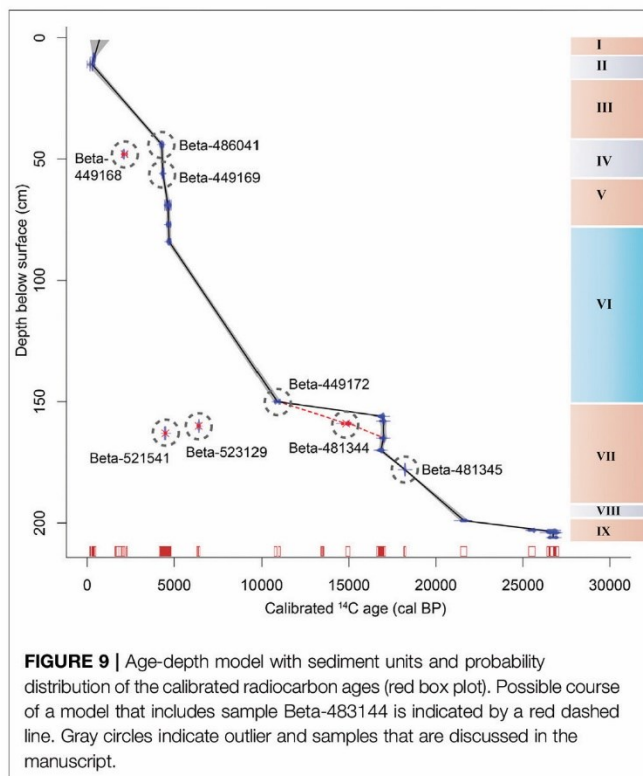
A modifiable classical age depth model was generated with the help of the clam2.3.5 package in RStudio. The model uses a linear interpolation technique with calculated accumulation rates to illustrate the changing deposition processes within the rockshelter. In Figure 9 the mentioned human settlement phases accumulated relatively fast. The intermitted archaeological sterile layers deposited comparably slow. Despite these similarities between the calculated ages and the age-depth model, several calibrated age ranges cannot be considered in the model, which are highlighted as “excl.” (Table 1). This includes the sample COL3149.1.1, COL3150.1.1, COL3153.1.1, which were taken during the test excavations of 2015 when no total station was available to record the exact location of the samples. The samples Beta-434190 and Beta-449173 are sieve finds and had to be excluded as well, since an exact field depth could not be measured. Samples that have been included in the model but clearly show a significant age

deviation are marked as outliers. In Figure 9, a “plateau” is shown between 10.8 and 17 ka, which is due to the fact that the sample Beta-481344 is considered an outlier. If the Beta-481344 was included in the model, two other samples (Beta-449174 and Beta-434192) would have to be excluded to prevent a reverse chronology (Figure 9). This illustrates how variable the sediment deposition is within Sodicho Rockshelter and how difficult it is to develop a reliable model.

## Archaeological Finds

The analysis of the archaeological finds is still ongoing and only preliminary results based on the analysis of artifacts from square F35 & G35 can be presented in this chapter. The preservation conditions for bones are extremely bad, due to the volcanic and moist environment of the shelter. The acid character of the sediments in combination with leakage water caused the destruction of any bones older than some hundred years. Pottery is also restricted to the recent surface layer and the youngest Stone Age occupation. This confirms the general picture of a late appearance of pottery in the southwestern Ethiopian Highlands around 2000 years ago (Gutherz et al., 2002; Hildebrand and Brandt, 2010; Schepers et al., 2020).

In all other cultural layers are stone artifacts the only cultural remains. The broad division of the stone artifact assemblages



reflects the general sedimentological differentiation of an upper sediment package, which is separated by a sterile, reddish-brown deposit (Unit VI) from a basal sediment package. Chronologically, this division can be correlated with the Late Holocene and the Late Pleistocene, separated by a Middle to Early Holocene occupational gap.

Raw material for the production of stone tools is in all assemblages almost exclusively obsidian. First microprobe analysis results verify the exploitation of two local sources and of the large Bantuu outcrop, which was also used by the occupants of the rockshelter Mochena Borago. In addition, several up to now unknown raw-material sources have been used (pers. communication B. Nash). The two cultural layers in the upper part of the stratigraphy (Unit III and Unit V) are both characterized by microlithic stone tools, mainly backed tools, which are type forms of the African microlithic Later Stone Age (LSA). The main difference between the two assemblages is the number of artifacts. Only 69 pieces (without chips) from the upper LSA assemblage in square F35 stand in contrast to 531 pieces from the older LSA assemblage. The small number of stone artifacts of the upper LSA assemblage, which dates between ~1800 and ~2,100 cal BP, accounts for the low number of retouched tools. Despite two fragments of backed microliths that cannot be further classified, two segments are the only characteristic type-forms. The older assemblage, which dates between ~4,300 and ~4,800 cal BP, comprised 11 segments (Figure 10), seven micro-points and six double micro-points (following the definition of type-forms in Schepers et al., 2020). Single pieces are one scraper, one backed point and one drill.

However, the percentage of retouched stone tools in comparison to the total number of stone artifacts is in both assemblages similar. The greater variation in type-forms of the older microlithic assemblage might be simply due to the higher total number of artifacts. Regarding the small sample size coming from a very restricted area of the shelter, further analysis has to verify, if the different spectrum of tools reflects any cultural or functional distinctions and if the number of finds reflects different settlement intensities.

A sediment package without any cultural remains (Unit VI) represents an occupational gap between these younger, microlithic assemblages and the Late Pleistocene assemblages. Repeated occupation of the shelter is testified between ~27,000 and ~13,500 cal BP. Preliminary analysis of the lithic assemblages shows a surprising uniformity of the stone artifacts. Obsidian is still the dominant raw-material for the production of stone tools, but also cryptocrystalline silices were used in small numbers. All assemblages are dominated by the production of bladelets and the analyzed sample completely lacks any retouched tools (Figure 11). Settlement phases dating around 17 to 15 ka cal BP and 27 to 22 ka cal BP coincide with the arid or rather hyper-arid climatic phases of the Heinrich event 1 and 2 (H1, H2) (Hemming, 2004) and the Last Glacial Maximum (Mark and Osmaton, 2008).

## DISCUSSION

### Interpretation of Multiproxy Analyses

Our sedimentological and geochemical results revealed major changes of the sediment sources and indicate a combination of different geogenic and anthropogenic processes that influenced the deposits in the Sodicho Rockshelter. Our data revealed that the sedimentological units preserved within Sodicho Rockshelter accumulated in different depositional environments. Based on field observation and analyses we distinguished a total of nine sedimentological units, which can be grouped in four sediment facies:

**Autochthonous geogenic deposits** are mainly characterized by trachytic clasts and boulders, that could derive most likely from the rockshelter walls and the roof itself. This type of deposit is omnipresent in almost all sediment units. A rockfall layer located in the upper part of the Unit VII, right below the sterile Unit VI, consists of trachytic boulders with a maximum diameter of up to 70 cm (Figure 4). The upward facing surface of the boulders is rounded. This indicates that the boulders were not rapidly covered by sediment and persistent weathering dissolved the fine feldspar matrix.

**Allochthonous geogenic deposits** predominantly consist of well sorted volcanic tephra and ash, which were ejected during past volcanic eruptions in the region and deposited in the shelter by aeolian transport. These Units II, IV and VI are easily identifiable as thicker, light color sediment layers or lenses, with an increased mean grain size. The grain size analyses revealed low ratios of the 90th and 10th percentiles and a higher amount of particle with the grain size that can be associated to an aeolian transport. These results and the field observation indicate major changes in sediment origin during

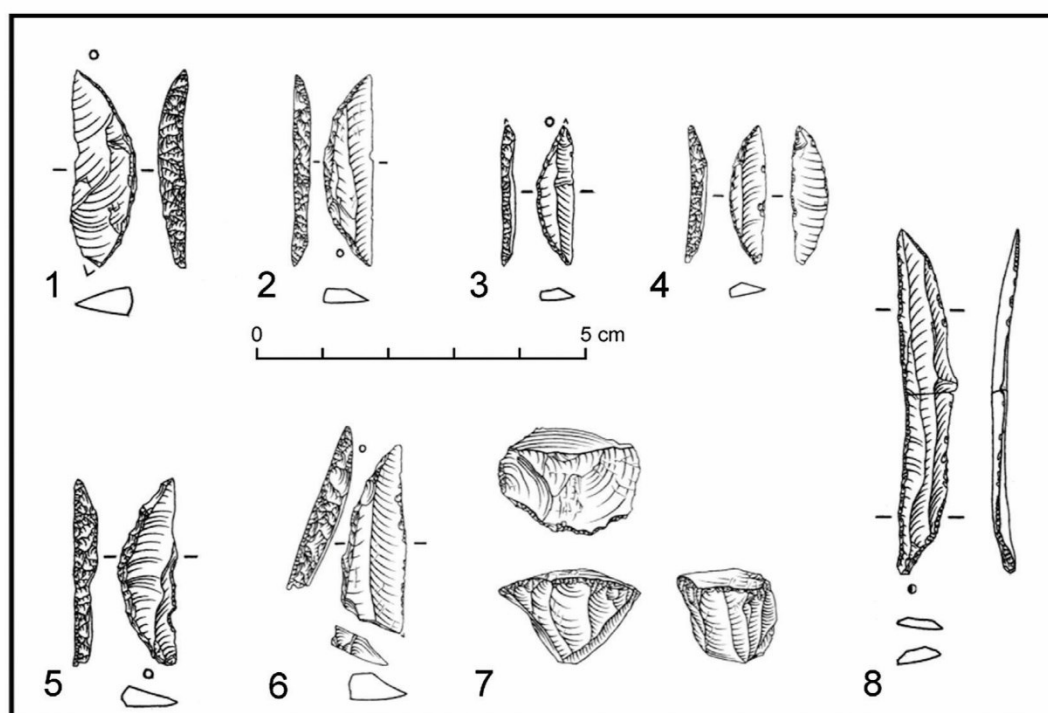


**FIGURE 10** | Microlithic LSA lithics: Segments (1–5), backed point (6), prismatic bladelet core (7), broken bladelet with use-wear (8).

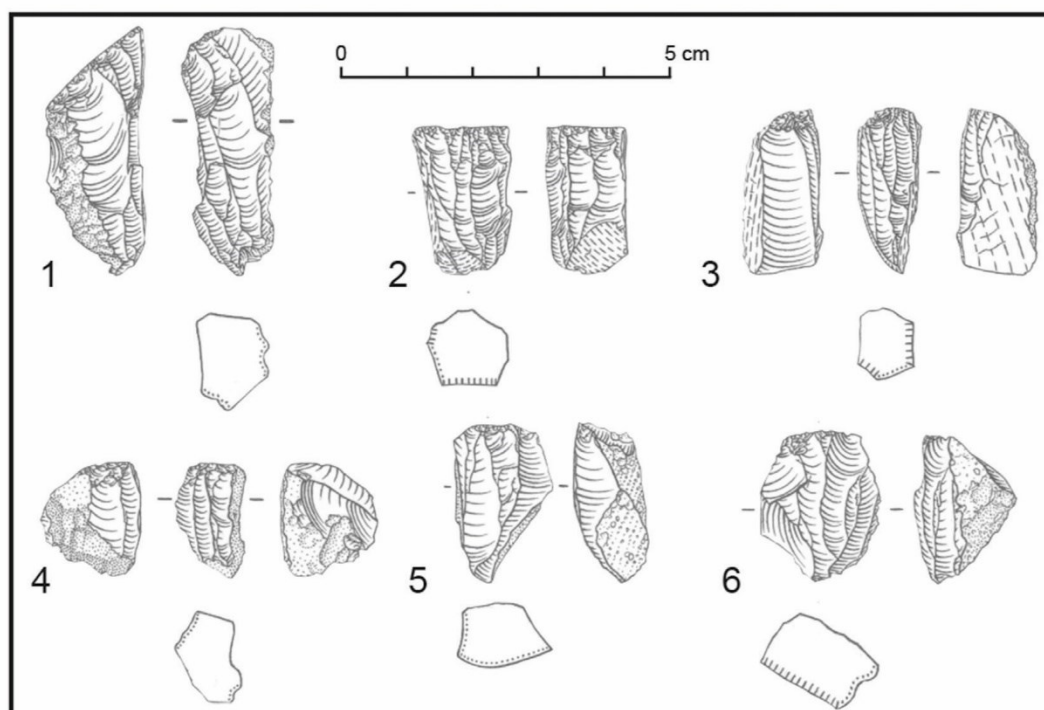


**FIGURE 11** | Late Pleistocene lithics: Bladelet cores (1–6).

deposition with the highest aeolian input in Units II, IV, and partly in III. Geochemical analyses point to a potassium and chlorine enriched felsic tephra, that is distinguishable from the surrounding sediment. This geochemical fingerprint allows the identification of altered volcanic tephra within samples, as identified in Unit VI and VIII. The source volcanos of the tephra remain undefined, even though we identified the geochemical composition. It can be assumed that this type of allochthonous geogenic deposits of volcanic origin were deposited relatively abrupt, which is shown by the sharp boundaries to lower deposits.

**Mixed autochthonous and allochthonous geogenic deposits** are the result of weathering of the trachytic rock and water percolation through the sediment. This type is common in the sterile Unit VI, that differs from all the other sediment units in both sample columns. The poor sorting in these deposits indicate polygenic sediment origins. The high CIA index as well as low K/Ti, K/Rb values refer to increased (Kehl et al., 2014). The reddish-brown deposits are characterized by an increased clay content and peaks in the redness index that correspond with a higher Fe<sub>2</sub>O<sub>3</sub> content (Figure 5). Particularly noticeable is the decrease in magnetic susceptibility and most other geochemical proxies. Nevertheless, Ti and Al content are increased since they are often bound to clay (Okrusch and Matthes, 2010). Based on its high Fe<sub>2</sub>O<sub>3</sub>, Ti and AL content, we argue that Unit VI originated from the weathering of the local bedrock in a moist environment, leading to the formation of authigenic clay minerals. Alternatively, the increased clay content and the different geochemical composition of this sediment could be the result of fine-grained soil material that was washed in the site through fissures in the ceiling of the rockshelter.

**Anthropogenic deposits** are identifiable by the concentration of archaeological finds, such as obsidian artifacts and charcoal from hearths, as observed in Units I, III, V, VII and IX. Moreover, the deposits have a certain sedimentological and geochemical fingerprint that is characterized by a poor sorting, high values of magnetic susceptibility and an increased content of Mn, P and TOC (Figure 4–7). Manganese and Phosphorous are released into the soil by the decay of deposited organic matter or inorganic compounds, as in phosphate minerals, that accumulate at the site by human occupation (Holliday and Gartner, 2007; Karkanas, 2017). Furthermore, the high percentage of TOC in Unit VII and IX can perhaps be explained by higher weathering of the lower levels of the stratigraphy and therefore the decomposing of the organic matter. The high values of the magnetic susceptibility most certainly derived from thermally alteration of the sedimentary substrate, due to burning activity. Chemical changes of magnetic minerals induce the development of ferrimagnetic mineral, such as maghemite that increases the magnetizability of the sediment (Le Borgne, 1955; Herrejón Lagunilla et al., 2019). Furthermore, manganese shows paramagnetic properties, which contributes to the relatively high ratios of magnetic susceptibility in the cultural layers. This means that randomly distributed magnetic dipoles interact with the external field of the magnetic susceptibility measurement, which orients the dipoles in one field direction, and amplifying the whole field (Ivers-Tiffée and von Münch,

2007). The Mn/Fe ratio is increased in the anthropogenic Units I, III and V (Supplementary Figure S3), suggesting increased manganese content under redox conditions in the upper part of the stratigraphy.

Although the sedimentological and elemental fingerprints show clear signs for human occupation, we cannot exclude that these layers underwent diagenetic processes such as dissolution or oxidation. This can bias results about environmental condition during human occupations in the shelter. By comparing the geochemical data of profile F35 with profile G35, it is noticeable that the values of the sedimentological and geochemical graphs of the basal sediment levels below the sterile unit are not as pronounced, which indicates stronger alteration. This may be caused by a higher influence of water infiltration during the deposition of the sterile layer that can be dated to the AHP (~15–5 ka BP) and a possible post depositional alteration.

## Chronology and Human Occupation at the Rockshelter

We assigned the multiproxy results to the radiometric ages and via the age-depth model in order to understand site formation processes and to correlate them with the chronological succession of the cultural layer. Following the mentioned sedimentological and geochemical results we can distinguish nine sedimentological units, comprising of both natural and anthropogenic accumulations (Figure 8). The following chronological phases of human occupation are described in stratigraphic order. It is important to note that the calculated age-depth model cannot reflect the complete depositional conditions and their variations in the Sodicho Rockshelter, as these processes vary within the different excavation quadrants. The model is intended as a simplification to illustrate phases of human settlement.

Mount Sodicho is probably one of the silicic domes associated to the Wagebeta Caldera Complex that developed 3.6- to 4.2 Ma ago (WoldeGabriel et al., 1990; WoldeGabriel et al., 1992). The exact time for the formation of the Sodicho Rockshelter and the beginning of sediment deposition is not yet clear. Therefore, further investigations and excavations down to the bedrock are needed. The rockshelter increased in size as time progressed due to solution of silica in the trachytic rock by water that flowed in through fissures and cracks in the weathered rock shelter roof, which are still visible today.

As discussed above, the lowermost investigated Unit IX with an approximate age range of about ~27 to 22 ka cal PB represents an anthropogenic layer (Figure 8). Charcoal fragments and lithic artifacts as well as the characteristic anthropogenic deposits with increased magnetic susceptibility, higher manganese and phosphorus content indicate human occupation. The base of this layer has not been reached yet. The excavation unit GE35-SE-37 is represented only by a single date (Beta-481347) in the age-depth model, although two other samples (Beta-487731, Beta-486039) derive from this level (Figure 9). Their different age can be explained by the presence of a coarser-grained and lighter colored band in Unit VIII, with increased values of Al/Ti, which indicates a variation of the sediment source. The influence of post-depositional processes such as bioturbation cannot

be excluded, which has to be a focus of future micromorphological investigations.

Sediment Unit IX is covered by a brownish layer, representing a distinct anthropogenic unit (VII), which lies below the archaeological sterile unit. The lower part of the unit consists of a yellow brownish sediment with intermixed cultural findings. One radiocarbon sample that was collected from this section dates between 21,392 and 21,867 cal BP. The following settlement phase covers a period of about 17 to 15 ka cal BP. All radiocarbon samples were taken from sediment in-between and below the big trachytic boulders of the rockfall layer. Chronologically, the trachytic rock fall layer in the upper part of the unit cannot be assigned, as no datable material has been preserved directly above this layer. At the moment it is not possible to determine whether the collapse of the roof caused the end of this occupation phases or if the humans had already left the rockshelter. The stone artifact distribution in between and below the boulders points to a severe disturbance of the accumulated anthropogenic material. Another question is whether the larger rocks at the entrance of the rockshelter collapsed at the same time as the trachytic rocks in Unit VII, or if this was a different event. The absence of trachytic boulders in higher strata of the stratigraphy speaks for a simultaneous collapse of the rocks. Future analyses below the large rocks, blocking the entrance, could provide information about this. It can be assumed that the whole sedimentological unit has undergone post-depositional processes that led to disturbances and influenced the expression of some geochemical indicators. A possible influence of pedogenetic processes and temporary absence of human impact can be explained by the inconsistency of the magnetic susceptibility and the K/Rb ratio (Kehl et al., 2014). This indicates post-depositional disturbances and a possible displacement of radiocarbon samples. With this assumption in mind the two outliers (Beta-523129, Beta-521541) of this cultural phase, can be excluded from the model.

The following clayish Unit VI provides a unique indication for the prolonged absence of humans. Chronostratigraphically, this unit can be dated by one radiocarbon date (Beta-449172), that originates from the base of the unit, and by the dates of the cultural layer below and above it. Based on this, the dates of ~15 and 4.7 ka are the maximum, respectively minimum age of the deposition. This period can be assigned to the Early Holocene African Humid Period (Foerster et al., 2012; Foerster et al., 2015; Hildebrand et al., 2019). An exact dating of the deposits is not possible due to the lack of datable material within Unit VI (Figure 8). The duration of the deposition is unclear and it might have been a slow process over a long period or a rapid event. It can be assumed that there must have been fluctuations during the deposition. This is verified by the variations in the degree of sorting and by the distinctive yellowish, silty layer in the lower part of the unit.

The end of the archaeologically sterile Unit VI and thus the beginning of the anthropogenic unit V is verified by the presence of obsidian tools and charcoal, as well as by the abrupt change in sedimentological and geochemical features. In particular, the increased values of magnetic susceptibility, TOC, as well as the

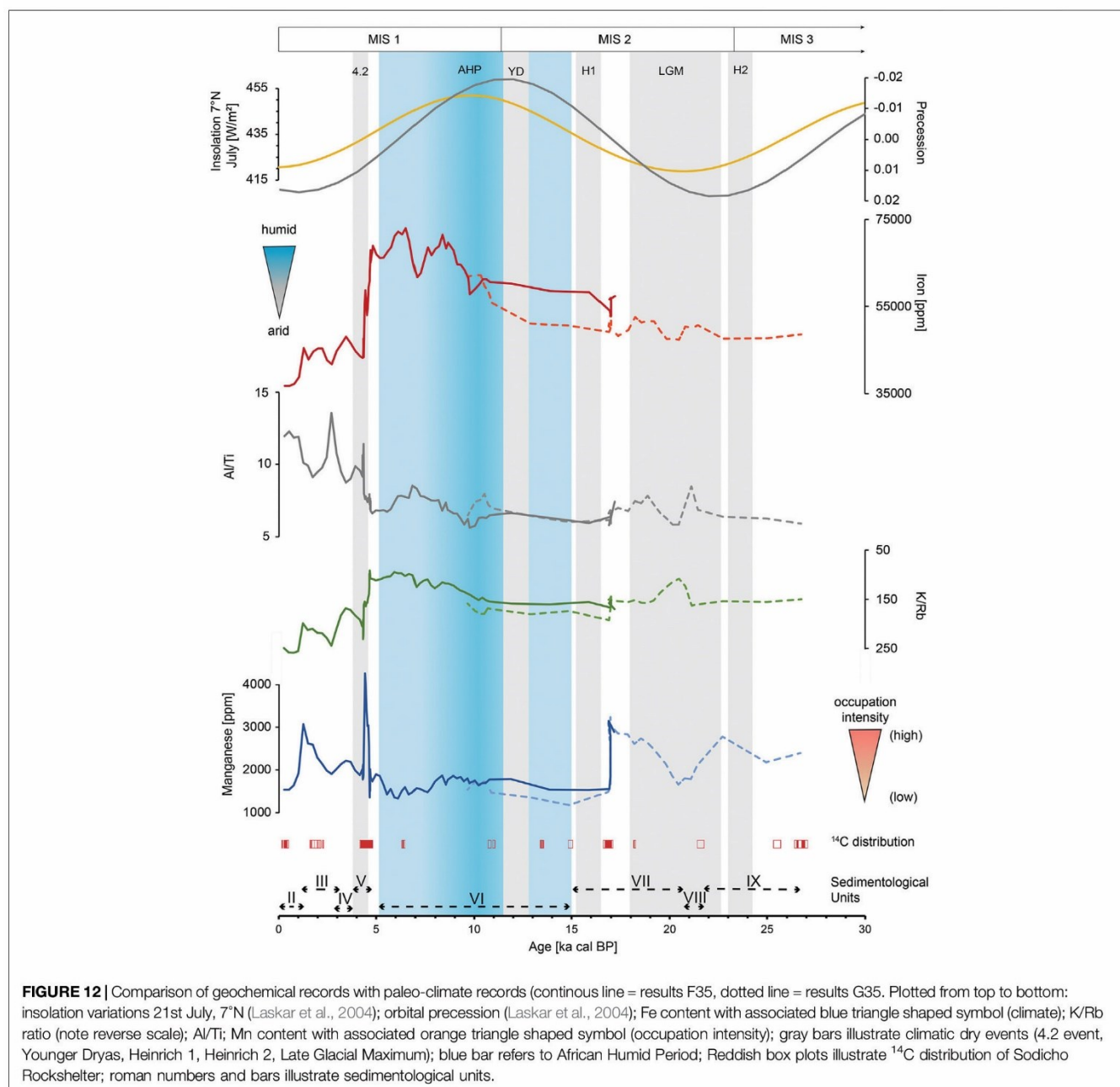
increase in manganese and phosphorus mark an intense re-occupation of the shelter by humans. Seed and charcoal samples date to an age range of about ~4.7–4.3 ka cal BP. Again, the accumulation rate of the anthropogenic impacted deposits in Unit V is higher than in the case of exclusively geogenic induced deposits in the Sodicho Rockshelter. Considering the sampling depth of the radiocarbon samples, the anthropogenic accumulations reach up to a field depth of 0.45 m. However, the samples Beta-486041 and Beta-449169, collected in excavation square G, are at the same depth as the sterile tephra of Unit IV in square F35, which is not visible in square G. These tephra layers can be geochemically identified by the coarser grain size, the increased potassium (K) amount and the maximum values of the Al/Ti proxies, which indicates a change in the sediment source (Kehl et al., 2014). In addition, sweeping and raking-out the surface may have been involved, as has already been observed in micromorphological studies at South African sites, like Sibudu Cave and Diepkloof Rock Shelter (Goldberg et al., 2009; Texier et al., 2010).

The radiocarbon sample Beta-449168 is marked as an outlier in the age-depth model because it was taken from a pit in excavation unit F34-NW-10 (Figure 9). Stratigraphically the sample is situated above sample Beta-486041 in Unit III (Table 1). This age discrepancy is the result of mixing and relocation of the sediment in the pit (Ossendorf et al., 2019). Nevertheless, the dated sample represents the anthropogenic Unit III, which is supported by cultural material and an increase in TOC and of manganese.

On the basis of the geochemical proxies alone, it can be assumed that the human occupation of the rockshelter was more pronounced in the periods above the sterile layer than in the stratigraphically older units. However, it should be pointed out that the proxies at the bottom of the sterile layer show weaker trends and were probably influenced by weathering. Considering the small size of the excavation trench, the artifact density might simply reflect differences in the spatial use of the shelter over time and is therefore an incidental result that cannot be considered as an indicator for settlement intensity.

## Regional Paleoenvironmental Implications

The sedimentological results indicate changes in the depositional conditions over time. As discussed above, some of the results, e.g., archaeological finds, magnetic susceptibility and the Mn content show clear signs of human impact. By plotting elemental ratios against the calculated age-depth model, it is possible to model these first results in relation to regional paleoenvironmental changes during the last 27 kilo years (Figure 12), covering periods like the Last Glacial Maximum (LGM,  $21 \pm 2$  ka) and the Early Holocene African Humid Period (AHP, ~15–5 ka). For the paleoenvironmental comparison we consider archaeological and sedimentological information from the rockshelter Mochena Borago, and paleoclimatic records from lacustrine sediments in Ethiopia. With our own data we observe local environmental fluctuations in sediment sources or weathering intensity caused by shifts in moisture availability.



### Phase 3: Unit VII–IX, ~27–15 Ka

The short distance of about 40 km to Mochena Borago provides a suitable basis for a local comparison of the past conditions. Chronologically, the currently excavated and dated cultural layers from Sodicho cannot be connected to the Late Pleistocene deposits of Mochena Borago, since layers from this period have not been excavated yet. Nevertheless, we see similarities in the changes of the lithostratigraphic sequences. The basal Pleistocene deposits of the stratigraphy of Mochena Borago offers one of the most complete records from the timeframe of 60–30 ka in Eastern Africa. The main trench at Mochena Borago revealed three major lithostratigraphic units

that preserved cultural remains dated between 36 and >50 ka (Brandt et al., 2017). The complex stratigraphy developed by multiphase, polygenetic accumulations of geogenic deposits, e.g., fluvial activities, volcanic eruptions, and anthropogenic depositional processes (Brandt et al., 2017). Several erosional activities resulted in a chronostratigraphic gap from ~36 to ~8 ka cal BP, erasing sedimentological history and possible cultural evidence until the Holocene (Brandt et al., 2012; Brandt et al., 2017). Although this archaeological and stratigraphic gap was recognized at other East African sites as well, e.g., Ziway-Shala basin and Goda Buticha (Tribolo et al., 2017), it is not found in Sodicho. In **Figure 12** the Mn record and the  $^{14}\text{C}$  dates illustrate

two anthropogenic Units IX and VII that preserved cultural material ranging from ~27 to ~16 ka cal BP. This makes Sodicho Rockshelter the first site in Ethiopia that partially reduces the chronostratigraphic gap. The two anthropogenic units partly cover the global short-term Heinrich event 2 (H2) and the prolonged high-latitude LGM with a decrease of the Mn values around 21 ka (Figure 12). On a regional level, both time ranges are pronounced dry and cold phases, that can be tracked by a drop in the K record of the Chew Bahir basin core (Foerster et al., 2012). In contrast to the geoarchaeological evidence from Mochena Borago indicating that prehistoric humans frequented the rockshelter during more humid conditions (Vogelsang and Wendt, 2018), the sedimentological and archaeological results at Sodicho point to multiple occupations during humid and arid periods. In fact, Sodicho is the first evidence for the use of highlands as a refugium during times of severe environmental stress in the lowlands. In the Rift Valley, human occupation is not traceable during Late Pleistocene arid phases, even not in the surroundings of lakes, such as the Ziway-Shalla Basin (Bon et al., 2013). Thus, highlands might have been the only retreats. Paleoclimate simulations indicate higher annual precipitation in the Ethiopian highlands during arid phases than in lower elevated regions in Ethiopia, and suggest that these regions were part of a warm and temperate savanna and remained covered by low growing vegetations and scrubs during the glacial aridity of the LGM (Basell, 2008; Willmes et al., 2017). Residual water in the highlands could have attracted animals and humans (Basell, 2008). The Mn value of Unit VII peaks around ~17 ka cal BP, followed by a rather extreme drop of the values, which was not evident in the raw data of the geochemical analyses of the stratigraphy (Figure 7). This indicates the end of the cultural settlement phase. At the same time the Fe values show a rather gradual change to more humid conditions. The rapid changes of the records can be explained by the calculated sediment rate of the age model, which is increased in this section. In addition, post-depositional processes, the rockfall event of Unit VII, and the human impact has to be considered. A further explanation is the sample Beta-481344 (14,812–15,122 cal BP), which was marked as an outlier in the calculated age depth model. When this dating would have been included in the age-depth model, the geochemical data does not show such a strong trend around 17 ka (Supplementary Figure S5). Nevertheless, the geochemical values would steadily decrease from 17 ka. Another possible explanation are stepwise abrupt changes to increasing precipitation. This observation is also preserved in the Chew Bahir basin record between ~19 and 15 ka, and further paleoclimatic records on the northern African continent (for detailed descriptions and references to these records, see Foerster et al., 2012). Overall, our geochemical data from this period around 17 to ~15 ka cal BP should be regarded with caution, since the age data are influenced by the plateau in the age-depth model (Supplementary Figure S5).

### Phase 2: Unit VI, ~15–4.7 ka

As mentioned before in Figure 12, a phase of prolonged human absence correlates with a shift to more intense moisture, expressed in low Mn content and higher Fe content. The overall moist signal is

recorded between a maximum age of ~17 ka cal BP and a minimum age of ~4.7 ka cal BP. Although Fe<sub>2</sub>O<sub>3</sub> record has a comparable trend as Fe (Figure 5), the graph of Fe was chosen, due to the higher sample density and the more precise detection of fluctuations. This increased Fe trend, enhanced input of clay minerals and the lower K/Rb ratio corresponds to intensive weathering influence (Figure 5). As mentioned before this phase is known as the Early Holocene African Humid Period, that occurred during low orbital precession and associated higher insolation values (Laskar et al., 2004). Comparable conditions were observed in the increasing trend of the K record of the Chew Bahir basin (Foerster et al., 2012; Foerster et al., 2015). Our geochemical results in Figure 12 show a gradual increase in humid conditions. In contrast, drier intervals like the Heinrich event 1 (H1, ~16 ka) and the Younger Dryas (YD, ~12 ka) are not visible in our geochemical record. This might be caused by one outlier sample that had to be excluded from our age model (see *Chronology and Human Occupation at the Rockshelter*). Nevertheless, a slight drop at 9.8 and 7 ka cal BP in the Fe values within the profile of F35 can be identified. These shifts can be explained by local changes in the sediment source region, as indicated by the fluctuations in the Al/Ti ratio. These intrusions correlate with a dry interval of 9.8–9.1 ka and a large-scale drought of around 7 ka observed at various sites throughout East Africa (Foerster et al., 2012). It is still unclear why the humans abandoned the rock shelter during the African Humid Period. Possibly the large lakes in the lowlands and Rift Valley offered preferred and easily accessible resources and the amount of energy needed to obtain food may have been lower there (Bon et al., 2013). Moreover, it can be assumed that the intense precipitation led to the formation of an extremely dense vegetation coverage, which impeded humans to live at the mountains slopes and use the highland ecosystems.

The termination of the AHP is a subject of current scientific discussions. These include the assumption of a slow gradual change to drier conditions (Kröpelin et al., 2008; Foerster et al., 2012) or a rather fast and relatively abrupt transition, which was also identified in several records, as according to water level reconstruction for the Turkana basin (Garcin et al., 2012). Furthermore, the role of humans as potential drivers for the end of the AHP is debated (Wright, 2017). These fundamental discussions go beyond the scope of this study that is based on a local data set. Regarding our analysis, after a maximum value of Fe around 6.5 ka cal BP a further weaker peak (4.8 ka cal BP) is followed by an abrupt drop in values, pointing to rather arid conditions. This abrupt change can also be seen in the other graphs of our figure. However, this is not an indication of the pace of termination of the AHP, since the sediment deposits at Sodicho are influenced by post-depositional processes. Furthermore, the deposition conditions in rockshelter settings are often somewhat more discontinuous, in comparison to other terrestrial or lacustrine deposits.

### Phase 1: Unit V-I, ~ 4.7–0 ka

With the rapid decrease of the Fe values, the anthropogenic influenced Unit V emerges. Geochemically this can be clearly identified by increased MS and Mn values around 4.4 ka. This settlement phase and the associated deposition processes may have disturbed the sediment of the former walking horizon and thus partly explain the strong fluctuating Fe values. The dating of this cultural layer is of interest with regard to global climatic events, as it may cover

a time range that correlates with the so-called 4.2 ka event. This hyperarid event was mainly investigated in the Mediterranean (Kaniewski et al., 2018) or Chinese region (Xiao et al., 2018). Furthermore, a lacustrine record from Abhe Lake in northern Ethiopia indicates a drastic drop in lake levels between 4.5 and 3.7 ka, with an increase in aeolian accumulations indicating a drier climate (Khalidi et al., 2020). This could further confirm that humans lived in the Sodicho Rockshelter during arid periods with more favorable conditions in the montane forests (Hildebrand et al., 2019).

The tephra layers separating sedimentological Units I, III and V in excavation square F35 represent again a purely geogenic deposit and thus a temporary absence of humans within the rockshelter. The question whether humans were forced to abandon the site due to the volcanic eruptions and the consequential temporary environmental changes in the area cannot be answered on the base of the present results. Based on archaeological and chronological analyses at Mochena Borago, it is assumed that humans were influenced by rapid shifts in local or even regional environment that may have made it impossible to stay in the area (Brandt et al., 2012). The graphs in **Figures 4, 6** of the sedimentological and geochemical analyses show that the deposition of the pyroclastic material occurred rapidly. Given the alternating tephra and cultural layers of the Sodicho stratigraphy, we can assume similar rapid changes influencing the surrounding landscape and the humans. In contrast we observe a rather slow change between Unit VII and the archaeologically sterile Unit VI. The geochemical analyses (slow decrease of MS and Mn content) may indicate that humans had already left the rockshelter.

## CONCLUSION

The sediment record of Sodicho Rockshelter contains a 27 ka record of repeated human occupation and local paleoenvironmental proxies. The study presents a first stratigraphic and chronological framework for the Sodicho Rockshelter that is an important new site for studying prehistoric settlement in East Africa during critical time frames, such as the Last Glacial Maximum (LGM,  $\sim 21 \pm 2$  ka) or the African Humid Period (AHP,  $\sim 15\text{--}5$  ka). Four sediment agents and the resulting site formation processes are identified. Purely geogenic accumulations differ significantly from anthropogenic induced deposits in terms of grain size distribution, sediment color and geochemical composition of the sediment. It is possible to indicate a higher intensity of human settlement phases during Unit V, according to the preliminary analyses of the lithic material, the results of magnetic susceptibility, and the content of Manganese and Phosphor. Archaeological sterile layers are identified with the help of sudden grain size variations and elemental ratios, like Al/Ti and K/Rb. These illustrate the deposition of volcanic fallout, changes of weathering intensity and shifts of major sediment sources. In particular, the Fe content reflects an increase in weathering caused by humid conditions between  $\sim 17$  and 4.7 ka cal BP. Furthermore, the values also indicate short-term dry spells that may correlate with dated dry intervals of climatic records from the Chew Bahir basin, situated about 300 km southwest of the rockshelter but affected by the climatic

conditions of the southwestern highlands. In total, our results verify human occupation in the highlands during humid and arid phases in the last 27 ka. This underlines the assumption that the highlands might have been used as part of larger settlement areas during times of favorable climatic conditions, but also as retreat under arid environmental conditions. However, a distinctive settlement gap is detected during the humid conditions of the AHP. Further excavations and investigations are needed to verify these first preliminary hypotheses. These would include micromorphological observations and the evaluation of phytoliths, which could offer a closer look into the microstratigraphical development of the site and the local paleo-vegetation. Nevertheless, the sediment record of the Sodicho Rockshelter reflects local environmental changes that correspond to the records of the Chew Bahir basin and to superregional climatic shifts. The sedimentological and archaeological records of Sodicho Rockshelter have the potential to be correlated to other archaeological and paleoenvironmental sites in eastern Africa and thus contribute to a supra-regional reconstruction of the settlement history and paleoenvironment. In particular, our study contributes to close the chronological gap of human occupation in north-eastern Africa around the times of the LGM.

## DATA AVAILABILITY STATEMENT

The datasets analyzed for this study can be found at the CRC 806 Database, <https://doi.org/10.5880/SFB806.55>.

## AUTHOR CONTRIBUTIONS

RV and OB developed the project framework within the CRC 806. RV and TN did archaeological excavation and preliminary stone tool analyze. EH performed sediment sampling in the field, sedimentological and geochemical analyses in the laboratory and developed the age-depth model with RStudio. EH developed the manuscript and figures. All co-authors contributed to, read, and approved the paper.

## FUNDING

This research has been supported by the Deutsche Forschungsgemeinschaft (DFG, German Research Foundation) (grant No. 57444011 – SFB 806).

## ACKNOWLEDGMENTS

We kindly thank the Authority for Research and Conservation of Cultural Heritage (ARCCH) of Ethiopia for their permission and general support, and the Ministry of Mines and Energy for the approval of our export permits. This study was conducted as a part of project A1 “Out of Africa – Late Pleistocene Rock Shelter Stratigraphies and Palaeoenvironments in Northeast Africa” in the framework of the Collaborative Research Center 806 (CRC 806) “Our way to Europe.” We thank the team of Beta Analytic Inc. and

our colleagues from the radiocarbon AMS lab of the University of Cologne for radiocarbon dating. We thank Marianne Dohms and her colleagues from the Institute of Geography of the RWTH Aachen for their help and instructions for sediment color and XRF measurements. We are very grateful Thomas Albert, Degene Bado, Dejenne Degena, Mesfin Gete, Solomon Gitaw, Habir Mohammed Kebir, Mareike Röhl, Christian Schepers, Desta Sinajew, Mehdanit Tamerat, Fitsum Tefera, Minassie Tekelemariam and Thorben Thenbruck for their

participation during various field seasons at Sodicho. Finally, we thank the local residents of Mt. Sodicho for their participation and support in field research.

## SUPPLEMENTARY MATERIAL

The Supplementary Material for this article can be found online at: <https://www.frontiersin.org/articles/10.3389/feart.2020.611700/full#supplementary-material>.

## REFERENCES

- Arnaud, F., Révillon, S., Debret, M., Revel, M., Chapron, E., Jacob, J., et al. (2012). Lake Bourget regional erosion patterns reconstruction reveals Holocene NW European Alps soil evolution and paleohydrology. *Quat. Sci. Rev.* 51, 81–92. doi:10.1016/j.quascirev.2012.07.025
- Barrón, V., and Torrent, J. (1986). Use of the kubelka–munk theory to study the influence of iron oxides on soil colour. *J. Soil Sci.* 37, 499–510. doi:10.1111/j.1365-2389.1986.tb00382.x
- Basell, L. S. (2008). Middle Stone Age (MSA) site distributions in eastern Africa and their relationship to Quaternary environmental change, refugia and the evolution of Homo sapiens. *Quat. Sci. Rev.* 27 (27), 2484–2498. doi:10.1016/j.quascirev.2008.09.010
- Benito-Calvo, A., De la Torre, I., Mora, R., Tibebe, D., Morán, N., and Martínez-Moreno, J. (2007). Geoarchaeological potential of the western bank of the Bilate River (Ethiopia). *Analele Universității din Oradea VII Seria Geographie*, 99–104.
- Berhanu, B., Melesse, A. M., and Seleshi, Y. (2013). GIS-based hydrological zones and soil geo-database of Ethiopia. *Catena* 104, 21–31. doi:10.1016/j.catena.2012.12.007
- Blaauw, M. (2010). Methods and code for ‘classical’ age-modelling of radiocarbon sequences. *Quat. Geochronol.* 5 (5), 512–518. doi:10.1016/j.quageo.2010.01.002
- Blott, S. J., and Pye, K. (2001). GRADISTAT: a grain size distribution and statistics package for the analysis of unconsolidated sediments. *Earth Surface Processes and Landforms*. 26 (11), 1237–1248. doi:10.1002/esp.261
- Bon, F., Dessie, A., Bruxelles, L., Daussy, A., Douze, K., Fauvelle-Aymar, F., et al. (2013). Prehistory of the central main Ethiopian rift (Ziway-Shala basin): establishing the late stone age sequence in eastern Africa. *An. Ethiopie*. 28, 405–407. doi:10.3406/ethio.2013.1552
- Bonini, M., Corti, G., Innocenti, F., Manetti, P., Mazzarini, F., Abebe, T., et al. (2013). Evolution of the Main Ethiopian Rift in the frame of Afar and Kenya rifts propagation. *Tectonics* 24, 1. doi:10.1029/2004TC001680
- Brandt, S. A., Fisher, E. C., Hildebrand, E. A., Vogelsang, R., Ambrose, S. H., Lesur, J., et al. (2012). Early MIS 3 occupation of Mochena Borago rockshelter, southwest Ethiopian highlands: implications for late Pleistocene archaeology, paleoenvironments and modern human dispersals. *Quat. Int.* 274, 38–54. doi:10.1016/j.quaint.2012.03.047
- Brandt, S., Hildebrand, E., Vogelsang, R., Wolfhagen, J., and Wang, H. (2017). A new MIS 3 radiocarbon chronology for Mochena Borago Rockshelter, SW Ethiopia: implications for the interpretation of Late Pleistocene chronostratigraphy and human behavior. *J. Archaeol. Sci. Report.* 11, 352–369. doi:10.1016/j.jasrep.2016.09.013
- Brown, E. T. (2011). Lake Malawi’s response to “megadrought” terminations: sedimentary records of flooding, weathering and erosion. *Palaeogeogr. Palaeoecol.* 303 (1–4), 120–125. doi:10.1016/j.palaeo.2010.01.038
- Chernet, T. (2011). Geology and hydrothermal resources in the northern Lake Abaya area (Ethiopia). *J. Afr. Earth Sci.* 61 (2), 129–141. doi:10.1016/j.jafrearsci.2011.05.006, 2011
- Corti, G. (2009). Continental rift evolution: from rift initiation to incipient break-up in the Main Ethiopian Rift, East Africa. *Earth Sci. Rev.* 96 (1–2), 1–53. doi:10.1016/j.earscirev.2009.06.005
- Corti, G., Sani, F., Philippon, M., Sokoutis, D., Willingshofer, E., and Molin, P. (2013). Quaternary volcano-tectonic activity in the Soddo region, western margin of the Southern Main Ethiopian Rift. *Tectonics* 32 (4), 861–879. doi:10.1002/tect.20052
- De la Torre, I., Benito-Calvo, A., Mora, R., Martínez-Moreno, J., Morán, N., and Tibebe, D. (2007). Stone age occurrences in the western bank of the Bilate River (southern Ethiopia) - some preliminary results. *Nyame Akuma*. 67, 14–25.
- Eckmeier, E., and Gerlach, R. (2012). Characterization of archaeological soils and sediments using VIS spectroscopy. *eTopoi. J. Ancient Stud.* 3, 285–290. doi:10.1002/gea.1004
- Fisher, E. (2010). *Late Pleistocene technological change and hunter-gatherer behavior at moche Borago rockshelter, sodo-wolayta, Ethiopia: flaked stone artifacts from the early OIS 3 (60–43 ka) deposits*. Gainesville, FL: University of Florida.
- Foerster, V., Junginger, A., Langkamp, O., Gebru, T., Asrat, A., Umer, M., et al. (2012). Climatic change recorded in the sediments of the Chew Bahir basin, southern Ethiopia, during the last 45,000 years. *Quat. Int.* 274, 25–37. doi:10.1016/j.quaint.2012.06.028
- Foerster, V., Vogelsang, R., Junginger, A., Asrat, A., Lamb, H. F., Schaebitz, F., et al. (2015). Environmental change and human occupation of southern Ethiopia and northern Kenya during the last 20,000 years. *Quat. Sci. Rev.* 129, 333–340. doi:10.1016/j.quascirev.2015.10.026
- Folk, R. L., and Ward, W. C. (1957). Brazos River bar [Texas]; a study in the significance of grain size parameters. *J. Sedim. Res.* 27 (1), 3–26. doi:10.1306/74d70646-2b21-11d7-8648000102e1865d
- Garcin, Y., Melnick, D., Strecker, M. R., Olago, D., and Tiercelin, J.-J. (2012). East African mid-Holocene wet–dry transition recorded in palaeo-shorelines of Lake Turkana, northern Kenya Rift. *Earth Planet. Sci. Lett.* 331–332, 322–334. doi:10.1016/j.epsl.2012.03.016
- Goldberg, P., and Bar-Yosef, O. (1998). “In site formation processes in kebara and hayonim caves and their significance in levantine prehistoric caves.” in *Neandertals and modern humans in western Asia*. Editors T. Akazawa, K. Aoki, and O. Bar-Yosef (Boston, MA: Springer US), 107–125. doi:10.1007/0-306-47153-1\_8
- Goldberg, P., Miller, C. E., Schiegl, S., Ligouis, B., Berna, F., Conard, N. J., et al. (2009). Bedding, hearths, and site maintenance in the Middle Stone age of Sibudu cave, KwaZulu-Natal, South Africa. *Archaeol. Anthropol. Sci.* 1, 95–122. doi:10.1007/s12520-009-0008-1
- Griffiths, J. (1972). “Ethiopian highlands,” in *World survey of climatology, in climates of Africa*. Editors H. Landsberg and N.L. Amsterda (New York, NY: Elsevier), Vol. 10, 369–381.
- Gutherz, X., Jallot, L., Lesur, J., Pouzolles, G., and Sordoillet, D. (2002). *Annales d’Éthiopie, De Boc-card/Centre Français des Études Éthiopiennes. Annales d’Éthiopie* 18, 181–190. doi:10.3406/ethio.2002.1019
- Hemming, S. R. (2004). Heinrich events: massive late Pleistocene detritus layers of the north atlantic and their global climate imprint. *Rev. Geophys.* 42, RG1005. doi:10.1029/2003RG000128
- Hensel, E. A., Bödeker, O., Bubenzer, O., and Vogelsang, R. (2019). Combining geomorphological–hydrological analyses and the location of settlement and raw material sites – a case study on understanding prehistoric human settlement activity in the southwestern Ethiopian Highlands. *E&G Quaternary Sci. J.* 68, 201–213. doi:10.5194/egqsj-68-201-2019
- Herrejón Lagunilla, Á., Carrancho, Á., Villalán, J. J., Mallol, C., and Hernández, C. M. (2019). An experimental approach to the preservation potential of magnetic signatures in anthropogenic fires. *PLoS One*. 14, e0221592. doi:10.1371/journal.pone.0221592
- Hildebrand, E. A., and Brandt, S. A. (2010). An archaeological survey of the tropical highlands of Kafa, southwestern Ethiopia. *J. Afr. Archaeol.* 8 (1), 43–63. doi:10.3213/1612-1651-10152

- Hildebrand, E. A., Brandt, S. A., Friis, I., and Demissew, S. (2019). "Paleoenvironmental reconstructions for the Horn of Africa: Interdisciplinary perspectives on strategy and significance," in *Trees, grasses and crops. People and plants in sub-saharan Africa and beyond*. Editors B. Eichorn and A. Höhn (Bonn, DE: Verlag Dr. Rudolf Habelt), 187–210.
- Holliday, V. T., and Gartner, W. G. (2007). Methods of soil P analysis in archaeology. *J. Archaeol. Sci.* 34 (2), 301–333. doi:10.1016/j.jas.2006.05.004
- Hunt, A. M., and Speakman, R. J. (2015). Portable XRF analysis of archaeological sediments and ceramics. *J. Archaeol. Sci.* 53, 626–638. doi:10.1016/j.jas.2014.11.031
- Inglis, R. H., French, C., Farr, L., Hunt, C. O., Jones, S. C., Reynolds, T., et al. (2018). Sediment micromorphology and site formation processes during the middle to later stone ages at the haa fteah cave, cyrenaica, Libya. *Geoarchaeology* 33 (3), 328–348. doi:10.1002/gea.21660
- Iuss Working Group Wrb (2014). *World Reference Base for Soil Resources International soil classification system for naming soils and creating legends for soil maps in World soil resources report*. Rome: FAO, 106, 188.
- Ivers-Tiffée, E., and von Münch, W. (2007). "Magnetische werkstoffe," in *Werkstoffe der Elektrotechnik*. Editors E. Ivers-Tiffée and W. von Münch (Wiesbaden (DE: B.G. Teubner Verlag) doi:10.1007/978-3-8351-9088-7\_6
- Junginger, A., and Trauth, M. H. (2013). Hydrological constraints of paleo-Lake Suguta in the Northern Kenya Rift during the African humid period (15–5 ka BP). *Global Planet. Change.* 111, 174–188. doi:10.1016/j.gloplacha.2013.09.005
- Kaniewski, D., Marriner, N., Cheddadi, R., Joel, G., and Campo, E. (2018). The 4.2 ka BP event in the Levant. *Clim. Past.* 14, 1529–1542. doi:10.5194/cp-14-1529-2018
- Karkanas, P. (2017). "Chemical alteration,," in *Encyclopedia of geoarchaeology. Encyclopedia of earth sciences series*. Editor A. S. Gilbert (Dordrecht, NL: Springer-Verlag) doi:10.1007/978-1-4020-4409-0\_126
- Kehl, M., Burow, C., Cantalejo, P., Domínguez-Bella, S., Durán, J. J., Henselowsky, F., et al. (2016). Site formation and chronology of the new Paleolithic site Sima de Las Palomas de Teba, southern Spain. *Quat. Res.* 85 (2), 313–331. doi:10.1016/j.yqres.2016.01.007
- Kehl, M., Eckmeier, E., Franz, S., Lehmkühl, F., Soler, J., Soler, N., et al. (2014). Sediment sequence and site formation processes at the Arbreca Cave, NE Iberian Peninsula, and implications on human occupation and climate change during the Last Glacial. *Clim. Past.* 10 (5), 1673–1692. doi:10.5194/cp-10-1673-2014
- Khalidi, L., Mologni, C., Ménard, C., Coudert, L., Gabriele, M., Davtian, G., et al. (2020). 9000 years of human lakeside adaptation in the Ethiopian Afar: Fisher-foragers and the first pastoralists in the Lake Abhe basin during the African Humid Period. *Quat. Sci. Rev.* 243, 106459. doi:10.1016/j.quascirev.2020.106459
- Klasen, N., Kehl, M., Mikdad, A., Brückner, H., and Weniger, G.-C. (2018). Chronology and formation processes of the Middle to Upper Palaeolithic deposits of Ifri n'Ammar using multi-method luminescence dating and micromorphology. *Quat. Int.* 485, 89–102. doi:10.1016/j.quaint.2017.10.043
- Kröpelin, S., Verschuren, D., Lézine, A.-M., Eggermont, H., Cocquyt, C., Francus, P., et al. (2008). Climate-driven ecosystem succession in the Sahara: the past 6000 years. *Science* 320, 765–768. doi:10.1126/science.1154913.5877
- Kuehn, D. D., and Dickson, D. B. (1999). Stratigraphy and noncultural site formation at the shurmai rockshelter (GnJm1) in the mukogodo hills of north-Central Kenya. *Geoarchaeology: Int. J.* 14 (1), 63–85. doi:10.1002/(SICI)1520-6548(199901)14:1<63::AID-GEA5>3.0.CO;2-F
- Laskar, J., Robutel, P., Joutel, F., Gastineau, M., Correia, A. C. M., and Levrard, B. (2004). A long-term numerical solution for the insolation quantities of the Earth. *A&A* 428 (1), 261–285. doi:10.1051/0004-6361:20041335
- Le Borgne, E. (1955). Susceptibilité magnétique anormale du sol superficiel. *Ann. Geophys.* 11, 399–419.
- Marean, C. W., Bar-Matthews, M., Fisher, E., Goldberg, P., Herries, A., Karkanas, P., et al. (2010). The stratigraphy of the middle stone age sediments at pinnacle point cave 13B (mossel bay, western cape province, South Africa). *J. Hum. Evol.* 59 (3–4), 234–255. doi:10.1016/j.jhevol.2010.07.007
- Mark, B. G., and Osmaton, H. A. (2008). Quaternary glaciation in Africa: key chronologies and climatic implications. *J. Quat. Sci.* 23, 589–608. doi:10.1002/jqs.1222
- Mentzer, S. M. (2017). "Rockshelter settings," in *Encyclopedia of geoarchaeology. Encyclopedia of earth sciences series*. Editor A. S. Gilbert (Dordrecht (NL): Springer-Verlag) doi:10.1007/978-1-4020-4409-0\_159
- Miller, C. E., Goldberg, P., and Berna, F. (2013). Geoarchaeological investigations at diepkloof rock shelter, western Cape, South Africa. *J. Archaeol. Sci.* 40 (9), 3432–3452. doi:10.1016/j.jas.2013.02.014
- Nesbitt, H., and Young, G. (1982). Early Proterozoic climates and plate motions inferred from major element chemistry of lutites. *Nature* 299 (5885), 715–717. doi:10.1038/299715a0
- Nicholson, S. E. (2018). The ITCZ and the seasonal cycle over equatorial Africa. *Bull. Am. Meteorol. Soc.* 99 (2), 337–348. doi:10.1175/BAMS-D-16-0287.1
- Okrusch, M., and Matthes, S. (2010). *Mineralogie*. Berlin, Germany: Springer-Verlag
- Ossendorf, G., Groos, A. R., Bromm, T., Tekelemariam, M. G., Glaser, B., Lesur, J., et al. (2019). Middle Stone Age foragers resided in high elevations of the glaciated Bale Mountains, Ethiopia. *Science* 365 (6453), 583–587. doi:10.1126/science.aaw8942
- Reimer, P., Austin, W., Bard, E., Bayliss, A., Blackwell, P., Bronk Ramsey, C., et al. (2020). The IntCal20 northern hemisphere radiocarbon age calibration curve (0–55 cal kBP). *Radiocarbon* 62 (4), 725–757. doi:10.1017/RDC.2020.41
- Schepers, C., Lesur, J., and Vogelsang, R. (2020). Hunter-gatherers of the high-altitude afro-montane forest – the Holocene occupation of Mount dendi, Ethiopia. *Azania* 55 (3), 329–359. doi:10.1080/0067270X.2020.1792709
- Segele, Z. T., Lamb, P. J., and Leslie, L. M. (2009). Large-scale atmospheric circulation and global sea surface temperature associations with Horn of Africa June–September rainfall. *Int. J. Climatol.* 29 (8), 1075–1100. doi:10.1002/joc.1751
- Stewart, B. A., and Jones, S. C. (2016). "Africa from MIS 6-2: the florescence of modern humans," in Africa from MIS 6-2: population dynamics and paleoenvironments. Editors S. C. Jones and B. A. Stewart (Dordrecht: Springer Netherlands), 1–20. doi:10.1007/978-94-017-7520-5\_1
- Texier, P. J., Porraz, G., Parkington, J., Rigaud, J. P., Poggenpoel, C., Miller, C., et al. (2010). From the Cover: a Howiesons Poort tradition of engraving ostrich eggshell containers dated to 60,000 years ago at Diepkloof Rock Shelter, South Africa. *Proc. Natl. Acad. Sci. USA.* 107, 6180–6185. doi:10.1073/pnas.0913047107
- Tierney, J. E., Lewis, S. C., Cook, B. I., LeGrande, A. N., and Schmidt, G. A. (2011). Model, proxy and isotopic perspectives on the east african Humid Period. *Earth Planet. Sci. Lett.* 307 (1–2), 103–112. doi:10.1016/j.epsl.2011.04.038
- Trauth, M. H., Asrat, A., Duesing, W., Foerster, V., Kraemer, K. H., Marwan, N., et al. (2019). Classifying past climate change in the Chew Bahir basin, southern Ethiopia, using recurrence quantification analysis. *Clim. Dynam.* 53 (5–6), 2557–2572. doi:10.1007/s00382-019-04641-3
- Tribolo, C., Asrat, A., Bahain, J. J., Chapon, C., Douville, E., Fragnol, C., et al. (2017). Across the gap: geochronological and sedimentological analyses from the Late Pleistocene-Holocene sequence of Goda Buticha, southeastern Ethiopia. *PLoS One.* 12 (1), e0169418. doi:10.1371/journal.pone.0169418
- Viste, E., and Sorteberg, A. (2013). Moisture transport into the Ethiopian highlands. *Int. J. Climatol.* 33, 249–263. doi:10.1002/joc.3409
- Vogelsang, R., and Wendt, K. P. (2018). Reconstructing prehistoric settlement models and land use patterns on Mt. Damota/SW Ethiopia. *Quat. Int.* 485, 140–149. doi:10.1016/j.quaint.2017.06.061
- Willmes, C., Becker, D., Brocks, S., Hütt, C., and Bareth, G. (2017). High resolution köppen-geiger classifications of paleoclimate simulations. *Trans. GIS.* 21, 57–73. doi:10.1111/tgis.12187
- WoldeGabriel, G., James, L. A., and Robert, C. W. (1990). Geology, geochronology, and rift basin development in the central sector of the Main Ethiopian Rift. *Geol. Soc. Am. Bull.* 102 (4), 439–485. doi:10.1130/0016-7606(1990)102<0439:GGARBD>2.3.CO;2
- WoldeGabriel, G., Walter, R. C., Aronson, J. L., and Hart, W. K. (1992). Geochronology and distribution of silicic volcanic rocks of Plio-Pleistocene age from the central sector of the Main Ethiopian Rift. *Quat. Int.* 13, 69–76. doi:10.1016/1040-6182(92)90011-P
- Wright, D. K. (2017). Humans as agent in the termination of the african Humid Period. *Front. Earth Sci.* 5, 4. doi:10.3389/feart.2017.00004
- Xiao, J., Zhang S., Fan, J., Wen, R., Zhai, D., Tian, Z., et al. (2018). The 4.2 ka BP event: multi-proxy records from a closed lake in the northern margin of the East Asian summer monsoon. *Clim. Past.* 14 (10), 1417–1425. doi:10.5194/cp-14-1417-2018

**Conflict of Interest:** The authors declare that the research was conducted in the absence of any commercial or financial relationships that could be construed as a potential conflict of interest.

Copyright © 2021 Hensel, Vogelsang, Noack and Bubenzer. This is an open-access article distributed under the terms of the Creative Commons Attribution License (CC BY). The use, distribution or reproduction in other forums is permitted, provided the original author(s) and the copyright owner(s) are credited and that the original publication in this journal is cited, in accordance with accepted academic practice. No use, distribution or reproduction is permitted which does not comply with these terms.

### 3.1 Supplement material

This supplementary material is published as part of the following open access publication:

Hensel, E. A., Vogelsang, R., Noack, T., and Bubbenzer, O. (2021). Stratigraphy and Chronology of Sodicho Rockshelter – A new sedimentological record of past environmental changes and human settlement phases in Southwestern Ethiopia. *Frontiers in Earth Science* 8(640). doi: <https://doi.org/10.3389/feart.2020.611700>.

## *Supplementary Material*

### 1 Supplementary Figures and Tables

The illustrations and the table shown here are a supplement to the results discussed in chapter 4 and to the discussion in chapter 5.3.

#### 1.1 Supplementary Table

**Table S1:** Field description of sedimentological units of the excavation quadrants F34, 35 and G34, 35. Information about grain size are according to the scale by Udden (1914) and Wentworth (1922).

<b>Unit</b>	<b>Description</b>
<b>I</b>	<p>Multi-layered anthropogenic surface unit: Grayish brown to light brown sediment with a main grain size of silt to fine sand and a moderate to poor sorting. The medium to coarse grained gravels are angular to subangular rounded with a high to medium sphericity. The gravels are identified as trachytic rock, from the common bed rock. The main sediment is compact and crumbly with firm aggregates. Macroscopic grading or bedding are absent.</p> <p>Only few charcoal fragments but also unburned botanical remains. Sherds of recent, black-colored pottery. The few obsidian lithics seem to be displaced. This is the only anthropogenic layer where bones are preserved. A pit filled with charcoal, ash and potsherds in square F35 extends down to Unit III.</p>
<b>II</b>	<p>Multi-layered geogenic unit with an upper light brownish grayish layer, a lighter colored tephra in the middle and a bright white to light gray tephra at the bottom of the unit. The upper layer has a main grain size of coarse silt to fine sand (medium sand). The coloration of this layer differs within the excavation squares, e.g. the brownish gray color in square G35 is much darker. Sediment aggregates and brown round lenses are included in a low frequency.</p> <p>The transition to the lower layer is gradual in F35, with thin brownish, discontinuous and horizontal microlamination (up to 2 mm thick). The lower situated tephra is thicker and lighter colored and has also a fine sand to coarse sand grain size. Brownish angular lenses (silt grains size) are less frequent and the main sediment is firm and seems well sorted and homogenous. The boundary to the lower layer is undulated and sharp.</p> <p>The lowest layer is not continuous, partly eroded and only exposed in square F34 and F35. The white to white gray colored tephra is very well sorted and homogenous. The main grain size is fine sand to medium sand.</p> <p>This unit is archaeological sterile.</p>

<b>III</b>	<p>Multi-layered anthropogenic unit with a dark greenish brown upper layer, a bright reddish-brown layer and a lower darker greenish brown layer. There is a sharp boundary to the above situated Unit II. The upper layer of this Unit III consists of clayish silt mixed with fine reddish lenses (0.5 - 1.0 cm) and charcoal (&lt; 0.5 mm) particles. The reddish sediment layer also occurs as bright red and even orange red in square F35 and G35. This layer consists of particles with main grains size of fine sand to silt. Brownish angulate lenses are unevenly distributed in this layer. The lowest greenish-brown layer consists of fine silt with charcoal fragments and is enriched in organic material. This layer can be addressed as a transition area to the underlying unit IV, since thin volcanic ash lenses are intermingled. The change appears to be gradual.</p> <p>The sediment of this unit is very firm. Especially the bright red layers seem cemented and were hard to sample (sedimentology). Macroscopic bedding or grading are absent. The lower section of this unit is characterized by inhomogeneous distributed volcanic ash lenses (angular shape), that are comparable to the volcanic ash of Unit IV. Here the sediment seems disturbed.</p> <p>Archaeological finds are mainly obsidian stone artefacts and only few potsherds. Concentrations of charcoal fragments with some larger pieces up to 1 cm indicate the location of fireplaces. One hearth is bordered with big trachyte gravels. An artificial pit is documented in profile G35 and another pit filled with charcoal is preserved in square F35. Both pits extend into the underlying sediment Unit IV.</p>
<b>IV</b>	<p>Two-layered geogenic unit consisting of tephra with an upper greenish-gray layer and a lower grayish-white layer. This unit is discontinuous and tilts slightly in north direction (~10 %) as can be seen in the east profile of F35. Its thickness varies throughout the excavation squares. In square G35 the tephra layers are no longer a separate unit, but disturbed and mixed with the overlying anthropogenic sediment unit. The upper tephra has a main grain size of silty sand to medium sand and its boundary to the overlying unit is gradual with a color transition from gray to brown-gray. The frequency of intermingled brownish angular lenses decreases with increasing depth.</p> <p>A discontinuous transition with fine, brownish lamination (1mm thick) separates the upper layer from the lower part. The laminae have a fine clayish silt grain size. Single well-preserved charcoal pieces (<math>\leq 1</math> cm) are distributed in the transition area.</p> <p>The lower layer of this unit is very well sorted and homogeneous. It has a main grain size of coarse silt to fine sand (medium sand). Grading or bedding is absent. Gravels or rock fragments are also absent. The boundary to the underlying Unit V is sharp and marked by a reddish-brown band (~ 0.5 mm) that has a clayish silt grain size.</p> <p>The origin of the charcoal is not yet clear, since there are no further archaeological remains in the layers. For this reason, this unit can be considered as archaeological sterile.</p>
<b>V</b>	<p>Multi-layered anthropogenic unit, with a clayish silt grain size. The main sediment of the upper layer is dark brown and relatively firm. Small gravels and single big subangular gravels with a medium to high sphericity are included. Their frequency is lower than in</p>

	<p>the above situated units. Isolated light-colored tephra lenses (2-4 cm thick) are found in the upper part of the unit. The tephra lenses have a similar composition as the tephra of Unit IV and seem to be displaced.</p> <p>The lower part of this unit is characterized by concentrations of charcoal fragments (up to 1.5 cm), indicating fireplaces. The sediment below the charcoal concentrations is red colored showing the impact of heat. Restricted to square F35 a discontinuous, irregular lens of light-colored tephra is situated directly underneath the reddish colored sediment below the hearth. The tephra seems dislocated and partly eroded. There is an extremely high density of archaeological finds, almost exclusively stone artefacts made of obsidian, in connection with the fireplaces. Remarkable are a large number of charred fruit kernels that were found in the fireplaces.</p> <p>The transition to the underlying Unit VI is gradual with an increase in clay content and red sediment color. It seems that both units V and VI are mixed in this transition area.</p>
<b>VI</b>	<p>Multi-layered geogenic unit. The thicker, upper layer is brown to reddish brown, followed by a yellowish layer and a brownish red layer.</p> <p>The sediment of the upper layer has a fine grain size from clayish silt to fine sandy silt. It is firm (cohesive), but with a crumbly and polyhedral fabric, caused by high clay content. The sediment is inhomogeneous with several lighter colored disturbances. The sediment is fine grained throughout, with a few isolated angular small gravels identified as trachyte.</p> <p>A slightly rounded trachytic boulder of 20 cm diameter with high sphericity marks the boundary to the underlying layer. This is brown colored with the same grain size as above, but with several small gravels. This layer is followed by a not continuous yellowish, firm layer with silt grain size that inclines slightly in square F35. The whole layer has a blocky structure, with thin brownish sediment in between the aggregate.</p> <p>This unit is archaeological sterile.</p>
<b>VII</b>	<p>Multi-layered anthropogenic unit. The upper part of this unit in square F35 and G35 is characterized by a rockfall layer of trachytic boulders with a maximum diameter of up to 70 cm (fig. 4). The boulders are irregular shaped, with a rounded upper surface and an angular lower surface. The finer grained (coarse silt to fine sand) sediment around the boulders includes several angular coarse gravels with a medium sphericity. There is a high density of lithic artefacts between and underneath the boulders, but only scattered charcoal pieces. In contrast to all other archaeological layers, the orientation of most stone artefacts is not horizontal but inclined.</p> <p>The sediment below is relative firm with a brown color and clayish silt to fine sandy silt grain size. It is not homogenous, with intermixed tephra in the lower part and seems disturbed. With increasing depth, the frequency of coarse gravel increases.</p>
<b>VIII</b>	<p>Thin light brownish geogenic unit with a sandy silt grainsize. The sediment is very firm with intermixed charcoal fragments. The frequency of angulate small gravels is much lower than in the unit above and the unit below. The lower section of this unit is</p>

	<p>characterized by several horizontal, yellow to gray colored layers, with a maximum thickness of &lt; 0.5 mm. In some areas, these are interrupted by disturbances from the overlying anthropogenic Unit VII.</p> <p>The origin of the charcoal is not yet clear, since there are no further archaeological remains in the layers. For this reason, this unit can be considered as archaeological sterile.</p>
<b>IX</b>	<p>Multi-layered anthropogenic unit with a clayish silt to fine sandy silt grain size. The reddish-brown sediment is not homogeneous and seems slightly disturbed. This unit is very firm and includes medium to big angular/subangular trachytic gravels.</p> <p>Cultural material includes lithic artefacts mainly made of obsidian but also chert gains in importance as raw material for the stone tool production. Charcoal is rare but sometimes also larger pieces (<math>\leq 1</math> cm) occur.</p>

## 1.2 Supplementary Figures

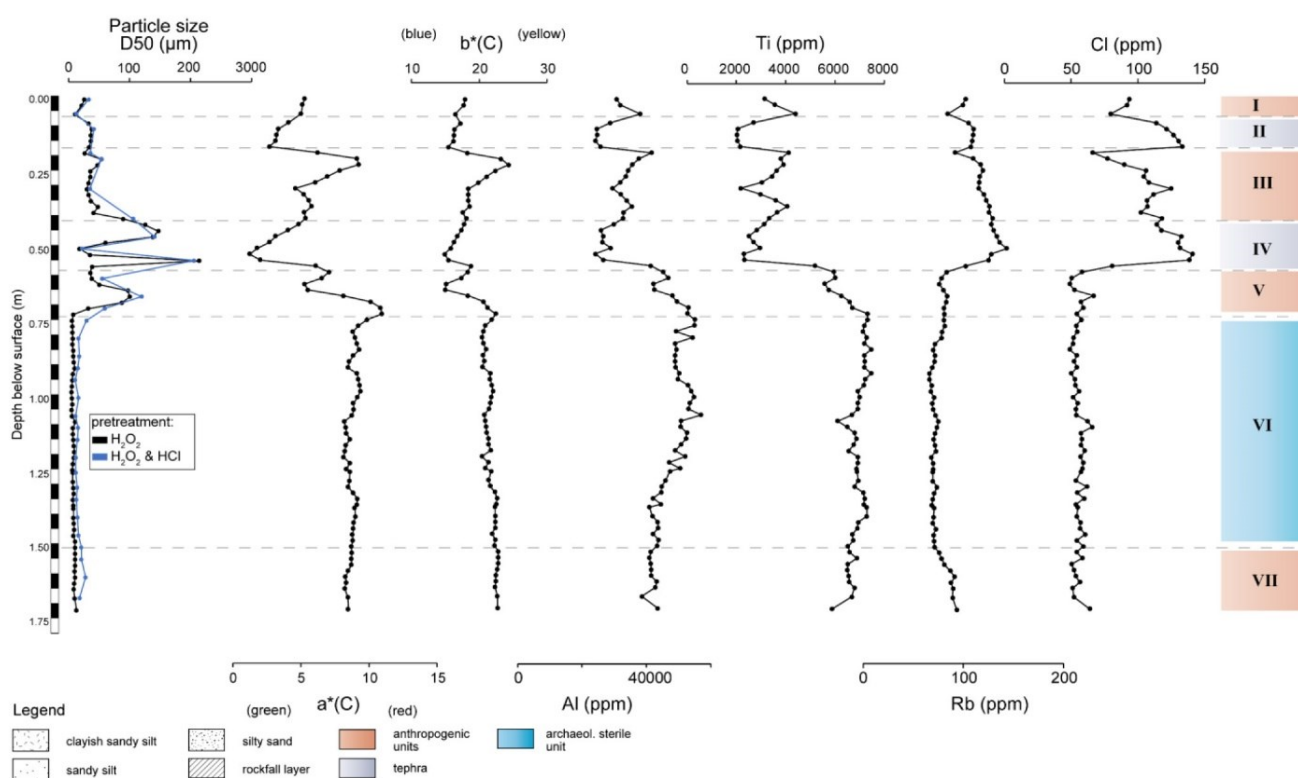


**Figure S1.** Further sedimentological and geochemical properties of the profile F35 at the Sodicho Rockshelter: median of particle size (pretreatment with  $\text{H}_2\text{O}_2$  or  $\text{H}_2\text{O}_2$  &  $\text{HCl}$ ); CIELab color values  $a^*$  and  $b^*$ ; element trends (Al, Ti, Rb, Cl).

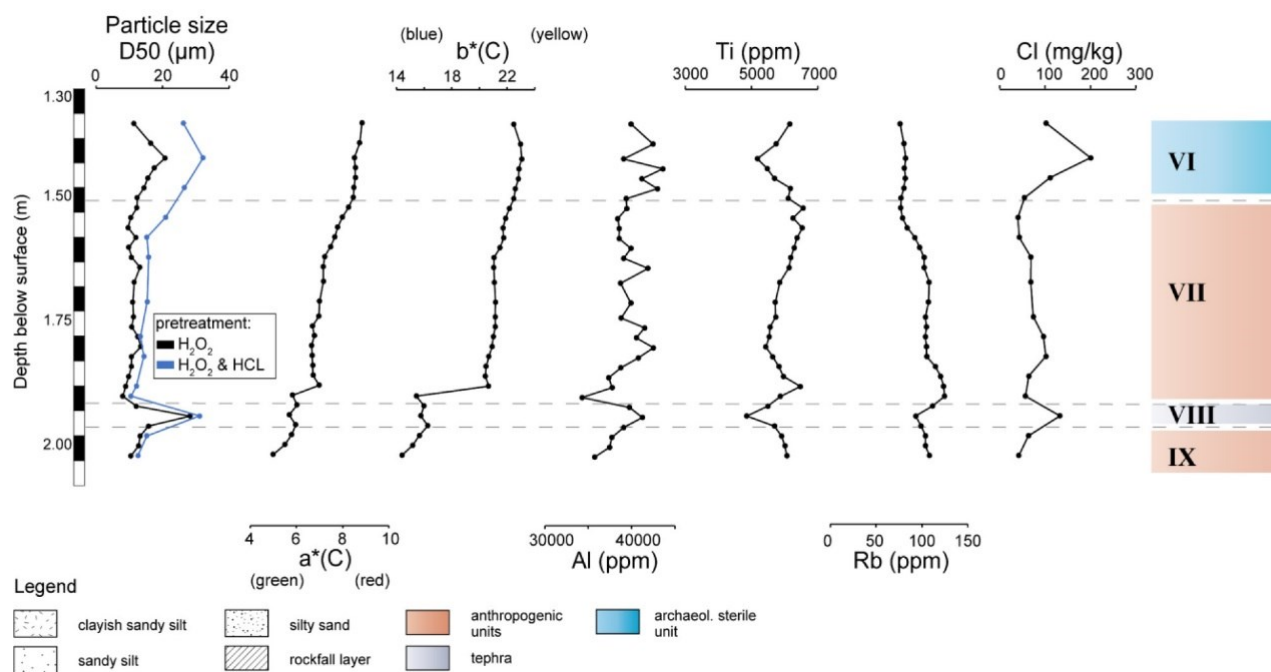


**Figure S2.** Further sedimentological and geochemical properties of the profile G35: median of particle size (pretreatment with H<sub>2</sub>O<sub>2</sub> or H<sub>2</sub>O<sub>2</sub> & HCl); CIELab color values a\* and b\*; element trends (Al, Ti, Rb, Cl).

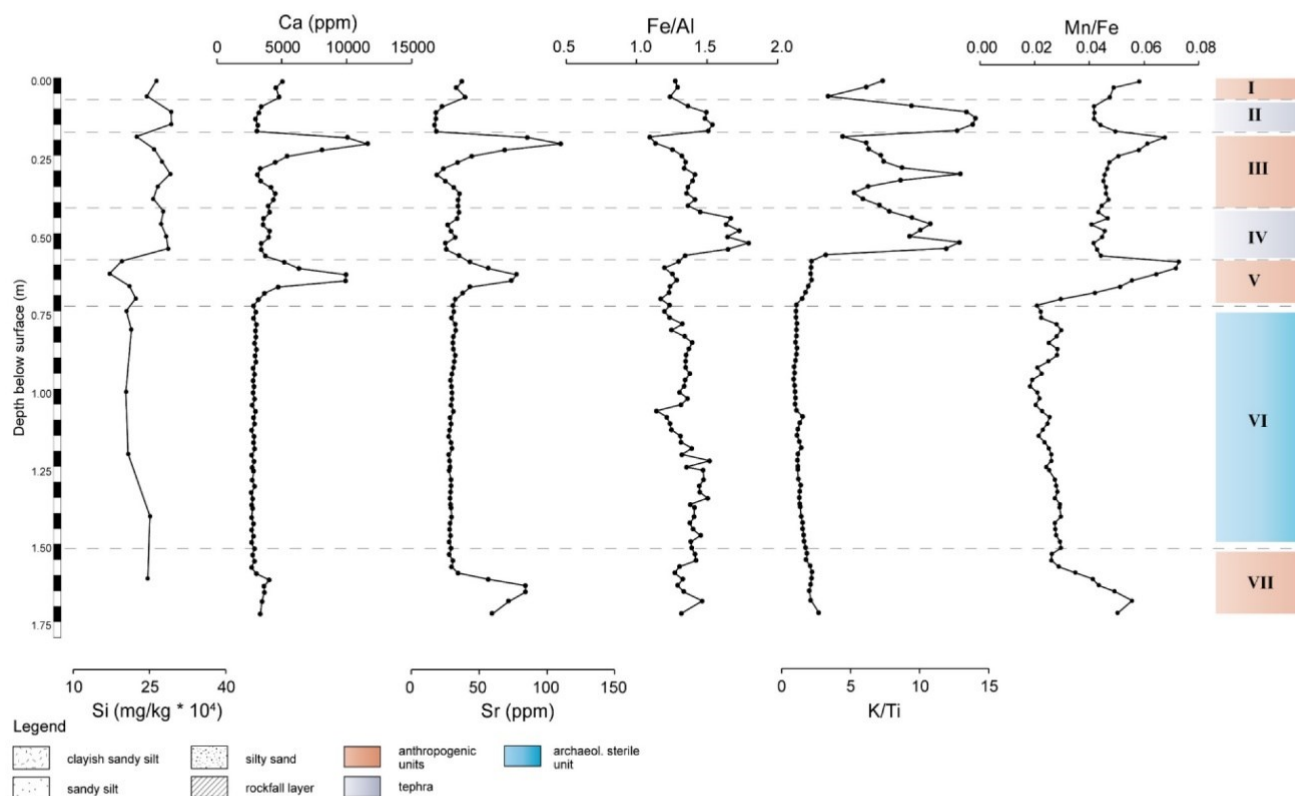


**Figure S3.** Further sedimentological and geochemical properties of the profile F35: element trends (Si, Ca, Sr); element ratios (Fe/Al, K/Ti, Mn/Fe).

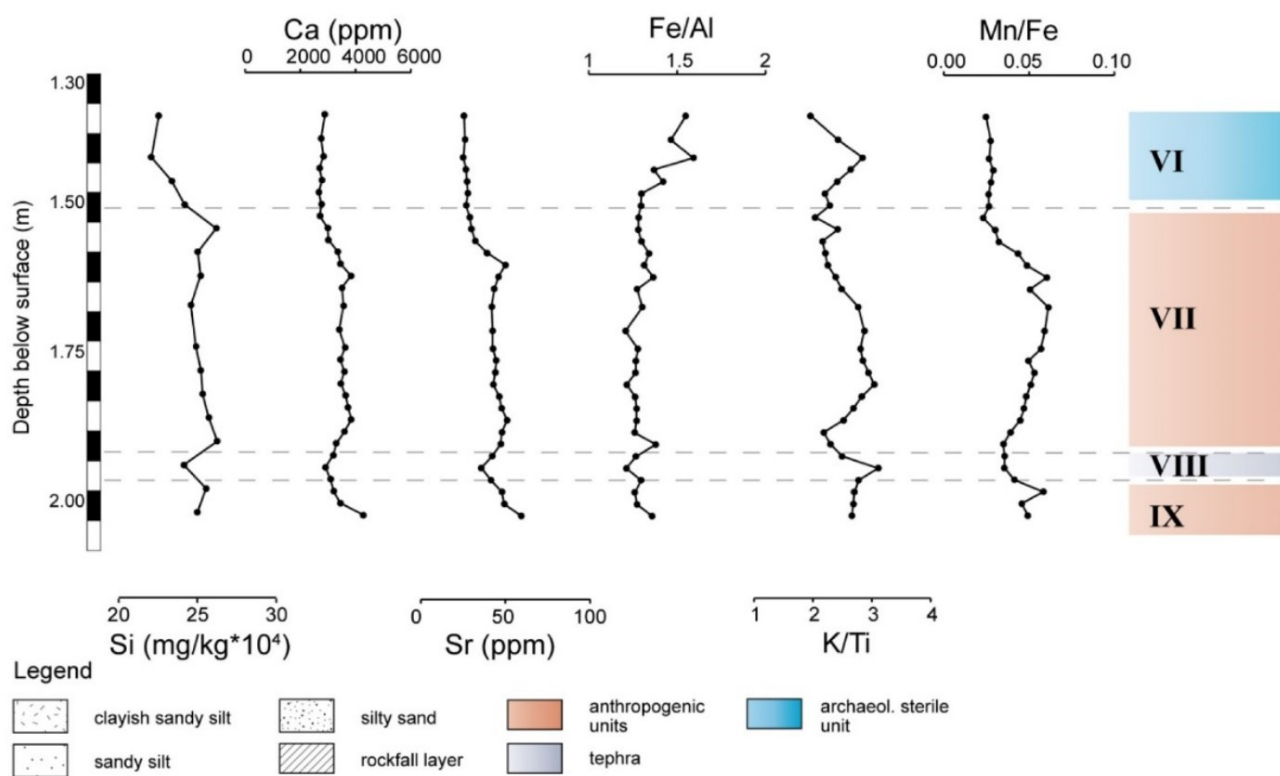


**Figure S4.** Further sedimentological and geochemical properties of the profile G35: element trends (Si, Ca, Sr); element ratios (Fe/Al, K/Ti, Mn/Fe).

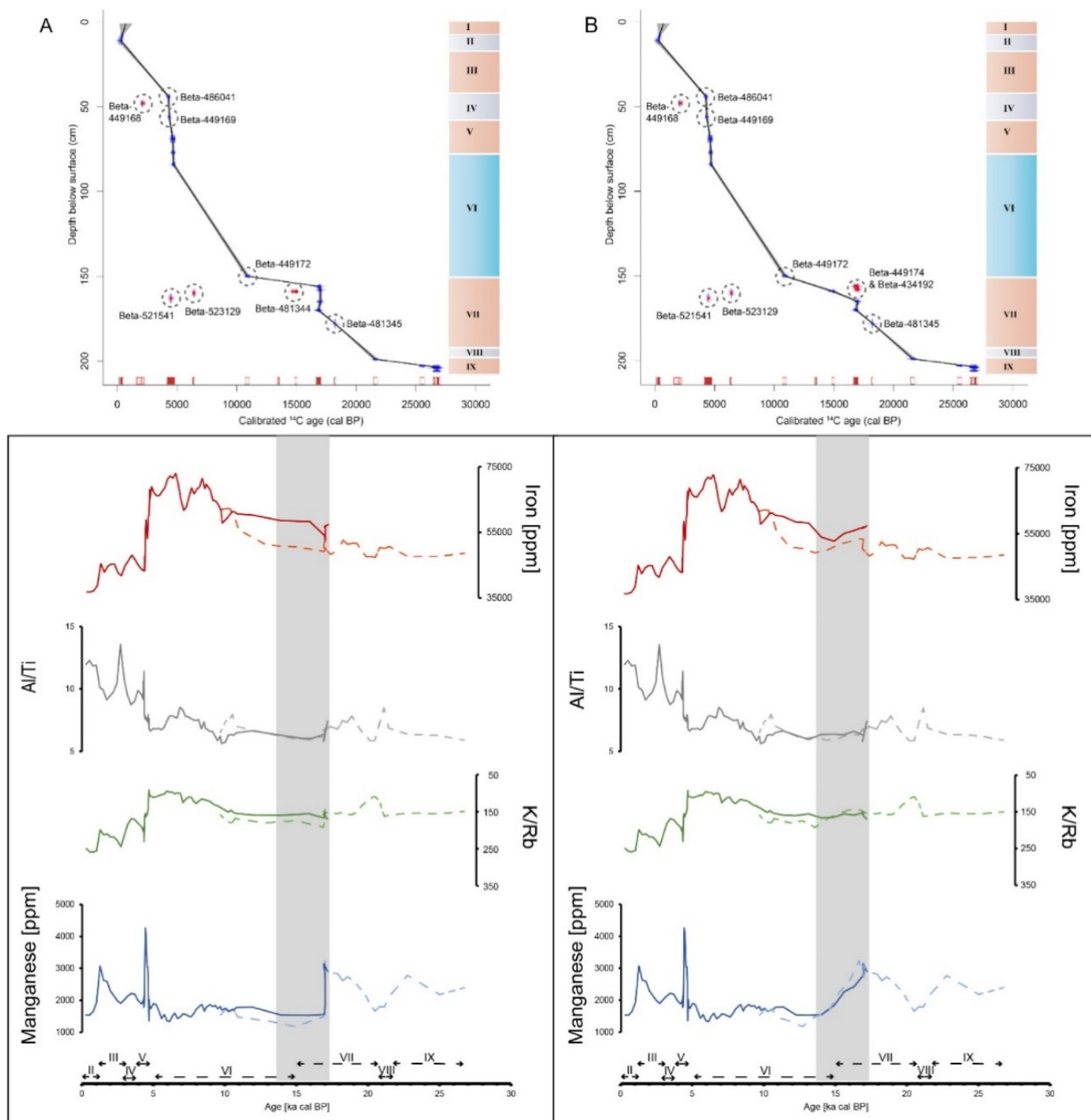


**Figure S5.** Comparison of two classical age-depth models for the Sodicho Rockshelter and the comparison of geochemical records calculated with the age data of the models; (A) For the age-depth model the sample Beta-481344 was excluded, resulting in a drop of Mn values and an increase in Fe values at ~ 17 ka cal BP; (B) For the age-depth model the sample Beta-481344 was included and the samples Beta-449174 and Beta-434192 were excluded, resulting in a gradual decrease in Mn values and a fluctuating increase in Fe values. There are only minor differences between the Al/Ti and K/Rb geochemical diagrams in A and B between 17 ka and 14 ka cal BP.

---

## Chapter IV

### 4. A Multi-Method Approach for Deciphering Rockshelter Microstratigraphies — The Role of the Sodicho Rockshelter (SW Ethiopia) as a Geoarchaeological Archive

Elena A. Hensel<sup>1\*</sup>, Martin Kehl<sup>1</sup>, Luisa Wöstehoff<sup>2</sup>, Katharina Neumann<sup>3</sup>, Ralf Vogelsang<sup>4</sup> and Olaf Bubenzer<sup>5</sup>

*1 Institute of Geography, University of Cologne, Cologne, Germany*

*2 Institute of Crop Science and Resource Conservation - Soil Science and Soil Ecology, University of Bonn, Bonn, Germany*

*3 Institute of Archaeological Sciences, Goethe University, Frankfurt am Main, Germany*

*4 Institute of Prehistoric Archaeology, University of Cologne; Germany*

*5 Institute of Geography and Heidelberg Center for the Environment (HCE), Heidelberg University, Heidelberg, Germany*

Published in *Geosciences* 12(2), 92, 1–36, 2022

doi: <https://doi.org/10.3390/geosciences12020092>

Special Issue: *Pleistocene Hunter-Gatherers Geoarchaeology*

*Keywords: geoarchaeology, Ethiopia, micromorphology, black carbon, phytoliths, pedogenic oxides*

Note: The following pages originate from the original peer-reviewed article published at *Geosciences*.

## Article

# A Multi-Method Approach for Deciphering Rockshelter Microstratigraphies—The Role of the Sodicho Rockshelter (SW Ethiopia) as a Geoarchaeological Archive

Elena A. Hensel <sup>1,\*</sup>, Martin Kehl <sup>1</sup>, Luisa Wöstehoff <sup>2</sup>, Katharina Neumann <sup>3</sup>, Ralf Vogelsang <sup>4</sup>  and Olaf Bubbenzer <sup>5</sup> 

<sup>1</sup> Institute of Geography, University of Cologne, 50923 Cologne, Germany; kehlm@uni-koeln.de

<sup>2</sup> Institute of Crop Science and Resource Conservation—Soil Science and Soil Ecology, University of Bonn, 53113 Bonn, Germany; luisa.woestehoff@gmail.com

<sup>3</sup> Institute of Archaeological Sciences, Senckenberg Research Institute, Goethe University, 60323 Frankfurt am Main, Germany; k.neumann@em.uni-frankfurt.de

<sup>4</sup> Institute of Prehistoric Archaeology, University of Cologne, 50931 Cologne, Germany; r.vogelsang@uni-koeln.de

<sup>5</sup> Heidelberg Center for the Environment (HCE), Institute of Geography, Heidelberg University, 69120 Heidelberg, Germany; olaf.bubbenzer@uni-heidelberg.de

\* Correspondence: elena.hensel@uni-koeln.de; Tel.: +49-(0)-221-470-6524



**Citation:** Hensel, E.A.; Kehl, M.; Wöstehoff, L.; Neumann, K.; Vogelsang, R.; Bubbenzer, O. A Multi-Method Approach for Deciphering Rockshelter Microstratigraphies—The Role of the Sodicho Rockshelter (SW Ethiopia) as a Geoarchaeological Archive.

*Geosciences* **2022**, *12*, 92. <https://doi.org/10.3390/geosciences12020092>

Academic Editors:

Rossana Sanfilippo and  
Jesus Martinez-Frias

Received: 14 December 2021

Accepted: 8 February 2022

Published: 17 February 2022

**Publisher's Note:** MDPI stays neutral with regard to jurisdictional claims in published maps and institutional affiliations.



**Copyright:** © 2022 by the authors. Licensee MDPI, Basel, Switzerland. This article is an open access article distributed under the terms and conditions of the Creative Commons Attribution (CC BY) license (<https://creativecommons.org/licenses/by/4.0/>).

**Abstract:** The Sodicho Rockshelter in the southwestern Ethiopian Highlands presents a unique site that contains sediments of Upper Pleistocene and Holocene occupation phases of hunter-gatherer communities. Excavations and previous geoarchaeological research provided a first <sup>14</sup>C chronostratigraphic framework for the last 27 ka cal BP, which supports the hypothesis of a potential environmental refugium during the Late Glacial Maximum (LGM, ~21 ± 2 ka). Nonetheless, it is necessary to extend the preliminary interpretation of stone tool assemblages, and the geoarchaeological analyses carried out so far to provide in-depth information on prehistoric human behavior at the site under changing climatic and environmental conditions. In this study, we reinvestigate the complex stratigraphy and the paleoclimatic context of Sodicho in order to expand the knowledge about site formation, post-depositional disturbances, weathering influences, and the anthropogenic impact on the sediment deposits. Micromorphological observations and the determination of active pedogenic oxides offered a more detailed look at the microstratigraphic record in relation to shifting moisture conditions during the African Humid Period (AHP, ~15 – 5 ka). Sediment alteration and reworking are connected to the influence of sheet flow, biological activity, and human impacts such as dumping activity and site maintenance. A comparison with black carbon (BC) analyses and a qualitative phytolith ratio (quantification of dark and light phytoliths) provided evidence for variations in human fire intensity. Our collaborative and multidisciplinary approach demonstrates how the complex formation of a rockshelter site in a tropical setting with changing climatic and anthropogenic impacts can be tackled.

**Keywords:** geoarchaeology; Ethiopia; rockshelter; Upper Pleistocene; Holocene; micromorphology; black carbon; phytoliths; pedogenic oxides

## 1. Introduction

The sediment deposits at the Sodicho Rockshelter, a volcanic rockshelter in the southwestern Ethiopian Highlands, provide important evidence for hunter-gatherer occupation over the last 27 ka years, thereby partly closing one of the major chronological gaps associated with the time range of Marine Isotope Stage 2 (MIS 2) [1]. Located near the Mochena Borago Rockshelter, a key site documenting Upper Pleistocene hunter-gatherer communities [2–4], Sodicho offers a complementary stratigraphy. Since the bedrock has not yet been reached during the excavations, further deposits are expected at Sodicho.

The stratigraphy of an archaeological site, ideally in an intact and undisturbed state, illustrates the occupational history and behavior of past inhabitants, as well as past environmental conditions. Often, rockshelters provide excellent sediment traps. Nevertheless, stratigraphies can be influenced by changing depositional environments and post-depositional impacts [5]. Particularly, this holds true for stratigraphies of rockshelters in tropical regions, which are often subject to changing moisture conditions [5,6]. This can complicate the identification of sedimentary sources and depositional processes at these sites.

Geoarchaeological methods, such as sediment analyses, micromorphology, or geochemical investigations, allow the study of various depositional processes and add a geomorphological and geoscientific perspective to archaeological investigations. In particular, micromorphological observations allow conclusions about sediment alteration, translocation processes, and human activity at a site [7].

Prior geoarchaeological research at Sodicho revealed a complex depositional history, influenced by depositional circumstances of the Late Glacial Maximum (LGM,  $\sim 21 \pm 2$  ka) and the Early Holocene African Humid Period (AHP,  $\sim 15 - 5$  ka BP) [1,8,9]. Past humans used the rockshelter repeatedly, probably during both dryer and wetter phases. However, an in-depth microscopic analysis of the deposits that would offer a better understanding of the stratigraphy and possible human–environment interactions had not been carried out yet. Therefore, we conducted a multi-method approach to specify human behavior, such as the use of fire. First, we employed micromorphological thin section analysis to determine the composition and the spatial structure of identified features that are not visible to the naked eye [7,10]. Especially regarding site formation processes and activity of prehistoric humans in caves and rockshelters, micromorphological studies have proven to be an essential tool. Among many in-depth studies, the interplay of geogenic, biogenic, and anthropogenic processes were studied at several sites, for instance, in southern [11–13] and northern Africa [14–16], the Levant [17,18], the Iberian Peninsula [19], central Europe [20], Western Australia [21], central Asia [22], and southern Siberia [23,24]. These studies emphasized the significance of humans as depositional agents and allowed a better understanding, in particular about palaeoenvironmental changes, human activity zones, combustion practice, combustion bi-products, and synsedimentary human activity, such as trampling and site maintenance.

In this study, black carbon (BC) measurements are used as a proxy for fire residue input and past human–fire interactions. The term BC describes the sum of pyrogenic organic matter and may comprise all charred residues, charcoal, and soot particles [25]. The aromatic structures [26,27] render BC recalcitrant to decomposition so that it can remain in soil and sediments for several thousands of years (e.g., [28–30]). To quantify the total amount of BC and also its properties (the latter to indicate changes in fire temperature), we determined benzene polycarboxylic acids (BPCAs) as specific tracers [31–33].

Further verification of fire residue input provides a preliminary qualitative phytolith analysis in order to develop a simple ratio of burned and unburned phytoliths. Opal phytoliths, as inorganic silicate bodies, are produced in plant cells or the cell wall through polymerization of monosilicic acid ( $\text{H}_4\text{SiO}_4$ ) taken up by plant roots [34–36]. Dark discoloration of the phytoliths is often caused by exposure to a fire, which burns occluded natural carbon or plant organic tissue, suggesting either natural bushfire or human-induced fire activity [10,34,35,37].

Finally, we determined the concentration of active iron (Fe), silicon (Si), aluminum (Al), and manganese (Mn) in an acidified ammonium oxalate (AO) extract [38,39]. In soil science, the AO method has been regarded as quantifying poorly crystalline or amorphous pedogenic (hydr)oxides formed after deliberation of the metals by silicate weathering. However, other species, such as organic associations or poorly crystalline aluminosilicates, may be dissolved by the AO extract as well [40].

The main aims of this study are (a) the extension of knowledge about the site formation processes and post-depositional alteration of the stratigraphy during the last 27 ka years,

(b) the identification of microscopic evidence on the degree of weathering under the influence of changing humidity within the rockshelter, (c) the determination of human activities with emphasis on the reconstruction of human fire activity, and finally (d) to demonstrate that such a geoarchaeological multi-method approach allows tackling complex rockshelter stratigraphies in a tropical environment in general.

## 2. The Site: Setting and Background

Sodicho Rockshelter is a ~30 m deep cavity on the southern flank of the trachytic Mount Sodicho, a volcanic mountain in the southwest Ethiopian Highlands (E 37°36'44 and N 7°15'21). The research area lies west of the southern Main Ethiopian Rift and the southern Ethiopian Plateau, east of the Omo River Canyon, and south of the three circular Wagebeta Calderas (Figure 1a). It is characterized by past volcanic activity and tectonic stress that occurred during the late development of the Ethiopian rift system [41–44]. The natural vegetation of Mount Sodicho is subject to drastic changes as a result of recent human impact. Nowadays, dense settlement, agriculture and cattle farming, human-induced deforestation, and massive soil erosion are characteristic, in particular at the relatively flat summit and the slopes. The average precipitation is 2000 mm per year. Still, annual and inter-annual precipitation changes have an effect on the vegetation cover (Figure 1b,c).

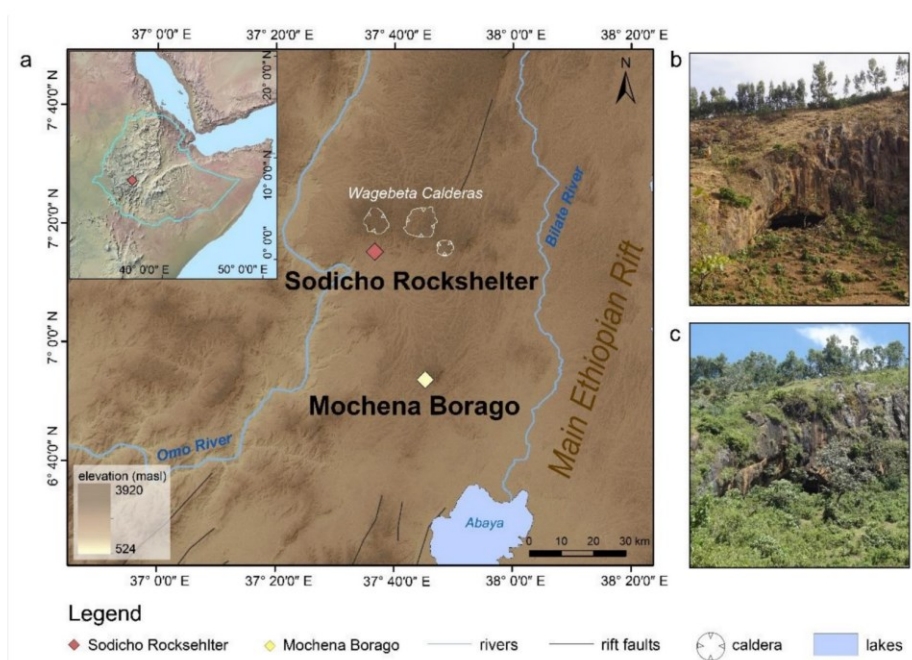


**Figure 1.** (a) Map of the study area in the Southwestern Ethiopian Highlands (DEM data by ASTER GDEM and Natural Earth raster map data); (b) During the dry season, natural plant growth is significantly reduced (photo by R. Vogelsang, 16 February 2016); (c) Mount Sodicho is heavily vegetated after the main rainy season (photo by E. Hensel, 18 November 2018).

The mountain itself has an irregular dome structure affected by an episodic and permanent hydrological system [44]. River erosion and gully formation are common phenomena, leading to the exposure of scattered obsidian raw material. Recent soil erosion exposed relatively fertile, red-colored, and kaolinite-rich humic Nitisols, typical for the tropical highlands [45,46].

The south-facing opening of the rockshelter is located below steep rock walls. Large boulders (3–4 m) prevent direct access to the cave and thus the direct influence of weather

conditions. The trachytic bedrock is grey to yellowish in color and erodes easily in certain places. During and immediately after the rainy season, the shelter is affected by the water dripping down the ceiling, resulting in constant dripping areas, the formation of shallow pools and drip holes, as well as weathering of large boulders within the cave. The rock surface of the walls is affected by dark staining, alveolar weathering (honeycomb weathering), and uneven exfoliation. During dry periods, evidence of residual moisture is limited to damp areas in the rear of the rockshelter.

The Sodicho Rockshelter, first visited by our team during surveys in 2012, lies ~40 km away from the key site Mochena Borago Rockshelter located on the southwestern slope of Mt. Damota. Mochena Borago has been well investigated since 1998 and contains Upper Pleistocene sedimentary units and cultural remains dated to >50 ka to ~36 ka and the Holocene [2,3,47,48]. The excavations at Sodicho were undertaken annually from 2015 to 2018 in the backward area of the rockshelter, starting with two test pits of 50 × 50 cm (Figure 2). The main pit was extended to 4 m<sup>2</sup> down with a maximum depth of ~2 m without reaching the bedrock. In 2016, a third pit (50 × 50 cm) with a depth of 60 cm was added [1].

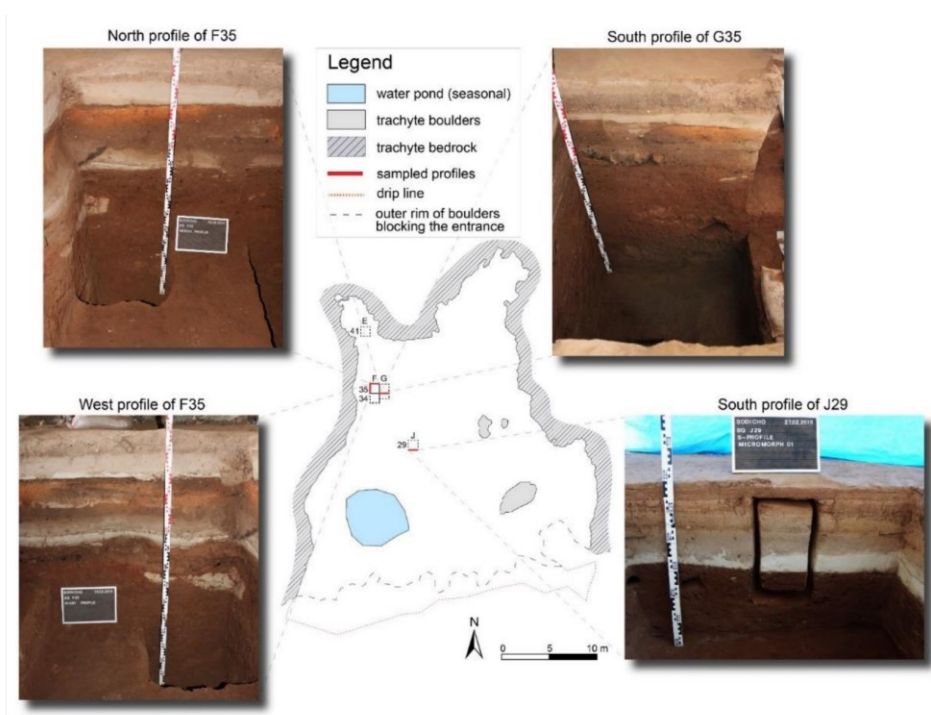


**Figure 2.** Floorplan of the Sodicho Rockshelter showing images of the excavation pits mentioned in the text (photos by R. Vogelsang, February 2016).

The most recent geoarchaeological investigations at Sodicho Rockshelter comprise a selection of sedimentological and geochemical analyses and the establishment of a chronological framework with <sup>14</sup>C dating. So far, a complex stratigraphy with nine sediment units was identified that include five anthropogenic units (in terms of geogenic sediment deposits impacted by human activity during occupation phases I, III, V, VII, and IX), three distinct allochthonous tephra units (II, IV, VIII) and a thick clayey archaeologically sterile unit (VI) (Figure 3) [1].

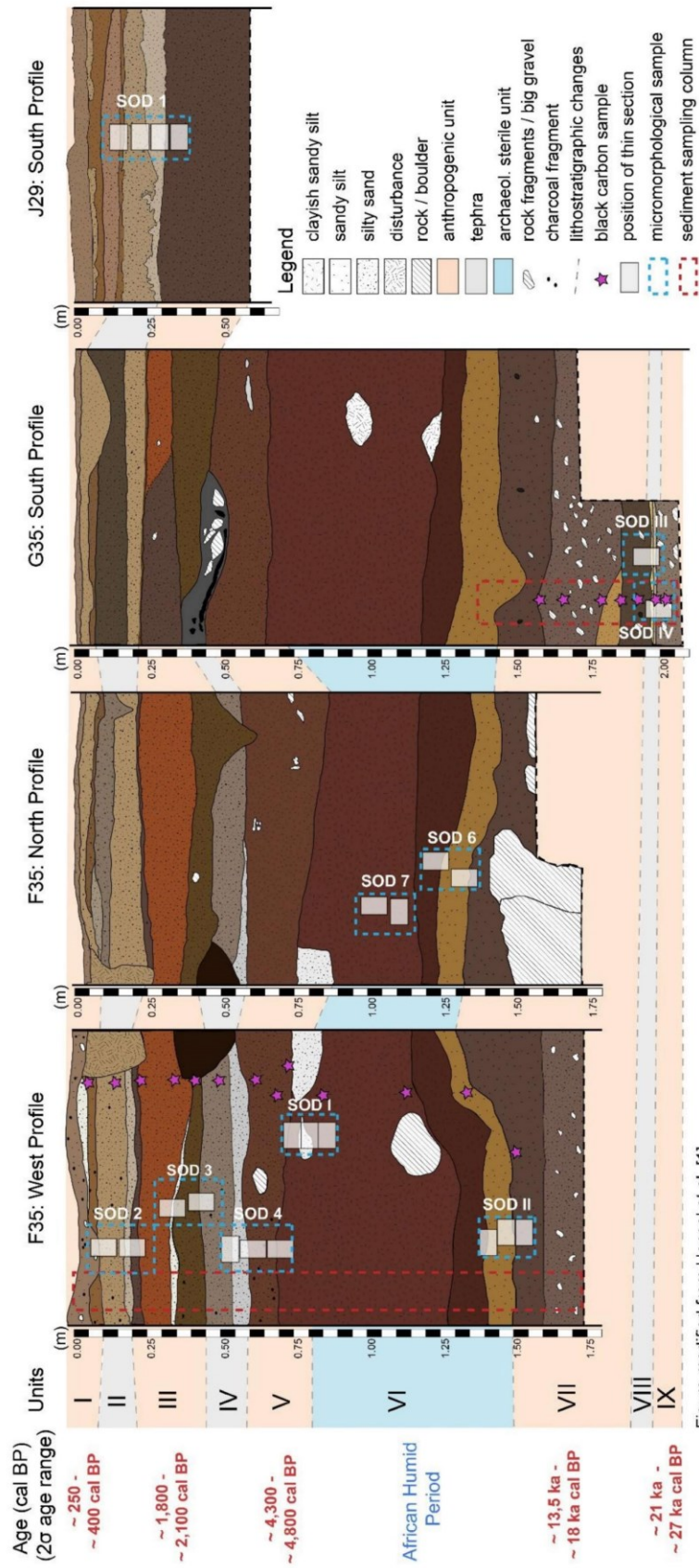
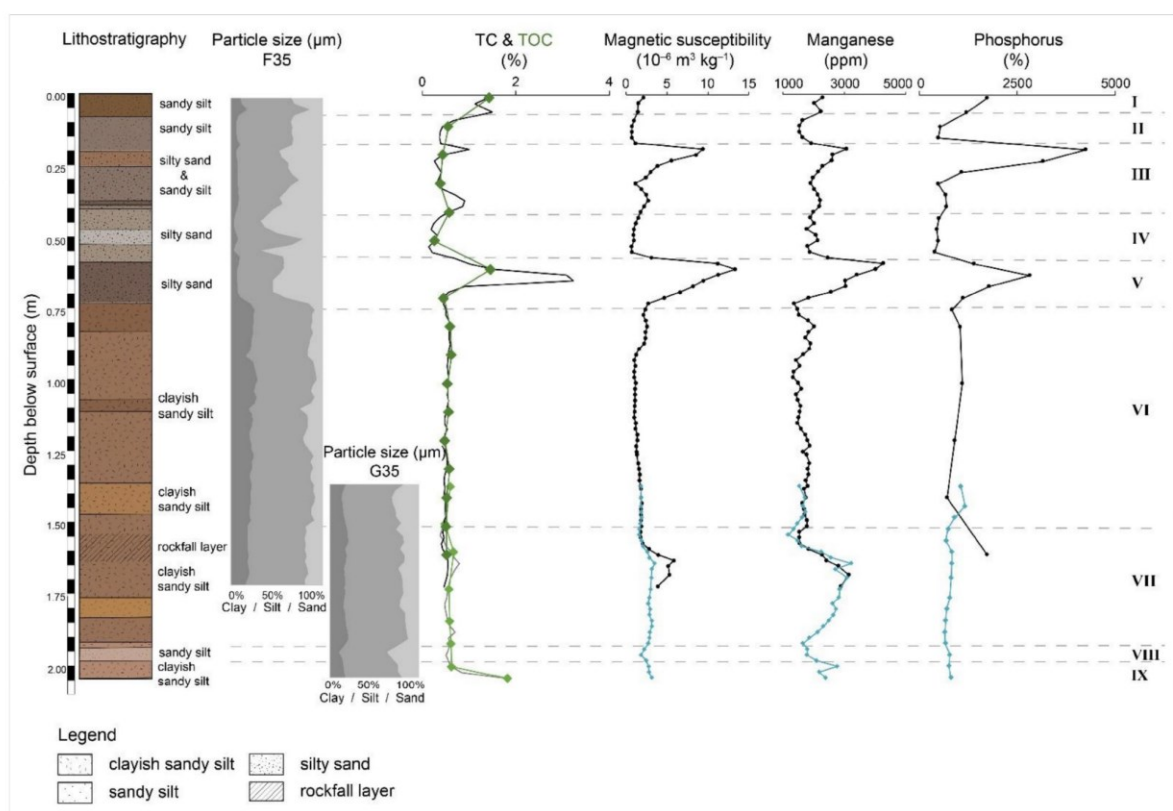


Figure modified from Hensel et al. [1].

**Figure 3.** Schematic illustration of the excavation profiles F35 west and north, G35 south and J29 south. Red ages refer to calibrated <sup>14</sup>C age range of 31 radiocarbon samples. Sediment samples are indicated in red, micromorphological sample blocks in blue, thin sections as whitish squares and BC samples as stars. A rockfall layer is in the upper part of Unit VII is illustrated in square F35 as white crosshatched boulders. The relative thicknesses of the sediment units are indicated in the background by different colors (mod. [1]).

According to macroscopic observations in the field, the deposits are slightly tilted to the northern backwall of the shelter. The occupational layers are recognized by a mostly dark brownish sediment color with an average grain size of silt and fine sand. In addition, some layers of these units show sediment rubification. Cultural remains and structures include lithic obsidian artifacts, macroscopic charcoal, hearths, and pits. Bone material has not been preserved in layers older than some hundred years due to the moist and acidic milieus of the sediments. The cultural units have a certain sedimentological fingerprint, characterized by higher values of total organic carbon (TOC), magnetic susceptibility (MS), manganese (Mn), and phosphorus (P) (Figure 4) [1]. The presence of hearth features and the lateral distribution of macroscopic evidence for fire residue in Unit III and V [1] represent in situ burning events as known from other rockshelter sites [49].



**Figure 4.** Sedimentological and geochemical properties of the profile F35 (black graphs) and G35 (grey graphs): carbon content with TC and TOC (green graph); magnetic susceptibility, element trends (manganese and phosphorus) (mod. [1]).

Radiocarbon measurements, mainly of charcoal, date the upper anthropogenic units between ~1800 and ~2100 cal BP (Unit III) and ~4300 and ~4800 cal BP (Unit V) [1]. Both units contain obsidian microlithic stone tools such as backed microliths, characteristic of the African Later Stone Age (LSA). Pottery and bone are also present but are limited to the youngest Later Stone Age assemblage (Unit III) and the surface layer (Unit I). Stratigraphically lower settlement layers date between ~13,500 and ~27,000 cal BP (Unit VII and IX) and contain predominantly obsidian artifacts. A rockfall layer with trachytic boulders (max. 70 cm in diameter) is located in the upper part of Unit VII. The boulders are weathered with a rounded upward-facing surface, indicating a slow covering with sediment. Allochthonous geogenic deposits (tephra layers, Unit II, IV, VII) are recognizable

by their light coloration and coarser grain size from fine sand to coarse sand [1]. Tephra units are mostly multi-layered, with a slightly darker upper layer often containing brown angular lenses. In Units II and IV, transitional layers are found underneath, which contain fine gradation/lamination visible to the naked eye. The mentioned archaeologically sterile Unit VI is a ~60 cm thick deposit of autochthonous and allochthonous geogenic sediment that can be dated to the African Humid Period. It is characterized by increased clay content and a continuous reddish-brown coloration. Increased values of Fe<sub>2</sub>O<sub>3</sub>, aluminum (Al), and titanium (Ti), and a lower K/Rb ratio point to intense weathering of this unit [1].

### 3. Material

The material for this study was sampled during the annual excavations in 2016 to 2018. In the following, the individual sampling strategy and the position within the stratigraphy are described. A detailed description of the methodology can be found in Appendix A.

A sampling of undisturbed sediment blocks for the micromorphological investigation was conducted at four excavation profiles (F35 North, F35 West, G35 South, J29 South) (Figure 3). Thin sections of samples taken in 2016 are labeled with Arabic numerals and those taken in 2018 with Roman numerals. The samples were taken from sediment units and across layer boundaries to ensure a sampling of the variety of depositional processes and to detect (environmental) transition zones. A large boulder, which only became visible when attempting to remove the sample block SOD\_III, considerably complicated the sampling. The lower part of this sample might be disturbed, which was considered in the following interpretations. The thin sections are classified into predominant facies types according to the stratigraphic description of Sodicho by Hensel et al. [1] and the defined deposition units. In this process, we distinguish individual micromorphological subunits by color, composition, compaction, and changes in grain size fractions.

A total of 20 sediment samples were taken from two excavation squares F35 and G35 (Table A1), for the analysis of black carbon (BC) covering anthropogenic deposits, light-colored tephra, and the archaeologically sterile section. For the phytolith study, ca. 10 g of thirteen bulk sediment samples were collected from excavation squares F35, and seven samples were taken from G35. To determine AO extractable Fe, Si, Al, and Mn, 20 reference bulk sediment samples were selected from the stratigraphy.

## 4. Results

### 4.1. Micromorphology

The most important features of each unit are described in stratigraphic order beginning with the lowest unit IX. Detailed results of the thin section analyses are presented in Table S1. The defined stratigraphic units within each thin section were divided into subunits, according to macroscopic boundaries detected in the flat bed scans (Figure 5).

Overall, the micromorphological observation verified the diverse stratigraphy with repetitive occupation layers, alternating with volcanic ash (tephra) or non-anthropogenic clayey layer. Independent of the sedimentological units, the following features can be identified in the majority of the thin sections. According to the micromorphological investigations, major coarse components (>10 µm in diameter) in the cultural layer (Units I, III, V, VII, and IX) and the archaeologically sterile unit VI are trachytic rock fragments of the bedrock of the shelter, feldspar mineral grains, brown clay and silt granules, and varying amounts of opal phytoliths with a whitish to bluish-white interference color under oblique incident light (OIL). Volcanic glass is the predominant coarse material within the tephra in Units II, IV, and VIII and within weathered tephra in Unit VI. Beyond that, volcanic glass particles are also mixed into the matrix within the other stratigraphic units but in different states of weathering. Anthropogenic coarse features are fragments of obsidian, bone, and charcoal. The following descriptions of the micromorphological results are presented from the bottom (Unit IX) to top (Unit I):

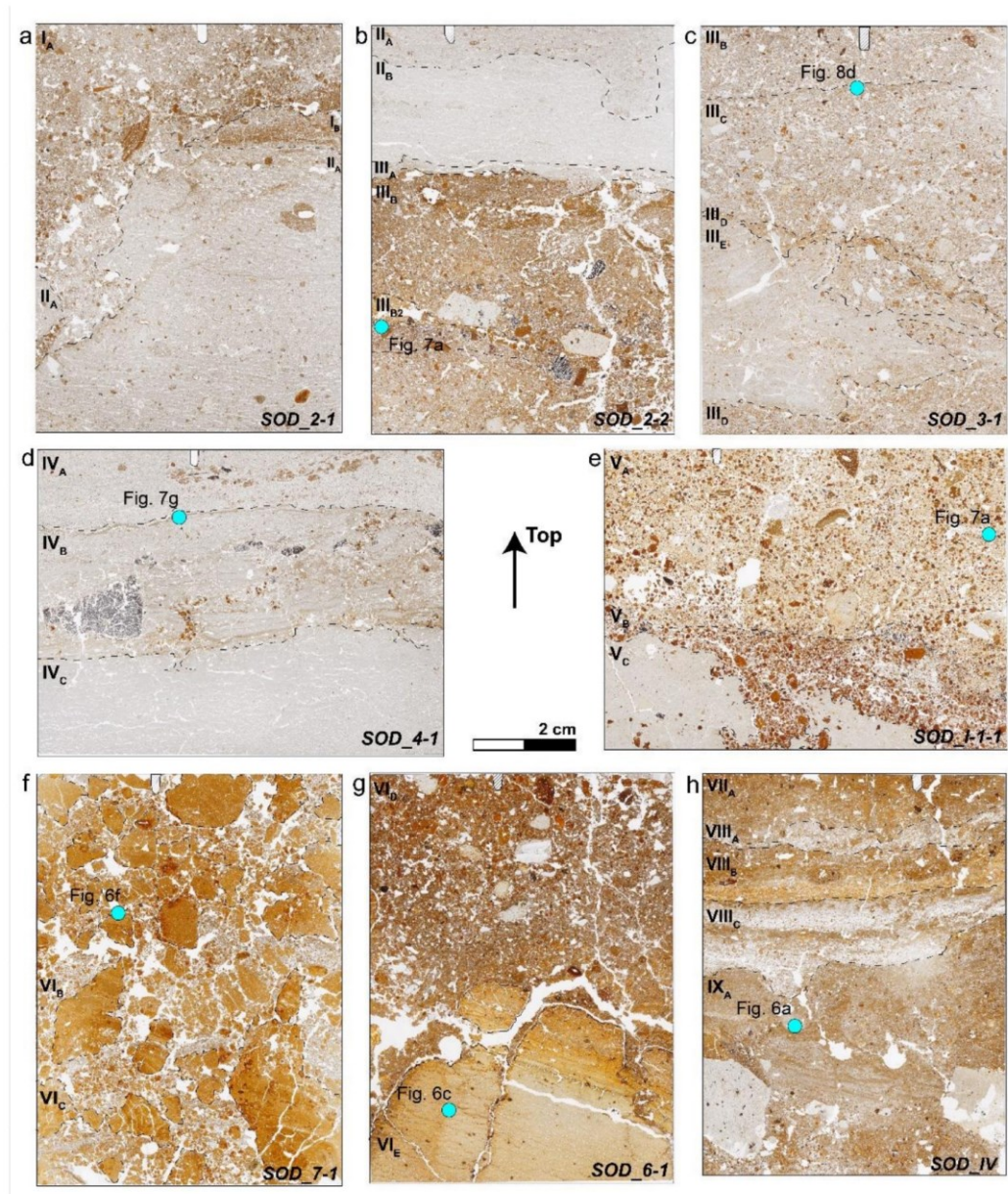


**Figure 5.** Flatbed scans of representative thin sections from Sodicho Rockshelter captured in transmitted light mode; subunits are indicated with Roman numerals and in subscript; green dots refer to figures mentioned in the text. (a) Transition between Unit II and I in SOD\_2-1. (b) Sharp boundary between anthropogenic Unit III and tephra (Unit II) in SOD\_2-2. (c) Disturbed tephra within the anthropogenic Unit III in SOD\_3-1. (d) Multi-layered tephra (Unit IV) in SOD\_4-1. (e) Fragments of charcoal and burned bone above a disturbed tephra in SOD\_I-1-1 (Unit V). (f) Fragmented and deformed tephra in SOD\_7-1 (Unit VI). (g) Yellow, weathered tephra in the lower part of SOD\_6-1 (Unit VI). (h) Multi-layered and disturbed tephra (Unit VIII) in the lowermost micromorphological sample SOD\_IV.

#### 4.1.1. Unit IX

The anthropogenic Unit IX is represented in the lower parts of the thin sections SOD\_IV and SOD\_III (Figure 5h). Microscopically, the deposits show a vughy microstructure. Coarse features consist mainly of individual feldspar mineral grains, fragmented charcoal particles, trachytic rock fragments with a fluidal feldspar texture, and bigger feldspar phenocrysts. Fine layered aggregates of volcanic glass particles and aggregates with phytoliths, as well as fragmented aggregates with finely graded bedding, are included. A large number of well-preserved light and a few dark phytoliths are found in a 0.5 cm depression-shaped accumulation, which also contains brown clay aggregates in the same fine particle size (Figure 8a). Main pedofeatures are fragments of bright yellow-orange colored clay coatings and limited bioturbation, indicated by biogenic pores. All included components and aggregates are intermixed within a brownish, dotted, and speckled micro-mass. The boundary to the overlying subunit VIII<sub>C</sub> is sharp.

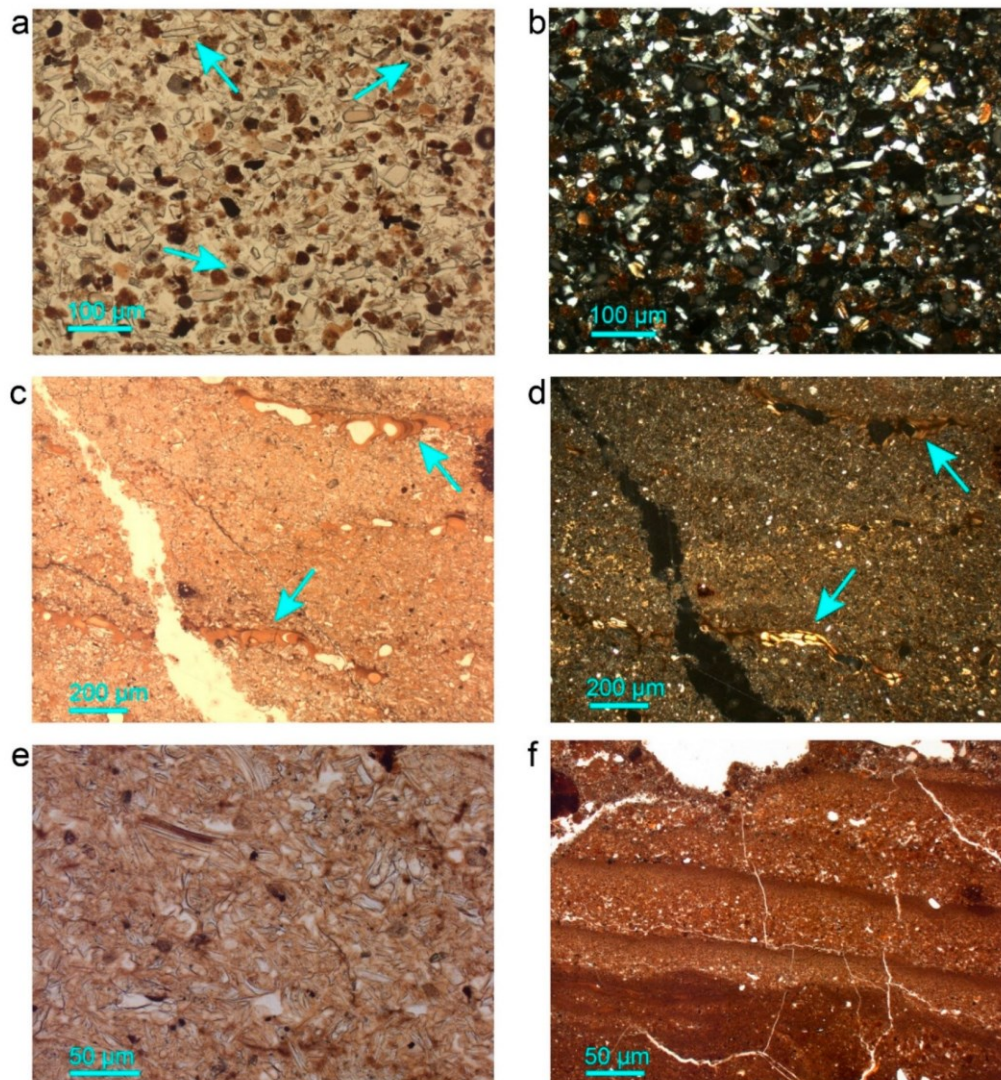
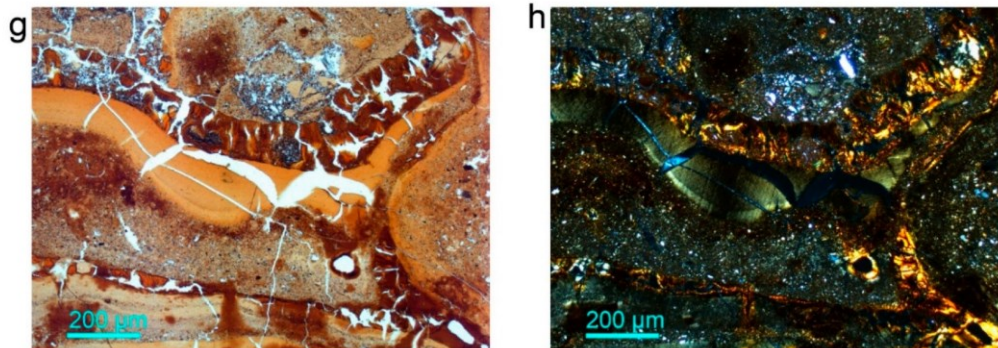


Figure 6. Cont.



**Figure 6.** Microscopic images of thin sections from the Sodicho Rockshelter. (a) Aggregation of light phytoliths (green arrows), brownish clay aggregates and rounded feldspar particles within subunit IX<sub>A</sub> (SOD\_IV, PPL). (b) Optically isotropic phytoliths remain black under XPL, same as Figure 8a (XPL). (c) Highly weathered tephra with an abundance of yellowish clay (green arrows) (SOD\_6-1, PPL). (d) Limpid clay coatings with yellowish golden color, same as Figure 8c (XPL). (e) Weathering of the volcanic glass particles in a yellow clayey micromass (SOD\_6-1, PPL). (f) Graded silt and clay bedding in an aggregate (SOD\_7-1, PPL). (g) Reddish crystallized Fe-(hydr)oxides coatings on top of yellow clay coating along voids (SOD\_7-2, PPL). (h) Differences in birefringence colors are obvious, same as Figure 8g (XPL).

#### 4.1.2. Unit VIII

The geogenic Unit VIII, approximately three cm thick, has a complex structure with a sequence of three thin subunits, which are preserved in thin section SOD\_III and particularly well in SOD\_IV. In these subunits, the coarse components consist of volcanic glass particles in different states of weathering. The lowest subunit (VIII<sub>C</sub>) appears very loose with large porosity and includes two white tephra layers with intermixed brownish-grey sediment. The layers are separated by a brownish silty layer containing only a few sharp-edged volcanic glass particles. The upper part of this subunit ends with a compacted crust of light pale clay, followed by a subunit (VIII<sub>B</sub>) of yellowish tephra. The lower part consists almost entirely of weathered volcanic glass and yellowish clay coatings (textural pedofeature) (Figure 5h). The micromass of this subunit has a speckled limpidity and grano-, porostriated b-fabric. The uppermost subunit VIII<sub>A</sub> is characterized by volcanic glass particles mixed in a brownish-grey matrix. The most prominent pedofeatures of this unit are yellowish clay coatings with bright interference colors.

#### 4.1.3. Unit VII

The sediment of anthropogenic Unit VII seems relatively uniform and cannot be subdivided, according to the micromorphological observations. As the sediment of this unit and the features contained within the thin sections are similar, only one subunit is described. The unit is visible in thin sections SOD\_6-2, SOD\_II\_3-3, SOD\_III, and SOD\_IV. Coarse components consist of slightly rounded trachytic rock fragments, charcoal fragments, and rounded granules in a reddish-brown clayey silt matrix. Fine volcanic glass with rounded edges and phytoliths are common within the brownish dotted micromass. Biogenic pedofeatures consist of passage features and biogenic pores. Further pedofeatures include redoximorphic nodules, yellow limpid clay coatings, and clay papules (fragmented clay coatings). In addition, sporadic lenses of fine, compacted sediment (disturbed crust material) are common.

#### 4.1.4. Unit VI

The archaeologically sterile Unit VI can be divided into five subunits based on the micromorphological observations within the thin sections SOD\_I\_1-2, SOD\_I\_1-3, SOD\_I\_4-

1, SOD\_7-1, SOD\_7-2, SOD\_6-1, SOD\_6-2, SOD\_II\_3-1, and SOD\_II\_3-2. In the field, the color of the dark reddish-brown sediment appeared homogenous, but differences in composition and layering of Unit VI are evident on a microscopic scale. The only apparent subdivision is a yellowish tephra layer ( $VI_E$  and  $VI_{E2}$ ) in the lower area (Figure 5g), which is the sharp boundary to the underlying Unit VII. Several accommodating aggregates (10 to 20 cm thick) of yellow and heavily weathered tephra form the subunit  $VI_E$ . The aggregates have a vuhgy microstructure with a very high proportion of limpid clay coatings with a bright interference color and a grano- and porostriated b-fabric of the clayey micromass. Vesicle chambers and channels are aligned parallel to each other. Furthermore, there are a few coatings with undifferentiated limpidity. The volcanic glass, as the main component, is extremely weathered, with round edges and particle fragmentation. There are sections with finely graded bedding of volcanic glass of silty grain size.

The weathered tephra is followed by reddish-brown silty clay sediment (Unit  $VI_D$ ) with a dotted and speckled micromass and a stipple-speckled and partly undifferentiated b-fabric. In the thin sections SOD\_6-1, SOD\_II\_3-1, and SOD\_II\_3-2, the porosity is low. The proportion of coarse feldspar mineral grains is increased in SOD\_6-1, SOD\_6-2, and SOD\_II\_3-1. The subunit  $VI_C$  consists mainly of clayey-silty sediment, broken into yellow-reddish and brownish, rounded to subangular aggregates with a vuhgy microstructure. Several bigger (up to 2 cm diameter) aggregates are internally fragmented (accommodated to partly accommodated). The clayey to silty aggregates are very diverse in texture, especially within the thin sections SOD\_7-1 and SOD\_7-2. Some aggregates include well-developed rhythmic bedding of fine silt and clay as well as microlaminated illuvial clay coatings. In certain areas, the clay coatings are impure with a speckled limpidity. Redoximorphic features are observed as dark reddish-brown Fe/Mn oxide nodules, along with a mainly reddish-brown coloring of the groundmass. The aggregates increase in size towards the top and can reach sizes  $>1$  cm.

The sediment between the aggregates ( $VI_B$ ) in SOD\_7-1 and SOD\_7-2 appears more dispersed with higher porosity. Coarse components include trachyte fragments of the bedrock, feldspar mineral grains, and rare charcoal fragments in the upper part. There are also differences in the fine sediment between the aggregates. The main components are silty brown granules and an equal proportion of transparent volcanic glass, which are intermixed and fragmented. Furthermore, reddish needle-shaped coatings and a fanlike intergrowth are present in the samples SOD\_7-1, SOD\_7-2, and SOD\_I-1-3 (Figure 8g). The most prominent impregnative pedofeatures are Fe/Mn hypocoatings and redoximorphic nodules, which are particularly pronounced within the uppermost subunit  $VI_A$ . Biogenic pores are found in all subunits of Unit VI and especially pronounced in the samples SOD\_II\_3-1 and SOD\_7-1.

#### 4.1.5. Unit V

The anthropogenic Unit V can be divided into four subunits, which can be observed in thin sections SOD\_4-2, SOD\_4-3, SOD\_I-1-1, SOD\_I-1-2, and SOD\_I-4-1. The whole unit is affected by post-depositional disturbance indicated by passage features, reworked sediment, and lateral translocation of coarse components, e.g., charcoal and bone fragments. There is no horizontal orientation of elongated components. The lower subunit  $V_D$  occurs in SOD\_I-1-2 and SOD\_I-4-1 from the west profile F35 and consists of reddish-brown silt and clay sediment. Some granules (angular blocky microstructure) show fine graded bedding and lamination, resembling the sediment of Unit VI.

The micromorphological sample SOD\_I is unique as it contains fire residues such as charcoal and rubified sediment ( $V_B$ ), overlying a redeposited light-colored tephra ( $V_C$ ) (Figure 7a,b). In addition, colorless calcined bone fragments are observed in PPL, which appear with dull interference colors under XPL. Within subunit  $V_B$ , calcitic ash was not found, and burned materials were mixed with unburned. The term redeposited is used because the tephra is not a continuous layer in the stratigraphy but rather lies in a kind

of depression. An accumulation of feldspar mineral grains with pellicular alteration (Figure 7c,d) is found below the tephra ( $V_D$ ).

The uppermost subunit  $V_A$  has a vughy microstructure and is characterized by a mainly pale yellowish isotropic groundmass (Figure 5e) with a dotted limpidity and an undifferentiated b-fabric. Coarser components in this subunit are trachytic rock, feldspar mineral grains, obsidian artifacts, charcoal fragments, calcined bone fragments, and rounded silty clay granules. Biogenic silicate is also found in the form of dark phytoliths and clustered SPHEROID ORNATE phytoliths (Figure 8a). In addition, volcanic tephra lenses ( $V_{A2}$ ) are observed in this subunit  $V_A$ , showing graded bedding of rounded volcanic glass particles. Pedofeatures comprise passage features, limpid clay coatings, and brownish silt-clay coatings around bigger trachytic fragments.

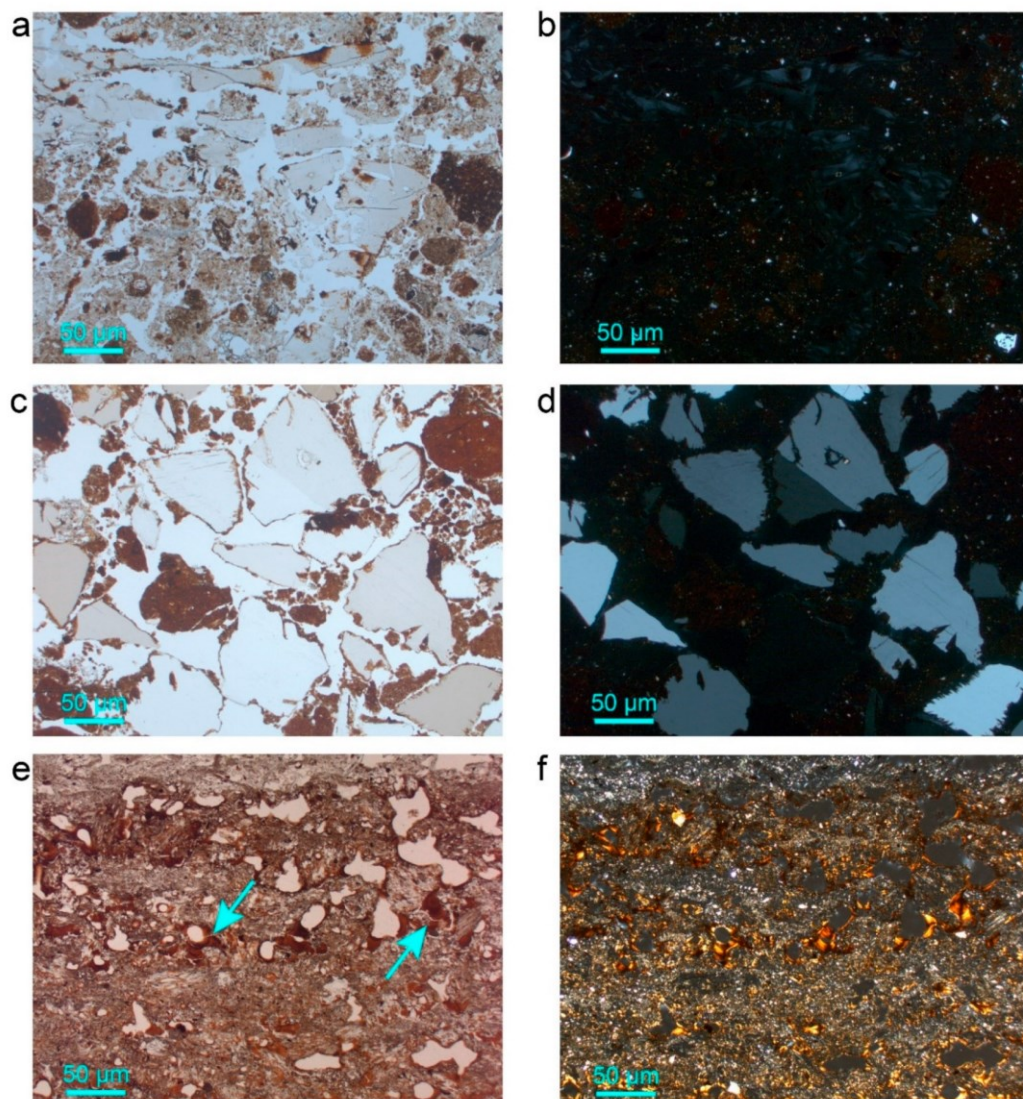
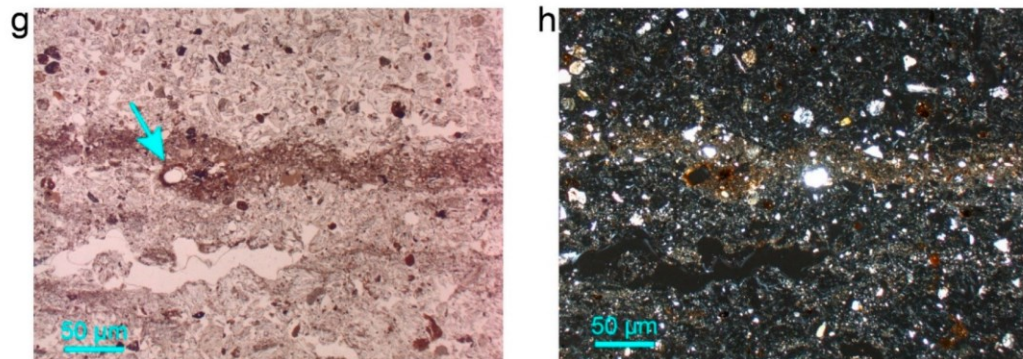
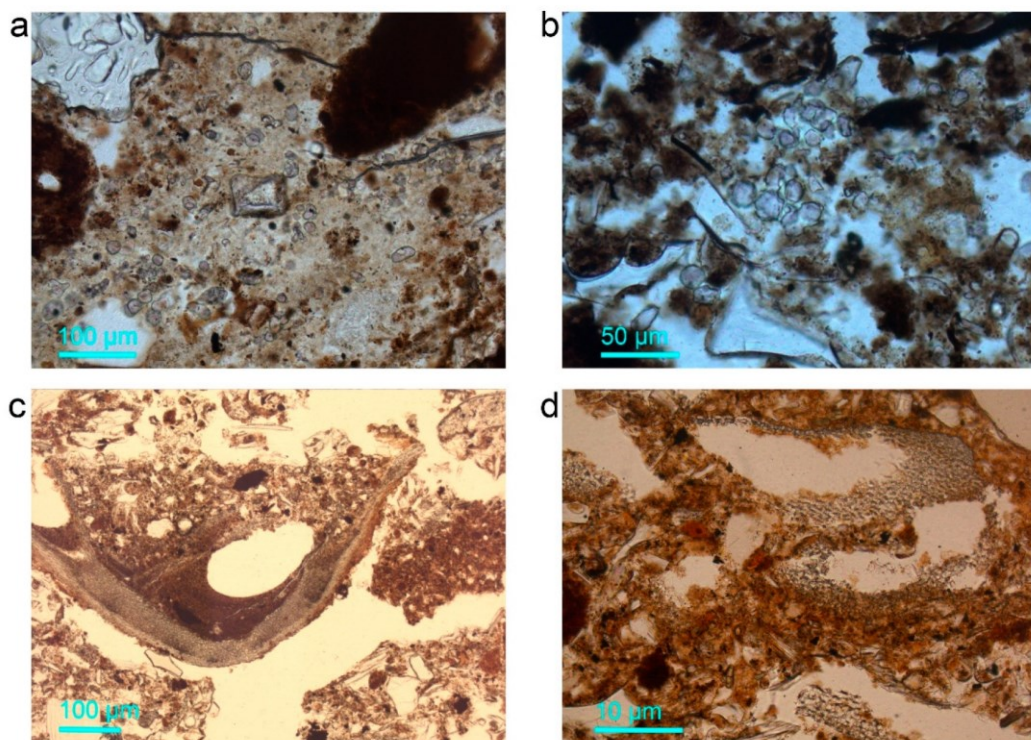


Figure 7. Cont.



**Figure 7.** Microscopic images of thin sections from the Sodicho Rockshelter. (a) Fragmented and calcinated bone within fire residue (SOD\_I-1-1, PPL). (b) Bone fragments show very weak interference colors, same as Figure 7a (XPL). (c) Accumulation of altered feldspar mineral grains (SOD\_I-4-1, PPL). (d) Same as Figure 7c (XPL). (e) Weathered volcanic glass and reddish-brown clay coatings (green arrows) (SOD\_4-2, PPL) (f) Clay coatings with reddish-golden interference colors, same as Figure 7e (XPL). (g) Fine brownish banding within tephra and brownish clay coatings (green arrow) (SOD\_4-1, PPL). (h) Same as Figure 7g (XPL).



**Figure 8.** *Cont.*

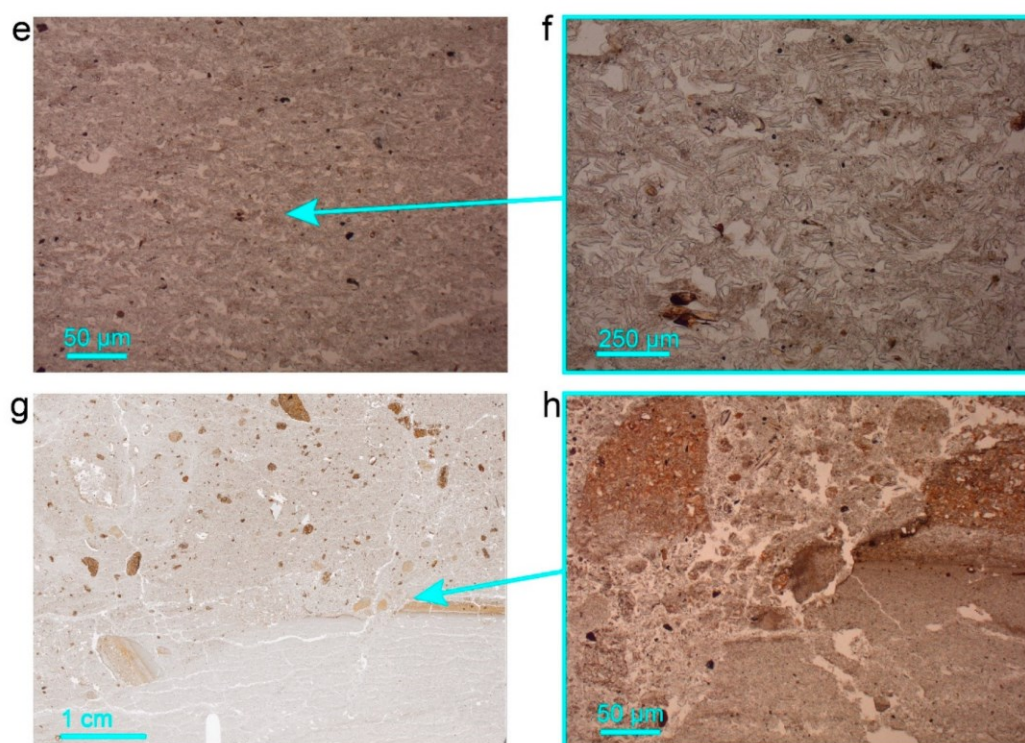


**Figure 8.** Microscopic images of thin sections from the Sodicho Rockshelter. (a) Spherical phytoliths within yellowish sediment of Unit V (SOD\_I\_1-1, PPL). (b) Magnification of spherical phytoliths within organic-rich sediment of Unit III (SOD\_2-2, PPL). (c) Fragment of undefined fruit seed coats/shells (SOD\_3-1, PPL). (d) Magnification of fine seed coat fragments (SOD\_3-1, PPL). (e) Light tephra with brownish sediment particles (SOD\_1-3, PPL). (f) Magnification of the same section (SOD\_1-3, PPL). (g) Two tephra layers are separated by a yellow clay crust (SOD\_1-2, PPL). (h) Magnification of the clay crust and an erosional contact (SOD\_1-2, PPL).

#### 4.1.6. Unit IV

The geogenic Unit IV, visible in thin sections SOD\_3-1, SOD\_4-1, and SOD\_4-2, can be divided into four subunits. The lowest subunit IV<sub>D</sub> consists mainly of weathered volcanic glass and reddish-brown crescent clay coatings (limpid and speckled) with reddish and golden yellow interference colors. It is about 5 mm thick and appears as a yellowish-brownish boundary layer to the underlying Unit V (Figure 7e). The overlying tephra (subunit IV<sub>C</sub>) also consists of a light grey silty sediment and comparatively fresh volcanic glass. This is followed by a tephra layer (IV<sub>B</sub>) containing larger charcoal fragments (up to max. 2 cm in diameter) and dark and light phytoliths. In addition, several slightly displaced and non-continuous laminations (graded bedding) of volcanic glass can be observed (Figure 5d). The uppermost subunit (IV<sub>A</sub>) is again a mix of slightly rounded volcanic glass, mineral particles, and brownish sediment granules, with a comparable high porosity. The speckled micromass of this unit has a mostly undifferentiated b-fabric, while a stipple-speckled b-fabric is present exclusively in subunit VI<sub>D</sub>.

#### 4.1.7. Unit III

The predominant anthropogenic Unit III is characterized by several layers of brown silty sediment, rubified silty sediment, and pale white lateral spreading lenses, which can be identified as tephra. The unit can be subdivided into six subunits, in varying thickness within the thin sections SOD\_1-3, SOD\_1-4, SOD\_3-2, SOD\_3-1, and SOD\_3-2. The

components seem mixed and reworked. Coarse components consist of obsidian artifacts, slightly rounded trachyte, feldspar mineral grains, rounded clay, and silt granules. In addition, there are a few charcoal fragments, very few slightly burned bone fragments, crust aggregates (silty clay, finely graded bedding), and a high abundance of single phytoliths (dark and light) as well as partly articulated to completely disarticulated phytoliths.

In the field, the boundary to the lower tephra layer (Unit IV) is very smooth, with an almost steady increase in reddish-brown sediment. The sediment appears reworked, indicated by passage features, incorporation of the sediment from Unit IV, and the fact that the coarse features are not positioned horizontally. The lowermost subunit (III<sub>F</sub>), seen in thin section SOD\_3-2, can be addressed as a transitional zone between the lower subunit (IV<sub>A</sub>) and the following anthropogenic unit. It consists of volcanic glass that is slightly mixed into brownish silty clay sediment. Several tephra lenses (III<sub>E</sub>) appear randomly. They are affected by disturbance and show signs of lateral spreading (Figure 5c). Towards the top, the content of brownish sediment, as well as amounts of brownish clay coatings, increase. In the upper subunits (III<sub>B</sub>, III<sub>C</sub>), highly weathered and fragmented volcanic glass with brownish-red hypocastings in vacuoles (intergranular pores) is still present. Subunit III<sub>B</sub> and III<sub>C</sub> are characterized by phosphatic features, lateral spread of charcoal fragments, dark and light phytoliths, and undefined fragments of fruit seed coats/seed shells. Furthermore, clusters of spherical phytoliths are found within subunit III<sub>B</sub>, with high transparency or masked by dark organic-rich material (Figure 8b). This unit has a light brownish dotted micromass with an undifferentiated b-fabric, which is especially prominent in subunit III<sub>B</sub>. Disturbance of the sediment, fragmentation of features, and sediment infilling in channels can be observed. The thin uppermost Unit (III<sub>A</sub>), a transition area to Unit II, is characterized by brownish autogenic clay coatings around pumice fragments. The coatings are optically isotropic or anisotropic with very low interference colors and mostly without lamination. Their color varies from yellow to bright brown due to the presence of organic pigments or iron oxides. Pedofeatures such as passage features, borrows, and silty clay infillings are included in all subunits, especially within the two uppermost subunits III<sub>B</sub> and III<sub>C</sub>.

#### 4.1.8. Unit II

The geogenic Unit II, consisting of two subunits, is well preserved in the excavated profiles and visible in the thin sections SOD\_1-1, SOD\_1-2, SOD\_1-3, SOD\_2-1, and SOD\_2-2. Even though there is the transition layer (III<sub>A</sub>) to Unit III, the boundary is abrupt (Figure 5b). The lower subunit II<sub>B</sub> consists of almost pure volcanic glass particles, with a few darker sediment clasts. The upper part of this subunit is compacted and capped by a thin clay-rich crust (II<sub>B2</sub>), which is only preserved in SOD\_1-3 and has been partly eroded and displaced by the overlying subunit II<sub>A</sub>. Fine crust fragments are also found in subunit II<sub>A</sub>, within the thin section SOD\_2-2. This reddish yellow layer II<sub>B2</sub> consists mainly of weathered volcanic glass and authigenic clay coatings, which are present along the voids and chambers. The upper subunit II<sub>A</sub> consists of volcanic glass, sediment granules, burned plant material, and weathered trachytic rock fragments. Some of the coarse components show a brownish coating (armed pyroclasts [50]). The micromass of this unit has an undifferentiated b-fabric. Pedofeatures, such as bioturbation and redoximorphic nodules, are found in the subunits II<sub>A</sub> and II<sub>B</sub>.

#### 4.1.9. Unit I

The surface Unit I can be divided into two subunits represented by thin sections SOD\_1-1 and SOD\_2-1. The subunit I<sub>B</sub> is a transitional layer between the lower tephra and the surface unit (Figure 5a). Within the brownish silty sediment, weathered volcanic glass and laminations are visible, as well as clay coatings and horizontally oriented and approximately parallel channels. The proportion of organic matter and the degree of weathering of the volcanic glasses increases with height within the upper Unit I<sub>A</sub>. The brownish micromass has an undifferentiated b-fabric. Coarse components are trachytic

rock fragments and pieces of charcoal. Biogenic features are passage features and botanic remains (root residues, phytoliths, seed coating fragments).

#### 4.2. Black Carbon Contents and Quality

Fire residue input was quantified by black carbon (BC) content as calculated from the yields of BPCAs.

##### 4.2.1. Profile F35

The BC contents vary across the stratigraphy of profile F35, ranging from <0.01 to 1.53 g BC per kg sediment (Table A1), with three samples peaking in Units I, III, and V. Moderate BC amounts are found in Unit II and the upper part of Unit III, whereas the remaining samples display BC contents near or below the detection limit. The B5CA/B6CA ratios range between 0.59 and 1.28.

##### 4.2.2. Profile G35

BC amounts range between 0.17 and 0.97 g BC per kilogram sediment (180–1579 g BC per kg C<sub>org</sub>) (Table A1). Within the profile, elevated BC contents occur in the upper part of Unit VII and then decline with depth so that BC contents are comparatively small in the lower part of Unit VII, VIII and IX. The B5CA/B6CA-ratio ranges between 0.76 and 0.85 with one distinctive peak in Unit VII (ratio value: 1.58).

#### 4.3. Phytoliths

In other studies it has already been observed that strongly heated and burned phytoliths obtain a brown to black discoloration or a black core caused by heated carbon inclusions [10,34,35,37]. The phytolith ratio (Table A2) shows that there are dark (burned) and (light) unburned types in almost all samples.

Three categories can be distinguished:

1. The dominance of light phytoliths: Within the samples SOD\_002, SOD\_027, SOD\_060, SOD\_103, SOD\_106, and SOD\_18\_03, the light phytoliths dominate, with a rough ratio of ~80:20% of light to dark. The samples originate from geogenic but also anthropogenic sediment units (Units I, IV, VI, VII, VIII). The most common morphotype within the light phytoliths is ELONGATE;
2. Roughly balanced: A rather balanced ratio of ~50:50% ( $\pm 10\%$ ) between light and dark types can be found in the samples SOD\_006, SOD\_013, SOD\_018, SOD\_039, SOD\_050, SOD\_071, SOD\_081, and SOD\_096. These samples originate primarily from anthropogenic units (III, VII, VIII) and the archaeologically sterile unit (VI). Except for the two samples from Unit III, in which the dark morphotypes are relatively evenly distributed, the ELONGATE morphotype is most common in the other samples, followed by the ACUTE type;
3. The dominance of dark phytoliths: Dark phytoliths, with the three morphotypes equally represented, dominate with a relative ratio of ~5:95% light to dark within the samples SOD\_009, SOD\_025, SOD\_031, and SOD\_087. The highest values are found within the anthropogenic sediment Units III and V, followed by a sample from the lower part of the sterile Unit VI. Remarkable is also a high proportion within a geogenic layer that can be associated with the middle section of tephra IV (SOD\_025).

The combined results also illustrate differences within the sediment units from which several samples have been examined: The lower two samples of the anthropogenic Unit VII show a higher proportion of light phytoliths (SOD\_103, SOD\_106), and a balanced ratio within the upper two samples (SOD\_071, SOD\_096). Variations in the ratio are also observed in five samples of the sterile Unit VI (SOD\_039, SOD\_050, SOD\_060, SOD\_071) and Unit IV (SOD\_025, SOD\_027). Within the predominantly anthropogenic Unit III, the upper sample (SOD\_009) shows a higher proportion of dark phytoliths, whereas the samples below show an equal ratio (SOD\_013, SOD\_018). Even though a lot of well-preserved phytoliths are present within the thin sections, corresponding to Unit IX, the stratigraphically lowest

sample (SOD\_18\_07) could not be counted due to a high content of fine organo-mineral compounds that were not dissolved during sample preparation.

#### 4.4. Metals in Ammonium Oxalate Extract

The content of  $\text{Fe}_\text{O}$  ranges from 1.77 g/kg to 8.15 g/kg with peaks in the cultural units (I, II, V) and the highest value in the sterile Unit VI (Table A3). The  $\text{Mn}_\text{O}$  values are lower compared to  $\text{Fe}_\text{O}$ , varying between 0.44 g/kg and 2.77 g/kg, with the highest values in the anthropogenic units (I, III, V, and VII).  $\text{Al}_\text{O}$  has the highest values compared to all extracted oxides, with values ranging from 0.77 g/kg in the tephra (Unit II) to 17.07 g/kg in Unit V. The trend of  $\text{Si}_\text{O}$  is similar to that of  $\text{Al}_\text{O}$ , with values ranging from 0.31 to 5.96 g/kg. The highest values occur in Unit V. The ratio of  $\text{Al}_\text{O}:\text{Si}_\text{O}$ , which is an indicator for the presence of allophane content [51,52], varies between 2:1 (Unit I, VI) and 3:1 (Units II, V).

## 5. Discussion

The materials and samples investigated in this study represent excavation areas F35, G35, and J29 on the northwestern side of the rockshelter, and therefore a comparatively small area of deposits within the cave. Even though the sediment deposits vary throughout the entire rockshelter, the following interpretation of the micromorphological observations, black carbon (BC) analyses, phytolith ratio, and the AO extractable metals help to understand the general depositional processes and post-depositional alterations as well as the human impact on the deposits.

### 5.1. Processes of Sediment Accumulation and Post-Depositional Alteration

The following discussion of the depositional processes and post-depositional alterations is based on the new results of the individual units and subunits while considering the preliminary study on site formation based on sedimentological and geochemical analyses by Hensel et al. [1]. The preliminary reconstruction revealed that the accumulation of predominantly autochthonous geogenic, allochthonous geogenic, and anthropogenic deposits in the Sodicho Rockshelter was not uniform and discontinuous [1]. The in-depth microscopic analysis offers new potential for interpreting sedimentary sources and depositional alterations.

The onset of sedimentation within Sodicho Rockshelter is not yet known, as the bedrock has not been reached during excavation. The deepest exposed strata of anthropogenic Unit IX contains stone tool and charcoal fragments and is dated to ~27 ka cal BP [1]. Abundant trachytic clasts and boulders are derived from the trachytic rock walls and the roof (Figure 5h). These trachytic rock fragments contain feldspar crystals in various stages of weathering. Generally, minerals are subject to weathering, especially under a given tropical climate, which typically increases alteration rates [53]. This is also the case within the deposits of rockshelters, as within Sodicho Rockshelter, which are at least partly exposed to the climatic conditions outside of the shelter. A variety of alkali feldspar mineral grains in the sediment groundmass represent the phenocrysts weathered from the fine ground matrix of the trachyte. Fine-grained feldspar alters into clay minerals, such as kaolinite, illite, or vermiculite [53,54]. At Sodicho, this can be observed by the destruction of trachytic rock. Microscopically, Unit IX appears mechanically loosened, and the coarse components are mixed with aggregates of a finer brownish matrix with a high content of organic matter. The disturbance is most probably due to human impact. Furthermore, biogenic pores point to bioturbation as a post-depositional influence. Fragmented aggregates with finely graded bedding suggest deposition by low energy sheet-flow, capable of transporting and reworking fine grained material. Here, sheet-flow is described as a probable slow movement of sediment down the slope, initiated by water entering the shelter through fissures in the walls and ceiling.

The following multi-layered Unit VIII illustrates a series of different geogenic depositional processes, which in turn are interrupted by post-depositional alteration, as in slight bioturbation and unweathered tephra layers, which are intercalated with strongly

weathered deposits (Figure 5h). As an example, the individual volcanic glass particles within a brown matrix (subunit VIII<sub>C</sub>) and the two thin layers of almost exclusively volcanic glass indicate tephra that was moved by eolian transport and subsequently relocated by possible sheet flow. The latter is indicated by a few sharp-edged volcanic glass particles in a brownish silty layer, separating two thin layers. Clay coatings with distinct stipple-speckled limpidity, as well as grano- and porostriated b-fabric of the micromass within the subunit VIII<sub>B</sub>, illustrate highly weathered tephra (Table S1). Subunit VIII<sub>A</sub> is comparable to subunit VIII<sub>C</sub> in its composition and features. However, this fine layer shows signs of disturbance due to the influence of water (sheet flow). The input of macroscopic anthropogenic material (e.g., lithics) within Unit VII refers to a human impact on subunit VIII<sub>A</sub> as well. The phytolith ratio is characterized by a high proportion (~83%) of light phytoliths (Figure 9) that most likely entered the shelter together with the tephra. Thus, they are representative of the local or regional vegetation outside of the rockshelter, which was obviously not subject to fire. This thin geogenic unit is located chronologically between the two dated anthropogenic Units IX (21–27 ka cal BP) and Unit VII (13.5–18 ka cal BP) [1] and thus still in the time range of the LGM. Any signs of anthropogenic habitation within this very thin tephra are missing, indicating that humans were absent from the rockshelter.

The deposits in the thin sections of the predominantly anthropogenic Unit VII seem to be disturbed mainly by biogenic activity (abundance of biogenic pores) and human action, indicated by anthropogenic finds. A further cause of the disturbance could have been the impact of the trachytic boulders of the rockfall layer. The partial collapse of the ceiling may be caused by an increased water impact on fissures in the ceiling, related to the onset of the AHP. Macroscopic changes within the sediment sequence were observed during excavation, e.g., lenses of weathered tephra in excavation square G35 (Figure 3). Furthermore, dotted brownish coatings are found, which may be masked by organic material (humus) [10]. Based on the micromorphological observations, no further subunits could be distinguished for this unit. However, the geochemical analyses show increased magnetic susceptibility and higher values of Mn and P (Figure 4) in the upper part of the unit [1], which correlates with higher values of dark phytoliths (sample SOD\_081 and SOD\_096). This shows that the human influence and burning activity is more pronounced in the upper part of the unit. Light-colored phytoliths are predominant in the sediment samples of the lower area. We suggest that dark-colored phytoliths indicate that these were introduced by humans due to fire activity.

A mixture of autochthonous and allochthonous geogenic sediment is common in Unit VI, the deposit dated to the African Humid Period [1], a phase characterized by increased precipitation but also including short dry periods [55–58]. Previous geochemical and sedimentological studies revealed a high influence of weathering, with an increased clay content, characterized by a lower K/Rb ratio (weathering ratio) and increased Fe<sub>2</sub>O<sub>3</sub> [1]. The ammonium oxalate extraction of the study at hand verifies this observation. A direct comparison of the corresponding curves of Fe<sub>XRF</sub> and Fe<sub>O</sub> clearly indicates higher contents of Fe and increased precipitation of amorphous pedogenic iron (hydr)oxides within the archaeologically sterile Unit VI (Figure 10). Here, the total Si content (XRF) is very low and Si<sub>O</sub> content low to moderate, caused by the increased influence of precipitation in the highlands, associated with increased weathering and leaching of Si within the sediment [6,59]. Formation of halloysite or kaolinite at Sodicho is likely, indicated by Si leaching.

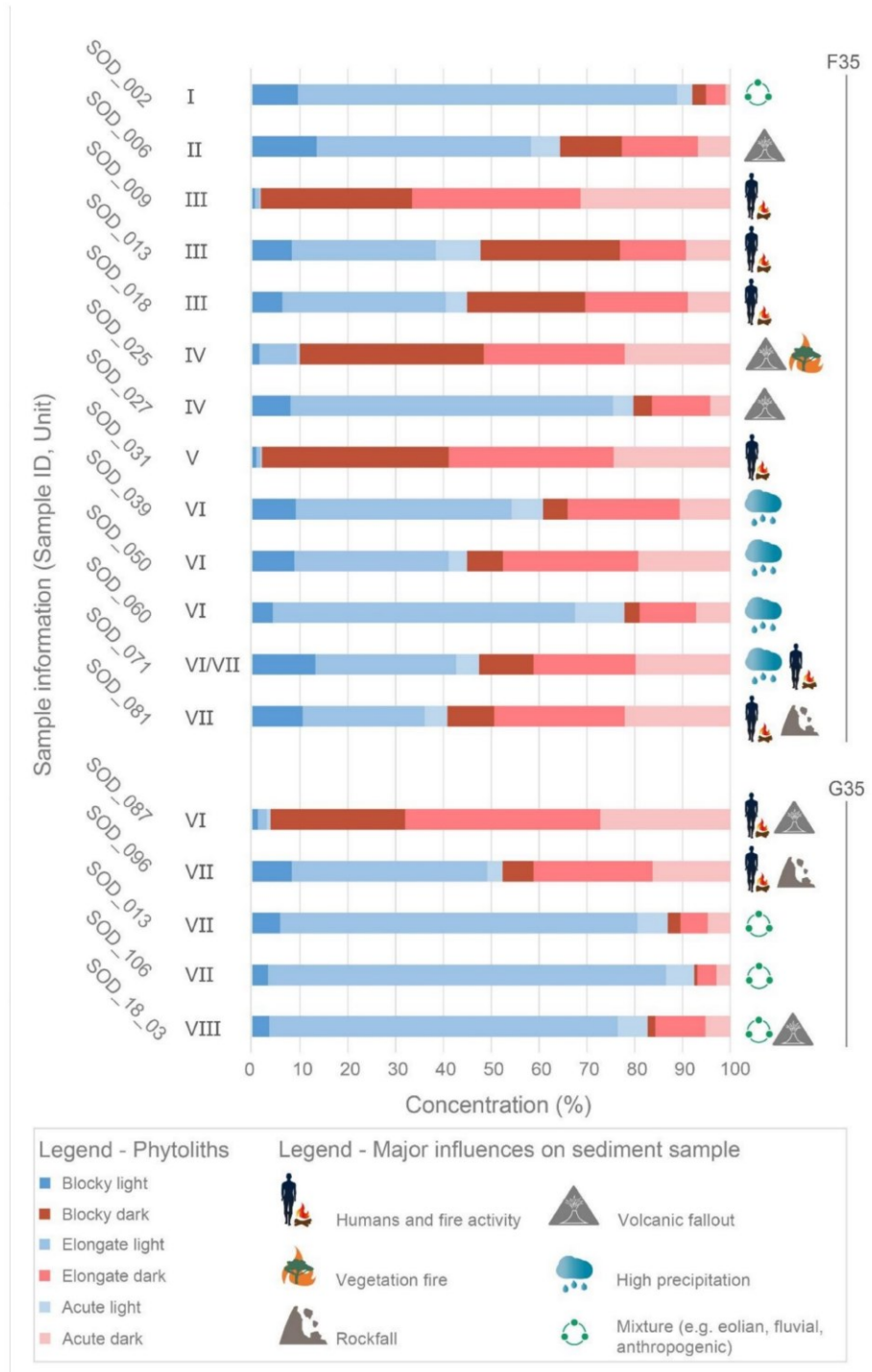


**Figure 9.** Interpretation of influences on sediment samples and phytolith ratio: sample counts of dark (burned; red) and light (unburned; blue) in percentage. Samples are arranged based on the stratigraphic position of the sedimentological units (roman numbers) for both excavation square F35 and G35. The depth of each sample can be found in Table A2.

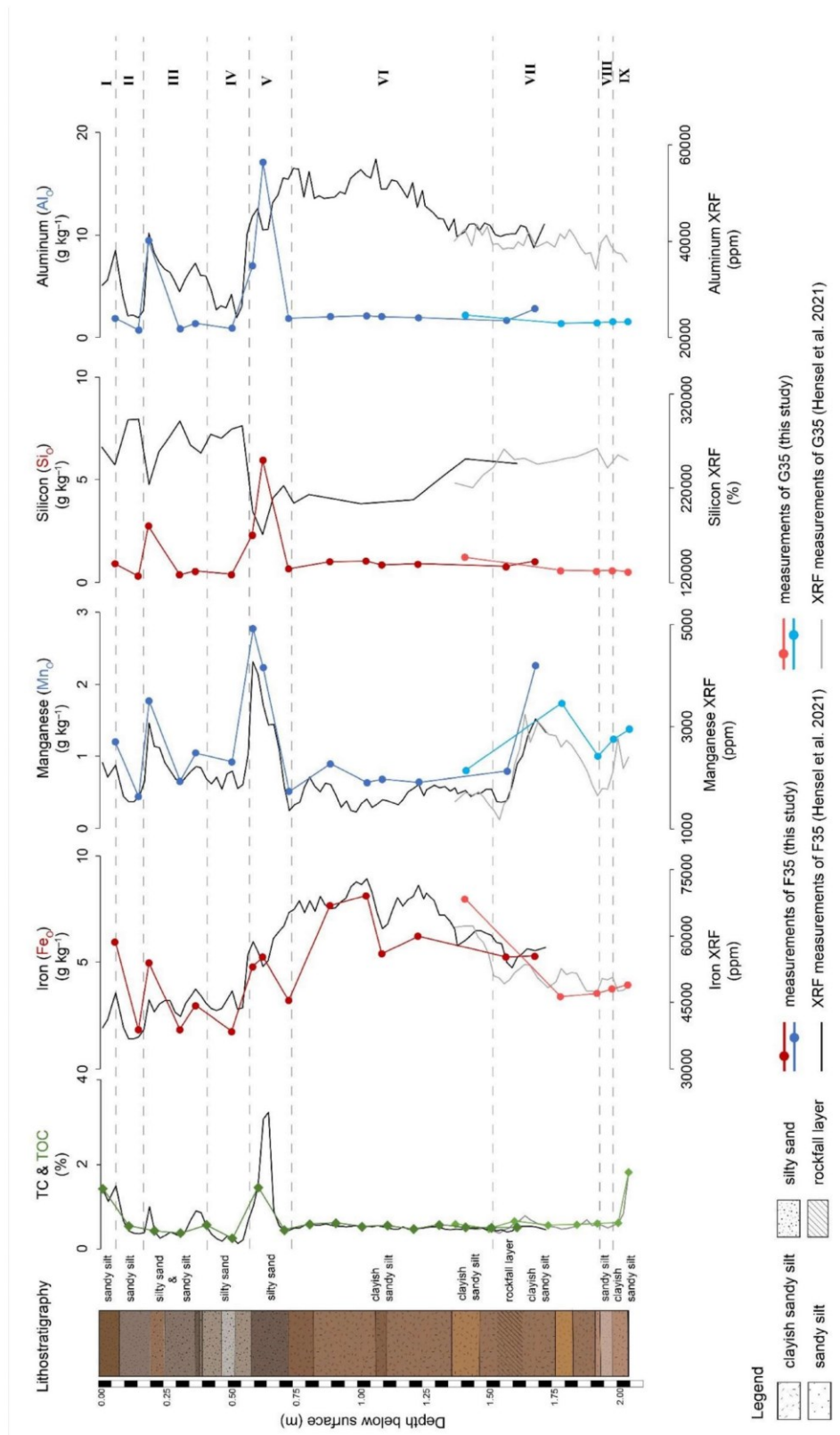


**Figure 10.** Comparison of new results of the oxalate extract of Fe<sub>o</sub>, Mn<sub>o</sub>, Si<sub>o</sub> and Al<sub>o</sub> (colored graphs) with the geochemical results from Hensel et al. [1]: carbon content (TC and TOC), total values of Fe, Mn and Al determined with a portable XRF and Si with XRF (black-grey graphs) (mod. [1]).

Micromorphological investigations identified five subunits of Unit VI. They probably represent different phases with changing moisture conditions during the African Humid Period. The lowermost subunit VI<sub>E</sub> represents strongly weathered tephra in the shape of accommodating aggregates (Figure 8g). The aggregates contain volcanic glass in a clayey micromass with a bright interference color. The formation process of this layer probably occurred through several successive steps. It is possible that the volcanic ash was blown into the rockshelter and was redeposited by low-energy sheet flow, evident in the silty graded beddings within subunits VI<sub>E2</sub> and VI<sub>E</sub> in.

The Al<sub>2</sub>O<sub>3</sub>:SiO<sub>2</sub> ratio, with a value of 1.78:1 (Table A3), is comparatively narrow within the heavily weathered subunit VI<sub>E</sub>. The weathering process of the silicon-rich tephra has progressed so far that more stable secondary clay minerals such as halloysite or kaolinite could have formed. These clay minerals, with a similar aluminosilicate composition and bright interference color, have a Al<sub>2</sub>O<sub>3</sub>:SiO<sub>2</sub> ratio of 1:1 and generally tend to form in silicon-rich environments [6,60]. As sediment from subunit VI<sub>D</sub> is found in the gaps between the aggregates, the redeposition of the tephra most probably took place during the deposition of subunit VI<sub>D</sub>. Considering the phytolith ratio of two samples (SOD\_071, SOD\_087) derived from subunit VI<sub>E</sub>, a dominant proportion of dark phytoliths is noticeable in sample SOD\_087, further illustrating the taphonomic processes that altered the sediment between the tephra aggregates and influenced local phytolith composition. Thus, the dark phytoliths result most likely from translocated anthropogenic combustion features associated with past occupation (Unit VII). Subunit VI<sub>D</sub> also shows signs of mechanical disturbance, with rounded sediment granules and aggregates and fragmented limpid clay coatings. Volcanic glass is most likely weathered and is very rare.

Changes in moisture availability during the AHP are evident within the subunits VI<sub>C</sub>, VI<sub>B</sub>, and VI<sub>A</sub> through shrink and swell processes and disturbed sediment aggregates, as well as the possible formation of Fe-(hydr)oxides (e.g., goethite) coatings along voids and channels, due to temporal dehydration [61,62]. Increased Fe levels in rockshelter deposits have been related to the high anthropogenic input of organic matter, which later decomposed [63]. Organic matter contents of Unit VI at Sodicho are not increased, and there are no further indications (e.g., artifacts, charcoal) that humans were present during the accumulation of this unit. We thus assume that Fe was enriched in Unit VI in the course of silicate weathering in- or outside of the rockshelter. Altered iron oxides, such as the association of hematite and goethite, are common for alteration in a tropical environment in acidic sediment [6], conditions similar to those at Sodicho. Here, yellow, homogenous clay coatings are directly overlain by banded radiating, acicular Fe-(hydr)oxide needles in samples SOD\_7-1 and SOD\_7-2. Such combined layers of clay (often kaolinite) and goethite are known to develop a boxwork fabric (network structure) or even a fanlike intergrowth [10,64,65] but their genesis is not completely clarified. At Sodicho, the well-crystallized Fe-(hydr)oxide needles illustrate the advanced stage of weathering, which led to an increased release of Fe and a subsequent development of the needle structure. In other cases, the presence of Fe-(hydr)oxides also indicates a development under water unsaturated (vadose) conditions and is therefore indicative for temporal dehydration of the sediment [61,62].

The subaqueous deposition is indicated by layers and aggregates with graded bedding of silt and clay particles [66]. Redoximorphic pedofeatures such as Fe/Mn nodules, reddish-brown staining and hypocoatings, and especially the abundance of clay lamination are signs of the influence of water [67,68]. These mentioned indicators are found within subunit VI<sub>C</sub>. It is likely that precipitation was extremely high over longer periods of time. Thus, the water could not drain quickly enough or percolate through the sediment, leading to an accumulation of water in shallow pools and possibly complete waterlogging. By using a Predictive Vegetation Model, linked to a Lake Balance Model of lake Chew Bahir, the recent study by Fischer et al. [69] determined an increase in moisture availability of 25–40% during the AHP, compared to today's values. This observation of increased moisture conditions emphasizes calm water deposition at Sodicho for this time period.

But, these deposition conditions were interrupted by phases of disturbance. Reworked sediment layers within the same Unit VI are probably caused by shrink and swell processes, as indicated by fragmented and contorted aggregates, especially within the subunits VI<sub>C</sub> and VI<sub>B</sub> in the thin sections SOD\_7-1 and SOD\_7-2 (Figure 5f). Very similar observations were made in the lower most and archaeologically sterile unit of Wonderwerk Cave in southern Africa [66]. In addition, to the shrink and swell processes in Unit VI, an abundance of biogenic pores points to a disturbance by bioturbation. Mesofauna (0.1–2 mm) probably used existing physical voids and actively modified them by, e.g., enlargement, as described for structure-formers [70].

The phytolith ratio of the samples from Unit VI shows a relatively balanced value of light and dark morphotypes (except for sample SOD\_60 with dominant light phytoliths). For this unit, we suggest that the phytoliths were brought naturally by eolian processes or sheet flow into the site and thus reflect the past natural environment. Since this unit is archaeologically sterile, an entry by humans can be ruled out. Therefore, the dark phytoliths could derive from vegetation fire ignited by hot volcanic ash fall. The identified depositional processes of this unit are evidence of the abandonment of the shelter due to extremely wet and uninhabitable conditions during the AHP.

According to the previous geoarchaeological studies at Sodicho Rockshelter, the anthropogenic influence increases again at around 4.7 ka cal BP [1], corresponding with the probable termination of the African Humid Period in this region [55]. Micromorphologically, this is indicated by the occurrence of obsidian artifacts, charcoal, and other fire residues within thin section SOD\_I-1-2 from Unit V. Likewise, the high abundance of dark phytoliths (~98%) indicates human occupation and intense fire activity. A further interruption of human occupation coincides with an increase in water influence on the deposits, as seen in the redistributed fragments of limpid clay coatings and tephra lenses (V<sub>A2</sub>) with graded bedding and rounded volcanic glass particles in subunit V<sub>A</sub>.

The elevated values of the two manganese curves (Mn<sub>XRF</sub> and Mn<sub>O</sub>) (Figure 10) within this and also the other anthropogenic layers probably indicate the decay of organic matter or inorganic compounds that accumulated during human occupation [1,63]. This correlates with increased TOC values and increased amorphous organic matter in the groundmass. The Al<sub>O</sub> values are particularly high in the uppermost part of Unit V, where geochemical observations proved a high BC (Figure 11) and TOC content. The absorption of Si by Al-oxides could explain the high Si content in the anthropogenic units. The increase in the Al<sub>O</sub>:Si<sub>O</sub> ratio (~3:1) within the anthropogenic units (Figure 11) suggests a possible formation of allophane or imogolite. A large part of released Si may thus be converted to secondary silicates, but this did not result in the accumulation of total Si, which is depleted in anthropogenic Units V and III relative to other layers. However, other studies showed that Al is more easily incorporated into organic complexes than it is available for allophane or imogolite formation [6,60]. For Sodicho, it appears thus more likely that the increased Al<sub>O</sub> originates from metal-organic matter complexes.

The following Unit IV is composed of lighter colored tephra, thus allochthonous geogenic deposits that deposited relatively abruptly. This tephra is only exposed within the excavation square F35 and is not visible in square G [1]. The main proportion of the tephra (Unit IV) entered the rockshelter via eolian transport during an initial phase of deposition. A coarse monic microstructure with homogeneous composition of sharp-edged volcanic glass particles within subunits IV<sub>C</sub> illustrates this (Figure 8g). Evidence of increased moisture and weathering intensity can be found in the highly weathered subunit IV<sub>D</sub> with golden yellow colored clay and a stipple-speckled birefringence (Figure 7e). An Al<sub>O</sub>:Si<sub>O</sub> ratio of 2:1 suggests the presence of imogolite-like or proto-imogolite allophanes [6,71]. Indications for this formation, based on an undifferentiated b-fabric, i.e., the absence of interference colors, are found in this less-weathered subunit.

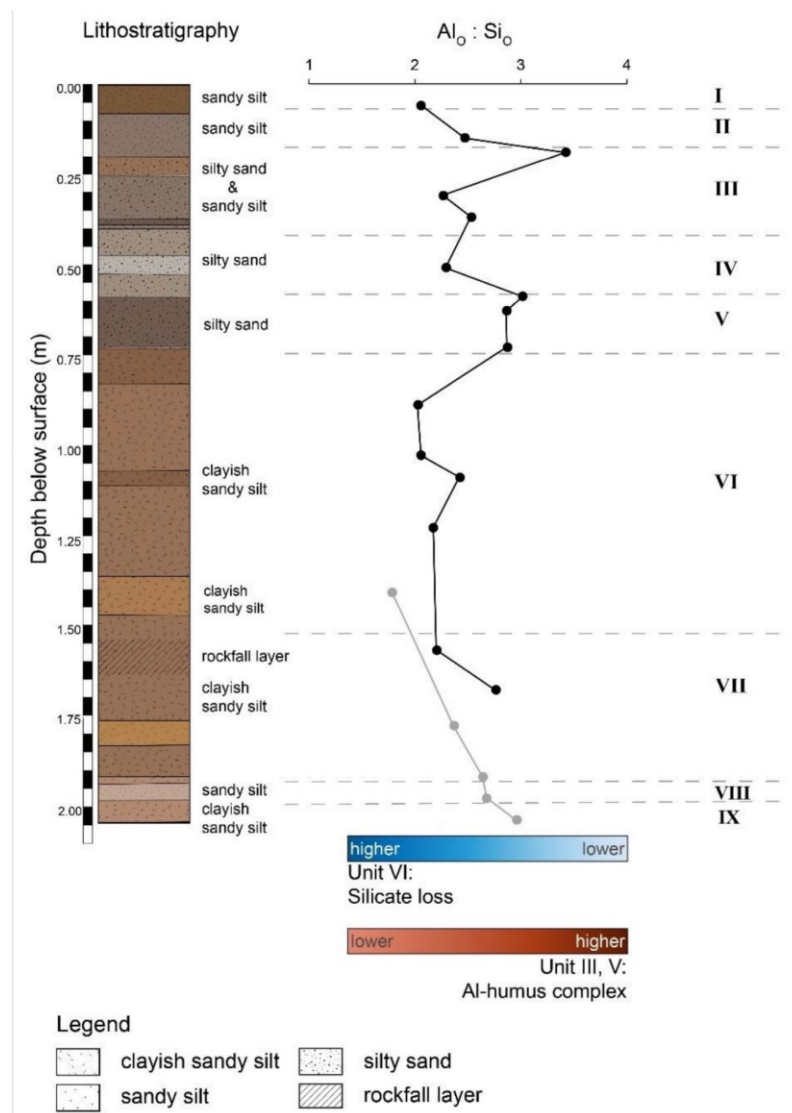


**Figure 11.** Illustration of the discussed factors (silicate loss; Al-humus complex formation) affecting the  $Al_2O_3:SiO_2$  ratio and allophane estimation for Sodicho. Silicate loss is accompanied by the formation of clays in Unit V. Formation of Al-humus complexes in the anthropogenic layers.

Subunit IV<sub>B</sub> shows indication for redeposition of the tephra by low-velocity flow, as in intermixing fine brownish gradations rounded volcanic glass, partial compaction, graded bedding, rounded sediment granules, as well as bigger and slightly fragmented charcoal pieces (Figure 5d). These investigations of slow-moving fluvial deposition can be compared to observations at the nearby Mochena Borago site. In this context, the observation of fine brownish lamination within the Yellow Brown Tephra (YBT) can be attributed to low-energy flow and accumulation in small water pools [2]. Comparison between Mochena Borago and Sodicho Rockshelter illustrates comparable depositional settings, influenced by changing moisture availability on a millennial scale, even though there is a temporal offset between

the two sites. The phytolith sample SOD\_025 corresponding to this subunit contains about 90% dark phytoliths, in contrast to the sample (SOD\_27) corresponding to subunit IV<sub>C</sub> that contains only 20%. Given that the bigger charcoal pieces and a high proportion of dark phytoliths are preserved in the middle of a purely geogenic layer, they most probably indicate non-anthropogenic burning events, such as natural forest or bush fires [68,72], initiated by hot gas clouds or lava flow.

The following settlement phase (Unit III) can be radiocarbon dated to 2.1 to 1.8 ka cal BP [1]. The micromorphological observations revealed a rather smooth transition (subunit III<sub>F</sub>) with increasing evidence of human occupation. The upper parts of the unit (III<sub>B</sub> and III<sub>C</sub>) are bright reddish in color and more cemented than the lower parts of the unit. Subunit III<sub>B</sub> has a dark-brownish-colored groundmass due to higher organic content. The Al<sub>2</sub>O<sub>3</sub>:SiO<sub>2</sub> ratio has its highest value in this subunit, indicating a high proportion of Al-humus complexes. The typical features observed in the previous anthropogenic units, such as stone artifacts and evidence of fire residue, are further discussed in Section 5.2. Three phytolith samples derived from subunits III<sub>D</sub> (SOD\_018) and III<sub>B/C</sub> (SOD\_013, SOD\_009) reflect the pattern of elevated geochemical values in this unit (Figures 4 and 10). Thus, an abundance of burned phytoliths in the upper part of the unit indicates intensified human impact. As a result of human activity on the former surface, such as the digging of pits, construction of hearths, and probably site maintenance, the deposits of subunit IV<sub>A</sub> were partly incorporated into Unit III. This is particularly apparent from the large proportion of volcanic glass in the lower part of the unit (III<sub>F</sub> and III<sub>D</sub>) and from the laterally distributed tephra lenses (III<sub>E</sub>) in F35 (Figure 2). Despite the post-depositional disturbance and slight compaction, the lenses are micromorphologically similar to tephra from Unit IV in terms of groundmass color, size of volcanic glass particles, brownish sedimentary granules, and occasional non-continuous laminations. The uppermost subunit III<sub>A</sub> can be described as a transition layer, despite the sharp color distinction between Unit III and II. Here, the transition was not smooth from one unit to the other, as observed between Units IV and III. It consists of bioturbated sediment, in which parts of the brownish silty and clayey sediment from Unit III are incorporated into the channels, borrows, and chambers of the tephra in Unit II.

The following Unit II is divided into two subunits, with the lower subunit II<sub>B</sub> as light-colored tephra, which was introduced by eolian transport. Within the sample SOD\_1-3, a yellow crust of clay and silt (subunit II<sub>B2</sub>) with a few slightly rounded volcanic glass particles overlay the slightly compacted upper part of subunit II<sub>B</sub> (Figure 8g). Here, compaction is interpreted as the result of water dripping from the rockshelter ceiling. Laboratory studies have shown that structural surface crusts with reduced porosity and reduced permeability can form on tephra during a phase of stable surface conditions under simulated rainfall [73,74]. At Sodicho, this crust on top of subunit II<sub>B</sub> is an indication of a rather stable surface. The features of reworking (e.g., intermixing with sediment aggregates) in the overlying tephra II<sub>A</sub> illustrate remobilization of the sediment. Simultaneous degradation of the yellowish clayey crust is possible (Figure 8h). Given that the subunit is subject to bioturbation, this process also contributed to the destruction of the crust. The phytoliths in subunit II<sub>A</sub> (SOD\_06) were transported into the rockshelter together with the tephra and represent the vegetation outside.

The onset of the predominantly anthropogenic surface Unit I, and thereby the most recent occupation, is indicated by a transition to brown and organic-rich sediment with limpid clay coatings, fine charcoal fragments, and indicators of mechanical disturbance (subunit I<sub>B</sub>). Within subunit I<sub>A</sub> there are well preserved biological components such as roots and seed coat fragments. Indications for bioturbation as in passage features are present throughout the entire Unit I. Thus, partly intermixing with geogenic subunit II<sub>A</sub> was observed. This explains the presence of ~35% dark phytoliths in the sediment samples corresponding to subunit II<sub>A</sub>. In contrast to this, a phytolith ratio with 90% light phytoliths indicates the decreasing presence of humans in this young (250–400 cal BP) sediment Unit I.

### 5.2. Human Behavior and Fire Activity at Sodicho

Identifying human activity and interpreting human behavior in a micromorphological context is fundamental for the study of archaeological sediments [75]. With the help of the applied methods, in-depth insight into the behavior of prehistoric humans can be provided, especially with regard to the use of fire. Combustion features at archaeological rockshelters not only speak for starting and controlling of fire but also indicate the need for light, heat, and of course, the use of the fire for food preparation as kind of a short-term human activity event [18,49]. At the Sodicho Rockshelter, evidence of human activity can be seen macroscopically by hearths, pits, and lithic artifacts [1]. The most prominent indirect evidence for burning at Sodicho is the abundance of charcoal fragments within the anthropogenic units. Microscopic evidence of reworked fire residue, such as charcoal (fragments), slightly burned or even calcined bones, as well as rubification of sediment, was observed in almost all anthropogenic units. Slightly burned and calcined bone fragments can either indicate that fires at Sodicho were used for food preparation and/or that the bones were used as burning material. It is also possible that bone fell into the fire by coincidence or that it was disposed of as waste. Three parted combustion features, including ash, charcoal, and rubified sedimentary layers, are apparent within two slightly disturbed hearths in G34 (south) and G35 (south) (Figure 2), which were not sampled for micromorphology. Carbonate ash layers, a typical overlying by-product of burning [49], are not contained in the thin sections from Sodicho. This means that decalcification occurred, influenced by the dissolution of acidic trachyte bedrock of the rockshelter. Decalcification is often associated with the formation of Al phosphates in clay-rich sediments [49,76]. In Sodicho, these elevated Al values correlate with increased phosphates values [1]. These observations strengthen the assumptions that reworking and leaching processes took place at Sodicho. Evidence of fire residue is particularly evident in sample SOD\_I-1-1 in Unit V, which exhibits the mentioned features above a relocated and partially eroded tephra (Figure 5e). Slightly burned bone and calcinated bone fragments that had not been visible macroscopically [1] are included as single fragments or as larger coherent fragments, suggesting a slight displacement (Figure 7a). Dark matter at the lightly burned bone fragments within subunit V<sub>A</sub> can be interpreted as char [11,49,77]. The displacement and fragmentation of sediment in anthropogenic layers of Sodicho reflect trampling and rake-out (sweep-out) processes in the center or around a fireplace, scattering the burned material laterally and intermixing it with unburned material as described by various authors [49,78]. This is also indicated by rounded aggregates of the rubified sediment and the oblique truncation of the tephra. Whether this light-colored tephra was previously relocated by humans or even intentionally dumped into a pit cannot be clarified at this point of the research. However, it is obvious that the tephra does not seem to be in-situ at this position, as the edges of the layer appear angular in profile F35 North (Figure 3). In addition, fine charcoal particles and distorted sediment aggregates are included. This means that the origin of the bright tephra is unknown, as no comparable tephra layer has been excavated at this stratigraphic level before.

According to other studies, the rubefaction of sediments depends on the organic and mineralogical composition of the substrate, the sediment moisture, and the duration of burning [49,79]. There are two types of rubification within the anthropogenic units of Sodicho. First, there is reddening activity caused by the oxidation of Fe<sup>2+</sup> to Fe<sup>3+</sup> and the development of iron oxides (such as hematite) [49,80], which is connected to anthropogenic fire, observed in the sample SOD\_I-1-1 in Unit V. Secondly, reddening appears in Unit III, probably due to the combination of human fire activity and the alteration of volcanic glass. According to the study of Ferralsols of the Canary Islands analyzed by Rodríguez-Rodríguez et al. [81], discussed in Stoops et al. [50], volcanic glass alters into a yellowish isotropic product. With increasing alteration, the destruction and fissuring increase, followed by a rubification with dark red optically isotropic alteromorphs. Within the thin sections from Unit III (such as SOD\_3-1), increased fragmentation and red brownish coatings are present in vacuoles of the volcanic glass. In addition, red-colored humic

Nitisols, the typical soils of the region, occur outside of the shelter. It seems possible that this red soil material (clay and silt size) has been transported from outside into the Sodicho Rockshelter by low energy sheet flow or through fissures in the rockshelter walls and incorporated into the archaeological sediment [1] as assumed for other rockshelter sites [49,72,82–84].

As previously mentioned, charcoal is found in all human-influenced units. The question arises whether we can detect differences in fire use between the units, and thus temporal differences, that may indicate changes in human behavior. For this purpose, we use the information from the BC analyses and the phytolith ratio, as well as the results of sedimentological and geochemical analyses by Hensel et al. [1]. The BC content, as a proxy for fire residue input, correlates with the increased MS and Mn values in the anthropogenic Units III, V, and VII (Figure 12) and thus complements the findings of charcoal, burned bone, and calcinated bone fragments.

The absence of BC in the preferentially geogenic units can therefore be seen as an additional indication for the absence of humans since the BC particles would have been distributed within the rockshelter even if the inhabitants used fire in another part of the shelter. At the same time, the higher fire activity in these occupation periods was accompanied by an increased degree of BC condensation due to higher fire temperature, as indicated by comparatively low B5CA/B6CA ratios. This is particularly useful when aiming, for instance, at distinguishing hot hearths with low ratios of penta- to hexacarboxylic benzoic acid (B5CA/B6CA) from cool vegetation fires, e.g., natural grass or forest ground fires, with higher B5CA/B6CA ratios [33,85,86]. Thus, the BPCA ratios from Sodicho support other indicators of anthropogenic fire, such as burned bone fragments and stone tools, providing evidence for food preparation [87]. Lower B5CA/B6CA ratios and thus comparatively higher temperatures are found within Unit III, which has been dated to a period of 1.8–2.1 cal BP. The older Unit V (4.3–4.8 ka cal BP) shows slightly higher ratios, especially when samples with low BC values are included. By comparing these observations for the defined units with the results of the phytolith ratio, it is noticeable that the upper sample in Unit III (subunit III<sub>B</sub>) shows only a slightly higher proportion of dark phytoliths compared to the values in the other anthropogenic units. Within both units, a strong abundance of dark phytoliths is found (~98%). Therefore, no difference in human fire intensity can be determined based on the counting of phytoliths alone. However, the abundance of discoloration in phytoliths is without doubt caused by burning activity, as it is more pronounced in units containing fire residue features.

Unit III shows a phosphate-rich groundmass with preserved fire residue, such as charcoal and black char with a vesicular structure, supporting the hypothesis of the use of wood as a fuel. However, the large proportion of dark phytoliths of the ACUTE morphotype in sample SOD\_009 indicates that grass was used as a burning material as well.

Small transparent phytoliths, identified as SPHEROIDAL ORNATE, are found in great abundance in Unit III (Figure 8b). These also occur in Unit V, but to a much lesser extent, and individually or in cell association in the areas of combusted matter. SPHEROID ORNATE phytoliths with an irregular surface are common in monocots and woody dicots [88]. In our thin sections, SPHEROID ORNATE occurs in cell clusters which likely are parts of seeds (Figure 8b) but were not observed during phytolith analyses. This is due to the close cell association which was not dissolved during sample preparation.

The phosphate-rich groundmass in Unit III correlates with elevated phosphate values, determined by X-ray fluorescence (XRF) (Figure 4) [1]. Due to poor bone preservation, with the exception of small bone fragments identified in the thin section, no definite conclusions can be drawn regarding the use of the rockshelter by animals. Phosphate can be introduced in various forms, such as human activity, bird guano, or excrements [76]. Since the human-influenced units were partly reworked, a biogenic input could be possible as well. Although the origin of the phosphorus cannot be unambiguously clarified, Unit III represents a settlement phase based on our sedimentological and geochemical findings as well as the occurrence of archaeological artifacts.

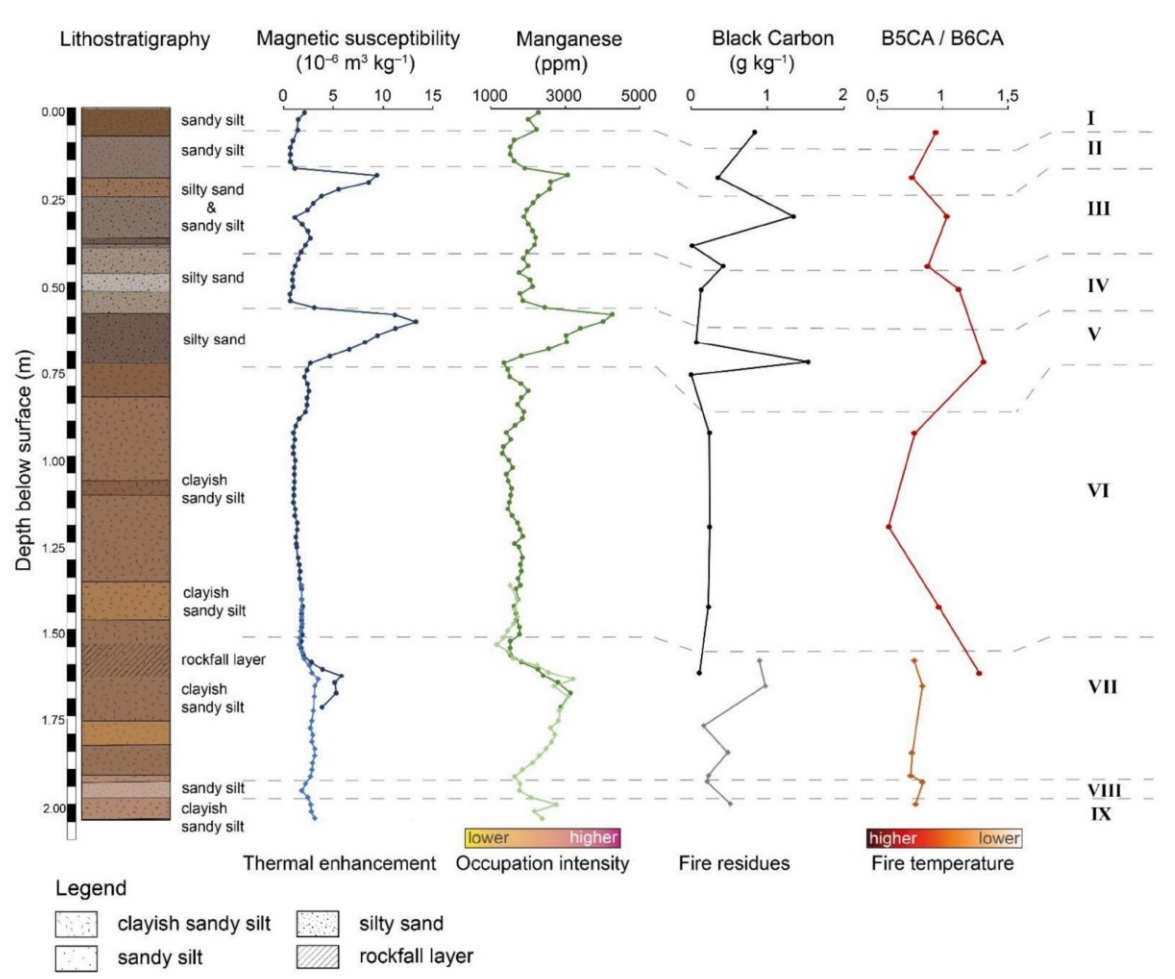


**Figure 12.** Comparison of the new BC results with the geochemical results from Hensel et al. [1]. Geochemical properties of the profile F35 and G35 (left to right): lithostratigraphy according to grain size analysis and sediment color measurement; magnetic susceptibility; manganese value (mod. [1]); BC content; B5CA/B6CA ratio values; sedimentological units. Grey dashed lines indicate association to the units. Note that the lines of BC content and B5CA/B6CA ratio values are staggered because the samples were taken from two excavation squares (F35 and G35).

The questions arise, whether the limited evidence of a changing fire temperature could have been caused by degradation or even leaching and, therefore, how the degree of weathering can affect the preserved information in the archaeological deposits. It is noticeable that BC and the phytolith ratio peaks within the upper anthropogenic units (III and V) and that no micromorphological features were observed within these units that could indicate the mentioned extreme weathering processes as observed in Unit VI, corresponding to the AHP. Furthermore, no trend between the BC content and increasing depth or sediment age was detected, which makes distinct pedogenic processes such as percolation by water less likely in the anthropogenic units.

## 6. Conclusions

The combined results of this study not only confirmed previous geoarchaeological investigations on site formation, post-depositional alteration, and human impact at Sodicho

Rockshelter. In addition, they provide deeper insights into weathering processes and the identification of prehistoric human behavior under shifting environmental and climatic settings. The combination of the different methods allowed a more precise subdivision of the units and the determination of individual depositional processes. In particular, the intercalated tephra layers display a clear interruption of human occupation at Sodicho. Given the high proportion of weathered and unweathered volcanic glass particles within the entire stratigraphy, we cannot clearly determine the allophane content, but we assume a partial allophane (proto-imogolite), imogolite, and even halloysite and kaolinite formation, respectively. Furthermore, clay minerals are formed by the weathering of the local trachytic bedrock but could also have been washed in from outside as clayey soil material [1].

Significant changes in moisture conditions on the substrate and the associated impact on depositional and post-depositional alteration processes (e.g., sheet flow, shrink and swell processes) are especially pronounced during the conditions of the AHP. On the other hand, bioturbation partly disturbed the original stratification of the deposits and therefore affected the preservation of environmental and archaeological information. The depositional processes identified for the AHP verify that the rockshelter was abandoned at this time, probably due to wet and uninhabitable conditions. In contrast, the combination of the archaeological finds and the microscopic evidence from layers dated to the time range of the LGM [1] verify that humans visited the rockshelter repeatedly.

Human occupation contributed significantly to site formation and post-depositional disturbance of the sediment. The microscopic identification of calcined and slightly burned bone fragments within fire residue and indications for trampling (compaction and bone fragmentation), dumping activity, and site maintenance verify that inhabitants of Sodicho were able to start, maintain and control fire. The combination of micromorphological observations and BC analyses yielded consistent results and thus allowed the identification of temporal changes in fire activity. Consequently, changes in BC contents and composition are interpreted as changes in the human-induced input of fire residues. It was not possible to differentiate fire intensity between the anthropogenic units based on the phytolith ratio. However, the combined analyses allowed the identification of human fire activity (Unit III, V) and the differentiation of natural vegetation fire (Unit IV) through the abundance of dark phytoliths. Light phytoliths that entered the site naturally provide the first evidence for the reconstruction of local vegetation changes at Mount Sodicho. In conclusion, this case study contributes to the development of comprehensive, methodical approaches to tackle and disentangle challenging stratigraphies in the tropical highlands of Ethiopia.

**Supplementary Materials:** The following are available online at <https://www.mdpi.com/article/10.3390/geosciences12020092/s1>, Table S1: Electronic Supplement: Overview of micromorphological results.

**Author Contributions:** Conceptualization, E.A.H., R.V. and O.B.; methodology, E.A.H., L.W. and K.N.; validation, E.A.H., M.K., L.W., K.N., R.V. and O.B.; formal analysis, E.A.H., L.W. and K.N.; investigation, E.A.H., L.W. and K.N.; resources, E.A.H., M.K., L.W., K.N., R.V. and O.B.; data curation, E.A.H., L.W. and K.N.; writing—original draft preparation, E.A.H.; writing—review and editing, E.A.H., M.K., L.W., K.N., R.V. and O.B.; visualization, E.A.H.; supervision, M.K., R.V. and O.B.; project administration, R.V. and O.B.; funding acquisition, R.V. and O.B. All authors have read and agreed to the published version of the manuscript.

**Funding:** This research was funded by the Deutsche Forschungsgemeinschaft (DFG, German Research Foundation), grant number 57444011—SFB 806.

**Institutional Review Board Statement:** Not applicable.

**Data Availability Statement:** The data presented in this study are available in Appendix B—Results and the supplementary material here.

**Acknowledgments:** We kindly thank the Authority for Research and Conservation of Cultural Heritage (ARCCCH) of Ethiopia for their permission and general support and the Ministry of Mines and Energy for the approval of our export permits. The Deutsche Forschungsgemeinschaft (DFG, German

Research Foundation) supported this research as part of project A1 “Out of Africa—Late Pleistocene Rock Shelter Stratigraphies and Palaeoenvironments in Northeast Africa” in the framework of the Collaborative Research Centre 806 (CRC 806) “Our way to Europe” (grant no. 57444011—SFB 806). We thank K. Greef for guidance and assistance during the oxalate extraction and Th. Beckmann for the preparation of the micromorphological thin sections. We are very grateful to Thomas Albert, Degene Bado, Dejenne Degena, Mesfin Gete, Solomon Gitaw, Habir Mohammed Kebir, Tom Noack, Mareike Röhl, Christian Schepers, Desta Sinajew, Mehdanit Tamerat, Fitsum Tefera, Minassie Tekelemariam, and Thorben Thenbruck for their participation during various field seasons at Sodicho. Finally, we thank the local residents of Mt. Sodicho for their participation and support in field research.

**Conflicts of Interest:** The authors declare no conflict of interest.

## Appendix A. Methods

### Appendix A.1. Micromorphology

Microscopic observations of soil and sediment thin sections have been crucial methods since they were established by W.L. Kubiëna in the 1930s to identify the spatial structure of features on a microscopic scale [7,10]. At Sodicho, the sediment blocks were secured with gypsum bandages. The samples from the excavations in 2016 had to be bandaged again with gypsum after a one-year storage phase to ensure further transport to the thin section laboratory. In the process, sample Sodicho\_6 was damaged at the upper right edge. This incident was also considered in the analysis and interpretation. The impregnation of the sediment monoliths, as well as the preparation of the <30 µm thick, thin sections, followed the instructions of Beckmann [89]. The description of the thin sections followed the guidelines and terminology of Stoops [10]. The thin sections were flatbed scanned (Canoscan 9000F, Canon) to document the overall composition and to detect subunits on a mesoscopic level [90]. The detailed microscopic examination was carried out with a polarizing microscope Axiolab (Zeiss) and the digital image capture software Axiovision (Zeiss) under plain-polarized, cross-polarized, and oblique incident light.

### Appendix A.2. Fire Residue (Black Carbon) Analysis

All samples were dried (40 °C), sieved (>2 mm), and milled prior to analysis. Organic carbon (OC) contents were determined with a Soli TOC Cube (Elementar Analysensysteme, Hanau, Germany) according to Mörchen et al. [91]. Samples preparation followed the protocols of Glaser et al. [32] and Brodowski et al. [31]. Black carbon (BC) content and composition were determined by oxidation of BC to benzene polycarboxylic acids (BPCA). To avoid the contribution of BPCAs from non-pyrogenic matter, the evaluation was limited to five- and six-times carboxylated BPCAs (benzene pentacarboxylic acid and mellitic acid, B5CA/B6CA), and a threshold of 5 mg organic carbon per sample was strictly maintained [92]. While the sum of BPCAs informs on BC quantity (comp. [31,32]), its composition, i.e., the degree of aromatic condensation, provides additional information about changes in combustion temperatures: the hotter a fire burns, the more benzene with 6 carboxyl rings are isolated from the combustion residue (comp. [33,85,93]). Hence, the ratio of B5CA/B6CA was used as a proxy for changes in combustion temperatures [33,85].

Samples were measured using a gas chromatograph equipped with a flame ionization detector (FID; Packard 6890 gas chromatograph, Hewlett Packard GmbH, Waldbronn, Germany), and an HP-5 capillary column (30 m × 0.32 mm i.d., 0.25 mm film thickness, Macherey-Nagel, Düren, Germany; for oven program see Brodowski et al. [31]). Citric acid was used as the first and biphenylene-dicarboxylic acid as the second internal standard to quantify the recovery of citric acid (average recovery: 72%). The BC amounts are expressed relative to kilogram sediment. As proposed by Glaser et al. [32], BPCA yield was corrected for CO<sub>2</sub> loss and insufficient conversion of BC to BPCAs using the factor 2.27, which provides a conservative, minimum estimate of total BC in soil [32]. Note that the B5CA/B6CA ratio was excluded from the evaluation if a sample contained less than 0.10 g BC kg<sup>-1</sup> as interpretation may not be reliable in this case; this applies to samples BC4, BC7 and BC9.

### Appendix A.3. Phytoliths

Phytoliths were extracted from ca. 10 g of sediment from each sample in the laboratory of the Senckenberg Research Institute, Frankfurt, using a modified protocol after Piperno [89] (pp. 90–93):

1. Deflocculation with EDTA;
2. Sieving for removal of coarse sediment and modern plant remains;
3. Clay removal with Stoke's Law gravity separation;
4. Carbonate destruction using HCl;
5. Organic matter removal with HNO<sub>3</sub> and KClO<sub>3</sub>;
6. Heavy liquid separation with sodium polytungstate.

Small amounts of each extracted phytolith sample were mounted on microscopic slides in immersion oil and counted at 400× magnification. At least 300 phytoliths were counted for each sample. In this study, light stands for the absence of any recognizable fire influence and thus for a light/transparent appearance. In the study by Parr [37], it was observed in experimental fire studies that phytoliths take on a dull and opaque color under oxidative conditions. We subsumed as 'dark' phytoliths those with a complete brown to black appearance as well as those with a dark core. Because our interest in this study was mainly to reconstruct the impact of fire on the rockshelter sediments, we restricted counting to three most conspicuous and common morphotypes, following the nomenclature after Neumann et al. [36], the guidelines of International Code for Phytolith Nomenclature (ICPN) 2.0 [36]:

- ELONGATE (ELO): Rectilinear phytoliths with variable sizes and edges (entire, sinuate, etc.). These phytoliths were observed as single-celled or articulated;
- BLOCKY (BLO): Compact phytoliths with length/width <2 and equal width and thickness;
- ACUTE BULBOSUS (ACU\_BUL): Unarticulated phytoliths with a wider antapex that narrows down to an acute apex.

The light and dark samples of each morphotype were counted separately. For each sample, the ratio of light (absence of fire influence) vs. dark phytoliths (contact with fire) phytoliths was calculated.

### Appendix A.4. Ammonium Oxalate Extractable Fe, Mn, Al, and Si

Moderate acidic reactions, initiated by acidified ammonium oxalate, are used to dissolve active non-crystalline oxides, organically bonded oxides and Fe, and Al and Si from allophane and allophane-like components. Allophane and imogolite are metastable aluminosilicates that form mainly on easily weathered volcanic glass or other recently deposited volcanic material (e.g., rocks, pumic) [60,94]. Opal and crystalline iron oxides such as hematite or goethite are not dissolved, although this may vary with sample properties [40]. Laboratory procedures followed the instructions of Tamm [38] and Schwertmann [39]. For the ammonium oxalate extraction solution, 28.42 g of (NH<sub>4</sub>)<sub>2</sub>C<sub>2</sub>O<sub>4</sub> × H<sub>2</sub>O and 18.01 g of the anhydrous oxalic acid (H<sub>2</sub>C<sub>2</sub>O<sub>4</sub>) are admixed with 1 L of ultrapure water. For the analysis, 20 reference samples were selected from the stratigraphy, and 0.5 g of dry fine sediment (<2 mm) was mixed with 50 mL of extraction solution, shaken for 2 h in the dark, and then centrifuged. The extract was filtered with qualitative filters, and the determination was carried out in an atomic absorption spectrometer in an Inductively Coupled Plasma Optical Emission Spectrometry (ICP-OES) (Thermo XSeries 2, Accela Pump). The results are given in mg metal/kg of sediment based on the sample weight. The Al<sub>2</sub>O<sub>3</sub>:SiO<sub>2</sub> ratio in the AO extract is a commonly used indicator for metastable aluminosilicates such as allophane or imogolite within volcanic soils and sediment [60,94]. According to Churchman and Lowe [6], a linear relationship between oxalate extracted Si and Al, which has been observed in New Zealand soil samples, indicates allophane concentration in the sediment. The availability of Si and Al in the sediment solution is therefore essential to clarify whether allophane, imogolite or halloysite is formed [51,52]. The AO extract thus provides a mea-

sure of both the formation of poorly crystalline oxides as well as of the presence of poorly crystalline aluminosilicates and thus may shed light on diachronic changes in weathering intensities

## Appendix B. Results

**Table A1.** Results of the BC content and the ratio of B5CA/B6CA. For samples labeled “excl.”, ratio values are excluded from further interpretation due to the low BC content.

Profile F35							
Sample ID	Depth (m b.s.)	Unit	BC (g kg <sup>-1</sup> )	STD	B5CA/B6CA	STD	
BC1	0.07	I	0.84	0.08	0.95	0.05	
BC2	0.20	II	0.35	0.05	0.77	0.08	
BC3	0.31	III	1.34	0.27	1.03	0.25	
BC4	0.40	III	0.02	0.00	1.36	0.25	excl.
BC5	0.45	III	0.42	0.08	0.89	0.00	
BC6	0.52	IV	0.14	0.04	1.12	0.03	
BC7	0.67	V	0.07	0.00	1.95	1.13	excl.
BC8	0.73	V	1.53	0.44	1.31	0.42	
BC9	0.76	V	0.0033	0.00	1.67	0.00	excl.
BC10	0.93	VI	0.24	0.06	0.79	0.12	
BC11	1.20	VI	0.24	0.03	0.59	0.07	
BC12	1.43	VI	0.23	0.01	0.97	0.10	
BC13	1.62	VII	0.11	0.00	1.28	0.67	
Profile G35							
Sample ID	Depth (m b.s.)	Unit	BC (g kg <sup>-1</sup> )	STD	B5CA/B6CA	STD	
BC14	1.59	VII	0.89	0.08	0.78	0.02	
BC15	1.66	VII	0.97	0.17	0.84	0.08	
BC16	1.77	VII	0.17	0.02	1.78	0.98	excl.
BC17	1.85	VII	0.48	0.08	0.77	0.11	
BC18	1.92	VII	0.23	0.00	0.76	0.13	
BC19	1.93	VIII	0.21	0.01	0.85	0.08	
BC20	2.00	IX	0.52	0.10	0.79	0.12	

**Table A2.** Results of the phytolith ratio for both squares F35 and G35. The classification was made according to the three fundamental morphotypes: ELONGATE (ELO), BLOCKY (BLO), ACUTE BULBOSUS (ACU\_BUL). Samples that could not be counted correctly are marked with the abbreviation n.c.

Profile F35											
Sample ID	Depth (m b.s.)	Unit	BLO light	ELO light	ACU_BUL light	BLO dark	ELO dark	ACU_BUL dark	Sum	% light	% dark
SOD_002	0.03	I	30	250	10	9	13	3	315	92.1	7.9
SOD_006	0.13	II	44	146	20	42	52	22	326	64.4	35.6
SOD_009	0.19	III	2	3	1	105	117	104	335	1.8	98.2
SOD_013	0.27	III	26	94	29	91	43	29	312	47.8	52.2
SOD_018	0.37	III	20	108	14	78	68	28	316	44.9	55.1
SOD_025	0.51	IV	5	25	2	124	95	71	322	9.9	90.1
SOD_027	0.55	IV	25	210	13	12	38	13	310	79.7	20.3
SOD_031	0.63	V	3	3	1	133	117	83	340	2.1	97.9
SOD_039	0.79	VI	32	158	23	18	82	37	350	60.9	39.1
SOD_050	1.01	VI	33	121	14	28	106	72	374	44.9	55.1
SOD_060	1.21	VI	15	220	36	11	41	25	348	77.9	22.1
SOD_071	1.43	VI (VII)	44	98	16	38	71	66	333	47.4	52.6
SOD_081	1.63	VII	32	78	14	30	83	67	310	40.3	59.7

Table A2. Cont.

Profile G35											
Sample ID	Depth (m b.s.)	Unit	BLO light	ELO light	ACU_BLO light	BLO dark	ELO dark	ACU_BLO dark	Sum	% light	% dark
SOD_087	1.44	VI (VII)	5	8	3	117	170	113	416	3.8	96.2
SOD_096	1.62	VII	28	138	11	22	84	55	338	52.4	47.6
SOD_103	1.8	VII	20	257	22	9	20	16	344	86.9	13.1
SOD_106	1.86	VII	10	253	18	2	12	9	303	92.7	7.3
SOD_18_03	1.96	VIII	11	223	19	5	32	16	306	82.7	17.3
SOD_18_07	2.04	IX	n.c.	n.c.	n.c.	n.c.	n.c.	n.c.	n.c.	n.c.	n.c.

Table A3. Results of ammonium oxalate extraction showing standard deviation (s) and AlO:SiO ratio. Samples SOD\_003 to 083 originate from profile F35 and SOD\_86 to SOD\_18\_07 from profile G35.

Profile F35											
Sample ID	Depth (m b.s.)	Unit	Al <sub>o</sub> (g kg <sup>-1</sup> )	Al <sub>o</sub> s (g kg <sup>-1</sup> )	Fe <sub>o</sub> (g kg <sup>-1</sup> )	Fe <sub>o</sub> s (g kg <sup>-1</sup> )	Mn <sub>o</sub> (g kg <sup>-1</sup> )	Mn <sub>o</sub> s (g kg <sup>-1</sup> )	Si <sub>o</sub> (g kg <sup>-1</sup> )	Si <sub>o</sub> s (g kg <sup>-1</sup> )	Al <sub>o</sub> :Si <sub>o</sub>
SOD_003	0.06	I	1.91	0.07	5.97	0.23	1.20	0.19	0.93	0.02	2.06
SOD_007	0.15	II	0.77	0.03	1.84	0.15	0.44	0.00	0.31	0.02	2.47
SOD_009	0.19	III	9.45	0.26	4.98	0.02	1.77	0.01	2.76	0.05	3.42
SOD_015	0.31	III	0.84	0.02	1.87	0.03	0.66	0.01	0.37	0.01	2.26
SOD_018	0.37	III	1.40	0.07	2.98	0.26	1.05	0.11	0.55	0.04	2.53
SOD_025	0.51	IV	0.90	0.12	1.77	0.24	0.92	0.17	0.39	0.06	2.29
SOD_029	0.59	V	7.00	0.39	4.80	0.37	2.77	0.10	2.32	0.28	3.02
SOD_031	0.63	V	17.07	0.45	5.25	0.39	2.23	0.17	5.96	0.42	2.86
SOD_036	0.73	V/VI	1.92	0.03	3.21	0.18	0.51	0.01	0.67	0.03	2.87
SOD_044	0.89	VI	2.07	0.08	7.66	0.16	0.89	0.15	1.02	0.00	2.03
SOD_051	1.03	VI	2.17	0.11	8.15	0.96	0.64	0.09	1.06	0.10	2.06
SOD_054	1.09	VI	2.08	0.05	5.41	0.27	0.68	0.06	0.86	0.05	2.42
SOD_061	1.23	VI	1.98	0.15	6.24	0.76	0.64	0.13	0.91	0.11	2.17
SOD_078	1.57	VII	1.70	0.04	5.26	0.10	0.80	0.09	0.77	0.03	2.20
SOD_083	1.68	VII	2.85	0.11	5.30	0.14	2.26	0.06	1.03	0.04	2.76

Profile G35											
Sample ID	Depth (m b.s.)	Unit	Al <sub>o</sub> (g kg <sup>-1</sup> )	Al <sub>o</sub> s (g kg <sup>-1</sup> )	Fe <sub>o</sub> (g kg <sup>-1</sup> )	Fe <sub>o</sub> s (g kg <sup>-1</sup> )	Mn <sub>o</sub> (g kg <sup>-1</sup> )	Mn <sub>o</sub> s (g kg <sup>-1</sup> )	Si <sub>o</sub> (g kg <sup>-1</sup> )	Si <sub>o</sub> s (g kg <sup>-1</sup> )	Al <sub>o</sub> :Si <sub>o</sub>
SOD_086	1.41	VI	2.23	0.11	7.98	0.57	0.80	0.09	1.25	0.09	1.78
SOD_102	1.78	VII	1.39	0.01	3.40	0.11	1.74	0.02	0.59	0.01	2.37
SOD_18_01	1.92	VII	1.47	0.06	3.56	0.30	1.00	0.11	0.56	0.05	2.64
SOD_18_04	1.98	VIII	1.57	0.11	3.77	0.33	1.24	0.15	0.59	0.05	2.68
SOD_18_07	2.04	IX	1.56	0.07	3.96	0.09	1.37	0.03	0.53	0.02	2.96

## References

- Hensel, E.A.; Vogelsang, R.; Noack, T.; Bubenzer, O. Stratigraphy and Chronology of Sodicho Rockshelter—A New Sedimentological Record of Past Environmental Changes and Human Settlement Phases in Southwestern Ethiopia. *Front. Earth Sci.* **2021**, *8*. [[CrossRef](#)]
- Brandt, S.A.; Fisher, E.C.; Hildebrand, E.A.; Vogelsang, R.; Ambrose, S.H.; Lesur, J.; Wang, H. Early MIS 3 occupation of Mochena Borago Rockshelter, Southwest Ethiopian Highlands: Implications for Late Pleistocene archaeology, paleoenvironments and modern human dispersals. *Quat. Int.* **2012**, *274*, 38–54. [[CrossRef](#)]
- Brandt, S.; Hildebrand, E.; Vogelsang, R.; Wolfhagen, J.; Wang, H. A new MIS 3 radiocarbon chronology for Mochena Borago Rockshelter, SW Ethiopia: Implications for the interpretation of Late Pleistocene chronostratigraphy and human behavior. *J. Archaeol. Sci. Rep.* **2017**, *11*, 352–369. [[CrossRef](#)]
- Vogelsang, R.; Wendt, K.P. Reconstructing prehistoric settlement models and land use patterns on Mt. Damota/SW Ethiopia. *Quat. Int.* **2018**, *485*, 140–149. [[CrossRef](#)]
- Waters, M.R. *Principles of Geoarchaeology: A North American Perspective*; University of Arizona Press: Tucson, AZ, USA, 1992; ISBN 0-8165-1770-3.
- Churchman, G.J.; Lowe, D.J. Alteration, Formation, and Occurrence of Minerals in Soils. In *Handbook of Soil Sciences: Properties and Processes*; CRC Press: Boca Raton, FL, USA, 2012; pp. 1–72.
- Stoops, G.; Nicosia, C. Introduction. In *Archaeological Soil and Sediment Micromorphology*; Nicosia, C., Stoops, G., Eds.; John Wiley & Sons, Ltd.: Chichester, UK, 2017; pp. 1–5.
- Mark, B.G.; Osmaston, H.A. Quaternary glaciation in Africa: Key chronologies and climatic implications. *J. Quat. Sci.* **2008**, *23*, 589–608. [[CrossRef](#)]
- Junginger, A.; Trauth, M.H. Hydrological constraints of paleo-Lake Suguta in the Northern Kenya Rift during the African Humid Period (15–5kaBP). *Glob. Planet. Chang.* **2013**, *111*, 174–188. [[CrossRef](#)]

10. Stoops, G. *Guidelines for Analysis and Description of Soil and Regolith Thin Sections*; John Wiley & Sons: Hoboken, NJ, USA, 2021; Volume 184.
11. Goldberg, P.; Miller, C.E.; Schiegl, S.; Ligouis, B.; Berna, F.; Conard, N.J.; Wadley, L. Bedding, hearths, and site maintenance in the Middle Stone Age of Sibudu Cave, KwaZulu-Natal, South Africa. *Archaeol. Anthropol. Sci.* **2009**, *1*, 95–122. [[CrossRef](#)]
12. Marean, C.W.; Bar-Matthews, M.; Fisher, E.; Goldberg, P.; Herries, A.; Karkanas, P.; Nilssen, P.J.; Thompson, E. The stratigraphy of the Middle Stone Age sediments at Pinnacle Point Cave 13B (Mossel Bay, Western Cape Province, South Africa). *J. Hum. Evol.* **2010**, *59*, 234–255. [[CrossRef](#)]
13. Miller, C.E.; Goldberg, P.; Berna, F. Geoarchaeological investigations at Diepkloof Rock Shelter, Western Cape, South Africa. *J. Archaeol. Sci.* **2013**, *40*, 3432–3452. [[CrossRef](#)]
14. Inglis, R.H.; French, C.; Farr, L.; Hunt, C.O.; Jones, S.; Reynolds, T.; Barker, G. Sediment micromorphology and site formation processes during the Middle to Later Stone Ages at the Haua Fteah Cave, Cyrenaica, Libya. *Geoarchaeology* **2017**, *33*, 328–348. [[CrossRef](#)]
15. Klasen, N.; Kehl, M.; Mikdad, A.; Brückner, H.; Weniger, G.-C. Chronology and formation processes of the Middle to Upper Palaeolithic deposits of Ifri n’Ammar using multi-method luminescence dating and micromorphology. *Quat. Int.* **2018**, *485*, 89–102. [[CrossRef](#)]
16. Potì, A.; Kehl, M.; Broich, M.; Marco, Y.C.; Hutterer, R.; Jentke, T.; Linstädter, J.; López-Sález, J.A.; Mikdad, A.; Morales, J.; et al. Human occupation and environmental change in the western Maghreb during the Last Glacial Maximum (LGM) and the Late Glacial. New evidence from the Iberomaurusian site Ifri El Baroud (northeast Morocco). *Quat. Sci. Rev.* **2019**, *220*, 87–110. [[CrossRef](#)]
17. Goldberg, P.; Bar-Yosef, O. Site Formation Processes in Kebara and Hayonim Caves and Their Significance in Levantine Prehistoric Caves. In *Neandertals and Modern Humans in Western Asia*; Akazawa, T., Aoki, K., Bar-Yosef, O., Eds.; Springer: Boston, MA, USA, 2005; pp. 107–125.
18. Albert, R.M.; Berna, F.; Goldberg, P. Insights on Neanderthal fire use at Kebara Cave (Israel) through high resolution study of prehistoric combustion features: Evidence from phytoliths and thin sections. *Quat. Int.* **2012**, *247*, 278–293. [[CrossRef](#)]
19. Kehl, M.; Burow, C.; Cantalejo, P.; Domínguez-Bella, S.; Durán, J.J.; Henselowsky, F.; Klasen, N.; Linstädter, J.; Medianero, J.; Pastoors, A.; et al. Site formation and chronology of the New Paleolithic Site Sima de Las Palomas de Teba, Southern Spain. *Quat. Res.* **2016**, *85*, 313–331. [[CrossRef](#)]
20. Miller, C.E. *A Tale of Two Swabian Caves: Geoarchaeological Investigations at Hohle Fels and Geißenklösterle*; Kerns Verlag: Tübingen, Germany, 2015; ISBN 3-935751-19-2.
21. Whitau, R.; Vannieuwenhuyse, D.; Dotte-Sarout, E.; Balme, J.; O’Connor, S. Home Is Where the Hearth Is: Anthracological and Microstratigraphic Analyses of Pleistocene and Holocene Combustion Features, Riwi Cave (Kimberley, Western Australia). *J. Archaeol. Method Theory* **2018**, *25*, 739–776. [[CrossRef](#)] [[PubMed](#)]
22. Brancaleoni, G.; Shnaider, S.; Osipova, E.; Danukalova, G.; Kurbanov, R.; Deput, E.; Kyzy, S.A.; Abdykanova, A.; Krajcarz, M.T. Depositional history of a talus cone in an arid intermontane basin in Central Asia: An interdisciplinary study at the Late Pleistocene–Late Holocene Obishir-I site, Kyrgyzstan. *Geoarchaeology* **2021**, 1–24. [[CrossRef](#)]
23. Morley, M.W.; Goldberg, P.; Uliyanov, V.A.; Kozlikin, M.B.; Shunkov, M.V.; Derevianko, A.P.; Jacobs, Z.; Roberts, R.G. Hominin and animal activities in the microstratigraphic record from Denisova Cave (Altai Mountains, Russia). *Sci. Rep.* **2019**, *9*, 13785. [[CrossRef](#)] [[PubMed](#)]
24. Kolobova, K.A.; Roberts, R.G.; Chabai, V.P.; Jacobs, Z.; Krajcarz, M.T.; Shalagina, A.V.; Krivoshapkin, A.I.; Li, B.; Uthmeier, T.; Markin, S.V.; et al. Archaeological evidence for two separate dispersals of Neanderthals into southern Siberia. *Proc. Natl. Acad. Sci. USA* **2020**, *117*, 2879–2885. [[CrossRef](#)] [[PubMed](#)]
25. Goldberg, E.D. *Black Carbon in the Environment: Properties and Distribution*; John Wiley and Sons: New York, NY, USA, 1985.
26. Schmidt, M.W.I.; Noack, A.G. Black carbon in soils and sediments: Analysis, distribution, implications, and current challenges. *Glob. Biogeochem. Cycles* **2000**, *14*, 777–793. [[CrossRef](#)]
27. Keiluweit, M.; Nico, P.S.; Johnson, M.G.; Kleber, M. Dynamic Molecular Structure of Plant Biomass-Derived Black Carbon (Biochar). *Environ. Sci. Technol.* **2010**, *44*, 1247–1253. [[CrossRef](#)]
28. Masiello, C.A.; Druffel, E.R.M. Black Carbon in Deep-Sea Sediments. *Science* **1998**, *280*, 1911–1913. [[CrossRef](#)] [[PubMed](#)]
29. Scott, A.C.; Glasspool, I.J. The diversification of Paleozoic fire systems and fluctuations in atmospheric oxygen concentration. *Proc. Natl. Acad. Sci. USA* **2006**, *103*, 10861–10865. [[CrossRef](#)] [[PubMed](#)]
30. Wolf, M.; Lehdorff, E.; Mrowald, M.; Eckmeier, E.; Kehl, M.; Frechen, M.; Pätzold, S.; Amelung, W. Black carbon: Fire fingerprints in Pleistocene loess–palaeosol archives in Germany. *Org. Geochem.* **2014**, *70*, 44–52. [[CrossRef](#)]
31. Brodowski, S.; Rodionov, A.; Haumaier, L.; Glaser, B.; Amelung, W. Revised black carbon assessment using benzene polycarboxylic acids. *Org. Geochem.* **2005**, *36*, 1299–1310. [[CrossRef](#)]
32. Glaser, B.; Haumaier, L.; Guggenberger, G.; Zech, W. Black carbon in soils: The use of benzenecarboxylic acids as specific markers. *Org. Geochem.* **1998**, *29*, 811–819. [[CrossRef](#)]
33. Wolf, M.; Lehdorff, E.; Wiesenberger, G.; Stockhausen, M.; Schwark, L.; Amelung, W. Towards reconstruction of past fire regimes from geochemical analysis of charcoal. *Org. Geochem.* **2013**, *55*, 11–21. [[CrossRef](#)]
34. Vrydaghs, L.; Devos, Y.; Pető, Á. Opal Phytoliths. In *Archaeological Soil and Sediment Micromorphology*; John Wiley & Sons, Ltd.: Chichester, UK, 2017; pp. 155–163.

35. Kaczorek, D.; Vrydaghs, L.; Devos, Y.; Petó, Á.; Effland, W.R. Biogenic Siliceous Features. In *Interpretation of Micromorphological Features of Soils and Regoliths*, 2nd ed.; Stoops, G., Marcelino, V., Mees, F., Eds.; Elsevier: Amsterdam, The Netherlands; Oxford, UK, 2018; pp. 157–176, ISBN 978-0-444-63522-8.
36. Neumann, K.; Strömberg, C.A.E.; Ball, T.; Albert, R.M.; Vrydaghs, L.; Cummings, L.S. International Code for Phytolith Nomenclature (ICPN) 2.0. *Ann. Bot.* **2019**, *124*, 189–199. [[CrossRef](#)]
37. Parr, J.F. Effect of fire on phytolith coloration. *Geoarchaeology* **2006**, *21*, 171–185. [[CrossRef](#)]
38. Tamm, O. Über die Oxalatmethode in der chemischen Bodenanalyse. *Med. Följer Skogsvårdsföreningens Tidskr.* **1932**, *27*, 1–20.
39. Schwertmann, U. Der einfluss einfacher organischer anionen auf die bildung von goethit und hämatit aus amorphen Fe(III)-Hydroxid. *Geoderma* **1970**, *3*, 207–214. [[CrossRef](#)]
40. Rennert, T. Wet-chemical extractions to characterise pedogenic Al and Fe species—A critical review. *Soil Res.* **2019**, *57*, 1–16. [[CrossRef](#)]
41. Woldegabriel, G.; Aronson, J.L.; Walter, R. Geology, geochronology, and rift basin development in the central sector of the Main Ethiopia Rift. *GSA Bull.* **1990**, *102*, 439–458. [[CrossRef](#)]
42. WoldeGabriel, G.; Walter, R.C.; Aronson, J.L.; Hart, W.K. Geochronology and distribution of silicic volcanic rocks of Plio-Pleistocene age from the central sector of the Main Ethiopian Rift. *Quat. Int.* **1992**, *13–14*, 69–76. [[CrossRef](#)]
43. Chernet, T. Geology and hydrothermal resources in the northern Lake Abaya area (Ethiopia). *J. Afr. Earth Sci.* **2011**, *61*, 129–141. [[CrossRef](#)]
44. Hensel, E.A.; Bödeker, O.; Bubenzer, O.; Vogelsang, R. Combining geomorphological–hydrological analyses and the location of settlement and raw material sites—A case study on understanding prehistoric human settlement activity in the southwestern Ethiopian Highlands. *E&G Quat. Sci. J.* **2019**, *68*, 201–213. [[CrossRef](#)]
45. Berhanu, B.; Melesse, A.M.; Seleshi, Y. GIS-based hydrological zones and soil geo-database of Ethiopia. *Catena* **2013**, *104*, 21–31. [[CrossRef](#)]
46. IUSS Working Group WRB. *World Reference Base for Soil Resources 2014: International Soil Classification System for Naming Soils and Creating Legends for Soil Maps*; FAO: Rome, Italy, 2015; Volume 106.
47. Guthertz, X.; Jallot, L.; Lesur, J.; Pouzolles, G.; Sordoillet, D. Les fouilles de l’abri sous-roche de Moche Borago (Soddo-Wolayta). Premier bilan. *Ann. D’ethiopie* **2002**, *18*, 181–190. [[CrossRef](#)]
48. Fisher, E.C. Late Pleistocene Technological Change and Hunter Gatherer Behavior at Moche Borago Rockshelter, Sodo-Wolayta, Ethiopia: Flaked Stone Artifacts from the Early OIS 3 (60–43 Ka) Deposits. Ph.D. Thesis, University of Florida, Gainesville, FL, USA, 2010.
49. Mentzer, S.M. Microarchaeological Approaches to the Identification and Interpretation of Combustion Features in Prehistoric Archaeological Sites. *J. Archaeol. Method Theory* **2014**, *21*, 616–668. [[CrossRef](#)]
50. Stoops, G.; Sedov, S.; Shoba, S. Regoliths and Soils on Volcanic Ash. In *Interpretation of Micromorphological Features of Soils and Regoliths*, 2nd ed.; Elsevier: Amsterdam, The Netherlands; Oxford, UK, 2018; pp. 721–751.
51. Parfitt, R.L.; Furkert, R.J.; Henmi, T. Identification and Structure of Two Types of Allophane from Volcanic Ash Soils and Tephra. *Clays Clay Miner.* **1980**, *28*, 328–334. [[CrossRef](#)]
52. Farmer, V.C.; McHardy, W.J.; Robertson, L.; Walker, A.; Wilson, M.J. Micromorphology and sub-microscopy of allophane and imogolite in a podzol Bs horizon: Evidence for translocation and origin. *J. Soil Sci.* **1985**, *36*, 87–95. [[CrossRef](#)]
53. Churchman, G.J.; Velde, B. *Soil Clays: Linking Geology, Biology, Agriculture, and the Environment*; CRC Press: Boca Raton, FL, USA, 2019; ISBN 0-429-53224-5.
54. Gillhuber, S.; Lehrberger, G.; Thuro, K. Teplá Trachyte Weathering Phenomena and Physical Properties of a Rare Volcanogenic Building Stone. *Geol. Soc. Lond.* **2006**, *469*, 1–11.
55. Foerster, V.; Junginger, A.; Langkamp, O.; Gebru, T.; Asrat, A.; Umer, M.; Lamb, H.F.; Wennrich, V.; Rethemeyer, J.; Nowaczyk, N.; et al. Climatic change recorded in the sediments of the Chew Bahir basin, southern Ethiopia, during the last 45,000 years. *Quat. Int.* **2012**, *274*, 25–37. [[CrossRef](#)]
56. Foerster, V.; Vogelsang, R.; Junginger, A.; Asrat, A.; Lamb, H.; Schaebitz, F.; Trauth, M. Environmental change and human occupation of southern Ethiopia and northern Kenya during the last 20,000 years. *Quat. Sci. Rev.* **2015**, *129*, 333–340. [[CrossRef](#)]
57. Hildebrand, E.A.; Brandt, S.A.; Friis, I.; Demissew, S. Paleoenvironmental Reconstructions for the Horn of Africa: Interdisciplinary Perspectives on Strategy and Significance. In *Trees, Grasses and Crops. People and Plants in Sub-saharan Africa and Beyond*; Verlag Dr. Rudolf Habelt: Bonn, Germany, 2019; pp. 187–210, ISBN 3-7749-4221-8.
58. Trauth, M.H.; Asrat, A.; Duesing, W.; Foerster, V.; Kraemer, K.H.; Marwan, N.; Maslin, M.; Schaebitz, F. Classifying past climate change in the Chew Bahir basin, southern Ethiopia, using recurrence quantification analysis. *Clim. Dyn.* **2019**, *53*, 2557–2572. [[CrossRef](#)]
59. Chadwick, O.A.; Gavenda, R.T.; Kelly, E.F.; Ziegler, K.; Olson, C.G.; Elliott, W.; Hendricks, D.M. The impact of climate on the biogeochemical functioning of volcanic soils. *Chem. Geol.* **2003**, *202*, 195–223. [[CrossRef](#)]
60. Parfitt, R.; Henmi, T. Comparison of an oxalate-extraction method and an infrared spectroscopic method for determining allophane in soil clays. *Soil Sci. Plant Nutr.* **1982**, *28*, 183–190. [[CrossRef](#)]
61. Stoops, G.; Marcelino, V. Lateritic and Bauxitic Materials. In *Interpretation of Micromorphological Features of Soils and Regoliths*, 2nd ed.; Stoops, G., Marcelino, V., Mees, F., Eds.; Elsevier: Amsterdam, The Netherlands; Oxford, UK, 2018; pp. 691–720.

62. Kühn, P.; Aguilar, J.; Miedema, R.; Bronnikova, M. Textural Pedofeatures and Related Horizons. In *Interpretation of Micromorphological Features of Soils and Regoliths*, 2nd ed.; Stoops, G., Marcelino, V., Mees, F., Eds.; Elsevier: Amsterdam, The Netherlands; Oxford, UK, 2018; pp. 377–423, ISBN 978-0-444-63522-8.
63. Karkanias, P. Chemical Alteration. In *Encyclopedia of Geoarchaeology*; Gilbert, A.S., Ed.; Springer: Dordrecht, The Netherlands, 2017; pp. 129–138, ISBN 978-1-4020-4409-0.
64. Stoops, G.; Mees, F. Groundmass Composition and Fabric. In *Interpretation of Micromorphological Features of Soils and Regoliths*, 2nd ed.; Stoops, G., Marcelino, V., Mees, F., Eds.; Elsevier: Amsterdam, The Netherlands; Oxford, UK, 2018; pp. 73–125.
65. Vepraskas, M.J.; Lindbo, D.L.; Stolt, M.H. Redoximorphic Features. In *Interpretation of Micromorphological Features of Soils and Regoliths*, 2nd ed.; Stoops, G., Marcelino, V., Mees, F., Eds.; Elsevier: Amsterdam, The Netherlands; Oxford, UK, 2018; pp. 425–445, ISBN 978-0-444-63522-8.
66. Goldberg, P.; Berna, F.; Chazan, M. Deposition and Diagenesis in the Earlier Stone Age of Wonderwerk Cave, Excavation 1, South Africa. *Afr. Archaeol. Rev.* **2015**, *32*, 613–643. [[CrossRef](#)]
67. Villagran, X.S.; Balbo, A.L.; Madella, M.; Vila, A.; Estevez, J. Experimental micromorphology in Tierra del Fuego (Argentina): Building a reference collection for the study of shell middens in cold climates. *J. Archaeol. Sci.* **2011**, *38*, 588–604. [[CrossRef](#)]
68. Mallol, C.; Mentzer, S.M.; Miller, C.E. Combustion Features. In *Archaeological Soil and Sediment Micromorphology*; John Wiley & Sons, Ltd.: Chichester, UK, 2017; pp. 299–330.
69. Fischer, M.L.; Bachofer, F.; Yost, C.L.; Bludau, I.J.E.; Schepers, C.; Foerster, V.; Lamb, H.; Schäbitz, F.; Asrat, A.; Trauth, M.H.; et al. A Phytolith Supported Biosphere-Hydrosphere Predictive Model for Southern Ethiopia: Insights into Paleoenvironmental Changes and Human Landscape Preferences since the Last Glacial Maximum. *Geosciences* **2021**, *11*, 418. [[CrossRef](#)]
70. Kooistra, M.J.; Pulleman, M.M. Features Related to Faunal Activity. In *Interpretation of Micromorphological Features of Soils and Regoliths*, 2nd ed.; Stoops, G., Marcelino, V., Mees, F., Eds.; Elsevier: Amsterdam, The Netherlands; Oxford, UK, 2018; pp. 447–469, ISBN 978-0-444-63522-8.
71. Parfitt, R.L. Allophane and imogolite: Role in soil biogeochemical processes. *Clay Miner.* **2009**, *44*, 135–155. [[CrossRef](#)]
72. Goldberg, P.; Holliday, V.T.; Ferring, C.R. *Earth Sciences and Archaeology*; Kluwer Academic/Plenum Publishers: New York, NY, USA, 2001; ISBN 978-0-306-46279-5.
73. Tarasenko, I.; Bielders, C.L.; Guevara, A.; Delmelle, P. Surface crusting of volcanic ash deposits under simulated rainfall. *Bull. Volcanol.* **2019**, *81*, 30. [[CrossRef](#)]
74. Williams, G.T.; Jenkins, S.F.; Lee, D.W.J.; Wee, S.J. How rainfall influences tephra fall loading—An experimental approach. *Bull. Volcanol.* **2021**, *83*, 42. [[CrossRef](#)]
75. Goldberg, P.; Aldeias, V. Why does (archaeological) micromorphology have such little traction in (geo)archaeology? *Archaeol. Anthr. Sci.* **2018**, *10*, 269–278. [[CrossRef](#)]
76. Karkanias, P.; Goldberg, P. Phosphatic Features. In *Interpretation of Micromorphological Features of Soils and Regoliths*, 2nd ed.; Stoops, G., Marcelino, V., Mees, F., Eds.; Elsevier: Amsterdam, The Netherlands; Oxford, UK, 2018; pp. 323–346, ISBN 978-0-444-63522-8.
77. Lambrecht, G.; de Vera, C.R.; Jambrina-Enríquez, M.; Crevecoeur, I.; Gonzalez-Urquijo, J.; Lazuen, T.; Monnier, G.; Pajović, G.; Tostevin, G.; Mallol, C. Characterisation of charred organic matter in micromorphological thin sections by means of Raman spectroscopy. *Archaeol. Anthr. Sci.* **2021**, *13*, 13. [[CrossRef](#)] [[PubMed](#)]
78. Homsey, L.K.; Capo, R.C. Integrating geochemistry and micromorphology to interpret feature use at Dust Cave, a Paleo-Indian through middle-archaic site in Northwest Alabama. *Geoarchaeology* **2006**, *21*, 237–269. [[CrossRef](#)]
79. Canti, M.; Linford, N. The Effects of Fire on Archaeological Soils and Sediments: Temperature and Colour Relationships. *Proc. Prehist. Soc.* **2000**, *66*, 385–395. [[CrossRef](#)]
80. Röpke, A.; Dietl, C. Burnt Soils and Sediments. In *Archaeological Soil and Sediment Micromorphology*; John Wiley & Sons, Ltd.: Chichester, UK, 2017; pp. 173–180.
81. Rodríguez-Rodríguez, A.; Fedoroff, N.; Tejedor-Salguero, M.L.; Fernández-Caldas, E. Observaciones Preliminares Sobre La Alteración En Los Suelos Fersialíticos Sobre Materiales Volcánicos (Islas Canarias). *An. Edafol. Agrobiol.* **1980**, *39*, 1923–1939.
82. Goldberg, P. Micromorphology of Pech-de-l’Azé II sediments. *J. Archaeol. Sci.* **1979**, *6*, 17–47. [[CrossRef](#)]
83. Goldberg, P. Some Observations on Middle and Upper Palaeolithic Ashy Cave and Rockshelter Deposits in the Near East. In *More than Meets the Eye: Studies on Upper Palaeolithic Diversity in the Near East*; Oxbow Books: Oxford, UK, 2003; pp. 19–32.
84. Dibble, H.; Berna, F.; Goldberg, P.; McPherron, S.; Mentzer, S.; Niven, L.; Richter, D.; Sandgathe, D.; Théry-Parisot, I.; Turq, A. A Preliminary Report on Pech de l’Azé IV, Layer 8 (Middle Paleolithic, France). *PaleoAnthropology* **2009**, *2009*, 182–219. [[CrossRef](#)]
85. Schneider, M.P.; Hilf, M.; Vogt, U.F.; Schmidt, M.W. The benzene polycarboxylic acid (BPCA) pattern of wood pyrolyzed between 200 °C and 1000 °C. *Org. Geochem.* **2010**, *41*, 1082–1088. [[CrossRef](#)]
86. Lehdorff, E.; Linstädter, J.; Kehl, M.; Weniger, G.-C. Fire history reconstruction from Black Carbon analysis in Holocene cave sediments at Ifri Oudadane, Northeastern Morocco. *Holocene* **2015**, *25*, 398–402. [[CrossRef](#)]
87. Braadbaart, F.; Poole, I. Morphological, chemical and physical changes during charcoalification of wood and its relevance to archaeological contexts. *J. Archaeol. Sci.* **2008**, *35*, 2434–2445. [[CrossRef](#)]
88. Piperno, D.R. *Phytoliths: A Comprehensive Guide for Archaeologists and Paleoecologists*; AltaMira Press: Lanham, MD, USA, 2006; ISBN 0-7591-1446-3.
89. Beckmann, T. Präparation Bodenkundlicher Dünnschliffe Für Mikromorphologische Untersuchungen. *Hohenh. Bodenkd. Hefte* **1997**, *40*, 86–103.

90. Arpin, T.L.; Mallol, C.; Goldberg, P. Short contribution: A new method of analyzing and documenting micromorphological thin sections using flatbed scanners: Applications in geoarchaeological studies. *Geoarchaeology* **2002**, *17*, 305–313. [[CrossRef](#)]
91. Mörchen, R.; Lehdorff, E.; Diaz, F.A.; Moradi, G.; Bol, R.; Fuentes, B.; Klumpp, E.; Amelung, W. Carbon accrual in the Atacama Desert. *Glob. Planet. Chang.* **2019**, *181*, 102993. [[CrossRef](#)]
92. Kappenberg, A.; Blasing, M.; Lehdorff, E.; Amelung, W. Black carbon assessment using benzene polycarboxylic acids: Limitations for organic-rich matrices. *Org. Geochem.* **2016**, *94*, 47–51. [[CrossRef](#)]
93. Hammes, K.; Schmidt, M.W.I.; Smernik, R.J.; Currie, L.A.; Ball, W.P.; Nguyen, T.H.; Louchouart, P.; Houel, S.; Gustafsson, Ö.; Elmquist, M.; et al. Comparison of quantification methods to measure fire-derived (black/elemental) carbon in soils and sediments using reference materials from soil, water, sediment and the atmosphere. *Glob. Biogeochem. Cycles* **2007**, *21*, GB3016. [[CrossRef](#)]
94. Harsh, J.; Chorover, J.; Nizeyimana, E. Allophane and Imogolite. In *Soil Mineralogy with Environmental Applications*; Soil Science Society of America: Madison, WI, USA, 2002; Volume 7, pp. 291–322.

## 4.1 Supplement material

This supplementary material is published as part of the following open access publication as Table S1: Electronic Supplement: Overview of micromorphological results:

Hensel, E. A., Kehl, M., Wöstehoff, L., Neumann, K., Vogelsang, R., Bubbenzer, O. (2022). A Multi-Method Approach for Deciphering Rockshelter Microstratigraphies—The Role of the Sodicho Rockshelter (SW Ethiopia) as a Geoarchaeological Archive. *Geosciences* 12(2), 92. doi: <https://doi.org/10.3390/geosciences12020092>

### Note:

For a better resolution, the reader is advised to access the online material at <https://www.mdpi.com/article/10.3390/geosciences12020092/s1>.







Block ID		Pedofeatures										Biogenic pedofeatures								
		Fine components					Micromass					Textural pedofeatures					Passage features			
		Thin sections	Subunit	Diatoms	Roots	Feldspar	Volcanic glass	Charcoal	Ash	Char	c/f-related distr.	Type of b-fabric	Hypocoating (Fe/Mn) (q-quasi)	Redoximorphic nodules	Clay coating	Impure brown yellow, speckled interference	Light (yellow), undiff. interference	Silt coating	Brown, undiff. interference	Gonbite coating
	IIIg2			•	••	••	••	•	•	Single-spaced porphyric	undifferentiated	-	-	••	••	(•)	-	-	-	-
SOD_3	3-1			•	•	•	•	(•)	•	Single-spaced porphyric	undifferentiated	(•)	•	•	-	-	-	•	-	-
	IIIc			•	••	••	•	-	•	Single-spaced porphyric	undifferentiated	(•)	(•)	••	•	-	-	••	-	-
	IIIp			•	•	•	•	-	•	Single-spaced porphyric	stipple-speckled	(•)	(•)	••	•	-	-	-	-	-
	IIIe			•	••	••	•	-	•	double spaced and open porphyric	undifferentiated	-	-	••	•	-	-	-	-	••
	IIIp			•	•	•	•	-	•	Single-spaced porphyric	undifferentiated	(•)	(•)	••	(•)	(•)	-	-	-	-
3-2	IIIp			•	•	•	•	-	•	double spaced and open porphyric	undifferentiated	•	(•)	•	-	-	-	-	-	•
	IIIf			•	•	•	-	-	•	open porphyric	undifferentiated	-	(•)	••	•	-	-	••	-	•
	IVa			•	•	•	-	-	•	coarse monic	stipple-speckled	-	(•)	-	-	-	-	-	-	-
SOD_4	4-1			•	•	•	•	-	•	coarse monic	stipple-speckled	-	(•)	-	-	-	-	-	-	-
	IVb			•	••	••	••	-	•	coarse monic	stipple-speckled	•	•	••	•	(•)	-	-	-	-
	IVc			•	•	••	••	-	•	coarse monic—all the same	(stipple-speckled)	-	-	-	-	(•)	-	-	-	-
4/2	IVc			•	•	••	••	-	•	coarse monic	(stipple-speckled)	-	-	-	•	(•)	-	-	-	(•)
	IVp			•	•	••	••	-	•	porostriated	porostriated	-	-	•••	•••	(•)	-	-	-	-
	Va			•	•	•	•	-	•	double spaced coarse enaulig, Single-spaced porphyric	undifferentiated	(•)	-	•	-	-	-	-	-	-
	Va2			•	••	••	••	-	•	-	stipple-speckled	-	(•)	••	••	?	-	-	-	-
4-3	Va			•	•	••	••	-	•	double spaced coarse enaulig, Single-spaced porphyric	undifferentiated	•	-	(•)	(•)	-	-	••	-	-
	Vb			•	•	-	-	-	•	double spaced coarse enaulig	undifferentiated	(•)	-	-	-	-	-	•	-	-
SOD_J	J_3-1			•	•	••	••	•	•	double spaced coarse enaulig	undifferentiated	•	(•)	-	-	-	-	•	-	•
	Vb			•	•	••	••	•	•	double spaced coarse enaulig	undifferentiated	•	-	•	-	-	-	•	-	•
	Vc			•	•	•	•	-	•	fine monic	undifferentiated	•	-	••	•	(•)	-	•	-	•
	Vc			•	•	•	•	-	•	fine monic	undifferentiated	•	-	•	-	-	-	•	-	•
	Vp			•	•	•	•	-	•	double spaced coarse enaulig	undifferentiated	•	-	••	•	(•)	-	••	-	••
	VIa			•	•	•	•	-	•	coarse monic and open porphyric (in aggregates)	undifferentiated	••••q	••	••	•	-	-	•	-	•

		Groundmass																		
		Coarse components																		
		Aggregation and voids																		
Block ID	Thin sections	Subunit	Aggregation			Voids			Microstructure			Biological and anthropogenic components								
			Degree of total textural porosity	Ped separation	Degree of developed pedality	Accommodation (accomm.)	Packing voids	Chambers	Channels	Planes	Vughs	Rock fragments	Trachyte fragments	Feldspar grains	Brown granules	Volcanic glass	Organic seeds coats	Charcoal	Bone fragment	Lithic
	L_1-3	V1A	strongly around aggregates	m, blocky peds and prism s, porous crumbs	w	(partly) accomm.	••	••	••	vughy	-	•	(•)	(•)	-	-	-	-	-	••
	L_4-1	Vb	strongly	subangular blocky beds	-	unaccomm.	•	•	-	vughy	-	(•)	••	•	-	-	(•)	-	-	••
		Vc	weakly	-	-	unaccomm.	•	•	-	vughy	-	-	-	•••	-	-	(•)	-	-	(•)
		Vd	moderately to strongly	s, porous crumbs subangular blocky beds	-	unaccomm.	•	•	-	vughy	-	(•)	•••	•	-	-	(•)	-	-	••
		V1A	weakly	m, blocky peds and prism	w	(partly) accomm.	••	••	••	vughy	-	•	(•)	(•)	-	-	-	-	-	••
		V1b	strongly	s, porous crumbs subangular blocky beds	-	unaccomm.	•	•	-	vughy	-	(•)	••	••	-	-	(•)	-	-	••
SOD_7	7-1	V1b	strongly	subangular blocky beds	-	unaccomm.	•	•	-	vughy	-	(•)	••	••	-	-	(•)	-	-	••
		V1c	moderately to strongly	m, blocky peds and prism	w	(partly) accomm.	••	••	••	vughy	-	•	(•)	(•)	-	-	-	-	-	••
	7-2	V1b	moderately to strongly	s, porous crumbs subangular blocky beds	-	unaccomm.	••	•	-	vughy	-	••	••	••	-	-	(•)	-	-	••
		V1c	moderately to strongly	m, blocky peds and prism	w	(partly) accomm.	••	••	••	vughy	-	•	(•)	(•)	-	-	-	-	-	••
SOD_6	6-1	V1b	weakly to moderately	s, porous crumbs subangular blocky beds	-	unaccomm.	••	•	-	vughy	-	••	••	•	-	-	(•)	-	-	••
	6-2	V1E	weakly	s, plates	m	(partly) accomm.	-	••	••	angular, subangular blocky peds	-	-	-	••	-	-	-	-	-	(•)
		V1E	weakly	s, plates	m	(partly) accomm.	-	••	••	vughy	-	-	-	••	-	-	-	-	-	(•)
		V1IA	weakly to moderately	s, porous crumbs subangular blocky beds	-	unaccomm.	••	•	-	vughy, crumb	-	••	•••	•	-	-	•	-	-	•••
SOD_II	II_3-1	V1b	weakly to moderately	s, porous crumbs subangular blocky beds	-	unaccomm.	••	•	-	vughy, crumb	-	••	•••	•	-	-	•	-	-	•••
		V1Ez	weakly to moderately	s, porous crumbs subangular blocky beds	-	unaccomm.	••	•	-	vughy, crumb, spongy	-	•	•	••	-	-	•	-	-	•••

		Pedofeatures																
		Fine components				Micromass				Impregnative pedofeatures				Textural pedofeatures				Biogenic pedofeatures
Block ID	Thin sections	Mineral components			Biological components			c/f-related distr.		Type of b-fabric	Hypo-coating (Fe/Mn) (q=quasi)	Redoximorphic nodules	Clay coating Limpid, orange-yellow, bright interference	Impure brown yellow, speckled interference	Light (yellow), undiff. interference	Silt coating Brown, undiff. interference	Goethite coating Acicular needles	Passage features
		Diatoms	Roots	Feldspar	Volcanic glass	Charcoal	Ash	Char										
	L_1-3	-	-	(*)	-	-	-	coarse monic and open porphyric (in aggregates)	undifferentiated	***q	**	**	**	.	-	.	.	**
	L_4-1	-	-	.	(*)	-	-	double spaced coarse enaulig	undifferentiated	.	(*)	.	.	.	-	.	-	**
	V_C	-	-	(*)	(*)	-	-	fine monic	undifferentiated	.	-	-	.	.	-	-	-	-
	V_D	-	-	**	.	(*)	-	single spaced coarse enaulig	undifferentiated	.	.	**	**	.	.	***	-	-
	V_Ia	-	-	(*)	-	-	-	fine monic and open porphyric (in aggregates)	undifferentiated	***+q	**	**	**	-	-	-	-	**
	V_Ib	-	-	.	(*)	-	-	double spaced coarse enaulig	undifferentiated	.	.	**	**	.	.	**	-	**
SOD_7	7-1	-	-	**	.	(*)	-	double spaced coarse enaulig	undifferentiated	.	.	**	**	-	-	.	-	**
	V_Ic	-	-	(*)	-	-	-	fine monic and open porphyric (in aggregates)	undifferentiated/stipple-speckled	***+q	**	**	**	-	-	.	-	.
	7-2	-	-	**	.	(*)	-	double spaced coarse enaulig	undifferentiated	.	.	**	**	-	-	**	-	**
	V_Ic	-	-	(*)	-	-	-	coarse monic and open porphyric (in aggregates)	undifferentiated/stipple-speckled	***+q	**	**	**	-	-	.	-	.
SOD_6	6-1	-	-	**	.	(*)	-	single spaced coarse enaulig	undifferentiated/stipple-speckled	.	.	**	**	-	-	-	-	**
	V_Ie	-	-	.	***	-	-	coarse monic	grano- and prostratated	.	**	**	**	-	-	-	-	-
	6-2	-	-	.	***	-	-	coarse monic	grano- and prostratated	-	.	**	**	-	-	-	-	-
	V_Ia	-	-	**	(*)	.	-	single spaced porphyric and coarse enaulig	stipple-speckled/undifferentiated	-	**	**	**	-	-	-	-	**
SOD_II	II_3-1	-	-	**	.	(*)	-	single spaced porphyric and coarse enaulig	stipple-speckled/undifferentiated	(*)	**	**	**	-	-	-	-	**
	V_Ib	-	-	**	***	-	-	single spaced porphyric and coarse enaulig	porostratated/undifferentiated	.	**	**	**	-	-	-	-	**
	V_Ie2	-	-	**	***	-	-	single spaced porphyric and coarse enaulig	porostratated/undifferentiated	.	**	**	**	-	-	-	-	**

		Groundmass																			
		Coarse components																			
Block ID	Thin sections	Subunit	Aggregation and voids																		
			Aggregation			Voids			Microstructure			Mineral components			Biological and anthropogenic components						
			Degree of total textural porosity	Ped separation	Degree of developed pedality	Accommodation (accomm.)	Packing voids	Chambers	Channels	Planes	Vughs	Rock fragments	Trachyte fragments	Feldspar grains	Brown granules	Volcanic glass	Organic seeds coats	Charcoal	Bone fragment	Lithic	Phytoliths
	IL_3-2	VI <sub>Ez</sub>	weakly to moderately	s, plates	m	(partly) accomm.	-	**	**	**	**	-	(*)	**	-	**	-	-	-	-	(*)
		VI <sub>E</sub>	moderately	m	w	(partly) accomm.	-	**	**	**	**	-	(*)	**	-	**	-	-	-	-	(*)
		VI <sub>b</sub>	moderately to strongly	s, porous crumbs subangular blocky beads	-	unaccomm.	**	*	-	-	**	-	**	**	**	*	-	*	-	-	**
	IL_3-3	VII <sub>A</sub>	weakly to moderately	s, porous crumbs subangular blocky beads	-	unaccomm.	-	*	-	-	**	-	**	**	**	*	-	*	-	-	**
SOD_III	III	VII <sub>A</sub>	weakly to (moderately)	-	-	unaccomm.	-	*	-	-	**	-	**	*	*	**	-	**	-	-	**
		VIII <sub>b</sub>	weakly to (moderately)	-	-	unaccomm.	-	*	-	-	**	-	*	*	*	**	-	-	-	-	*
		VIII <sub>c</sub>	moderately to strongly	-	-	unaccomm.	-	*	-	-	**	-	**	*	*	**	-	-	-	-	*
SOD_IV	IV	VI <sub>A</sub>	weakly	-	-	unaccomm.	-	*	-	-	**	-	**	*	*	*	-	**	-	-	**
	IV	VIII <sub>A</sub>	moderately to strongly	-	-	unaccomm.	-	*	-	-	**	-	**	*	*	**	-	-	-	-	**
	IV	VIII <sub>b</sub>	weakly to (moderately)	-	-	unaccomm.	-	*	-	-	**	-	*	*	*	**	-	-	-	-	**
	IV	VIII <sub>c</sub>	moderately to strongly	-	-	unaccomm.	-	*	-	-	**	-	**	*	*	**	-	-	-	-	**
	IV	IX <sub>A</sub>	weakly to moderately	-	-	unaccomm.	-	*	-	-	**	-	**	*	*	*	-	**	-	-	**

References:

Stoops, G. Guidelines for Analysis and Description of Soil and Regolith Thin Sections; John Wiley & Sons, 2021; Vol. 184; ISBN 0-89118-975-0.

Block ID	Thin sections	Subunit	Pedofeatures																	
			Fine components					Micromass			Impregnative pedofeatures			Textural pedofeatures				Biogenic pedofeatures		
			Diatoms	Roots	Feldspar	Mineral components	Biological components	Charcoal	Ash	Char	c/f-related distr.	Type of b-fabric	Hypocoating (Fe/Mn (q-quasi))	Redoximorphic nodules	Clay coating	Impure brown yellow, speckled interference	Light (yellow), undiff. interference	Silt coating	Goethite coating	Passage features
IL_3-2		V1 <sub>E2</sub>	-	-	•	•••	-	-	-	-	-	-	coarse monic	porostriated/undiff ereniated	•	••	-	-	-	••
		V1 <sub>E</sub>	-	-	•	•••	-	-	-	-	-	-	coarse monic	grano- and porostriated	•	••	-	-	-	••
		V1 <sub>b</sub>	-	-	••	•	-	-	-	-	-	-	single spaced porphyric and coarse enaull	stipple-speckled/undifferentiated	•	••	-	-	-	•
IL_3-3		VII <sub>A</sub>	-	-	••	••	-	-	-	-	-	-	single spaced porphyric and coarse enaull	stipple-speckled/undifferentiated	•	••	-	-	-	••
SOD_III	III	VII <sub>A</sub>	-	-	••	••	-	-	-	-	-	-	single spaced porphyric and coarse enaull	Undifferentiated grano- and porostriated	•	••	-	-	-	••
		VIII <sub>b</sub>	-	-	•	•	-	-	-	-	-	-	coarse monic	grano- and porostriated	•	••	-	-	-	-
		VIII <sub>c</sub>	-	-	•	(•)	-	-	-	-	-	-	coarse monic and open porphyric (in aggregates)	grano- and porostriated	-	•	-	-	-	-
SOD_IV	IV	VII <sub>A</sub>	-	-	•	••	-	-	-	-	-	-	single spaced porphyric and coarse enaull	stipple-speckled/undiffere niated	••	••	-	-	-	••
	IV	VIII <sub>A</sub>	-	-	•	•	-	-	-	-	-	-	coarse monic and open porphyric (in aggregates)	stipple-speckled/undiffere niated	-	•	-	-	-	-
	IV	VIII <sub>b</sub>	-	-	•	•	-	-	-	-	-	-	coarse monic	grano- and porostriated	•	••	-	-	-	-
	IV	VIII <sub>c</sub>	-	-	•	(•)	-	-	-	-	-	-	coarse monic and open porphyric (in aggregates)	grano- and porostriated	-	•	-	-	-	-
	IV	IX <sub>A</sub>	•	-	••	•	-	-	-	-	-	-	single spaced porphyric and coarse enaull	undifferentiated/ (stipple-speckled)	•	••	-	-	-	••

## Chapter V

### 5. Synoptic Discussion

This doctoral research bridges geoarchaeological investigations at the archaeological site Sodicho Rockshelter, and the geomorphological circumstances in its surroundings with evidence for the palaeoenvironmental and palaeoclimatological shifts in the southwestern Ethiopian Highlands. While considering different temporal and spatial scales, geoarchaeological research is able to investigate large-scale palaeolandscape changes. Even microscopic features within a sedimentary sequence can be examined, while addressing geological, geomorphological and archaeological research questions (Goldberg and Macphail 2006, French 2015, Siart et al. 2018). Within the following synthesis, the results and interpretations of the three peer-reviewed publications from chapter II to IV are combined and discussed, considering the objectives of the doctoral study, formulated in chapter I. In this study, the different scales of geoarchaeological research are considered (Fig. 5.1), starting with the local scale, which takes a closer look at site formation at the Sodicho Rockshelter, to reconstruct the human impact, the depositional development, and disturbances of the stratigraphy.

Further analyses were focused on a regional landscape scale, by combining satellite-based GIS evaluations of the hydrological system with mapped archaeological sites and lithic raw material sources. Based on the current geomorphological circumstances investigated, the question was raised whether it is possible to make assumptions about the past landscape dynamics, the impact on the accessibility of obsidian raw material sources and therefore human settlement history. By combining all these interpretations, connections are created that yield first implications for a supraregional scale, that allows to reconstruct palaeoenvironmental changes and contributes to the Mountain Refugium Hypothesis in the Ethiopian Highlands.

Considering the new results from Sodicho Rockshelter, this multi-method approach serves as a case study for tackling difficult sedimentary stratigraphies in tropical regions. It will be discussed to what extent (spatially and temporally) the results from Sodicho are transferable to other sites in the tropical highlands of Ethiopia as well as to rockshelters in general. It will also be pointed out which methodological approach can be used for different spatial and temporal scales, to ascertain the geoarchaeological context of a site by using a certain amount of significant and conclusive methods.

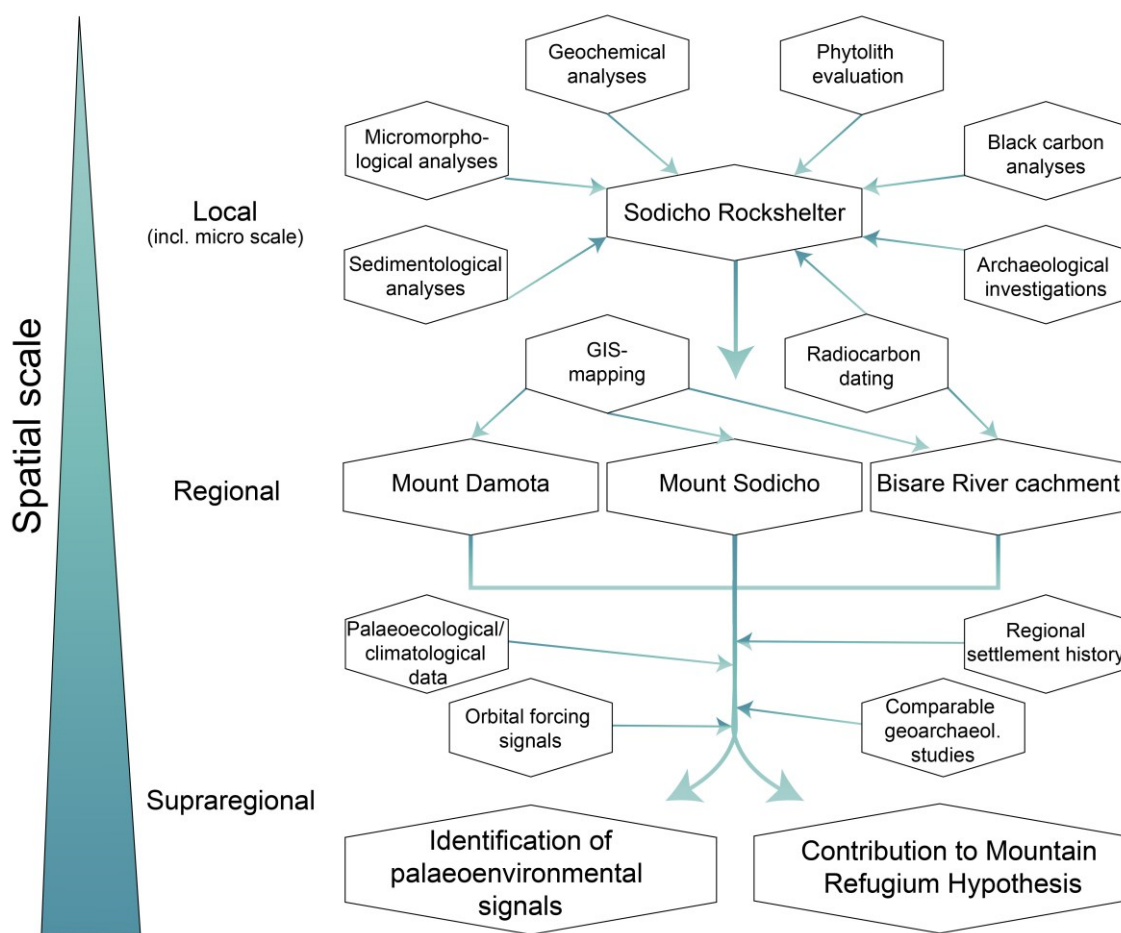


Figure 5.1 Flow chart showing the different spatial scales of applied geoarchaeological methods and the major scientific outcome of this research.

## 5.1 Local scale: Understanding site formation and human impact

To reconstruct the development of a sediment stratigraphy at an archaeological site several aspects have to be considered, such as geogenic and biogenic site formation processes and post-depositional disturbances, as well as past human impact. The formulated research objectives 2.1 to 2.3 relate to the understanding of the site formation (2.1), identifying the human context (2.2) and establishing a reliable chronological framework (2.3). It should be noted that for this investigation of the deposits at Sodicho Rockshelter, the local scale is applied, which includes the microscale. In this way, results of the sediment elemental composition can be combined with micromorphological investigations and macroscopic archaeological data.

A combination of sedimentological and geochemical analyses, micromorphological investigations, and the contribution of supporting studies have provided insights into the type and composition of the deposits and the site formation of the Sodicho Rockshelter. So far, as the stratigraphy has been excavated, 9 sediment units were identified. With

help of micromorphological analyses further subunits were defined. It is important to mention that these subunits were identified within the micromorphological thin sections and are not applicable within the entire stratigraphy.

A reliable chronological framework was established, via radiocarbon dating on mainly charcoal samples, which originate from cultural units. The upper units were dated between  $\sim 1800$  and  $\sim 2100$  cal BP (Unit III) and  $\sim 4300$  and  $\sim 4800$  cal BP (Unit V). The lower units date between  $\sim 13,500$  and  $\sim 27,000$  cal BP (Unit VII and IX) and cover therefore parts of the arid Last Glacial Maximum (LGM,  $\sim 21 \pm 2$  ka) (Hensel et al. 2021). A calculated age-depth model was plotted against elemental ratios, which illustrated changes in elemental composition of the sediments and therefore shifts of the sediment source and indications for paleoenvironmental changes during the last 27 ka.

With help of the macroscopic field study, micromorphological investigations, geochemical and sedimentological analyses, as well as the archaeological evidence, the following main depositional and post-depositional processes can be suggested. The most common type of autochthonous clastic fine sediment in rockshelters originate from the weathered rock surface on the rockshelter walls or the ceiling (Birndorfer et al. 2022). At the entrance, a part of the rockshelters that is under stronger influence of the natural elements, larger bedrock fragments and coarse blocks are often found (Mentzer et al. 2017).

At Sodicho Rockshelter disintegration of trachytic rock from the rockshelter ceiling and walls are very common in all units. Under today's tropical conditions, as prevailing in the southwestern Ethiopian Highlands, the influence of moisture is averagely very high (compare climate chart Fig. 1.12). Seepage water probably entered the cave through fissures and cracks and at the same time transported fine sediment and eroded the bedrock further. This means, that fine geogenic sediment originates from both eroded autochthonous trachytic bedrock and allochthonous fine soil particles, which developed above the rockshelter on the relatively flat hilltop. Similar circumstances with rock fragments and reworked soil particles in the groundmass were observed at the tropical rockshelter Beli-lena (Sri Lanka) via micromorphological investigations (Kourampas et al. 2009).

If we now consider to increase the local scale to a regional scale and compare the observations with a phase of increased precipitation such as the African Humid Period, the influence of increased moisture should also be visible in the sedimentological and geochemical properties of rockshelter deposits. The geogenic deposits of the reddish and archaeological sterile Unit VI from Sodicho, which were chronologically dated to the AHP, using radiocarbon dating (Hensel et al. 2021), are particularly recognizable for this case. The unit is characterized by sudden variations in grain size and elemental ratios,

such as Al/Ti, K/Rb and the CIA index (Hensel et al. 2021). Especially the Fe (and FeO<sub>2</sub>) values and the high abundance of limpid clay coatings, which were identified within the micromorphological samples, reflect increased weathering between 17 and 4.7 ka cal BP. Micromorphological studies have suggested that there is evidence for waterlogging, i.e. the relatively prolonged rainfall caused a large accumulation of water which could not drain quickly enough. This resulted in the formation of shallow water pools, which can be identified by graded bedding of silt and clay particles and redoximorphic pedofeatures. Micromorphologically, an enhanced impact of the reworking process, as a result of sheet wash, was also detected for this phase (Hensel et al. 2022). Within the deposits at the site Beli-lena, observations of episodic clay translocation correlate with increased drainage, which therefore indicates increased rainfall (Kourampas et al. 2009). At Sodicho this is indicated by an increase of more developed clay (like kaolinite) in Unit VI, which implies an increased weathering rate under humid conditions. According to these observations at Sodicho, it could be possible to use the clay mineral formation and the derived weathering state as an environmental proxy.

However, there are two objections that need to be considered. First, individual clay layers that would be identified as “episodes” are not observed in the Unit V. This is due to reworking, and observed shrink and swell processes. A further fact is, that clay is found in certain amounts in every unit of Sodicho’s stratigraphy. Secondly, in a case with less disturbed and well micro stratified sediment, an accurate representation of wet/ dry climatic cyclicity would still be difficult. As these fine cycles are limited by the chronological context of the fine sediments, a much denser sampling pattern for dating would be needed (Kourampas et al. 2009).

At Sodicho predominant geogenic units, which are archaeologically sterile, consist of the mentioned fine sediment, trachytic clasts and boulders. Furthermore, tephra represents a large part of allochthonous sediment, which was introduced into the shelter by aeolian transport and reworked by the influence of water. Multi-layered tephra units stand out by their pale coloration in the stratigraphy, with volcanic glass as predominant coarse material, and distinct boundary in certain areas. These sudden changes in the stratigraphy speak for a rapid deposition. The lower layers of the tephra units, often show a high homogeneity of sharp-edged volcanic glasses, indicating that the sediment in these layers has not been redeposited. The fact that layers of the tephra show signs of disturbance and reworking by water, indicates that postdepositional changes have occurred, and that the circumstances within the shelter changed.

At this stage of research, the volcanic source for the deposits and direction from which the distal tephra was blown into the rockshelter cannot be defined, yet the thickness of the tephra deposits (especially ash of subunit IV<sub>C</sub>) indicates an eruptive event in

proximity. While larger particles distribute closer to the eruptive center, the distal tephra is able to be transported further away, over hundreds to thousands square kilometers (Antos and Zobel 2005, Lane and Woodward 2017). However, based on the thickness of the homogeneous volcanic ash layers (max. 5 cm), it can be assumed that the deposits occurred comparable thick, if not even more intense outside of the rockshelter, with exception at the steep slopes at Mt. Sodicho. Fine charcoal fragments within the subunit IV<sub>B</sub> indicate an origin by vegetation fire. It can be assumed that the tephra was not hot enough to ignite the vegetation, but rather hot gas clouds or lava flow at the source volcano. This observation again supports the hypothesis of a volcanic eruption in near vicinity. It can be assumed that this was followed by drastic changes to the landscape, and affected flora and fauna. If the tephra was not partly washed out or completely eroded due to precipitation, a fine surface crust could have formed at the rather shallow slopes of the mountain. This could have restricted water permeability and thus severely limited growth of smaller plants (Tarasenko et al. 2019). Evidence of crust formation is found within micromorphological thin section (e.g., SOD\_1-2). These circumstances could have made the region uninhabitable for a certain period of time and forced humans to abandon the area to ensure their survival, i.e. food security, access to clean water, and shelter. In addition, fine volcanic ash particles in the air pose direct health hazards because of possible particles that are respirable (< 4 µm diameter) and finer grained volcanic aerosol particles (~ 0.2–0.5 µm), which can enter the lungs (Mather et al. 2003, Horwell 2007). It cannot be clarified whether the inhabitants left the region long before a volcanic eruption, or were still in the area at the time of the approaching ash cloud.

Roughly five settlement layers were detected with help of radiocarbon chronology. This observation is consistent with the results of the examined sediment samples. The anthropogenically influenced units were particularly well identified by macroscopic archaeological evidence, such as stone artifacts, charcoal, and evidence for fire use (Hensel et al. 2021). According to the sedimentological and geochemical analyses, these units are characterized by elevated values of manganese, phosphorus, TOC and distinct measurements of magnetic susceptibility and black carbon. Micromorphological observations revealed impacts such as fire activity, site maintenance, trampling and dumping (Hensel et al. 2022). The calculated accumulation rates of the age-depth-model (Hensel et al. 2021) showed the settlement layers accumulated relatively quickly, compared to the other sediment layers.

It is possible to understand Late Pleistocene and Holocene patterns of hunter-gatherer behavior for this study site, through the connection between the archaeological findings and the geoarchaeological results. During times of intensive use of the rockshelter, the deposits display local anthropogenic impact and human behavior. The last mentioned

includes observed combustion features and the introduction of lithic raw material for tool production. Another possible influence by humans inside the rock shelter is not limited to the contribution of site formation and post depositional disturbance, but also the impact on the shelter itself. In this case, a thermoclastic effect is created by the heat generated by the human fires. Hints for the phenomenon of wall disintegration was observed in the deposits in the tropical rockshelter Beli-lena (Kourampas et al. 2009).

Due to the limited excavation trench in Sodicho, it is not yet possible to make a statement on the spatial organization within the rockshelter. It is also not possible to determine whether the observed behavioral patterns have changed drastically over time, since the excavations did not reach the bedrock (Hensel et al. 2021). At this point of research, it is not possible to distinguish human behavioral zones for specific activities within Sodicho. In additions studies, e.g. Burns and Raber (2010), revealed that activity zones in smaller rockshelters overlap. Nevertheless, our study shows that the area of the excavation (north-eastern part of the rockshelter) is marked by fire activity and evidence of site maintenance. Lithic tool maintenance can be identified from the stone tool assemblage. The Late Pleistocene assemblage (13.5 to 27 ka cal BP) consists mainly of uniform obsidian artefacts and the LSA assemblage in the upper part (Unit III and Unit V) of a variation of microlithic stone tools (Hensel et al. 2021). The production of ceramic objects is only found in the upper anthropogenic units I and III. A strong biogenic influence can be neglected, as it is limited to microscopic features of bioturbation (passage features and biogenic pores) and small-scale botanical remains in the upper part of the stratigraphy (Hensel et al. 2022).

In summary, our research at the Sodicho Rockshelter shows that the combined use of sedimentological, geochemical, micromorphological analyses revealed a very complex sediment composition, influenced by several autochthonous and allochthonous processes as well as biogenic and anthropogenic impacts. By implementing the results of cooperative studies (see subchapter 1.5.6) such as archaeology, it was possible to determine site formation and prehistoric human behavior. This means that through the exclusive application, or focus on a local spatial scale essential geoarchaeological information were gained. However, in some cases, it is often necessary to include larger spatial scales, such as the inclusion of regional or even supraregional palaeoenvironmental data to understand certain variations in depositional processes.

## 5.2 Regional scale: Reconstructing past environmental signals, and regional settlement activity

Present landscape dynamics cannot be fully understood without the knowledge of past processes. Past morphodynamics have had an impact on the environment and human occupation in particular places. Two research objectives of chapter 1.4, which were addressed in the publication of chapter II, relate to the reconstruction of the recent hydrological system, via satellite imagery and geoinformations systems, to identify regional geomorphological processes (objective 1.1). Furthermore, the data was being compared to mapped archaeological survey data from the study areas, to imply the impact of the past hydrological system and to understand prehistoric settlement activity (objective 1.2). On the basis of the satellite imagery supported by geoinformation systems, it became apparent that the study area has a very active hydrological system (Hensel et al. 2019). This means that the system is very sensitive to external influences, such as fluctuations in water availability, caused by precipitation changes. This was observed in the formation of recent swamps at the Bisare River catchment, caused by sediment accumulation and damming of the stream during intensive erosion and active gullying. Within our study we assume for today's dynamics, that stronger gully erosion, land degradation, and badland formation is activated during wetter climatic phases. Studies by Fryirs and Brierley (2012), showed that processes like shallow landslides, soil erosion, and gullying are increased without native vegetation cover to support the system.

If we attempt to apply the observations of the current morphodynamic processes to the prehistoric past, the question arises whether the activity of the hydrological system and erosion processes had a comparable intensity in our study area during the Late Pleistocene and early Holocene? The geoarchaeological investigations of Sodicho have made it possible to identify past depositional processes under the influence of changing environmental conditions. These include, in particular, changes in the humidity of the sediment, which may indicate changes in the local precipitation. In this context, the 60 cm thick sediment Unit VI is striking, as it is radiocarbon dated to the time of the AHP (~ 15–5 ka cal BP). Based on the results of studies from palaeoclimatic records of Lake Chew Bahir by Fischer et al. (2021), a calculated Predictive Vegetation Model predicted an annual moisture increase of about 25–40 %, compared to today's conditions. Unfortunately, little is known about erosional processes of the past in Eastern Africa. According to a study of fluvio-lacustrine deposits from the Baragoi palaeo-delta, Tanzania, rapid changes in erosion rates during the AHP indicate an increase in the probability of runoff (Garcin et al. 2017). At the Baragoi palaeo-delta, erosivity is

increased in the time range of arid-to-humid transition at 15 ka or 12 ka cal BP. The micromorphological investigations of Sodicho suggested that an increase in humidity did not last during the whole period of the AHP, but was rather interrupted by shorter dry phases (Hensel et al. 2022), which roughly coincided with the identified dry spells in the lacustrine record of Chew Bahir (Foerster et al. 2012, 2015). The investigations prove that Sodicho and the surrounding landscape were affected by increased precipitation, which has promoted the degradation processes. Vegetation models predict an expansion of forests and an overall denser vegetation in southern Ethiopia (Fischer et al. 2021). Since the sediment unit at Sodicho, that can be assigned to the AHP are archaeologically sterile, it can be assumed that the increasingly dense vegetation had a great influence on the abandonment of the region. In addition, during this phase, the lowlands became more attractive as the lake systems expanded (Fischer et al. 2021)

This information in mind raises another question about the exposure of obsidian raw material through erosion processes, and whether increased availability has influenced human settlement in higher elevated regions such as our study area. The most dominant used raw material for stone tool production in Sodicho is a dark obsidian. Cryptocrystalline silices were used in smaller numbers and were only found within the Late Pleistocene units. Preliminary microprobe analysis showed that the raw material originates from the obsidian outcrops of the Bantuu region (Hensel et al. 2021). Studies from the nearby Mochena Borago proved that the same raw material outcrops were exploited, which is only 20 km southeast from the rockshelter (Brandt et al. 2017). Today, degradation processes such as gully erosion, sheet erosion and river erosion are widespread, especially pronounced at the southern part of the Bisare River. In our study Hensel et al. (2019), we suggest a relationship between widespread gully erosion, badland formation, and raw material availability. This means that this excessive form of soil erosion may have affected raw material outcrops. At Mt. Sodicho obsidian was observed as transported boulders or debris during a survey along the surrounding rivers and streams. Based on these observations, it can be assumed that erosion processes in the study area, especially on mountain slopes and river courses, have increased during wet periods such as the AHP. This may have further facilitated the exposure of already existing obsidian deposits.

Today the increased human presence at the mountain slopes and tops strongly impacts the landscape and cannot be completely ignored when thinking about the past. The clearance of the vegetation cover and transformation into cropland for teff farming and cattle grazing also effects the ecosystem. Increased erosional processes and soil loss are the consequences. Today obsidian outcrops are also exposed by roadworks, as in

the area of Fulasa, which is in proximity of Sodicho Rockshelter (Fig. 5.2) (Hensel et al. 2019). According to our study Hensel et al. (2019) we suggest that in the present time obsidian is exposed to the surface much more frequently due to higher runoff.

Obsidian was collected and processed in the past because of its good knapping properties and sharp edges, which can be easily produced (Rapp 2009). According to our study and other studies in the region (Brandt et al. 2012, Brandt et al. 2017, Vogelsang and Wendt 2018), obsidian probably has been almost constantly available in sufficient quantities. In other cases, people would have relied on other sources of raw material, which would have been reflected in the lithic inventory at Mochena and Sodicho.

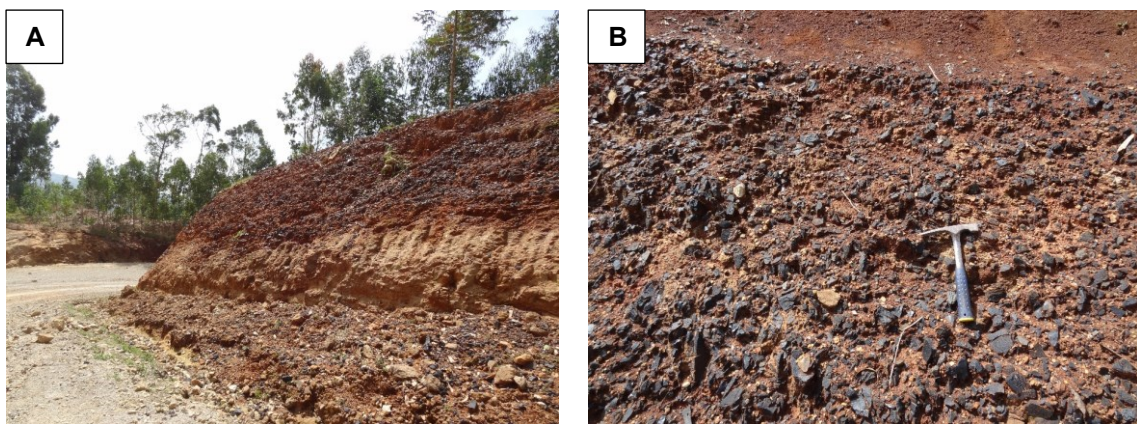


*Figure 5.2 (A) Road construction work along the steep mountainside exposed the obsidian raw material deposit of Fulasa. (B) Scattered obsidian, and obsidian gravels show signs for transport/reworking (Photos by E. Hensel).*

Obsidian is also the most common raw material used by hunter-gatherers which occupied the rockshelter DEN12-A01 (Mount Dendi) (Schepers et al. 2020). Within this study it is discussed, that an abundance in micro-points and segments illustrate short-termed stays of the inhabitants at the site and that foragers procured the raw material probably during their hunting trips (Vogelsang and Wendt 2018, Schepers et al. 2020). At the high elevated rockshelter site Fincha Habera, within the Bale Mountains, the prehistoric hunter-gatherer (cultural layers dated to 47–31 ka cal BP) collected their raw material at ice-free ridge along glaciers, which were situated 500 to 700 m above the shelter (Ossendorf et al. 2019). Even if Sodicho Rockshelter is not as elevated as Fincha Habera and the raw material procurement was comparatively easy, a comparison of the studies shows how prehistoric humans relied on good quality raw material and what they undertook to obtain it.

When all the observations are taken into consideration it is not easy to transfer the knowledge about modern morphodynamics into the past, since certain circumstances change over time and we cannot prove that mapped recent processes like the swamp formation, were active in the past. Due to today's human influence, we assume that obsidian raw material comes to the surface more frequently or even in larger quantities than in prehistory. Nevertheless, humans frequented this higher elevated area, because of sufficient water and food resources, shelter, and especially the access to obsidian raw material.

### **5.3 Supraregional Scale: Implications for settlement history and adaptation to the environmental shifts**

In order to grasp large-scale palaeoclimatic changes, both spatial and temporal, it is necessary to link the obtained data of the local and regional scale from the study area with data from a supraregional scales. A key objective of this research was to understand the local climatic and environmental variability and to identify the signals based on the existing data. The geoarchaeological research results of this study give a first impression of the local environmental changes and human presence in the study area.

The well-studied ~ 293 m long composite sediment core from Chew Bahir basin, provides a continuous record for reconstructing the past 200,000 years of palaeoclimatic change in southwestern Ethiopia (Schaebitz et al. 2021). Therefore, a comparison with our observations from our study area, with this palaeoclimatic records is useful. Several studies showed that hydroclimatic conditions at the study area are correlated to orbital eccentricity and therefore changes of the orbital insolation (Foerster et al. 2012, Foerster et al. 2015, Schaebitz et al. 2021, Fischer et al. 2021). The resulting climatic fluctuations, which intensified from 60 ka, influenced geomorphodynamics, sediment input into the basin, and thus hydrological system (Schaebitz et al. 2021). According to chronometric dating of the core record, a mean accumulation rate from 0.47 mm/a was calculated, but it dropped to a rate of about 0.1 mm/a during the MIS 2, corresponding to reduced sediment supply during the drier Late Glacial Maximum (Roberts et al. 2021).

With this context in mind, it is important to understand the push and pull factors for orographic mobility (Schaebitz et al. 2021), when it comes to the discussion about the refugial hypothesis, concerning the human retreat into the highlands of Ethiopia during harsher living conditions (Basell 2008, Brandt et al. 2012). The results of this study provide insights into the timing of relatively rapid environmental changes at the Sodicho Rockshelter, which must have forced early humans to adapt in the area.

As discussed above, the hunter-gatherer groups from Fincha Habera used to find their resources at the glaciers (Ossendorf et al. 2018). Even though there is a temporal offset between Fincha Habera and Sodicho, it illustrates the determination of prehistoric humans to cross rough terrain, in search of resources. The top of Mount Sodicho has an elevation of about 2000 m above sea level. This means that health risks such as high-altitude hypoxia, which begins at elevations of ~ 2500 m a.s.l., are not being considered for our study site (Aldenderfer 2006).

It is important to understand that some environmental changes proceed quickly (e.g. atmospheric shifts) and some slowly (e.g., soil formation). This means that changes in different pace have different impacts on humans, including fast or slow changing conditions impacting expansion and migration. With the radiocarbon dating of the sediment units XI to VII, which also span partly over the timeframe of the LGM, Sodicho is the first site in Ethiopia to date settlement during this dry time period. Now, recent geochronological studies on ostrich eggshell samples from the upper Middle Awash study area (Oulen Dorwa basin) point to an occupation prior to and during the Last Glacial Maximum (Niespolo et al. 2021). In our microstratigraphic record we see a short but intense eruptive event (comp. Fig. A. 11) between two dated cultural layers. This shows that the occupation during the LGM was shortly interrupted and humans left the site because of this probably rapid event. Apart from this "short" interruption, our results show that harsher, dry conditions of the LGM could have led to the movement into the mountainous area. This means that the retreat and the following reoccupation can be related to more favorable ecological conditions and available resources (e.g., water, food, shelter, and raw material).

The already mentioned study by Fischer et al. (2021), is discussing the human response to paleoenvironmental changes and the preferences for certain landscapes during the LGM, and also puts Sodicho Rockshelter in context of the results. The calculated vegetation model showed the vegetation during the LGM comprised of mainly grassland and further other vegetation types. This has probably led to the development of a mosaic of independent landscapes that people have been able to exploit. This hypothesis is consistent with the statement to human adaptation at Mochena Borago and Mt. Dendi. In these areas the humans exploited the diverse environment in different ecozones along the mountain flanks (Vogelsang and Wendt 2018, Schepers et al. 2020). According to Vogelsang (2021), the interior of Mochena Borago was big enough to have hold larger groups of hunter-gatherers, that could have occupied the site as a base camp for longer stays. The advantage in this complex habitat, also present on Mt. Dendi, was the accessibility of the mentioned resources in proximity and the advantage of short-distance

transport (e.g., obsidian raw material) (Vogelsang and Wendt 2018, Schepers et al. 2020). Due to the vicinity of Sodicho Rockshelter to Mochena Borago, it is plausible that the ecological conditions were similar.

With reference to the Mountain Refugium Hypothesis, it can be summarized that for the time frame investigated, major push factors for the migration were climatic and environmental driven. Pull factors were ecological stability, water, vegetation, animals, obsidian raw material and many others (Basell 2008). To what extent the migration was dependent on the individual human preferences and choices remains to be determined. Nevertheless, we assume that the region of the southwestern Ethiopian Highlands fulfilled the basic needs for a certain period of time, i.e. provided a variety of stable resources necessary for survival.

#### **5.4 Applicability of the multiscale study**

This thesis underlines the importance of geoarchaeological research to understand past human-environment interaction. In the Horn of Africa, and especially in Ethiopia, only very few sites have been investigated with help of a comprehensive, interdisciplinary research design, how it can be provided by geoarchaeology.

The geoarchaeological investigations at Sodicho Rockshelter confirm the importance and multiproxy approach different spatial and temporal scales, based on the preservation of archaeological finds and the key results on site formation, postdepositional changes and human behavior in a tropical rockshelter. The combined results are especially powerful, when they are correlated with external data from palaeoclimatic records. In this way it could be possible to interpret observed features, as local palaeoenvironmental proxies.

The applicability of the methodological approach can also be discussed in terms of potential costs. Of course, all scientific field and laboratory studies are quite cost-effective, but our study shows that with sufficient bulk sediment samples and micromorphological samples, the geoarchaeological processes can be deciphered. Of course, a narrow and continuous sampling of sediment stratigraphy is important.

The results of the research were linked to other research sites and especially to other rockshelter sites. Now the questions arise to what extent the chosen spatial and temporal scales are transferable for other sites. In this study, a set of basic methods was used for the investigation at each scale.

The local scale, which for this study also included a microscale, allows to identify a large part of the information on sedimentological processes, geochemical components, and the human impact (comp. chapter 5.1). In this context basic sedimentological fieldwork

and laboratory methods, a variety of geochemical analyses and micromorphological investigations were chosen (comp. chapter 1.5). However, it is necessary to include a larger spatial scale in a certain extent, as for example in the inclusion of external palaeoenvironmental data on the African Humid Period.

A similar concept also applies to the usage of the regional scale. The regional investigations placed the Sodicho Rockshelter in a broader spectrum and provided comparisons to surrounding phenomena. Geomorphological and archaeological surveys, and satellite data supported GIS analyses proven to be suitable. These new acquired insights into the regional morphodynamics were used for an interpretation of the observed features within the stratigraphy (local scale). In turn, the local microscale, such as the micromorphological identified rapid changes in deposition, can contribute to fill knowledge gaps in the regional scale, concerning fast environmental changes.

In this study, the temporal scale has not been applied to the same extent as the spatial scale. Nevertheless, it has been shown that by exceeding to a continental or global scale, globally identifiable phenomena are recognizable in the sediment record of a rockshelter. This was achieved by comparing geochemical data from Sodicho, with major shifts of a palaeoclimatic record and orbital cycles.

With the Sodicho's location in the tropical highlands, this site immediately faces two challenges that hinders the investigations and complicate the evaluation of the observations. However, the study has shown that the diverse methodological approach and the different perspectives on the research questions were comprehensive and effective in dealing with difficult environments. Sediment stratigraphies often show poor preservation of organic materials under moist tropical conditions. This occurs very often at open air-sites or when the substrate is very acidic (Cordova 2019). Exactly these conditions are found in the acidic trachytic bedrock of Sodicho. To cope with this issue, Phytoliths that have an inorganic silicate body and resist decomposition, were analyzed (Kaczorek et al. 2018). The preliminary study provided first insights into the differentiation of human induced fire activity and natural vegetation fire, as well as preliminary evidence for past vegetation changes in the area.

Geoarchaeologically interesting but also difficult to study are sites and especially stratigraphies in mountainous areas. With increased geomorphological dynamics, steep slopes and harsher terrain, the highlands do not seem inviting for human occupation. Nevertheless, this and other research from all around the globe (Rademaker et al. 2014, Chen et al. 2019, Ossendorf et al. 2019) showed that humans have been drawn to the highlands in the past. Increased weathering and erosional processes affect sediment deposits in these elevated archaeological sites and can prevent the preservation of important data about the past. In the course of this study, identified erosion processes

discordances in the stratigraphy had to be dealt with. However, by linking the onsite information on human and depositional circumstances with the observed processes in a wider landscape (and vice versa), “gaps” in the stratigraphy could be filled.

The study verified that the different scales are mutually dependent to each other in order to address the defined objectives and to exploit the full potential of geoarchaeological investigation.

## **5.5 Implementation of results into the context of the CRC 806**

Within 12 years, since the first funding period in 2009, the participating collaborators of “CRC 806 – Our Way to Europe” have collected important new results and fundamental insights into the cultural-environmental context of the dispersal of the anatomically modern humans (comp. Litt et al. 2021). Following the migration routes from the “source” in Africa to the “sink” in Central Europe, the focus was set to the main triggers of past climatic and environmental shifts, cultural development and transition, and population changes along the way.

Investigations of regional model project A1, that deal with rockshelter stratigraphies and human adaptation to palaeoenvironmental changes, led to Eastern Egyptian Desert and the highlands of Ethiopia. As part of A1, this study focused on working in the Ethiopian Highlands, and therefore a region that can be seen as the starting point for the CRC 806 research. In the past two funding phases the research in Ethiopia focused mainly on Mochena Borago (see chapter 1.3.1). The new site Sodicho Rockshelter was seen as a promising site with a comparable stratigraphic development and the potential to preserve useful information, that can be implemented into the framework of the CRC 806. The studies at the Sodicho Rockshelter provided new insights into the settlement history of the Ethiopian Highlands, contributed to the Mountain Refugium Hypothesis, and provided many more fundamental results on the investigation of sediment stratigraphies at tropical rockshelters (see chapters 5.1–5.3). Due to the limited excavation area, the cultural layers have only been dated to an age of about 27 ka. Therefore, there is still no chronological connection to Mochena Borago. Nevertheless, the similar depositional conditions for the two rockshelters can be compared.

Project A3, which focused on palaeoenvironmental and palaeoclimate archives in Ethiopian lakes, acquired a substantial amount of proxy data within a ~ 200 ka old record from Chew Bahir. Geochemical results from Sodicho show trends that are comparable to the most recent records. Thus, the results from Sodicho could be increased to a supraregional scale. In return project A3 has received information on the impact of

observed climatic and environmental changes on prehistoric humans in the southwestern highlands of Ethiopia.

Together with project E7 sediment samples from Sodicho Rockshelter were used for a black carbon analyses, which yielded consistent results. With help of this interdisciplinary work temporal changes in BC contents and composition were observed, that could be identified as changes in fire activity within the stratigraphy.

## **5.6 Critical review of this research: Limitations and future perspectives**

This doctoral research conducted at Sodicho Rockshelter has provided new insights into the human-environment interaction of the past 27 ka in the southwestern highlands of Ethiopia. The geoarchaeological studies allowed the reconstruction of the archaeological site development and the identification of geomorphological processes in its surroundings. Furthermore, the strength of a multiproxy approach in different spatial and temporal scales is highlighted. Considering past climatic and environmental changes, it has been possible to focus on the behavior of prehistoric humans.

A critical consideration of the methodological approach at the main study site enables several possibilities to validate existing data, to answer open research questions and to improve the approach. Although the bulk sediment sampling of the excavated profiles was precise (mostly 2 cm steps), further sediment samples could be taken to verify the existing data. In particular, within future excavation squares, but also targeted samples from macroscopic pits, hearths and the volcanic tephra layers. The correlation of the sedimentological and geochemical data with the micromorphological investigation resulted in a precise understanding of the microstratigraphy development and single depositional processes, since all the units and the boundaries have been sampled. In the future, the micromorphological sampling strategy could be targeted to special anthropogenic features, such as hearth and pits, to get a better understanding of combustion material and pit infillings.

Further studies on the micromorphological thin sections with the help of enhanced techniques, should be considered. This includes the usage of fluorescence microscopy (Stoops 2021) to study certain mineral accumulations or organic matter. A first mineralogical fingerprint analyses of the thin sections, using Raman spectroscopy, failed. For this reason, the methodology was not included in the introduction (comp. chapter 1.5). The “desired” Raman scattering, stimulated by laser in visible near infrared light, was completely masked by fluorescence of the sample material. The sources of

fluorescence are not yet clear, but it could be autofluorescent phosphate minerals or free aluminum ions absorbed on clay (Stoops 2017, Stoops 2021).

Numerous  $^{14}\text{C}$  dating of charcoal and seed samples have formed a robust chronostratigraphic framework that illustrated the settlement phases for Sodicho (Chapter 3). With the classical calculated age-depth model it is not possible to capture the variability of depositional conditions and accumulation fluctuations of the entire stratigraphy. By focusing on a specific sample of the excavation squares, the model must be seen as a simplification, that reflects a limited but no less profound view into the settlement history of Sodicho. A tephrochronology is not necessary for the upper tephra layer because of the radiocarbon dating. A detailed chemical investigation and a possible comparison with the geochemical fingerprint of documented volcanic eruptions (dated archives) could be interesting (Lane and Woodward 2017). Especially in context of the influence of volcanic fallouts on prehistoric human behavior/ mobility.

The existing data on the ratio of light to dark phytoliths, obtained from the relative abundance of three common morphotypes, contributed to the understanding of the origin and transport (aeolian, fluvial, anthropogenic) into to the volcanic rockshelter (chapter IV). In addition, the combination of this method with other geochemical and micromorphological parameters enabled the reconstruction of prehistoric human fire activity at the site. Although the occurrence of special morphotypes such as TRAPEZOID is low, it is consistent with decreasing local temperatures during the LGM, according to the preliminary studies. Still, a detailed analysis of all morphotypes and a comparison with modern specimens is needed to establish an understanding of past vegetation changes relative to climatic shifts in the study area.

The preliminary investigations of the lithic artifacts from Sodicho (chapter III), were constrained by the limited excavation area and depth. A lithic assemblage is one of the most important indicators for human behavior at an archaeological site, therefore further investigations are needed.

The study of the hydrological system and the geomorphological processes (chapter II) at Mount Sodicho, Mount Damota and the Bisare River catchment has revealed a dynamic system that is driven by recent climatic influences. A transfer of present knowledge about the actual morphodynamics into to past was not straightforward. The need for the analyses of several fluvial and colluvial sediment archives would be needed, as done by the geochronological and sedimentological studies in NE Morocco by Bartz et al. (2015 and 2017) within the framework of the CRC 806. Additional extended geomorphological surveys could help in this regard, as well as the investigation of additional drilling cores, that were taken during the survey in 2012 to 2015. The sediment

records could be improved by a selection of sedimentological and geochronological observations.

During the archaeological excavations the bedrock was not reached. Therefore, further explorations of deeper sediment layers are required. So far, the uncovered quadrants are very limited in their dimensions and consequently only a limited overview of the stratigraphy of Sodicho could be obtained. Also, the major site formation processes and post-depositional processes could be identified (Hensel et al. 2021), certain changes in layering or the erosion of units, which could indicate changes in local environmental conditions could remain hidden. The extensions of the excavation squares are needed to confirm our findings and to reach a temporal connection to the nearby Mochena Borago Rockshelter, as well. At this stage of research, there is a temporal gap of 10 ka between the two sites, with missing information about the time frames of MIS 2 and the beginning von MIS 3. With the help of further research, it could be possible to identify the overlap of occupation phases at both sites and to compare human behavior. In addition, the combined geoarchaeological archives would emphasize this area in the Ethiopian Highlands as one of the key regions for reconstructing regional settlement history and past human-environment interactions. The onset of sediment deposition within the Sodicho Rockshelter is not yet clear, nor is the thickness of the deposits. At Mochena Borago, non-destructive ground penetrating radar (GPR) and electrical resistivity tomography (ERT) surveys were carried out, which revealed the information on the thickness and progression of the sediment deposits within the rockshelter (Lanzarone et al. 2019). In the future a similar geophysical approach is possible for Sodicho. This would allow the determination of depositional thickness, sediment changes, surface shape of the bedrock and possibly the onset of human occupation. In addition, a comparison with the results of Mochena Borago might be possible in order to evaluate/ interpret depositional conditions under similar climatic circumstances within a volcanic rockshelter. The Sodicho Rockshelter is one of the few sites, that partly closes one major chronostratigraphic gap, that spans a time period covering the MIS 2 (Brandt et al. 2012, Tribolo et al. 2017), furthermore it is one of the first sites in eastern Africa to provide dated evidence for the habitation of the region during harsh climatic conditions, such as during the LGM (Hensel et al. 2021, Schaebitz et al. 2021). Thus, Sodicho is actively contributing to the Mountain Refugium Hypothesis, which deals with forced human migration to environmental refugia (Brandt et al. 2012, Stewart and Stringer 2012). Still, further comparing research could link hunter-gatherer mobility in mountainous areas with the influence of past climatic shifts. A comparison with further archaeological sites from the Horn of Africa (Fig. 5.3) would allow to study the environmental influences on past human communications, the expansion of AMH during

the MIS 3, as well as innovations in Late Pleistocene stone tool technology (such as technological development from MSA to LSA).

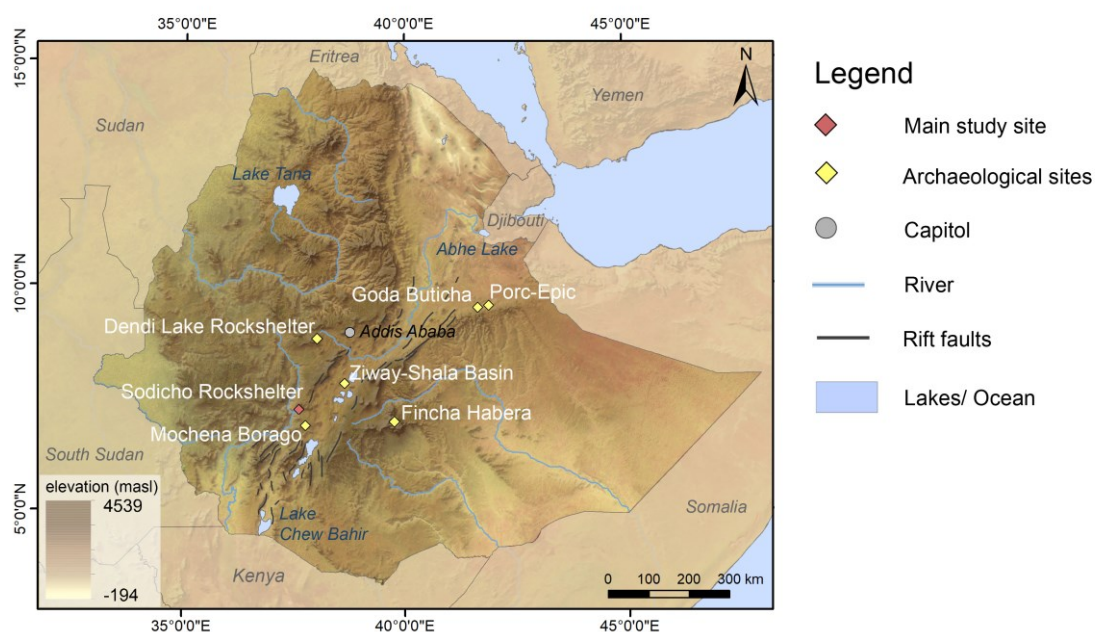


Figure 5.3 Map of the Horn of Africa showing the location of the main study site and important archaeological sites, situated in Ethiopia (DEM data by ASTER GDEM and Natural Earth raster map data) (modified from Hensel et al. 2021).

All of this research results and future results from this study area, as well as the results from the collaborating projects of the CRC 806 (see chapter 1.1), which provided data on human mobility, can be used for further studies, especially with regard to a larger spatial scale (e.g., continental scale). This could include anthropological models, such as agent-based modelling of the dispersal routes of the AMH within and out of Africa. All considered there is still a need for further collaboration between the different disciplines in the field and also in the laboratory. This is not only about joint planning and execution of field visits, method scopes and laboratory work, but also the opportunity for equal cooperation and contribution to the research. This enables to address common research questions from different angles but can also overcome inadequate investigations and research bias.

## Chapter VI

### 6. Conclusion

The geoarchaeological investigations undertaken in the southwestern Ethiopian Highlands and presented in this thesis provided first insights into the stratigraphic development and occupation at the new and promising site Sodicho Rockshelter, during the Late Pleistocene and Holocene. Based on a variation of geoarchaeological field and laboratory methods [e.g., sedimentology, geochemistry, micromorphology] as well as the contribution of supportive investigations [e.g., archaeology, phytolith analyses, palaeoclimate data] detailed information concerning the archaeological site itself and the surroundings could be gained for the first time. The most important results obtained include information about site formation processes, post depositional disturbances, human behavior, current landscape dynamics, occupation history, palaeoenvironmental signals and prehistoric human environment-interaction (Hensel et al. 2021, Hensel et al. 2022).

Within nine sedimentological units at Sodicho, four main sediment agents were responsible for the development of a complex stratigraphy under changing climatic and environmental conditions. Archaeological data, and the sedimentological/ geochemical composition of the deposits clearly mark several human settlement phases during the last 27 ka years. Up to now, in the Horn of Africa, and especially in Ethiopia, sedimentary and archaeological records are short and discontinuous and major chronostratigraphic gaps in the stratification are common. One period of archaeological uncertainties correlates with the critical transition from the Middle Stone Age (MSA) to the Late Stone Age (LSA), a timeframe that corresponds with the MIS 2 (Tribolo et al. 2019). With the lower dated occupation phases between ~ 13.5–18 ka cal BP (Unit VII) and ~ 21–27 cal BP (Unit VII and IX), an occupation phase during climatic critical Last Glacial Maximum (LGM, ~ 21 ± 2 ka) was determined. With this dating, Sodicho is given a unique position in science, as it is the only site in southwestern Ethiopia that shows that humans visited this area partly during this arid phase. In addition, this study highlights the Sodicho Rockshelter as the first site to provide initial evidence to partially reduce this chronostratigraphic gap. Although a transition between the MSA and LSA within the lithic material of Sodicho has not yet been identified, advanced geoarchaeological studies of this kind will help to fill major chronostratigraphic gaps.

Continuous and reliable terrestrial paleoenvironmental records are scarce in Ethiopia. However, in the recent years several sophisticated studies on lacustrine sediment records from Ethiopia and Kenya, provided useful data and predictive models for past varying environmental and climatic conditions for East Africa (e.g., Junginger and Trauth 2013, Foerster et al. 2015, Gebru Kassa 2015, Trauth et al. 2019, Fischer et al. 2021, Schaebitz et al. 2021, Schaebitz et al. 2021b). By applying the geoarchaeological methods at Sodicho Rockshelter on multiple spatial and temporal scales, the results could be incorporated into the mentioned supraregional palaeoenvironmental and palaeoclimatic studies, thus providing information on the occupation phases of the southwestern Ethiopian Highlands. In exchange, supraregional data were used to determine palaeoclimatic proxies within the local sedimentological and geochemical record of Sodicho. At the same time, this provided deeper insights into weathering processes. The radiocarbon dating of Sodicho provided a comprehensive chronostratigraphic framework that clearly highlights the settlement phases. Only by calculating an age-depth model, was it possible to correlate the geochemical data against time. This enabled a modelling of the results in relation to regional paleoenvironmental changes. In the process, it was possible to recognize supraregional to global climatic dry events (e.g., 4.2 ka event, Heinrich event 1, LGM) (Hensel et al. 2021).

While Mochena Borago was mainly occupied during rather humid phases (Brandt et al. 2017), the observations at Sodicho Rockshelter point to the settlement phases of prehistoric hunter-gatherers also during arid to hyper-arid periods. This contributes to the Mountain Refugium Hypothesis (Brandt et al. 2012), when humans left dryer lowland habitats and retreated to the highlands of Ethiopia, where they found an environmental refugium (Basell 2008).

An absence of humans from the study region, can be suggested according to the evidence within the stratigraphy of Sodicho. The clayish sterile unit, which was dated to the AHP period constitutes the largest gap of occupation. Palaeoecological and palaeoclimatic data from Chew Bahir records indicate an expansion of forest and dense vegetation in southern Ethiopia (Fischer et al. 2021, Schaebitz et al. 2021). This probably resulted in a thicker vegetation cover in the highlands, which must have hindered humans to occupy the rockshelters, let alone hunting under limited visibility.

In summary, the results highlight Sodicho Rockshelter as a new prime example for geoarchaeological, multiscale research approaches in East Africa. The observed archaeological features and palaeoenvironmental circumstances are useful for the reconstruction of past processes and human impact at other sites. The multimethodological practice enabled interdisciplinary cooperation and allowed the

investigations to use various spatial and temporal scales. This is especially suitable for challenging research sites, that are lacking comprehensive archaeological and terrestrial palaeoenvironmental archives, in regions such as the tropical highlands of Ethiopia. Furthermore, the research design and the multi-method approach are applicable for further geoarchaeological studies that deal with problematic/ critical stratigraphies in high elevated mountainous areas.

This research demonstrates that most of the basic geoarchaeological research questions that are asked at an archaeological study site or an archaeological important landscape, can to be answered with a multimethodological research design. The presented multi-method approach represents a solid tool to tackle difficult stratigraphies and to contribute to the reconstruction of past human-environment interaction. But even with the fulfilment of research aims and objectives, new and interesting research questions arise that allow new paths of science to be taken. For where one study ends, a new one begins. The question now is: **Where do we go from here?**

## 7. References

- Abbate, E., Bruni, P., and Sagri, M. (2015). Geology of Ethiopia: A Review and Geomorphological Perspectives. In P. Billi (Ed.), *Landscapes and Landforms of Ethiopia* (pp. 33–64). Dordrecht: Springer, Netherlands. doi: [https://doi.org/10.1007/978-94-017-8026-1\\_2](https://doi.org/10.1007/978-94-017-8026-1_2).
- Albert, R.M., Berna, F., and Goldberg, P. (2012). Insights on Neanderthal fire use at Kebara Cave (Israel) through high resolution study of prehistoric combustion features: Evidence from phytoliths and thin sections. *Quaternary International* 247, 278–293. doi: <https://doi.org/10.1016/j.quaint.2010.10.016>.
- Aldenderfer, M. (2006). Modelling Plateau Peoples: The Early Human Use of the World's High Plateaux. *World Archaeology* 38(3), 357–370. doi: <https://doi.org/10.1080/00438240600813285>.
- Antos, J.A., and Zobel, D.B. (2005). Plant Responses in Forests of the Tephra-Fall Zone. In V.H. Dale, F.J. Swanson and C.M. Crisafulli (Eds.), *Ecological Responses to the 1980 Eruption of Mount St. Helens* (pp. 47–58). New York: Springer New York, NY, USA. doi: [https://doi.org/10.1007/0-387-28150-9\\_4](https://doi.org/10.1007/0-387-28150-9_4).
- Aubert, M., Pike, A.W.G., Stringer, C., Bartsiokas, A., Kinsley, L., Eggins, S., et al. (2012). Confirmation of a late middle Pleistocene age for the Omo Kibish 1 cranium by direct uranium-series dating. *Journal of Human Evolution* 63(5), 704–710. doi: <https://doi.org/10.1016/j.jhevol.2012.07.006>.
- Arnaud, F., Révillon, S., Debret, M., Revel, M., Chapron, E., Jacob, J., et al. (2012). Lake Bourget regional erosion patterns reconstruction reveals Holocene NW European Alps soil evolution and paleohydrology. *Quaternary Science Reviews* 51, 81–92. doi: <https://doi.org/10.1016/j.quascirev.2012.07.025>.
- Arpin, T.L., Mallol, C., and Goldberg, P. (2002). Short contribution: a new method of analyzing and documenting micromorphological thin sections using flatbed scanners: applications in geoarchaeological studies. *Geoarchaeology: An International Journal* 17(3), 305–313. doi: <https://doi.org/10.1002/gea.10014>.
- Ayenew, T., and GebreEgziabher, M. (2015). Morphometric Characteristics and Hydrology of Selected Ethiopian Rift Lakes. In P. Billi (Ed.), *Landscapes and Landforms of Ethiopia* (pp. 275–287). Dordrecht: Springer, Netherlands. doi: [https://doi.org/10.1007/978-94-017-8026-1\\_16](https://doi.org/10.1007/978-94-017-8026-1_16).
- Barrón, V., and Torrent, J. (1986). Use of the Kubelka–Munk theory to study the influence of iron oxides on soil colour. *Journal of Soil Science* 37(4), 499–510. doi: <https://doi.org/10.1111/j.1365-2389.1986.tb00382.x>.
- Bartz, M., Klasen, N., Zander, A., Brill, D., Rixhon, G., Seeliger, M., et al. (2015). Luminescence dating of ephemeral stream deposits around the Palaeolithic site of Ifri n'Ammar (Morocco). *Quaternary Geochronology* 30, 460–465. doi: <https://doi.org/10.1016/j.quageo.2015.02.012>.
- Bartz, M., Rixhon, G., Kehl, M., El Ouahabi, M., Klasen, N., Brill, D., et al. (2017). Unravelling fluvial deposition and pedogenesis in ephemeral stream deposits in the vicinity of the prehistoric rock shelter of Ifri n'Ammar (NE Morocco) during the last 100ka. *CATENA* 152, 115–134. doi: <https://doi.org/10.1016/j.catena.2016.12.007>.
- Basell, L. S. (2008). Middle Stone Age (MSA) site distributions in eastern Africa and their relationship to Quaternary environmental change, refugia and the evolution of Homo sapiens. *Quaternary Science Reviews* 27(27), 2484–2498. doi: <https://doi.org/10.1016/j.quascirev.2008.09.010>.

- Basell, L. (2013). The Middle Stone Age of Eastern Africa. In P. Mitchell and P. Lane (Eds.), *The Oxford handbook of African Archaeology* (pp. 387–401). Oxford: Oxford University Press, UK. <https://doi.org/10.1093/oxfordhb/9780199569885.013.0027>.
- Beckmann, T., (1997). Präparation bodenkundlicher Dünnschliffe für mikromorphologische Untersuchungen. *Hohenheimer Bodenkundliche Hefte* 40, 89–103.
- Belay, A., Demissie, T., Recha, J.W., Oludhe, C., Osano, P.M., Olaka, L.A., et al. (2021). Analysis of Climate Variability and Trends in Southern Ethiopia. *Climate* 9(6), 96, 1–17. doi: <https://doi.org/10.3390/cli9060096>.
- Benito-Calvo, A., De la Torre, I., Mora, R., Tibebe, D., Morán, N., and Martínez- Moreno, J. (2007). Geoarchaeological potential of the western bank of the Bilate River (Ethiopia). *Analele Universit'at,ii din Oradea XVII Seria Geographie*, 99–104.
- Berhanu, B., Melesse, A.M., and Seleshi, Y. (2013). GIS-based hydrological zones and soil geodatabase of Ethiopia. *CATENA* 104, 21–31. doi: <https://doi.org/10.1016/j.catena.2012.12.007>.
- Billi, P. (2015). Geomorphological Landscapes of Ethiopia. In P. Billi (Ed.), *Landscapes and Landforms of Ethiopia* (pp. 3–32). Dordrecht: Springer, Netherlands. doi: [https://doi.org/10.1007/978-94-017-8026-1\\_1](https://doi.org/10.1007/978-94-017-8026-1_1).
- Billi, P., and Dramis, F. (2003). Geomorphological investigation on gully erosion in the Rift Valley and the northern highlands of Ethiopia. *CATENA* 50(2), 353–368. doi: [https://doi.org/10.1016/S0341-8162\(02\)00131-5](https://doi.org/10.1016/S0341-8162(02)00131-5).
- Birndorfer, T., Brückner, H., Bubbenzer, O., Dotterweich, M., Dreibrodt, S., Hadler, H., et al. (2022). Geoarchäologie in unterschiedlichen Landschaftsräumen. In C. Stolz and C.E. Miller (Eds.), *Geoarchäologie* (pp. 79–164). Berlin, Heidelberg: Springer, Germany. [https://doi.org/10.1007/978-3-662-62774-7\\_9](https://doi.org/10.1007/978-3-662-62774-7_9).
- Blaauw, M. (2010). Methods and code for 'classical' age-modelling of radiocarbon sequences. *Quaternary Geochronology* 5(5), 512–518. doi: <https://doi.org/10.1016/j.quageo.2010.01.002>.
- Blinkhorn, J., Timbrell, L., Grove, M., and Scerri, E.M.L. (2022). Evaluating refugia in recent human evolution in Africa. *Philosophical Transactions of the Royal Society B: Biological Sciences* 377(1849), 20200485. doi: <https://doi.org/10.1098/rstb.2020.0485>.
- Blott, S.J., and Pye, K. (2001). GRADISTAT: a grain size distribution and statistics package for the analysis of unconsolidated sediments. *Earth surface processes and Landforms* 26(11), 1237–1248. doi: <https://doi.org/10.1002/esp.261>.
- Bolten, A., Bubbenzer, O., and Darius, F. (2006). A digital elevation model as a base for the reconstruction of Holocene land-use potential in arid regions. *Geoarchaeology* 21(7), 751–762. doi: <https://doi.org/10.1002/gea.20137>.
- Bon, F., Dessie, A., Bruxelles, L., Daussy, A., Douze, K., Fauvelle-Aymar, F., et al. (2013). Prehistory of the central main Ethiopian rift (Ziway-Shala basin): Establishing the Late Stone Age sequence in eastern Africa. *Annales d'Ethiopie* 28, 405–407. doi: <https://doi.org/10.3406/ethio.2013.1552>.
- Bonini, M., Corti, G., Innocenti, F., Manetti, P., Mazzarini, F., Abebe, T., et al. (2005). Evolution of the Main Ethiopian Rift in the frame of Afar and Kenya rifts propagation. *Tectonics* 24(1), TC1007. doi: <https://doi.org/10.1029/2004tc001680>.
- Braadbaart, F. and Poole, I. (2008). Morphological, chemical and physical changes during charcoalification of wood and its relevance to archaeological contexts. *Journal of Archaeological Science* 35, 2434–2445. doi: <https://doi.org/10.1016/j.jas.2008.03.016>.

- Brancaleoni, G., Shnaider, S., Osipova, E., Danukalova, G., Kurbanov, R., Deput, E., et al. (2021). Depositional history of a talus cone in an arid intermontane basin in Central Asia: An interdisciplinary study at the Late Pleistocene–Late Holocene Obishir-I site, Kyrgyzstan. *Geoarchaeology* 37, 350–373. doi: <https://doi.org/10.1002/gea.21892>.
- Brandt, S.A., Fisher, E.C., Hildebrand, E.A., Vogelsang, R., Ambrose, S.H., Lesur, J., et al. (2012). Early MIS 3 occupation of Mochena Borago Rockshelter, Southwest Ethiopian Highlands: implications for Late Pleistocene archaeology, paleoenvironments and modern human dispersals. *Quaternary International* 274, 38–54. doi: <https://doi.org/10.1016/j.quaint.2012.03.047>.
- Brandt, S., Hildebrand, E., Vogelsang, R., Wolfhagen, J., and Wang, H. (2017). A new MIS 3 radiocarbon chronology for Mochena Borago Rockshelter, SW Ethiopia: Implications for the interpretation of Late Pleistocene chronostratigraphy and human behavior. *Journal of Archaeological Science: Reports* 11, 352–369. doi: <https://doi.org/10.1016/j.jasrep.2016.09.013>.
- van Breugel P, Kindt R, Lillesø JPB, Bingham M, Demissew S, Dudley C, Friis I, Gachathi F, Kalema J, Mbago F, Moshi HN, Mulumba, J, Namaganda M, Ndangalasi HJ, Ruffo CK, Védaste M, Jamnadass R and Graudal L (2015). Potential Natural Vegetation Map of Eastern Africa (Burundi, Ethiopia, Kenya, Malawi, Rwanda, Tanzania, Uganda and Zambia). Version 2.0. *Forest and Landscape*, (Denmark) and World Agroforestry Centre (ICRAF). URL: [//vegetationmap4africa.org](http://vegetationmap4africa.org)
- Brierley, G.J., and Fryirs, K. (1999). Tributary–trunk stream relations in a cut-and-fill landscape: a case study from Wolumla catchment, New South Wales, Australia. *Geomorphology* 28(1), 61–73. doi: [https://doi.org/10.1016/S0169-555X\(98\)00103-2](https://doi.org/10.1016/S0169-555X(98)00103-2).
- Brochier, J.É. (2002). Les sédiments anthropiques. *Géologie de la Préhistoire: Méthodes, Techniques et Applications. Méthodes d'étude et perspectives Géologie de la Préhistoire*, 453–473.
- Brodowski, S., Rodionov, A., Haumaier, L., Glaser, B., and Amelung, W. (2005). Revised black carbon assessment using benzene polycarboxylic acids. *Organic Geochemistry* 36(9), 1299–1310. doi: <https://doi.org/10.1016/j.orggeochem.2005.03.011>.
- Brown, E.T. (2011). Lake Malawi's response to “megadrought” terminations: sedimentary records of flooding, weathering and erosion. *Palaeogeography, Palaeoclimatology, Palaeoecology* 303(1-4), 120–125. doi: <https://doi.org/10.1016/j.palaeo.2010.01.038>.
- Burns, J.A., and Raber, P.A. (2010). Rockshelters in Behavioral Context: Archaeological Perspectives from Eastern North America. *North American Archaeologist* 31(3), 257–285. doi: <https://doi.org/10.2190/NA.31.3-4.b>.
- Canti, M.G., and Linford, N. (2000). The Effects of Fire on Archaeological Soils and Sediments: Temperature and Colour Relationships. *Proceedings of the Prehistoric Society* 66, 385–395. doi: <https://doi.org/10.1017/S0079497X00001869>.
- Carnicelli, S., Benvenuti, M., Ferrari, G., and Sagri, M. (2009). Dynamics and driving factors of late Holocene gully erosion in the Main Ethiopian Rift (MER). *Geomorphology* 103(4), 541–554. doi: <https://doi.org/10.1016/j.geomorph.2008.07.019>.
- Castillo, C., and Gómez, J.A. (2016). A century of gully erosion research: Urgency, complexity and study approaches. *Earth-Science Reviews* 160, 300–319. doi: <https://doi.org/10.1016/j.earscirev.2016.07.009>.
- Chadwick, O.A., Gavenda, R., Kelly, E., Ziegler, K., Olson, C., Elliott, W.C., et al. (2003). The impact of climate on the biogeochemical functioning of volcanic soils. *Chemical Geology* 202, 195–223. doi: <https://doi.org/10.1016/j.chemgeo.2002.09.001>.

- Chen, F., Welker, F., Shen, C.-C., Bailey, S.E., Bergmann, I., Davis, S., et al. (2019). A late Middle Pleistocene Denisovan mandible from the Tibetan Plateau. *Nature* 569(7756), 409–412. doi: <https://doi.org/10.1038/s41586-019-1139-x>.
- Chernet, T. (2011). Geology and hydrothermal resources in the northern Lake Abaya area (Ethiopia). *Journal of African Earth Sciences* 61(2), 129–141. doi: <https://doi.org/10.1016/j.jafrearsci.2011.05.006>.
- Churchman, G.J., and Lowe, D.J. (2012). Alteration, formation, and occurrence of Minerals in Soils. In P.M. Hnag, M. E. Sumner (Eds.), *Handbook of Soil Science (2), Vol. 1 Properties and Processes* (pp. 1–72). New York: CRC Press, Taylor & Francis Group, USA.
- Churchman, G.J., and Velde, B. (2019). *Soil Clays: Linking Geology, Biology, Agriculture, and the Environment*. CRC Press, Taylor & Francis Group: Boca Raton, FL, USA.
- Cordova, C. (2018). *Geoarchaeology: The Human-Environmental Approach*. London & New York: I.B.Tauris.
- Cornelissen, E. (2013). Hunting and Gathering in Africa's Tropical Forests at the End of The Pleistocene and in the Early Holocene. In P. Mitchell and P.J. Lane (Eds.), *The Oxford Handbook of African Archaeology* (pp. 402–417). Oxford: Oxford University Press, UK. doi: <https://doi.org/10.1093/oxfordhb/9780199569885.013.0028>.
- Corti, G. (2009). Continental rift evolution: From rift initiation to incipient break-up in the Main Ethiopian Rift, East Africa. *Earth-Science Reviews* 96(1), 1–53. doi: <https://doi.org/10.1016/j.earscirev.2009.06.005>.
- Corti, G., Sani, F., Philippon, M., Sokoutis, D., Willingshofer, E., and Molin, P. (2013). Quaternary volcano-tectonic activity in the Soddo region, western margin of the Southern Main Ethiopian Rift. *Tectonics* 32(4), 861–879. doi: <https://doi.org/10.1002/tect.20052>.
- Dearing, J. (1999): *Environmental magnetic susceptibility. Using the Bartington MS2 system*. Kenilworth: Chi Publishing.
- De la Torre, I., Benito-Calvo, A., Mora, R., Martínez-Moreno, J., Morán, N., and Tibebe, D. (2007). Stone age occurrences in the western bank of the Bilate River (southern Ethiopia) - some preliminary results. *Nyame Akuma*. 67, 14–25.
- Dibble, H., Berna, F., Goldberg, P., McPherron, S., Mentzer, S., Niven, L., et al. (2009). A Preliminary Report on Pech de l'Azé IV, Layer 8 (Middle Paleolithic, France). *PaleoAnthropology 2009*, 182–219. doi: <https://doi.org/10.4207/PA.2009.ART30>.
- Eckmeier, E., and Gerlach, R. (2012). Characterization of Archaeological Soils and Sediments Using VIS Spectroscopy. *eTopoi Journal for Ancient Studies* 3, 285–290.
- Farmer, V.C., McHardy, W.J., Robertson, L., Walker, A., and Wilson, M.J. (1985). Micromorphology and sub-microscopy of allophane and imogolite in a podzol Bs horizon: evidence for translocation and origin. *Journal of Soil Science* 36(1), 87–95. doi: <https://doi.org/10.1111/j.1365-2389.1985.tb00315.x>.
- Fassbinder, J. (2007). Unter Acker und Wadi: Magnetometerprospektion in der Archäologie. In G. Wagner (Ed.), *Einführung in die Archäometrie* (pp. 53–73). Berlin, Heidelberg: Springer, Germany. doi: [https://doi.org/10.1007/978-3-540-71937-3\\_4](https://doi.org/10.1007/978-3-540-71937-3_4).
- Fazzini, M., Bisci, C., and Billi, P. (2015). The Climate of Ethiopia. In P. Billi (Ed.), *Landscapes and Landforms of Ethiopia* (pp. 65–87), Dordrecht: Springer, Netherlands. doi: [https://doi.org/10.1007/978-94-017-8026-1\\_3](https://doi.org/10.1007/978-94-017-8026-1_3).

- Fischer, M.L., Bachofer, F., Yost, C.L., Bludau, I.J.E., Schepers, C., Foerster, V., et al. (2021). A Phytolith Supported Biosphere-Hydrosphere Predictive Model for Southern Ethiopia: Insights into Paleoenvironmental Changes and Human Landscape Preferences since the Last Glacial Maximum. *Geosciences* 11(10), 418. doi: <https://doi.org/10.3390/geosciences11100418>.
- Fisher, Erich C. (2010). Late Pleistocene technological change and hunter gatherer behavior at Moche Borago rockshelter, Sodo-Wolayta, Ethiopia: Flaked stone artifacts from the early OIS 3 (60–43 ka) deposits. (Ph.D. thesis), University of Florida, Gainesville, FL, USA (3532627).
- Fleagle, J.G., Assefa, Z., Brown, F.H., and Shea, J.J. (2008). Paleoanthropology of the Kibish Formation, southern Ethiopia: Introduction. *Journal of Human Evolution* 55(3), 360–365. doi: <https://doi.org/10.1016/j.jhevol.2008.05.007>.
- Foerster, V., Junginger, A., Langkamp, O., Gebru, T., Asrat, A., Umer, M., et al. (2012). Climatic change recorded in the sediments of the Chew Bahir basin, southern Ethiopia, during the last 45,000 years. *Quaternary International* 274, 25–37. doi: <https://doi.org/10.1016/j.quaint.2012.06.028>.
- Foerster, V., Vogelsang, R., Junginger, A., Asrat, A., Lamb, H.F., Schaebitz, F., et al. (2015). Environmental change and human occupation of southern Ethiopia and northern Kenya during the last 20,000 years. *Quaternary Science Reviews* 129, 333–340. doi: <https://doi.org/10.1016/j.quascirev.2015.10.026>.
- Folk, R.L., and Ward, W.C. (1957). Brazos River bar [Texas]; a study in the significance of grain size parameters. *Journal of Sedimentary Research* 27(1), 3–26. doi: <https://doi.org/10.1306/74d70646-2b21-11d7-8648000102c1865d>.
- French, C. (2015). *A handbook of geoarchaeological approaches to settlement sites and landscapes*. Oxford: Oxbow Books, UK.
- Friis, I., Sebsebe, D., and Breugel, P. (2010). *Atlas of the potential vegetation of Ethiopia*. Copenhagen: Det Kongelige Danske Videnskaberne Selskab, Denmark.
- Fryirs, K.A., and Brierley, G.J. (2012). *Geomorphic analysis of river systems: an approach to reading the landscape*. Chichester: John Wiley & Sons, UK.
- Fryirs, K.A. (2017). River sensitivity: a lost foundation concept in fluvial geomorphology. *Earth Surface Processes and Landforms* 42(1), 55–70. doi: <https://doi.org/10.1002/esp.3940>.
- Garcin, Y., Melnick, D., Strecker, M.R., Olago, D., and Tiercelin, J.-J. (2012). East African mid-Holocene wet–dry transition recorded in palaeo-shorelines of Lake Turkana, northern Kenya Rift. *Earth and Planetary Science Letters* 331–332, 322–334. doi: <https://doi.org/10.1016/j.epsl.2012.03.016>.
- Garcin, Y., Schildgen, T.F., Torres Acosta, V., Melnick, D., Guillemoteau, J., Willenbring, J., et al. (2017). Short-lived increase in erosion during the African Humid Period: Evidence from the northern Kenya Rift. *Earth and Planetary Science Letters* 459, 58–69. doi: <https://doi.org/10.1016/j.epsl.2016.11.017>.
- Gasse, F. (2000). Hydrological changes in the African tropics since the Last Glacial Maximum. *Quaternary Science Reviews* 19(1), 189–211. doi: [https://doi.org/10.1016/S0277-3791\(99\)00061-X](https://doi.org/10.1016/S0277-3791(99)00061-X).
- Gebru Kassa, T. (2015). Holocene Environmental History of Lake Chamo, South Ethiopia. (Ph.D. thesis), Universität zu Köln, <https://kups.ub.uni-koeln.de/6193/>.
- Garrison, E. (2016). *Techniques in Archaeological Geology*. Cham, Switzerland: Springer International Publishing AG.

- Gilbert, A.S., Goldberg, P., Holliday, V.T., Mandel, R.D., and Sternberg, R.S. (2017). *Encyclopedia of Geoarchaeology*. Dordrecht: Springer, Netherlands.
- Gillhuber S., Lehrberger G. and Thuro K. (2006). Teplá trachyte weathering phenomena and physical properties of a rare volcanogenic building stone. In M.G. Culshaw, H.J. Reeves, I. Jefferson, and T.W. Spink (Eds.) (2009). *IAEG2006 CD, in Engineering Geology for Tomorrow's Cities*. 469, (pp. 1–11). Nottingham: Geological Society of London 22, UK.
- Glaser, B., Haumaier, L., Guggenberger, G., and Zech, W., (1998). Black carbon in soils: the use of benzene carboxylic acids as specific markers. *Organic Geochemistry* 29, 811–819. doi: [https://doi.org/10.1016/S0146-6380\(98\)00194-6](https://doi.org/10.1016/S0146-6380(98)00194-6).
- Goldberg, E.D. (1985). *Black Carbon in the Environment*. New York: John Wiley & Sons, USA
- Goldberg, P. (1979). Micromorphology of Pech-de-l'Azé II sediments. *Journal of Archaeological Science* 6(1), 17–47. doi: [https://doi.org/10.1016/0305-4403\(79\)90031-1](https://doi.org/10.1016/0305-4403(79)90031-1).
- Goldberg, P. (2000). Micromorphology and site formation at Die Kelders Cave I, South Africa. *Journal of Human Evolution* 38(1), 43–90. doi: <https://doi.org/10.1006/jhev.1999.0350>.
- Goldberg, P. (2003). Some Observations on Middle and Upper Palaeolithic Ashy Cave and Rockshelter Deposits in the Near East. In: A.N. Goring-Morris and A. Belfer-Cohen (Eds.), *More than Meets the Eye: Studies on Upper Palaeolithic Diversity in the Near East* (pp. 19–32). Oxford: Oxbow Books, UK.
- Goldberg, P., and Bar-Yosef, O. (1998). Site Formation Processes in Kebara and Hayonim Caves and Their Significance in Levantine Prehistoric Caves. In T. Akazawa, K. Aoki and O. Bar-Yosef (Eds.), *Neandertals and Modern Humans in Western Asia* (pp. 107–125). Boston, MA: Springer, USA.
- Goldberg, P., Holliday, V.T., and Ferring, C.R. (2001). *Earth Sciences and Archaeology* Kluwer Academic/Plenum Publishers: New York, NY, USA.
- Goldberg, P., and Sherwood, S.C. (2006). Deciphering human prehistory through the geoarchaeological study of cave sediments. *Evolutionary Anthropology: Issues, News, and Reviews* 15(1), 20–36. doi: <https://doi.org/10.1002/evan.20094>.
- Goldberg, P., and Macphail, R. (2006). *Practical and theoretical geoarchaeology*. Blackwell publishing Oxford.
- Goldberg, P., Miller, C.E., Schiegl, S., Ligouis, B., Berna, F., Conard, N.J., et al. (2009). Bedding, hearths, and site maintenance in the Middle Stone age of Sibudu cave, KwaZulu-Natal, South Africa. *Archaeological and Anthropological Sciences* 1(2), 95–122. doi: <https://doi.org/10.1007/s12520-009-0008-1>.
- Goldberg, P., Berna, F., and Chazan, M. (2015). Deposition and Diagenesis in the Earlier Stone Age of Wonderwerk Cave, Excavation 1, South Africa. *African Archaeological Review* 32(4), 613–643. doi: <https://doi.org/10.1007/s10437-015-9192-9>.
- Goldberg, P., and Aldeias, V. (2018). Why does (archaeological) micromorphology have such little traction in (geo)archaeology? *Archaeological and Anthropological Sciences* 10(2), 269–278. doi: <https://doi.org/10.1007/s12520-016-0353-9>.
- Griffiths, JF. (1972). Ethiopian highlands. In H. Landsberg and N.L. Amsterda (Eds.), *World survey of climatology* 10 (pp. 369–381). New York, NY: Elsevier, USA.
- Gutherz, X., Jallot, L., Lesur, J., Pouzolles, G., and Sordoillet, D. (2002). D. Les fouilles de l'abri sous-roche de Moche Borago (Soddo-Wolayta). *Premier bilan. Annales d'Ethiopie* 18, 181–190. doi: <https://doi.org/10.3406/ethio.2002.1019>

- Harsh, J., Chorover, J., and Nizeyimana, E. (2002). Allophane and Imogolite. In J.B. Dixon and D.G. Schulze (Eds.), *Soil Mineralogy with Environmental Application (7)* (pp. 291–322). Madison, Wisconsin: Soil Science Society of America doi: <https://doi.org/10.2136/sssabookser7.c9>.
- Hammes, K., Schmidt, M.W.I., Smernik, R.J., Currie, L.A., Ball, W.P., Nguyen, T.H., et al. (2007). Comparison of quantification methods to measure fire-derived (black/elemental) carbon in soils and sediments using reference materials from soil, water, sediment and the atmosphere. *Global Biogeochemical Cycles* 21(3), 1–18, doi: <https://doi.org/10.1029/2006GB002914>.
- Hemming, S.R. (2004). Heinrich events: Massive late Pleistocene detritus layers of the North Atlantic and their global climate imprint. *Reviews of Geophysics* 42(1). doi: <https://doi.org/10.1029/2003RG000128>.
- Hensel, E.A., Bödeker, O., Bubenzer, O., and Vogelsang, R. (2019). Combining geomorphological– hydrological analyses and the location of settlement and raw material sites – a case study on understanding prehistoric human settlement activity in the southwestern Ethiopian Highlands. *E&G Quaternary Science Journal* 68, 201–213. doi: <https://doi.org/10.5194/egqsj-68-201-2019>.
- Hensel, E.A., Vogelsang, R., Noack, T., and Bubenzer, O. (2021). Stratigraphy and Chronology of Sodicho Rockshelter – A new sedimentological record of past environmental changes and human settlement phases in Southwestern Ethiopia. *Frontiers in Earth Science* 8(640). doi: <https://doi.org/10.3389/feart.2020.611700>.
- Hensel, E.A., Kehl, M., Wöstehoff, L., Neumann, K., Vogelsang, R., and Bubenzer, O. (2022). A Multi-Method Approach for Deciphering Rockshelter Microstratigraphies—The Role of the Sodicho Rockshelter (SW Ethiopia) as a Geoarchaeological Archive. *Geosciences* 12(2), 92. doi: <https://doi.org/10.3390/geosciences12020092>.
- Henselowsky, F., Kindermann, K., Willmes, C., Lammerich-Long, D., Bareth, G., and Bubenzer, O. (2022). Palaeoenvironments and landscape diversity in Egypt during the Last Interglacial and its implications on the dispersal of Homo sapiens. *Journal of Maps*, 1–11. doi: <https://doi.org/10.1080/17445647.2022.2064779>.
- Herrejón Lagunilla, Á., Carrancho, A., Villalaín, J., Mallol, C., and Hernández, C. (2019). An experimental approach to the preservation potential of magnetic signatures in anthropogenic fires. *PLOS ONE* 14, e0221592. doi: <https://doi.org/10.1371/journal.pone.0221592>.
- Hildebrand, E.A., Brandt, S.A., Friis, I., and Demissew, S. (2019). Paleoenvironmental reconstructions for the Horn of Africa: Interdisciplinary perspectives on strategy and significance. In B. Eichorn and A. Höhn (Eds.), *Trees, grasses and crops. People and plants in sub-saharan Africa and beyond* (pp. 187–210). Bonn: Verlag Dr. Rudolf Habelt, Germany.
- Holliday, V.T., and Gartner, W.G. (2007). Methods of soil P analysis in archaeology. *Journal of archaeological science* 34(2), 301–333. doi: <https://doi.org/10.1016/j.jas.2006.05.004>.
- Homsey, L.K., and Capo, R.C. (2006). Integrating geochemistry and micromorphology to interpret feature use at Dust Cave, a Paleo-Indian through middle-archaic site in Northwest Alabama. *Geoarchaeology* 21(3), 237–269. doi: <https://doi.org/10.1002/gea.20103>.
- Horwell, C.J. (2007). Grain-size analysis of volcanic ash for the rapid assessment of respiratory health hazard. *Journal of Environmental Monitoring* 9(10), 1107–1115. doi: <https://doi.org/10.1039/B710583P>.
- Hublin, J.-J., Ben-Ncer, A., Bailey, S., Freidline, S., Neubauer, S., Skinner, M., et al. (2017). New fossils from Jebel Irhoud, Morocco and the pan-African origin of Homo sapiens. *Nature* 546, 289–292. doi: <https://doi.org/10.1038/nature22336>.

- Hunt, A.M., and Speakman, R.J. (2015). Portable XRF analysis of archaeological sediments and ceramics. *Journal of Archaeological Science* 53, 626–638. doi: <https://doi.org/10.1016/j.jas.2014.11.031>.
- Inglis, R.H., French, C., Farr, L., Hunt, C.O., Jones, S.C., Reynolds, T., et al. (2018). Sediment micromorphology and site formation processes during the Middle to Later Stone Ages at the Haua Fteah Cave, Cyrenaica, Libya. *Geoarchaeology* 33(3), 328–348. doi: <https://doi.org/10.1002/gea.21660>.
- IUSS Working Group WRB (2015). World Reference Base for Soil Resources 2014: International soil classification system for naming soils and creating legends for soil maps in World soil resources report. 106, Rome: FAO Italy.
- Ivers-Tiffée, E., and von Münch, W. (2007). Magnetische Werkstoffe. In E. Ivers-Tiffée and W. von Münch (Eds.), *Werkstoffe der Elektrotechnik*. (pp. 183–208). Wiesbaden: Teubner Verlag. doi: [https://doi.org/10.1007/978-3-8351-9088-7\\_6](https://doi.org/10.1007/978-3-8351-9088-7_6).
- Junginger, A., and Trauth, M.H. (2013). Hydrological constraints of paleo-Lake Suguta in the Northern Kenya Rift during the African humid period (15–5 ka BP). *Global and planetary change* 111, 174–188. doi: <https://doi.org/10.1016/j.gloplacha.2013.09.005>.
- Junginger, A., Vonhof, H., and Foerster, V.E. (2016). AGU Fall Meeting Abstracts, How wet is wet? Strontium isotopes as paleo-lake level indicators in the Chew Bahir basin (S-Ethiopia), American Geophysical Union, Fall Meeting 2016, (abstract no. PP23A-2310).
- Kaboth-Bahr, S., Gosling, W.D., Vogelsang, R., Bahr, A., Scerri, E.M.L., Asrat, A., et al. (2021). Paleo-ENSO influence on African environments and early modern humans. *Proceedings of the National Academy of Sciences* 118(23), e2018277118. doi: <https://doi.org/10.1073/pnas.2018277118>.
- Kaczorek, D., Vrydaghs, L., Devos, Y., Petó, Á., and Effland, W.R. (2018). Biogenic Siliceous Features. In G. Stoops, V. Marcelino and F. Mees (Eds.), *Interpretation of Micromorphological Features of Soils and Regoliths (Second Edition)* (pp. 157–176). Amsterdam: Elsevier, Netherlands; Oxford: Elsevier, UK. doi: <https://doi.org/10.1016/B978-0-444-63522-8.00007-3>.
- Kaniewski, D., Marriner, N., Cheddadi, R., Joel, G., and Campo, E. (2018). The 4.2 ka BP event in the Levant. *Climate of the Past* 14, 1529–1542. doi: <https://doi.org/10.5194/cp-14-1529-2018>.
- Kappenberg, A., Bläsing, M., Lehndorff, E., and Amelung, W. (2016). Black carbon assessment using benzene polycarboxylic acids: Limitations for organic-rich matrices. *Organic Geochemistry* 94, 51–74. doi: <https://doi.org/10.1016/j.orggeochem.2016.01.009>.
- Karkanas, P. (2017). Chemical alteration. In A.S. Gilbert (Ed.), *Encyclopedia of Geoarchaeology. Encyclopedia of earth sciences series* (pp. 129–138). Dordrecht: Springer-Verlag, Netherlands. doi: [https://doi.org/10.1007/978-1-4020-4409-0\\_126](https://doi.org/10.1007/978-1-4020-4409-0_126).
- Karkanas, P., and Goldberg, P. (2018). *Reconstructing archaeological sites: Understanding the geoarchaeological matrix*. John Wiley & Sons.
- Karkanas, P., and Goldberg, P. (2018). Phosphatic Features. In: G. Stoops, V. Marcelino, and F. Mees (Eds.), *Interpretation of Micromorphological Features of Soils and Regoliths (Second Edition)* (pp. 323–346). Amsterdam: Elsevier, Netherlands. doi: <https://doi.org/10.1016/B978-0-444-63522-8.00012-7>.
- Kehl, M., Eckmeier, E., Franz, S., Lehmkuhl, F., Soler, J., Soler, N., et al. (2014). Sediment sequence and site formation processes at the Arbreda Cave, NE Iberian Peninsula, and implications on human occupation and climate change during the Last Glacial. *Climate of the Past* 10(5), 1673–1692. doi: <https://doi.org/10.5194/cp-10-1673-2014>.

- Kehl, M., Burow, C., Cantalejo, P., Domínguez-Bella, S., Durán, J.J., Henselowsky, F., et al. (2016). Site formation and chronology of the new Paleolithic site Sima de Las Palomas de Teba, southern Spain. *Quaternary Research* 85(2), 313–331. doi: <https://doi.org/10.1016/j.yqres.2016.01.007>.
- Keiluweit, M., Nico, P.S., Johnson, M.G., and Kleber, M. (2010). Dynamic molecular structure of plant biomass-derived black carbon (Biochar). *Environmental Science and Technology* 44, 1247–1253. doi: <https://doi.org/10.1021/es9031419>.
- Khalidi, L., Mologni, C., Ménard, C., Coudert, L., Gabriele, M., Davtian, G., et al. (2020). 9000 years of human lakeside adaptation in the Ethiopian Afar: Fisher-foragers and the first pastoralists in the Lake Abhe basin during the African Humid Period. *Quaternary Science Reviews* 243, 106459. doi: <https://doi.org/10.1016/j.quascirev.2020.106459>.
- Kindermann, K., Bubbenzer, O., and Peer, P. (2013). Geo-archaeological research on the Late Pleistocene of the Egyptian Eastern Desert: recent threats to the Sodmein Cave. *Antiquity* 87(337).
- Kindermann, K., Van Peer, P., and Henselowsky, F. (2018). At the lakeshore – An Early Nubian Complex site linked with lacustrine sediments (Eastern Desert, Egypt). *Quaternary International* 485, 131–139. doi: <https://doi.org/10.1016/j.quaint.2017.11.006>.
- Klasen, N., Kehl, M., Mikdad, A., Brückner, H., and Weniger, G.-C. (2018). Chronology and formation processes of the Middle to Upper Palaeolithic deposits of Ifri n'Amman using multi-method luminescence dating and micromorphology. *Quaternary International* 485, 89–102. doi: <https://doi.org/10.1016/j.quaint.2017.10.043>.
- Kolobova, K., Roberts, R., Chabai, V., Jacobs, Z., Krajcarz, M., Shalagina, A., et al. (2020). Archaeological evidence for two separate dispersals of Neanderthals into southern Siberia. *Proceedings of the National Academy of Sciences* 117, 201918047. doi: <https://doi.org/10.1073/pnas.1918047117>.
- Kooistra, M.J. and Pulleman, M.M. (2018). Features Related to Faunal Activity. In: G. Stoops, V. Marcelino and F. Mees (Eds.), *Interpretation of Micromorphological Features of Soils and Regoliths (Second Edition)* (pp. 447–469). Amsterdam: Elsevier, Netherlands. doi: <https://doi.org/10.1016/B978-0-444-63522-8.00016-4>.
- Kourampas, N., Simpson, I.A., Perera, N., Deraniyagala, S.U., and Wijeyapala, W.H. (2009). Rockshelter sedimentation in a dynamic tropical landscape: Late Pleistocene–Early Holocene archaeological deposits in Kitulgala Beli-lena, southwestern Sri Lanka. *Geoarchaeology* 24(6), 677–714. doi: <https://doi.org/10.1002/gea.20287>.
- Kröpelin, S., Verschuren, D., Lézine, A.-M., Eggermont, H., Cocquyt, C., Francus, P., et al. (2008). Climate-Driven Ecosystem Succession in the Sahara: The Past 6000 Years. *Science* 320(5877), 765–768. doi: <https://doi.org/10.1126/science.1154913>.
- Kuehn, D.D., and Dickson, D.B. (1999). Stratigraphy and noncultural site formation at the Shurmai Rockshelter (GnJm1) in the Mukogodo Hills of North-Central Kenya. *Geoarchaeology: An International Journal* 14(1), 63–85. doi: [https://doi.org/10.1002/\(SICI\)1520-6548\(199901\)14:1<63::AID-GEA5>3.0.CO;2-F](https://doi.org/10.1002/(SICI)1520-6548(199901)14:1<63::AID-GEA5>3.0.CO;2-F).
- Kühn, P., Aguilar, J., Miedema, R., and Bronnikova, M. (2018). Textural Pedofeatures and Related Horizons. In G. Stoops, V. Marcelino, and F. Mees (Eds.), *Interpretation of Micromorphological Features of Soils and Regoliths (Second)* (pp. 377–423). Amsterdam: Elsevier, Netherlands; Oxford, UK. doi: <https://doi.org/10.1016/B978-0-444-63522-8.00014-0>.
- Lane, C., and Woodward, J. (2017). Tephrochronology. In A.S. Gilbert (Ed.), *Encyclopedia of Geoarchaeology* (pp. 972–978). Dordrecht: Springer, Netherlands. doi: [https://doi.org/10.1007/978-1-4020-4409-0\\_185](https://doi.org/10.1007/978-1-4020-4409-0_185).

- Lanzarone, P., Seidel, M., Brandt, S., Garrison, E., and Fisher, E. (2019). Ground-penetrating radar and electrical resistivity tomography reveal a deep stratigraphic sequence at Mochena Borago Rockshelter, southwestern Ethiopia. *Journal of Archaeological Science: Reports* 26, 101915. doi: <https://doi.org/10.1016/j.jasrep.2019.101915>.
- Laskar, J., Robutel, P., Joutel, F., Gastineau, M., Correia, A.C.M., and Levrard, B. (2004). A long-term numerical solution for the insolation quantities of the Earth. *Astronomy & Astrophysics* 428(1), 261–285. doi: <https://doi.org/10.1051/0004-6361:20041335>.
- Lambrecht, G., Rodríguez de Vera, C., Jambrina-Enríquez, M., Crevecœur, I., Gonzalez-Urquijo, J., Lazuen, T., et al. (2021). Characterisation of charred organic matter in micromorphological thin sections by means of Raman spectroscopy. *Archaeological and Anthropological Sciences* 13(1), 13. doi: <https://doi.org/10.1007/s12520-020-01263-3>.
- Le Borgne, E. (1955). Susceptibilité magnétique anormale du sol superficiel. *Annals of Geophysics* 11, 399–419.
- Lehndorff, E., Linstädter, J., Kehl, M., and Weniger, G.C. (2015). Fire history reconstruction from Black Carbon analysis in Holocene cave sediments at Ifri Oudadane, Northeastern Morocco. *The Holocene* 25(2), 398–402. doi: <https://doi.org/10.1177/0959683614558651>.
- Leplongeon, A. (2021). Northeastern African Stone Age. Oxford University Press. *Oxford Research Encyclopedia of Anthropology*. doi: <https://doi.org/10.1093/acrefore/9780190854584.013.563>.
- Litt, T., Richter, J., and Schäbitz, F. (2021). *The Journey of Modern Humans from Africa to Europe. Culture-Environmental Interaction and Mobility*. Stuttgart: Schweizerbart, Germany.
- Machado, M.J. (2015). Geomorphology of the Adwa District. In P. Billi. (Ed.), *Landscapes and Landforms of Ethiopia* (pp. 163–178). Dordrecht: Springer Netherlands. doi: [https://doi.org/10.1007/978-94-017-8026-1\\_8](https://doi.org/10.1007/978-94-017-8026-1_8).
- Mallol, C., and Goldberg, P. (2017). Cave and rock shelter sediments. In: C. Nicosia and G. Stoops (Eds.), *Archaeological soil and sediment micromorphology* (pp. 359–381). Chichester: John Wiley & Sons, UK. doi: <https://doi.org/10.1002/9781118941065.ch34>.
- Mallol, C., Mentzer, S.M., and Miller, C.E. (2017). Combustion features. In: C. Nicosia and G. Stoops (Eds.), *Archaeological soil and sediment micromorphology* (pp. 299–330). Chichester: John Wiley & Sons, UK. doi: <https://doi.org/10.1002/9781118941065.ch31>.
- Mallol, C., and Mentzer, S.M. (2017). Contacts under the lens: Perspectives on the role of microstratigraphy in archaeological research. *Archaeological and Anthropological Sciences* 9(8), 1645–1669. doi: <https://doi.org/10.1007/s12520-015-0288-6>.
- Masiello, C.A., and Druffel, E.R.M. (1998). Black Carbon in Deep-Sea Sediments. *Science* 280(5371), 1911–1913. doi: <https://doi.org/10.1126/science.280.5371.1911>.
- Marcelino, V., Schaefer, C.E.G.R., and Stoops, G. (2018). Oxic and Related Materials. In G. Stoops, V. Marcelino, and F. Mees (Eds.), *Interpretation of Micromorphological Features of Soils and Regoliths (Second)* (pp. 663–689). Amsterdam: Elsevier, Netherlands. doi: <https://doi.org/10.1016/B978-0-444-63522-8.00023-1>.
- Marean, C.W., Bar-Matthews, M., Fisher, E., Goldberg, P., Herries, A., Karkanas, P., et al. (2010). The stratigraphy of the Middle Stone Age sediments at Pinnacle Point Cave 13B (Mossel Bay, Western Cape Province, South Africa). *Journal of Human Evolution* 59(3-4), 234–255. doi: <https://doi.org/10.1016/j.jhevol.2010.07.007>.
- Mark, B.G., and Osmaton, H.A. (2008). Quaternary glaciation in Africa: key chronologies and climatic implications. *Journal of Quaternary Science* 23, 589–608. doi: <https://doi.org/10.1002/jqs.1222>.

- Markl, G. (2008). *Minerale und Gesteine*. Heidelberg: Springer, Germany.
- Mather, T.A., Allen, A.G., Oppenheimer, C., Pyle, D.M., and McGonigle, A.J.S. (2003). Size-Resolved Characterisation of Soluble Ions in the Particles in the Tropospheric Plume of Masaya Volcano, Nicaragua: Origins and Plume Processing. *Journal of Atmospheric Chemistry* 46(3), 207–237. doi: <https://doi.org/10.1023/A:1026327502060>.
- McDougall, I., Brown, F.H., and Fleagle, J.G. (2005). Stratigraphic placement and age of modern humans from Kibish, Ethiopia. *Nature* 433(7027), 733–736. doi: <https://doi.org/10.1038/nature03258>.
- Mentzer, S.M. (2014). Microarchaeological Approaches to the Identification and Interpretation of Combustion Features in Prehistoric Archaeological Sites. *Journal of Archaeological Method and Theory* 21, 616–668. doi: <http://doi.org/10.1007/s10816-012-9163-2>.
- Mentzer, S.M. (2017). Rockshelter Settings. In A.S. Gilbert (Ed.), *Encyclopedia of Geoarchaeology* (pp. 725–743). Dordrecht: Springer Netherlands. doi: [https://doi.org/10.1007/978-1-4020-4409-0\\_159](https://doi.org/10.1007/978-1-4020-4409-0_159)
- Miller, C.E. (2015). *A tale of two Swabian caves: Geoarchaeological investigations at Hohle Fels and Geißenklösterle*. Tübingen: Kerns Verlag, Germany.
- Miller, C.E., Goldberg, P., and Berna, F. (2013). Geoarchaeological investigations at Diepkloof rock shelter, western Cape, South Africa. *Journal of Archaeological Science* 40(9), 3432–3452. doi: <http://doi.org/10.1016/j.jas.2013.02.014>.
- Mirazón Lahr, M. (2013). Why East Africa could be driving human evolution? <http://www.in-africa.org/origins-2/why-east-africa/>, Accessed August 2022.
- Mirazón Lahr, M., and Foley, R.A. (2016). Human Evolution in Late Quaternary Eastern Africa. In S.C. Jones and B.A. Stewart (Eds.), *Africa from MIS 6-2: Population Dynamics and Paleoenvironments* (pp. 215–231). Dordrecht: Springer, Netherlands. doi: [https://doi.org/10.1007/978-94-017-7520-5\\_12](https://doi.org/10.1007/978-94-017-7520-5_12).
- Mörchen, R., Lehndorff, E., Diaz, F.A., Moradi, G., Bol, R., Fuentes, B., et al. (2019). Carbon accrual in the Atacama Desert. *Global and Planetary Change* 181, 102993. doi: <https://doi.org/10.1016/j.gloplacha.2019.102993>.
- Morley, M.W., Goldberg, P., Uliyanov, V.A., Kozlikin, M.B., Shunkov, M.V., Derevianko, A.P., et al. (2019). Hominin and animal activities in the microstratigraphic record from Denisova Cave (Altai Mountains, Russia). *Scientific Reports* 9(1), 13785. doi: <http://doi.org/10.1038/s41598-019-49930-3>.
- Mukai, S. (2017). Gully Erosion Rates and Analysis of Determining Factors: A Case Study from the Semi-arid Main Ethiopian Rift Valley. *Land Degradation & Development* 28(2), 602–615. doi: <https://doi.org/10.1002/ldr.2532>.
- Nanson, G.C., and Croke, J.C. (1992). A genetic classification of floodplains. *Geomorphology* 4(6), 459–486. doi: [https://doi.org/10.1016/0169-555X\(92\)90039-Q](https://doi.org/10.1016/0169-555X(92)90039-Q).
- Neumann, K., Strömberg, C., Ball, T., Albert, R., Vrydaghs, L., and Scott Cummings, L. (2019). International Code for Phytolith Nomenclature (ICPN) 2.0. *Annals of Botany* 124, 189–199. doi: <http://doi.org/10.1093/aob/mcz064>.
- Nesbitt, H., and Young, G. (1982). Early Proterozoic climates and plate motions inferred from major element chemistry of lutites. *nature* 299(5885), 715–717. doi: <http://doi.org/10.1038/299715a0>.
- Nicholson, S.E. (2018). The ITCZ and the Seasonal Cycle over Equatorial Africa. *Bulletin of the American Meteorological Society* 99(2), 337–348. doi: <http://doi.org/10.1175/bams-d-16-0287.1>.

- Niespolo, E.M., WoldeGabriel, G., Hart, W.K., Renne, P.R., Sharp, W.D., Shackley, M.S., et al. (2021). Integrative geochronology calibrates the Middle and Late Stone Ages of Ethiopia's Afar Rift. *Proceedings of the National Academy of Sciences* 118(50), e2116329118. doi: <http://doi.org/10.1073/pnas.2116329118>.
- Nyssen, J., Poesen, J., Lanckriet, S., Jacob, M., Moeyersons, J., Haile, M., et al. (2015). Land Degradation in the Ethiopian Highlands. In P. Billi (Ed.), *Landscapes and Landforms of Ethiopia* (pp. 369–385). Dordrecht: Springer, Netherlands. doi: [https://doi.org/10.1007/978-94-017-8026-1\\_21](https://doi.org/10.1007/978-94-017-8026-1_21).
- Okrusch, M., and Matthes, S. (2010). *Mineralogie*. Berlin: Springer-Verlag, Germany.
- Ossendorf, G., Groos, A.R., Bromm, T., Tekelemariam, M.G., Glaser, B., Lesur, J., et al. (2019). Middle Stone Age foragers resided in high elevations of the glaciated Bale Mountains, Ethiopia. *Science* 365(6453), 583–587. doi: <http://doi.org/10.1126/science.aaw8942>.
- Parfitt, R.L. (2009). Allophane and imogolite: role in soil biogeochemical processes. *Clay Minerals* 44(1), 135–155. doi: <http://doi.org/10.1180/claymin.2009.044.1.135>.
- Parfitt, R.L., Furkert, R.J. and Henmi, T. (1980). Identification and structure of two types of allophane from volcanic ash soils and tephra. *Clays and Clay Minerals* 28(5), 328–334. doi: <http://doi.org/10.1346/CCMN.1980.0280502>.
- Parfitt, R.L. and Henmi, T. (1982). Comparison of an oxalate-extraction method and an infrared spectroscopic method for determining allophane in soil clay. *Soil Science and Plant Nutrition* 28(2), 183–190. doi: <http://doi.org/10.1080/00380768.1982.10432435>.
- Parfitt, R.L. and Wilson, L.H. (1985). Estimation of allophane and Halloysite in three sequences of volcanic soils, New Zealand. *Catena Supplement*, 1–8.
- Parr, J.F. (2006). Effect of fire on phytolith coloration. *Geoarchaeology* 21(2), 171–185. doi: <https://doi.org/10.1002/gea.20102>.
- Piperno, D.R. (2006). *Phytoliths: a comprehensive guide for archaeologists and paleoecologists*. Rowman Altamira Press: Lanham, MD, USA.
- Pleurdeau, D., Hovers, E., Assefa, Z., Asrat, A., Pearson, O., Bahain, J.-J., et al. (2014). Cultural change or continuity in the late MSA/Early LSA of southeastern Ethiopia? The site of Goda Buticha, Dire Dawa area. *Quaternary International* 343, 117–135. doi: <https://doi.org/10.1016/j.quaint.2014.02.001>.
- Poti, A., Kehl, M., Broich, M., Marco, Y.C., Hutterer, R., Jentke, T., et al. (2019). Human occupation and environmental change in the western Maghreb during the Last Glacial Maximum (LGM) and the Late Glacial. New evidence from the Iberomaurusian site Ifri El Baroud (northeast Morocco). *Quaternary Science Review* 220, 87–110. doi: <https://doi.org/10.1016/j.quascirev.2019.07.013>.
- Rademaker, K., Hodgins, G., Moore, K., Zarrillo, S., Miller, C., Bromley, G.R.M., et al. (2014). Paleoindian settlement of the high-altitude Peruvian Andes. *Science* 346, 6208, 466–469. doi: <http://doi.org/10.1126/science.1258260>.
- Ramsey, C.B., Scott, E.M., and van der Plicht, J. (2013). Calibration for Archaeological and Environmental Terrestrial Samples in the Time Range 26–50 ka cal BP. *Radiocarbon* 55(4), 2021–2027. doi: [http://doi.org/10.2458/azu\\_js\\_rc.55.16935](http://doi.org/10.2458/azu_js_rc.55.16935).
- Rapp, G. (2009) Lithic Materials. In G. Rapp (Ed.), *Archaeomineralogy, Natural Science in Archaeology* (pp. 60–90). Berlin, Heidelberg: Springer. doi: <https://doi.org/10.1007/978-3-540-78594-1>.

- Reimer, P.J., Bard, E., Bayliss, A., Beck, J.W., Blackwell, P.G., Ramsey, C.B., et al. (2013). IntCal13 and Marine13 Radiocarbon Age Calibration Curves 0–50,000 Years cal BP. *Radiocarbon* 55(4), 1869–1887. doi: [http://doi.org/10.2458/azu\\_js\\_rc.55.16947](http://doi.org/10.2458/azu_js_rc.55.16947).
- Reimer, P.J., Austin, W.E., Bard, E., Bayliss, A., Blackwell, P.G., Ramsey, C.B., et al. (2020). The IntCal20 Northern Hemisphere radiocarbon age calibration curve (0–55 cal kBP). *Radiocarbon*, 1–33. doi: <http://doi.org/10.1017/RDC.2020.41>.
- Rennert, T. (2019). Wet-chemical extractions to characterise pedogenic Al and Fe species – a critical review. *Soil Research* 57, 1–16. doi: <https://doi.org/10.1071/SR18299>.
- Roberts, H.M., Ramsey, C.B., Chapot, M.S., Deino, A.L., Lane, C.S., Vidal, C., et al. (2021). Using multiple chronometers to establish a long, directly-dated lacustrine record: Constraining >600,000 years of environmental change at Chew Bahir, Ethiopia. *Quaternary Science Reviews* 266, 107025. doi: <https://doi.org/10.1016/j.quascirev.2021.107025>.
- Rodríguez-Rodríguez, A., Fedoroff, N., Tejedor Salguero, M.L. and Fernández-Caldas, E., (1980). Observaciones preliminares sobre la alteracion en los suelos fersialíticos sobre materiales volcanicos (Islas Canarias). *Anales de Edafologia y Agrobiologia* 39, 1923–1940.
- Röpke, A., and Dietl, C. (2017). Burnt soils and sediments. In C. Nicosia. and G. Stoops (Eds.), *Archaeological soil and sediment micromorphology* (pp. 173–180). Chichester: John Wiley & Sons, Ltd., UK. doi: <https://doi.org/10.1002/9781118941065.ch21>.
- Sagri, M., Bartolini, C., Billi, P., Ferrari, G., Benvenuti, M., Carnicelli, S., et al. (2008). Latest Pleistocene and Holocene river network evolution in the Ethiopian Lakes Region. *Geomorphology* 94(1–2), 79–97. doi: <https://doi.org/10.1016/j.geomorph.2007.05.010>.
- Scerri, E., Chikhi, L., and Thomas, M. (2019). Beyond multiregional and simple out-of-Africa models of human evolution. *Nature Ecology & Evolution* 3, 1–3. doi: <https://doi.org/10.1038/s41559-019-0992-1>.
- Schaebitz, F., Asrat, A., Lamb, H.F., Cohen, A.S., Foerster, V., Duesing, W., et al. (2021). Hydroclimate changes in eastern Africa over the past 200,000 years may have influenced early human dispersal. *Communications Earth & Environment* 2(1), 123. doi: <https://doi.org/10.1038/s43247-021-00195-7>.
- Schaebitz, F., Lamb, H.F., Asrat, A., Trauth, M.H., Vogelsang, R., Viehberg, F.A. and Foerster, V. (2021b): Ethiopian lakes as paleoenvironmental and palaeoclimate archives. In: T. Litt, J. Richter, and F. Schaebitz (Eds.), *The Journey of Modern Humans from Africa to Europe. Culture-Environmental interaction and Mobility* (pp. 14–21). Stuttgart: Schweizerbart, Germany.
- Schepers, C., Lesur, J., and Vogelsang, R. (2020). Hunter-gatherers of the high-altitude Afromontane forest – the Holocene occupation of Mount Dendi, Ethiopia. *Azania: Archaeological Research in Africa* 55(3), 329–359. doi: <https://doi.org/10.1080/0067270X.2020.1792709>.
- Schneider, M.P.W., Hilf, M., Vogt, U.F., and Schmidt, M.W.I. (2010). The benzene polycarboxylic acid (BPCA) pattern of wood pyrolyzed between 200°C and 1000°C. *Organic Geochemistry* 41(10), 1082–1088. doi: <https://doi.org/10.1016/j.orggeochem.2010.07.001>.
- Schmidt, M.W.I., and Noack, A.G. (2000). Black carbon in soils and sediments: Analysis, distribution, implications, and current challenges. *Global Biogeochemical Cycles* 14(3), 777–793. doi: <https://doi.org/10.1029/1999GB001208>.
- Schütt, B., Thiemann, S., and Wenclawiak, B. (2005). Deposition of modern fluvio-lacustrine sediments in Lake Abaya, South Ethiopia-A case study from the delta areas of Bilate River and Gidabo River, northern basin. *Zeitschrift für Geomorphologie, Supplementband* 138, 131–151.

- Schwertmann, U. (1970). Der Einfluss einfacher organischer anionen auf die Bildung von Goethit und Hämatit aus amorphen Fe (III)-hydroxid. *Geoderma* 3(3), 207–214. doi: [https://doi.org/10.1016/0016-7061\(70\)90020-0](https://doi.org/10.1016/0016-7061(70)90020-0).
- Scott A.C. (2000). Pre-Quaternary history of fire. *Palaeogeography, Palaeoclimatology, Palaeoecology* 164, 297–345. doi: [https://doi.org/10.1016/S0031-0182\(00\)00192-9](https://doi.org/10.1016/S0031-0182(00)00192-9).
- Scott, A.C., and Glasspool, I.J. (2006). The diversification of Paleozoic fire systems and fluctuations in atmospheric oxygen concentration. *Proceedings of the National Academy of Sciences* 103(29), 10861–10865. doi: <https://doi.org/10.1073/pnas.0604090103>.
- Segele, Z.T., and Lamb, P.J. (2005). Characterization and variability of Kiremt rainy season over Ethiopia. *Meteorology and Atmospheric Physics* 89(1), 153–180. doi: 10.1007/s00703-005-0127-x.
- Segele, Z.T., Lamb, P.J., and Leslie, L.M. (2009). Large-scale atmospheric circulation and global sea surface temperature associations with Horn of Africa June–September rainfall. *International Journal of Climatology: A Journal of the Royal Meteorological Society* 29(8), 1075–1100. doi: <https://doi.org/10.1002/joc.1751>.
- Shafer, H. J. (2016). Research design and sampling techniques. In T.R. Hester, H.J. Schäfer and K.I. Feder (Eds.), *Field Methods in Archaeology* (pp. 21–40). Routledge: Oxford, England, UK.
- Siart, C., Forbriger, M., and Bubbenzer, O. (2018). Digital Geoarchaeology: Bridging the Gap Between Archaeology, Geosciences and Computer Sciences. In C. Siart, M. Forbriger and O. Bubbenzer (Eds.), *Digital Geoarchaeology: New Techniques for Interdisciplinary Human-Environmental Research* (pp. 1–7). Cham: Springer International Publishing, Switzerland. doi: [https://doi.org/10.1007/978-3-319-25316-9\\_1](https://doi.org/10.1007/978-3-319-25316-9_1).
- Stewart, B.A., and Jones, S.C. (2016). Africa from MIS 6-2: The Florescence of Modern Humans. In S.C. Jones and B.A. Stewart (Eds.), *Africa from MIS 6-2: Population Dynamics and Paleoenvironments* (pp. 1–20). Dordrecht: Springer, Netherlands. doi: [https://doi.org/10.1007/978-94-017-7520-5\\_1](https://doi.org/10.1007/978-94-017-7520-5_1).
- Stewart, J.R., and Stringer, C.B. (2012). Human Evolution Out of Africa: The Role of Refugia and Climate Change. *Science* 335(6074), 1317–1321. doi: <https://doi.org/10.1126/science.1215627>.
- Stoops, G. (2021). *Guidelines for analysis and description of soil and regolith thin sections*. John Wiley & Sons.
- Stoops, G. and Nicosia C. (2017). Introduction. In: C. Nicosia and G. Stoops (Eds.), *Archaeological soil and sediment micromorphology* (pp. 1–5). Chichester: John Wiley & Sons, Ltd., UK. doi: <https://doi.org/10.1002/9781118941065.ch0>.
- Stoops, G. and Marcelino, V., (2018). Lateritic and bauxitic materials. In G. Stoops, V. Marcelino and F. Mees (Eds.), *Interpretation of Micromorphological Features of Soils and Regoliths (Second)* (pp. 691–720). Amsterdam: Elsevier, Netherlands; Oxford, UK. doi: <https://doi.org/10.1016/B978-0-444-63522-8.00024-3>.
- Stoops, G., and Mees, F. (2018). Groundmass Composition and Fabric. In G. Stoops, V. Marcelino and F. Mees (Eds.), *Interpretation of Micromorphological Features of Soils and Regoliths (Second)* (pp. 73–125). Amsterdam: Elsevier, Netherlands; Oxford, UK. doi: <https://doi.org/10.1016/B978-0-444-63522-8.00005-X>.
- Stoops, G.; Sedov, S.; Shoba, S. (2018). Regoliths and Soils on Volcanic Ash. In G. Stoops, V. Marcelino and F. Mees (Eds.), *Interpretation of Micromorphological Features of Soils and Regoliths (Second)* (pp. 721–751). Amsterdam: Elsevier, Netherlands; Oxford, UK. doi: <https://doi.org/10.1016/B978-0-444-53156-8.00013-1>.

- Tamm, O. (1932). Über die Oxalatmethode in der Chemischen Bodenanalyse. *Med. följer Skogsvårdsföreningens Tidskrift. Häfte 27*, 1–20.
- Tarasenko, I., Bielders, C.L., Guevara, A., and Delmelle, P. (2019). Surface crusting of volcanic ash deposits under simulated rainfall. *Bulletin of Volcanology* 81(5), 30. doi: <https://doi.org/10.1007/s00445-019-1289-6>.
- Texier, P.-J., Porraz, G., Parkington, J., Rigaud, J.-P., Poggenpoel, C., Miller, C., et al. (2010). A Howiesons Poort tradition of engraving ostrich eggshell containers dated to 60,000 years ago at Diepkloof Rock Shelter, South Africa. *Proceedings of the National Academy of Sciences* 107(14), 6180–6185. doi: <https://doi.org/10.1073/pnas.0913047107>.
- Tierney, J.E., Russell, J.M., Huang, Y., Damsté, J.S.S., Hopmans, E.C., and Cohen, A.S. (2008). Northern Hemisphere Controls on Tropical Southeast African Climate During the Past 60,000 Years. *Science* 322(5899), 252–255. doi: <https://doi.org/10.1126/science.1160485>.
- Tierney, J.E., Lewis, S.C., Cook, B.I., LeGrande, A.N., and Schmidt, G.A. (2011). Model, proxy and isotopic perspectives on the East African Humid Period. *Earth and Planetary Science Letters* 307(1-2), 103–112.
- Trauth, M.H., Asrat, A., Duesing, W., Foerster, V., Kraemer, K.H., Marwan, N., et al. (2019). Classifying past climate change in the Chew Bahir basin, southern Ethiopia, using recurrence quantification analysis. *Climate Dynamics* 53(5-6), 2557–2572. doi: <https://doi.org/10.1007/s00382-019-04641-3>.
- Tribolo, C., Asrat, A., Bahain, J.J., Chapon, C., Douville, E., Fragnol, C., et al. (2017). Across the Gap: Geochronological and Sedimentological Analyses from the Late Pleistocene-Holocene Sequence of Goda Buticha, Southeastern Ethiopia. *PLOS One* 12(1), e0169418. doi: <https://doi.org/10.1371/journal.pone.0169418>.
- Vallejo Orti, M., Negussie, K., Corral-Pazos-de-Provens, E., Höfle, B., and Bubenzer, O. (2019). Comparison of Three Algorithms for the Evaluation of TanDEM-X Data for Gully Detection in Krumhuk Farm (Namibia). *Remote Sensing* 11(11), 1327. doi: <https://doi.org/10.3390/rs11111327>.
- Van den Hende, C., Van Schaeuybroeck, B., Nyssen, J., Van Vooren, S., Van Ginderachter, M., and Termonia, P. (2021). Analysis of rain-shadows in the Ethiopian Mountains using climatological model data. *Climate Dynamics* 56(5), 1663–1679. doi: <https://doi.org/10.1007/s00382-020-05554-2>.
- Vepraskas, M.J., Lindbo, D.L., and Stolt, M.H. (2018). Redoximorphic Features. In G. Stoops, V. Marcelino and F. Mees (Eds.), *Interpretation of Micromorphological Features of Soils and Regoliths (Second)* (pp. 425–445). Amsterdam: Elsevier, Netherlands; Oxford, UK. doi: <https://doi.org/10.1016/B978-0-444-63522-8.00015-2>.
- Villagran, X., Balbo, A., Madella, M., Vila, A., and Estévez Escalera, J. (2010). Experimental Micromorphology in Tierra del Fuego (Argentina): building a reference collection for the study of shell middens in cold climates. *Journal of Archaeological Science* 38, 604–588. doi: <https://doi.org/10.1016/j.jas.2010.10.013>.
- Viste, E., and Sorteberg, A. (2013). Moisture transport into the Ethiopian highlands. *International Journal of Climatology* 33(1), 249–263. doi: <https://doi.org/10.1002/joc.3409>.
- Vogelsang, R., and Wendt, K.P. (2018). Reconstructing prehistoric settlement models and land use patterns on Mt. Damota/SW Ethiopia. *Quaternary International* 485, 140–149. doi: <https://doi.org/10.1016/j.quaint.2017.06.061>.
- Vogelsang, R., Bubenzer, O., Kehl, M., Meyer, S., Richter, J., and Zinaye, B. (2018). When Hominins Conquered Highlands—an Acheulean Site at 3000 m a.s.l. on Mount Dendi/Ethiopia. *Journal of Paleolithic Archaeology* 1(4), 302–313. doi: <https://doi.org/10.1007/s41982-018-0015-9>.

- Vogelsang (2021). The role of tropical highlands in the dispersal of *Homo sapiens*. In: T. Litt, J. Richter, and F. Schaebitz (Eds.), *The Journey of Modern Humans from Africa to Europe. Culture-Environmental interaction and Mobility* (pp. 14–21). Stuttgart: Schweizerbart, Germany.
- Vrydaghs, L., Devos, Y., and Petó, Á. (2017). Opal phytoliths. In C. Nicosia and G. Stoops (Eds.), *Archaeological soil and sediment micromorphology* (pp. 155–163). Chichester: John Wiley & Sons Ltd., UK. doi: <https://doi.org/10.1002/9781118941065.ch18>.
- Waters, M.R. (1992). *Principles of geoarchaeology: A North American perspective*. University of Arizona Press.
- Whitau, R., Vannieuwenhuysse, D., Dotte-Sarout, E. et al. (2018). Home Is Where the Hearth Is: Anthracological and micromorphological Analyses of Pleistocene, Riwi Cave (Komberley, Western Australia). *Journal of Archaeological Method and Theory* 25, 739–776. doi: <https://doi.org/10.1007/s10816-017-9354-y>.
- White, T.D., Asfaw, B., DeGusta, D., Gilbert, H., Richards, G.D., Suwa, G., et al. (2003). Pleistocene *Homo sapiens* from Middle Awash, Ethiopia. *Nature* 423(6941), 742–747. doi: <https://doi.org/10.1038/nature01669>.
- Williams, G.T., Jenkins, S.F., Lee, D.W.J., and Wee, S.J. (2021). How rainfall influences tephra fall loading—an experimental approach. *Bulletin of Volcanology* 83(6), 42. doi: <https://doi.org/10.1007/s00445-021-01465-0>.
- Willmes, C., Becker, D., Brocks, S., Hütt, C., and Bareth, G. (2017). High Resolution Köppen-Geiger Classifications of Paleoclimate Simulations. *Transactions in GIS* 21(1), 57–73. doi: <https://doi.org/10.1111/tgis.12187>.
- Wolf, M., Lehndorff, E., Stockhausen, M., Schwark, L., and Amelung, W. (2013). Towards reconstruction of past fire regimes from geochemical analysis of charcoal. *Organic Geochemistry* 55, 11–21. doi: <https://doi.org/10.1016/j.orggeochem.2012.11.002>.
- Wolf, M., Lehndorff, E., Mrowald, M., Eckmeier, E., Kehl, M., Frechen, M., et al. (2014). Black carbon: Fire fingerprints in Pleistocene loess–palaeosol archives in Germany. *Organic Geochemistry* 70, 44–52. doi: <https://doi.org/10.1016/j.orggeochem.2014.03.002>.
- WoldeGabriel, G., Aronson, J.L., and Walter, R.C. (1990). Geology, geochronology, and rift basin development in the central sector of the Main Ethiopia Rift. *Geological Society of America Bulletin* 102(4), 439–458. doi: [https://doi.org/10.1130/0016-7606\(1990\)102<0439:GGARBD>2.3.CO;2](https://doi.org/10.1130/0016-7606(1990)102<0439:GGARBD>2.3.CO;2)
- WoldeGabriel, G., Walter, R.C., Aronson, J.L., and Hart, W.K. (1992). Geochronology and distribution of silicic volcanic rocks of Plio-Pleistocene age from the central sector of the Main Ethiopian Rift. *Quaternary International* 13, 69–76. doi: [https://doi.org/10.1016/1040-6182\(92\)90011-P](https://doi.org/10.1016/1040-6182(92)90011-P).
- Wright, D.K. (2017). Humans as Agents in the Termination of the African Humid Period. *Frontiers in Earth Science* 5(4). doi: <https://doi.org/10.3389/feart.2017.00004>.
- Xiao, J., Zhang, S., Fan, J., Wen, R., Zhai, D., Tian, Z., et al. (2018). The 4.2 ka BP event: multi-proxy records from a closed lake in the northern margin of the East Asian summer monsoon. *Climate of the Past* 14(10), 1417–1425. doi: <https://doi.org/10.5194/cp-14-1417-2018>.
- Yeshitela, K., and Bekele, T. (2002). Plant community analysis and ecology of Afromontane and transitional rainforest vegetation of southwestern Ethiopia. *SINET: Ethiopian Journal of Science*, 25(2), 155–175. doi: <https://doi.org/10.4314/sinet.v25i2.18078>.

- Zepner, L., Karrasch, P., Wiemann, F., and Bernard, L. (2021). ClimateCharts.net – an interactive climate analysis web platform. *International Journal of Digital Earth* 14(3), 338–356. doi: <https://doi.org/10.1080/17538947.2020.1829112>.

## Appendix A

### Sample and method overview

The following tables contain a brief summary of laboratory methodologies and their frequencies, performed on bulk sediment samples from the Sodicho Rockshelter. For the technical requirements and information on sample preparation, the reader is referred to Chapter 1.5. The following abbreviations are used in the table:

Sqm	Excavation square
Qsqm	Quarter square within excavation square
Depth	field depth in m b.s.
Sample ID	Major sample identification number
GS H <sub>2</sub> O <sub>2</sub>	Grain size analyses with hydrochloric acid (HCl 10 %) pretreatment
GS H <sub>2</sub> O <sub>2</sub> , HCl	Grain size analyses with hydrogen peroxide (H <sub>2</sub> O <sub>2</sub> 15 %) and hydrochloric acid (HCl 10 %) pretreatment
Spec CM-5	Sediment color determination with VIS spectrophotometer (Konica Minolta, CM-5)
TC	Total carbon content determination (Elementar Analysensysteme GmbH, vario EL cube)
TOC	Total organic carbon determination (pretreatment with HCl 10 %) (Elementar Analysensysteme GmbH, vario EL cube)
MS	Mass specific magnetic susceptibility measurement (Bartington MS2)
XRF XL3t	X-ray fluorescence determination (Thermo Scientific, handheld Niton™ XL3t XRF Analyzer)
XRF Spectro	X-ray fluorescence determination (Spectro, SPECTRO XEPOS)
Phy.	Phytolith analyses, determination of ratio (analyzed at the University of Frankfurt)
AO	Determination of active Fe, Si, Al, and Mn in an acidified ammonium oxalate extract

Table A 1: Summary of applied laboratory methods on the bulk sediment samples from profile F35 SW. Samples that were measured and included in the results of this doctoral thesis are marked with an X.

Spm	Qsmq	Depth [m b.s.]	Sample ID	GS H <sub>2</sub> O <sub>2</sub>	GS H <sub>2</sub> O <sub>2</sub> , HCl	Spec CM-5	TC	TOC	MS	XRF XL3t	XRF Spectro	Phy.	AO
F35	SW	0.01	SOD_SE_01	X	X	2X	X	X	2X	X	X		
F35	SW	0.03	SOD_SE_02	X		2X	X		2X	X		X	
F35	SW	0.06	SOD_SE_03	X	X	2X	X		2X	X	X		X
F35	SW	0.09	SOD_SE_04	X		2X	X		2X	X			
F35	SW	0.11	SOD_SE_05	X	X	2X	X	X	2X	X	X		
F35	SW	0.13	SOD_SE_06	X		2X	X		2X	X	X		
F35	SW	0.15	SOD_SE_07	X		2X	X		2X	X	X		X
F35	SW	0.17	SOD_SE_08	X		2X	X		2X	X			
F35	SW	0.19	SOD_SE_09	X	X	2X	X		2X	X	X		X
F35	SW	0.21	SOD_SE_10	X	X	2X	X	X	2X	X			
F35	SW	0.23	SOD_SE_11	X		2X	X		2X	X	X		
F35	SW	0.25	SOD_SE_12	X		2X	X		2X	X			
F35	SW	0.27	SOD_SE_13	X		2X	X		2X	X	X		
F35	SW	0.29	SOD_SE_14	X		2X	X		2X	X			
F35	SW	0.31	SOD_SE_15	X	X	2X	X	X	2X	X	X		X
F35	SW	0.33	SOD_SE_16	X		2X	X		2X	X			
F35	SW	0.35	SOD_SE_17	X		2X	X		2X	X	X		
F35	SW	0.37	SOD_SE_18	X		2X	X		2X	X		X	
F35	SW	0.39	SOD_SE_19	X		2X	X		2X	X	X		
F35	SW	0.41	SOD_SE_20	X	X	2X	X	X	2X	X			
F35	SW	0.43	SOD_SE_21	X		2X	X		2X	X	X		
F35	SW	0.45	SOD_SE_22	X		2X	X		2X	X			
F35	SW	0.47	SOD_SE_23	X	X	2X	X		2X	X	X		
F35	SW	0.49	SOD_SE_24	X		2X	X		2X	X			
F35	SW	0.51	SOD_SE_25	X	X	2X	X	X	2X	X	X	X	X
F35	SW	0.53	SOD_SE_26	X		2X	X		2X	X			
F35	SW	0.55	SOD_SE_27	X	X	2X	X		2X	X	X	X	
F35	SW	0.57	SOD_SE_28	X		2X	X		2X	X			
F35	SW	0.59	SOD_SE_29	X		2X	X		2X	X	X		X

Table A 2: Summary of applied laboratory methods on the bulk sediment samples from profile F35 SW; continuation of table A 1. Samples that were measured and included in the results of this doctoral thesis are marked with an X.

Spm	Qsmq	Depth [m b.s.]	Sample ID	GS H <sub>2</sub> O <sub>2</sub>	GS H <sub>2</sub> O <sub>2</sub> , HCl	Spec CM-5	TC	TOC	MS	XRF XL3t	XRF Spectro	Phy.	AO
F35	SW	0.61	SOD_SE_30	X	X	2X	X	X	2X	X			
F35	SW	0.63	SOD_SE_31	X		2X	X		2X	X	X	X	X
F35	SW	0.65	SOD_SE_32	X		2X	X		2X	X			
F35	SW	0.67	SOD_SE_33	X	X	2X	X		2X	X	X		
F35	SW	0.69	SOD_SE_34	X		2X	X		2X	X			
F35	SW	0.71	SOD_SE_35	X	X	2X	X	X	2X	X	X	X	
F35	SW	0.73	SOD_SE_36	X		2X	X		2X	X			X
F35	SW	0.75	SOD_SE_37	X	X	2X	X		2X	X	X		
F35	SW	0.77	SOD_SE_38	X		2X	X		2X	X			
F35	SW	0.79	SOD_SE_39	X		2X	X		2X	X		X	
F35	SW	0.81	SOD_SE_40	X	X	2X	X	X	2X	X	X		
F35	SW	0.83	SOD_SE_41	X		2X	X		2X	X			
F35	SW	0.85	SOD_SE_42	X		2X	X		2X	X			
F35	SW	0.87	SOD_SE_43	X	X	2X	X		2X	X			
F35	SW	0.89	SOD_SE_44	X		2X	X		2X	X		X	X
F35	SW	0.91	SOD_SE_45	X	X	2X	X	X	2X	X			
F35	SW	0.93	SOD_SE_46	X		2X	X		2X	X			
F35	SW	0.95	SOD_SE_47	X		2X	X		2X	X			
F35	SW	0.97	SOD_SE_48	X		2X	X		2X	X			
F35	SW	0.99	SOD_SE_49	X		2X	X		2X	X			
F35	SW	1.01	SOD_SE_50	X	X	2X	X	X	2X	X	X	X	
F35	SW	1.03	SOD_SE_51	X		2X	X		2X	X			X
F35	SW	1.05	SOD_SE_52	X		2X	X		2X	X			
F35	SW	1.07	SOD_SE_53	X	X	2X	X		2X	X			
F35	SW	1.09	SOD_SE_54	X		2X	X		2X	X			X
F35	SW	1.11	SOD_SE_55	X	X	2X	X	X	2X	X			
F35	SW	1.13	SOD_SE_56	X		2X	X		2X	X			
F35	SW	1.15	SOD_SE_57	X	X	2X	X		2X	X			
F35	SW	1.17	SOD_SE_58	X		2X	X		2X	X			

Table A 3: Summary of applied laboratory methods on the bulk sediment samples from profile F35 SW; continuation of table A 1. Samples that were measured and included in the results of this doctoral thesis are marked with an X.

Spm	Qsmq	Depth [m b.s.]	Sample ID	GS H <sub>2</sub> O <sub>2</sub>	GS H <sub>2</sub> O <sub>2</sub> , HCl	Spec CM-5	TC	TOC	MS	XRF XL3t	XRF Spectro	Phy.	AO
F35	SW	1.19	SOD_SE_59	X		2X	X		2X	X			
F35	SW	1.21	SOD_SE_60	X	X	2X	X	X	2X	X	X	X	
F35	SW	1.23	SOD_SE_61	X		2X	X		2X	X			X
F35	SW	1.25	SOD_SE_62	X		2X	X		2X	X			
F35	SW	1.26	SOD_SE_63	X	X	2X	X		2X	X			
F35	SW	1.29	SOD_SE_64	X		2X	X		2X	X			
F35	SW	1.31	SOD_SE_65	X	X	2X	X	X	2X	X			
F35	SW	1.33	SOD_SE_66	X		2X	X		2X	X			
F35	SW	1.35	SOD_SE_67	X	X	2X	X		2X	X			
F35	SW	1.37	SOD_SE_68	X		2X	X		2X	X			
F35	SW	1.38	SOD_SE_69	X		2X	X		2X	X			
F35	SW	1.41	SOD_SE_70	X	X	2X	X	X	2X	X	X		
F35	SW	1.43	SOD_SE_71	X		2X	X		2X	X		X	
F35	SW	1.45	SOD_SE_72	X		2X	X		2X	X			
F35	SW	1.47	SOD_SE_73	X	X	2X	X		2X	X			
F35	SW	1.49	SOD_SE_74	X		2X	X		2X	X			
F35	SW	1.51	SOD_SE_75	X	X	2X	X	X	2X	X			
F35	SW	1.53	SOD_SE_76	X		2X	X		2X	X			
F35	SW	1.55	SOD_SE_77	X	X	2X	X		2X	X			
F35	SW	1.57	SOD_SE_78	X		2X	X		2X	X			X
F35	SW	1.59	SOD_SE_79	X		2X	X		2X	X			
F35	SW	1.61	SOD_SE_80	X	X	2X	X	X	2X	X	X		
F35	SW	1.63	SOD_SE_81	X		2X	X		2X	X		X	
F35	SW	1.65	SOD_SE_82	X		2X	X		2X	X			
F35	SW	1.68	SOD_SE_83	X	X	2X	X		2X	X			X
F35	SW	1.72	SOD_SE_84	X		2X	X		2X	X			

Table A 4: Summary of applied laboratory methods on the bulk sediment samples from profile G35 SE. Samples that were measured and included in the results of this doctoral thesis are marked with an X.

Spm	Qsmq	Depth [m b.s.]	Sample ID	GS H <sub>2</sub> O <sub>2</sub>	GS H <sub>2</sub> O <sub>2</sub> , HCl	Spec CM-5	TC	TOC	MS	XRF XL3t	XRF Spectro	Phy.	AO
G35	SE	1.37	SOD_SE_85	X	X	2X	X	X	2X	X	X		
G35	SE	1.41	SOD_SE_86	X		2X	X		2X	X			X
G35	SE	1.44	SOD_SE_87	X	X	2X	X		2X	X	X	X	
G35	SE	1.46	SOD_SE_88	X		2X	X		2X	X			
G35	SE	1.48	SOD_SE_89	X	X	2X	X	X	2X	X	X		
G35	SE	1.50	SOD_SE_90	X		2X	X		2X	X			
G35	SE	1.52	SOD_SE_91	X		2X	X		2X	X			
G35	SE	1.54	SOD_SE_92	X		2X	X		2X	X			
G35	SE	1.56	SOD_SE_93	X	X	2X	X		2X	X	X		
G35	SE	1.58	SOD_SE_94	X		2X	X		2X	X			
G35	SE	1.60	SOD_SE_95	X	X	2X	X	X	2X	X	X		
G35	SE	1.62	SOD_SE_96	X		2X	X		2X	X		X	
G35	SE	1.64	SOD_SE_97	X	X	2X	X		2X	X			
G35	SE	1.66	SOD_SE_98	X		2X	X		2X	X			
G35	SE	1.69	SOD_SE_99	X		2X	X		2X	X	X		
G35	SE	1.73	SOD_SE_100	X	X	2X	X	X	2X	X			
G35	SE	1.76	SOD_SE_101	X		2X	X		2X	X			
G35	SE	1.78	SOD_SE_102	X		2X	X		2X	X			X
G35	SE	1.80	SOD_SE_103	X	X	2X	X		2X	X	X		
G35	SE	1.82	SOD_SE_104	X		2X	X		2X	X			
G35	SE	1.84	SOD_SE_105	X	X	2X	X	X	2X	X	X		
G35	SE	1.86	SOD_SE_106	X		2X	X		2X	X		X	
G35	SE	1.88	SOD_SE_107	X		2X	X		2X	X			
G35	SE	1.90	SOD_SE_108	X	X	2X	X		2X	X			
G35	SE	1.92	SOD_18_01	X	X	1x	X	X	2x	X	X		X
G35	SE	1.94	SOD_18_02	X		1x	X		2x	X			
G35	SE	1.96	SOD_18_03	X	X	1x	X		2x	X	X		
G35	SE	1.98	SOD_18_04	X		1x	X		2x	X			X
G35	SE	2.00	SOD_18_05	X	X	1x	X	X	2x	X	X		

Table A 5: Summary of applied laboratory methods on the bulk sediment samples from profile G35 SW; continuation of table A 4. Samples that were measured and included in the results of this doctoral thesis are marked with an X.

Spm	Qsmq	Depth [m b.s.]	Sample ID	GS H <sub>2</sub> O <sub>2</sub>	GS H <sub>2</sub> O <sub>2</sub> , HCl	Spec CM-5	TC	TOC	MS	XRF XL3t	XRF Spectro	Phy.	AO
G35	SE	2.02	SOD_18_06	X		1x	X		2x	X			
G35	SE	2.04	SOD_18_07	X	X	1x	X	X	2x	X	X	X	X

## Appendix B

### Stratigraphic position of the micromorphological samples

In the following the stratigraphic position of the micromorphological sample blocks and the thin sections analysed for this thesis are illustrated.

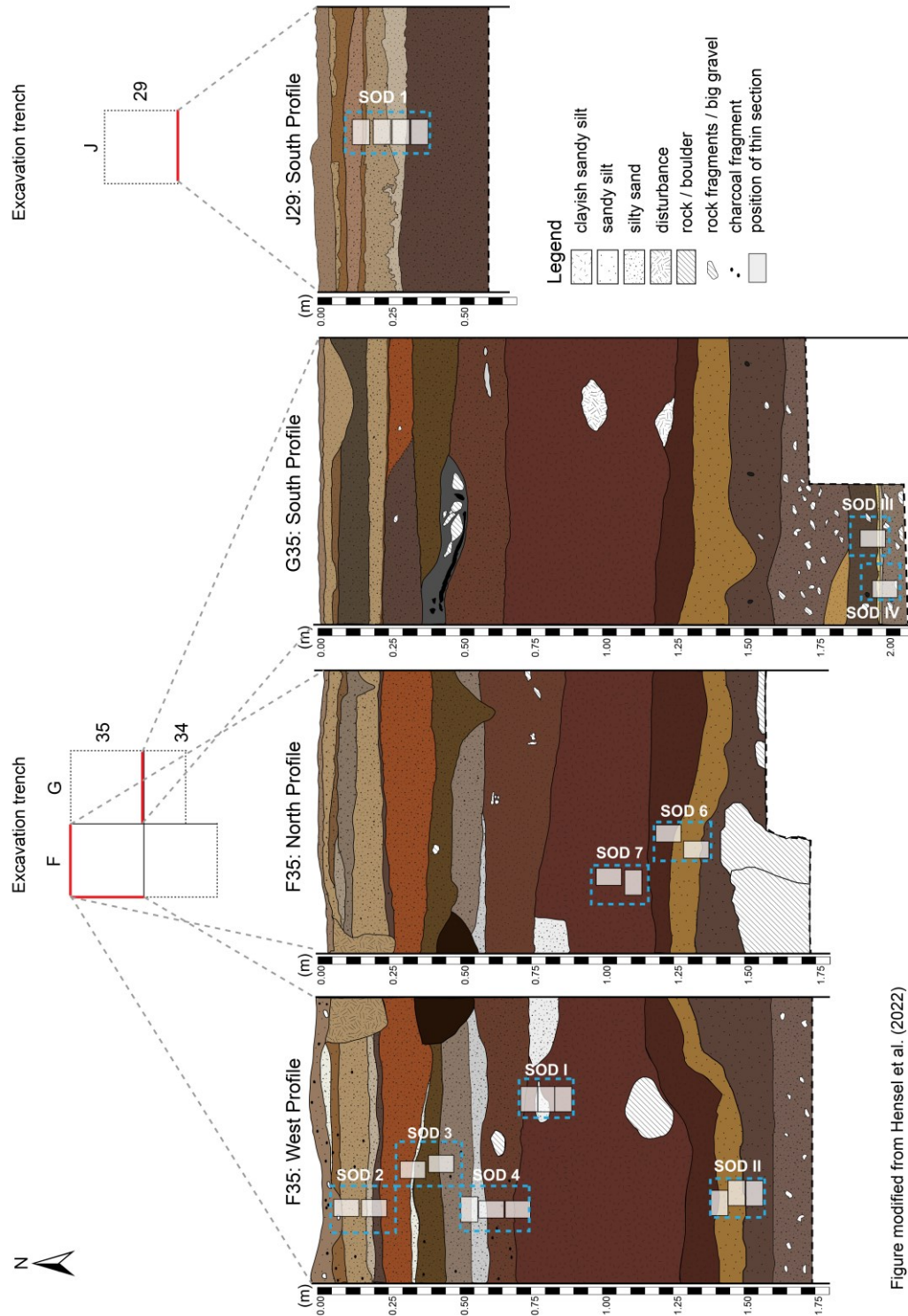


Figure modified from Hensel et al. (2022)

Figure A. 1 Schematic illustration of the excavation profiles F35 west and north, G35 south and J29 south. Blue blocks refer to micromorphological sample blocks and thin sections are indicated as whitish squares (mod. from Hensel et al. 2022).

### Micromorphological sample block SOD\_01

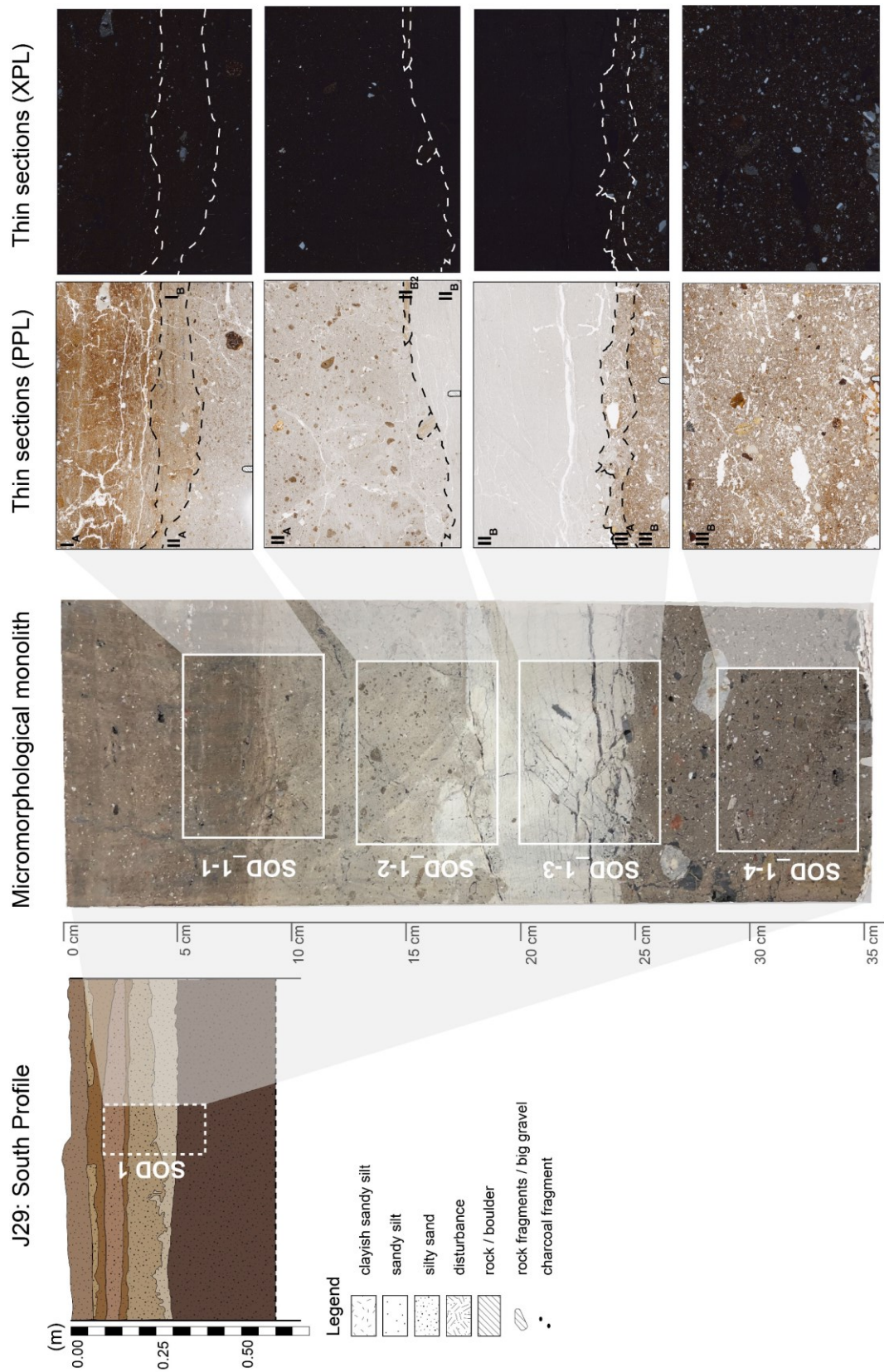


Figure A. 2 Schematic illustration of the micromorphological sample block SOD\_01, and the position of the thin sections (mod. from Hensel et al. 2022).

## Micromorphological sample block SOD\_02

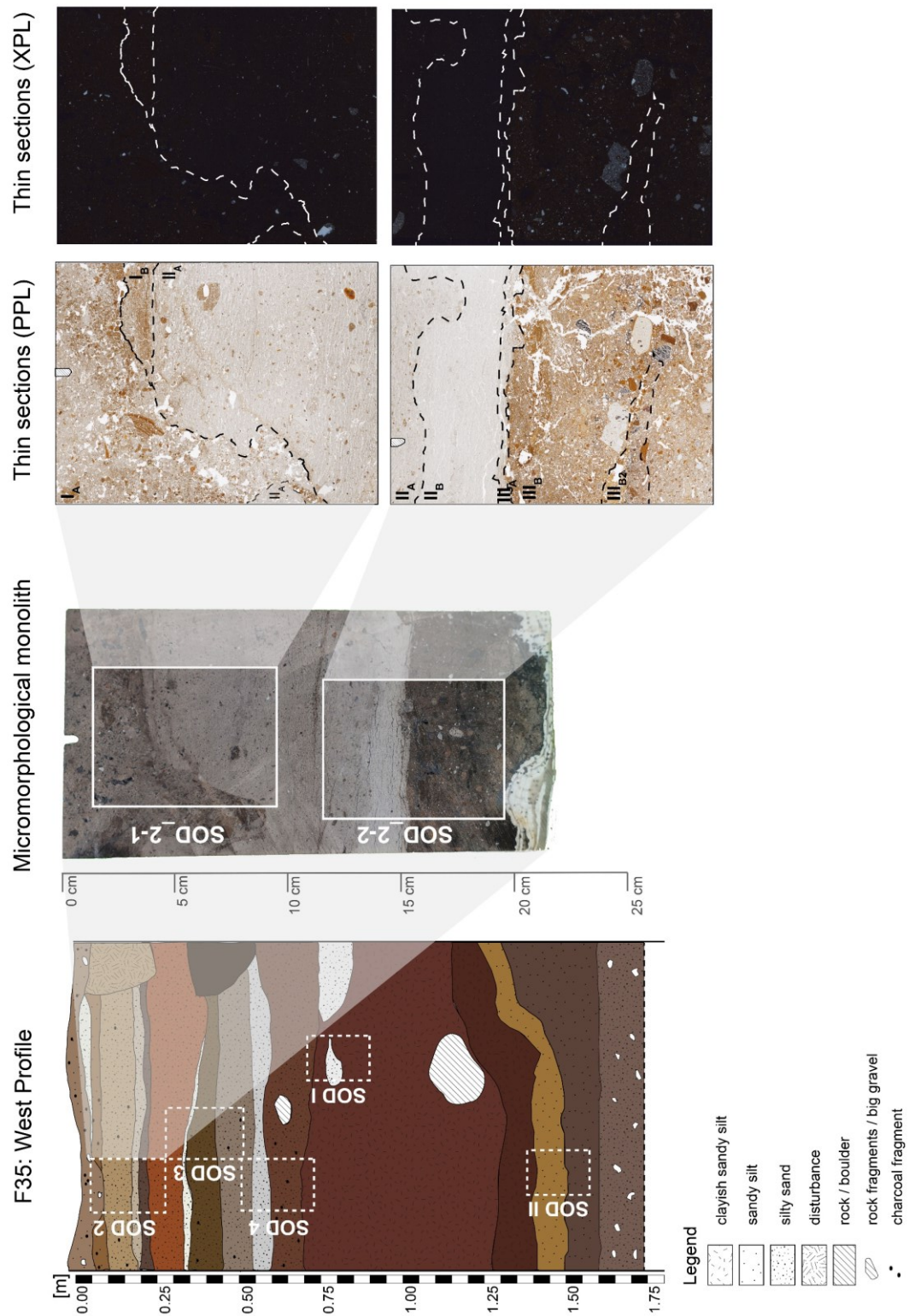


Figure A. 3 Schematic illustration of the micromorphological sample block SOD\_02, and the position of the thin sections (mod. from Hensel et al. 2022).

## Micromorphological sample block SOD\_03

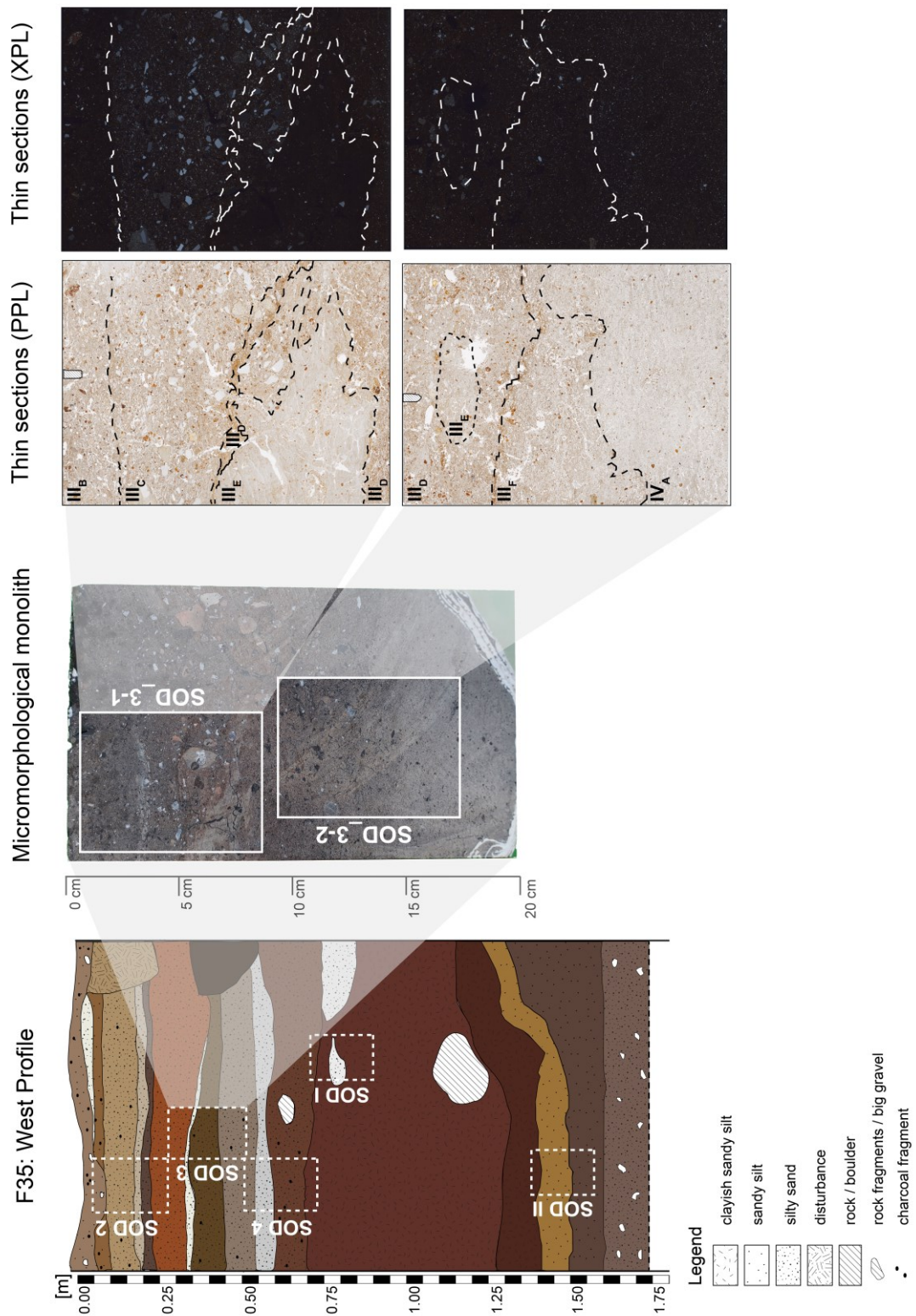


Figure A. 4 Schematic illustration of the micromorphological sample block SOD\_03, and the position of the thin sections (mod. from Hensel et al. 2022).

### Micromorphological sample block SOD\_04

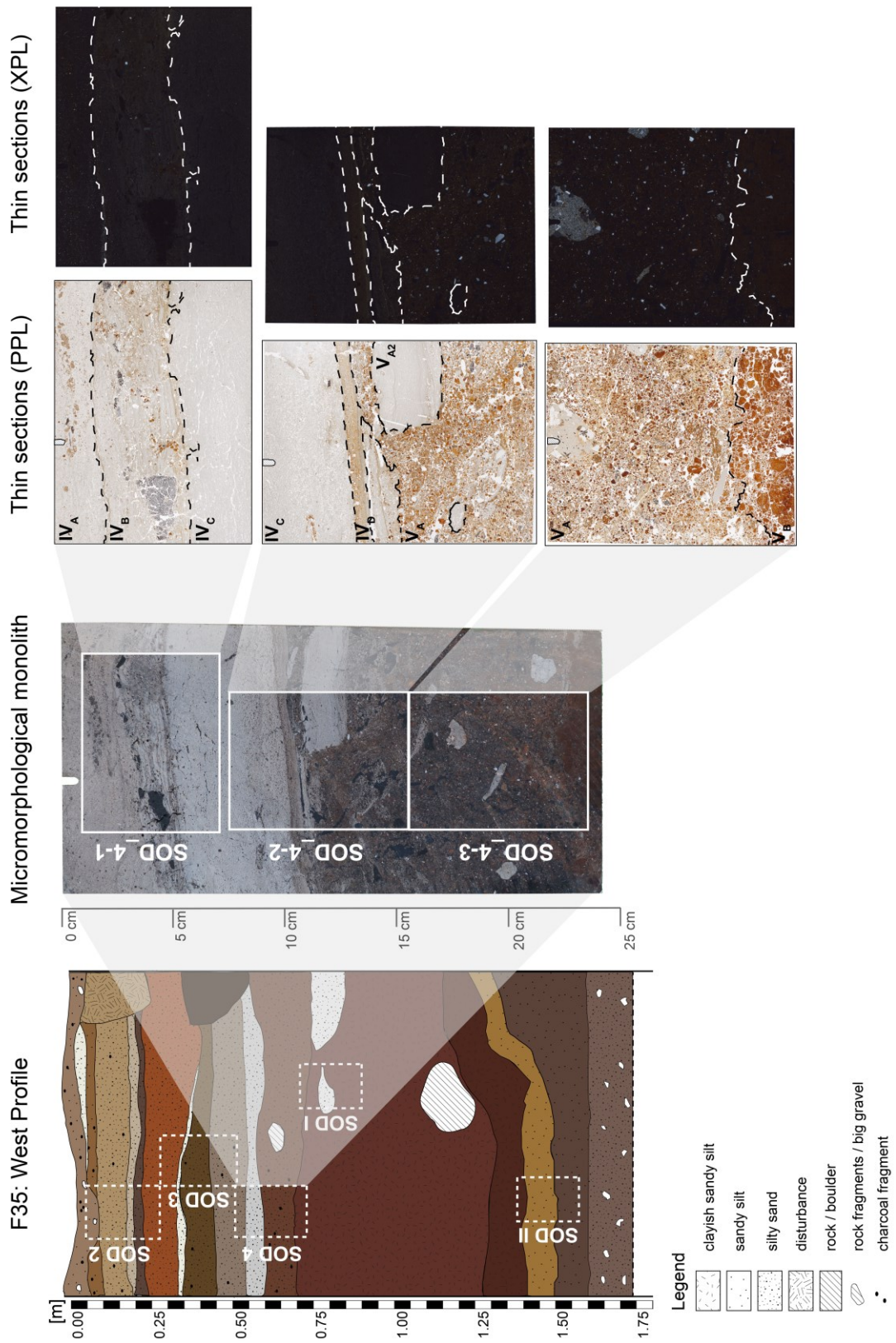


Figure A. 5 Schematic illustration of the micromorphological sample block SOD\_04, and the position of the thin sections (mod. from Hensel et al. 2022).

### Micromorphological sample block SOD\_I-1

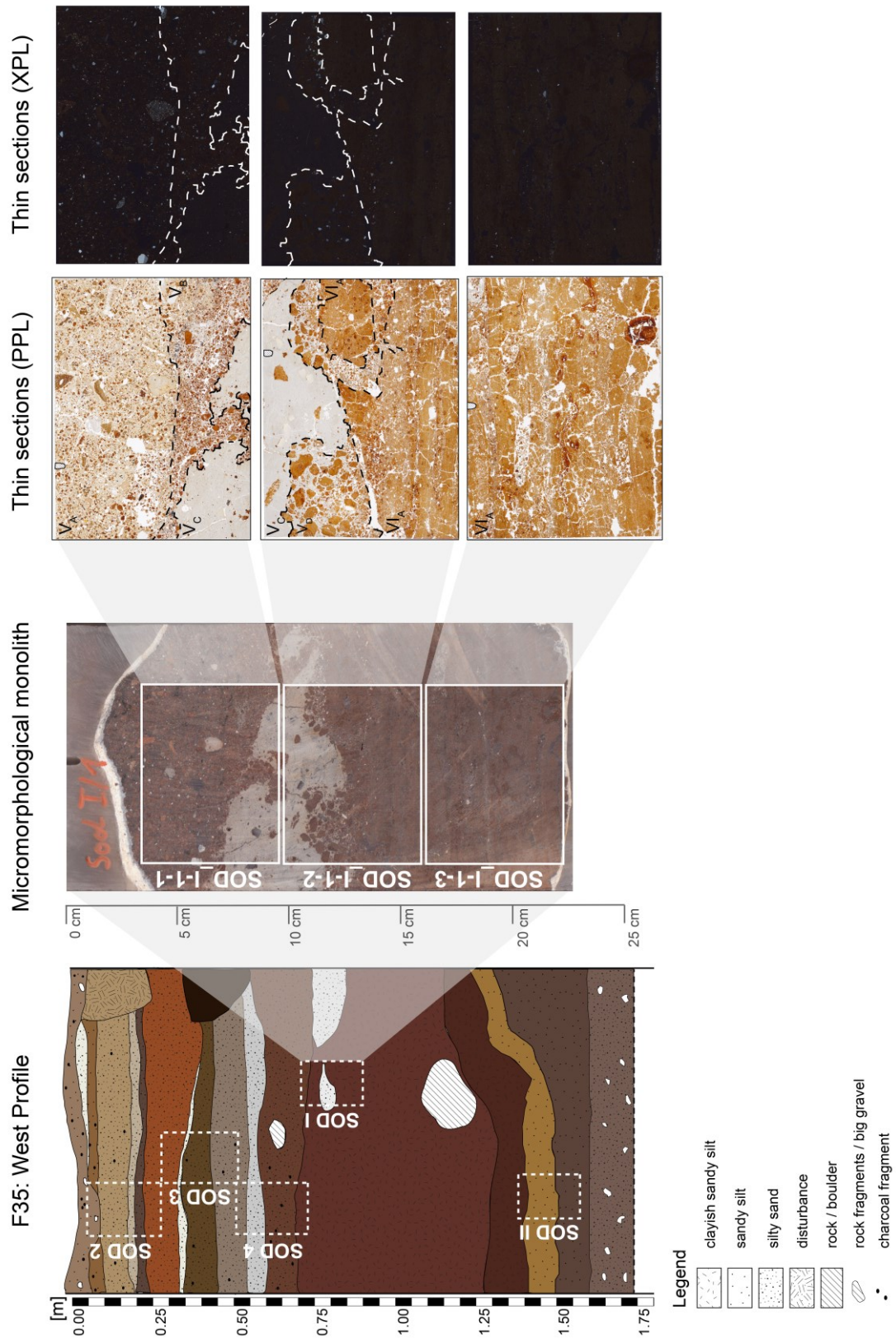


Figure A. 6 Schematic illustration of the micromorphological sample block SOD\_I-1, and the position of the thin sections (mod. from Hensel et al. 2022).

### Micromorphological sample block SOD\_I-4

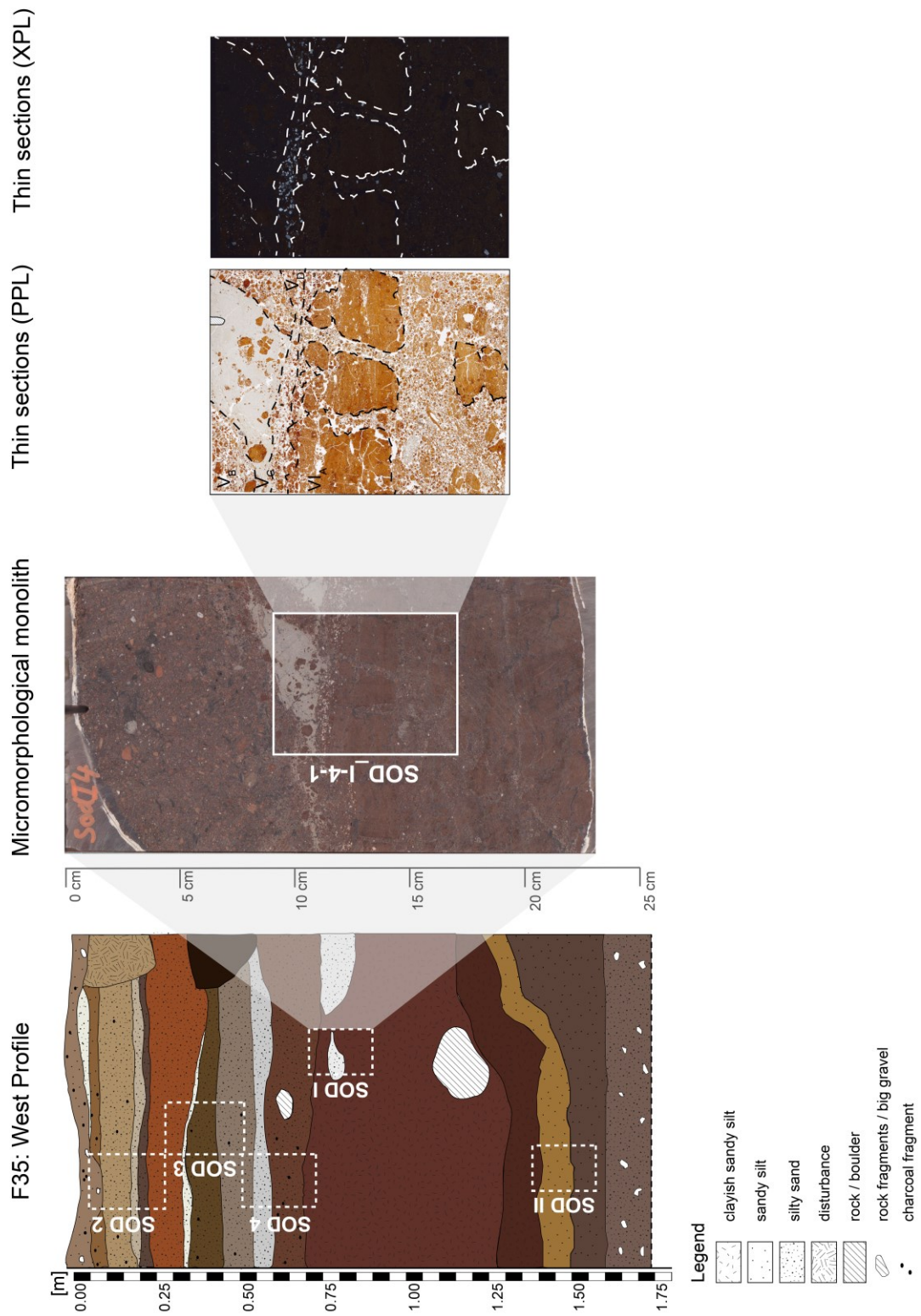


Figure A. 7 Schematic illustration of the micromorphological sample block SOD\_I-4, and the position of the thin sections (mod. from Hensel et al. 2022).

## Micromorphological sample block SOD\_II-3

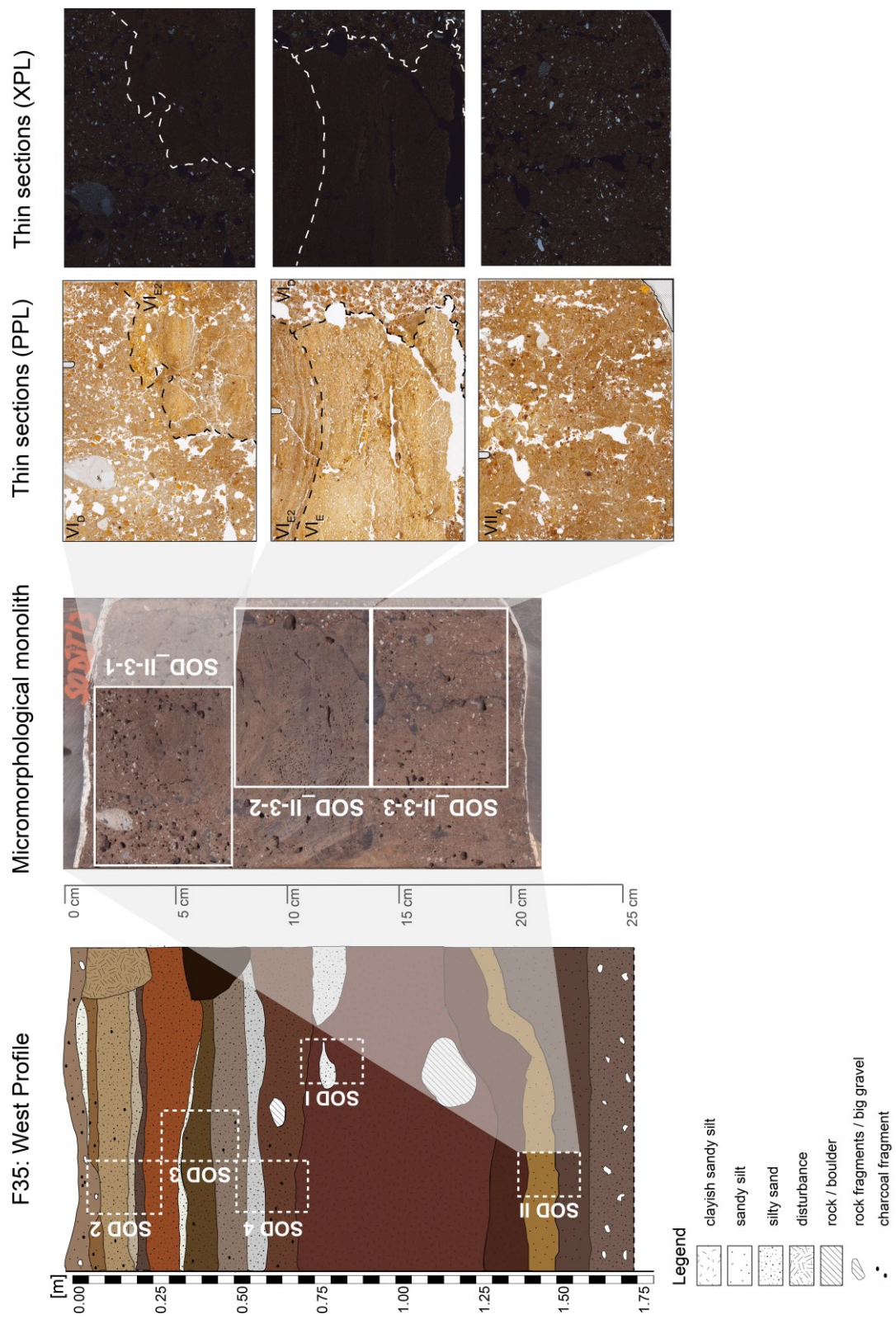


Figure A. 8 Schematic illustration of the micromorphological sample block SOD\_II-3, and the position of the thin sections (mod. from Hensel et al. 2022).

## Micromorphological sample block SOD\_7

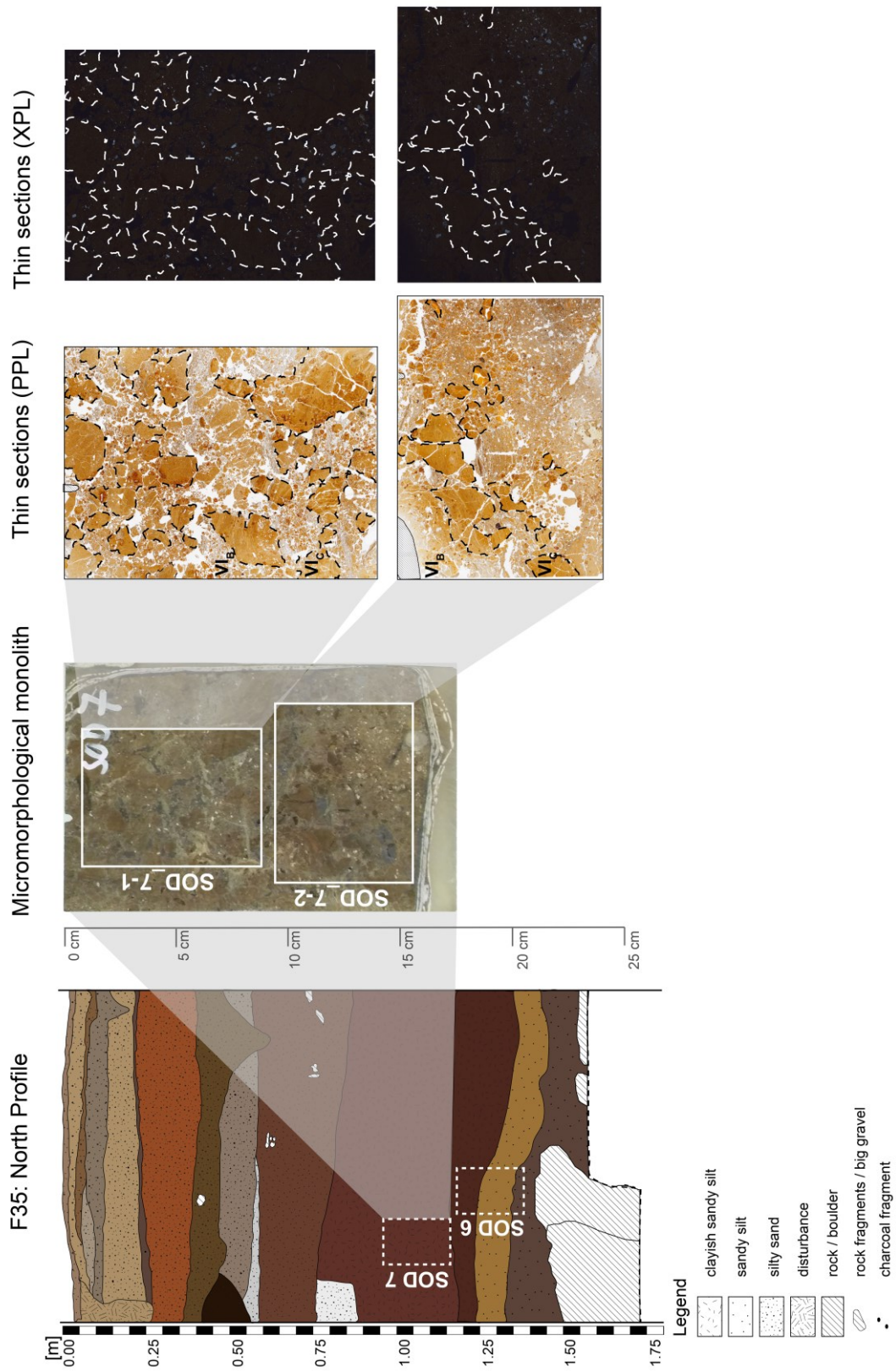


Figure A. 9 Schematic illustration of the micromorphological sample block SOD\_7, and the position of the thin sections (mod. from Hensel et al. 2022).

### Micromorphological sample block SOD\_6

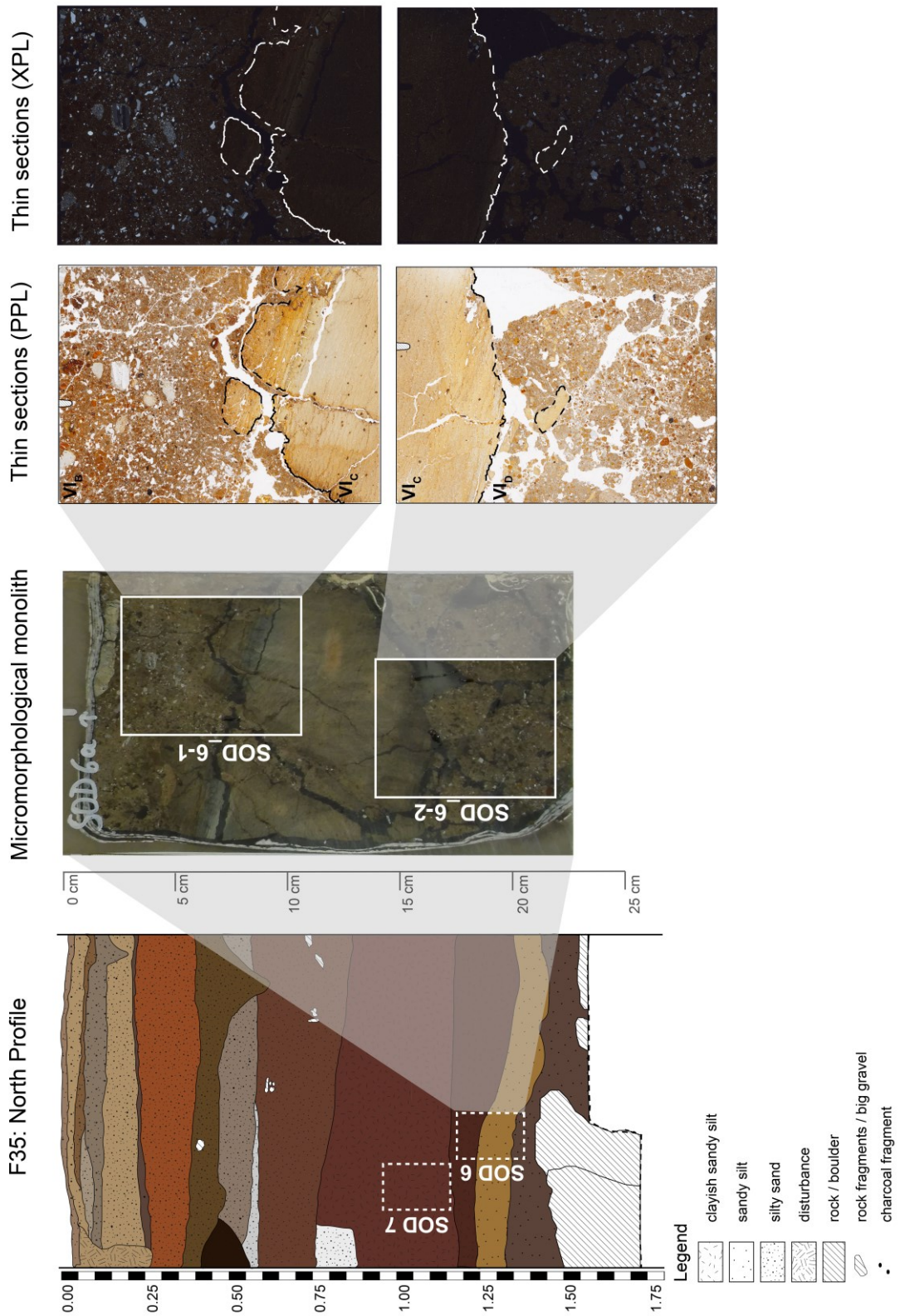


Figure A. 10 Schematic illustration of the micromorphological sample block SOD\_6, and the position of the thin sections (mod. from Hensel et al. 2022).

## Micromorphological sample blocks SOD\_III and SOD\_IV

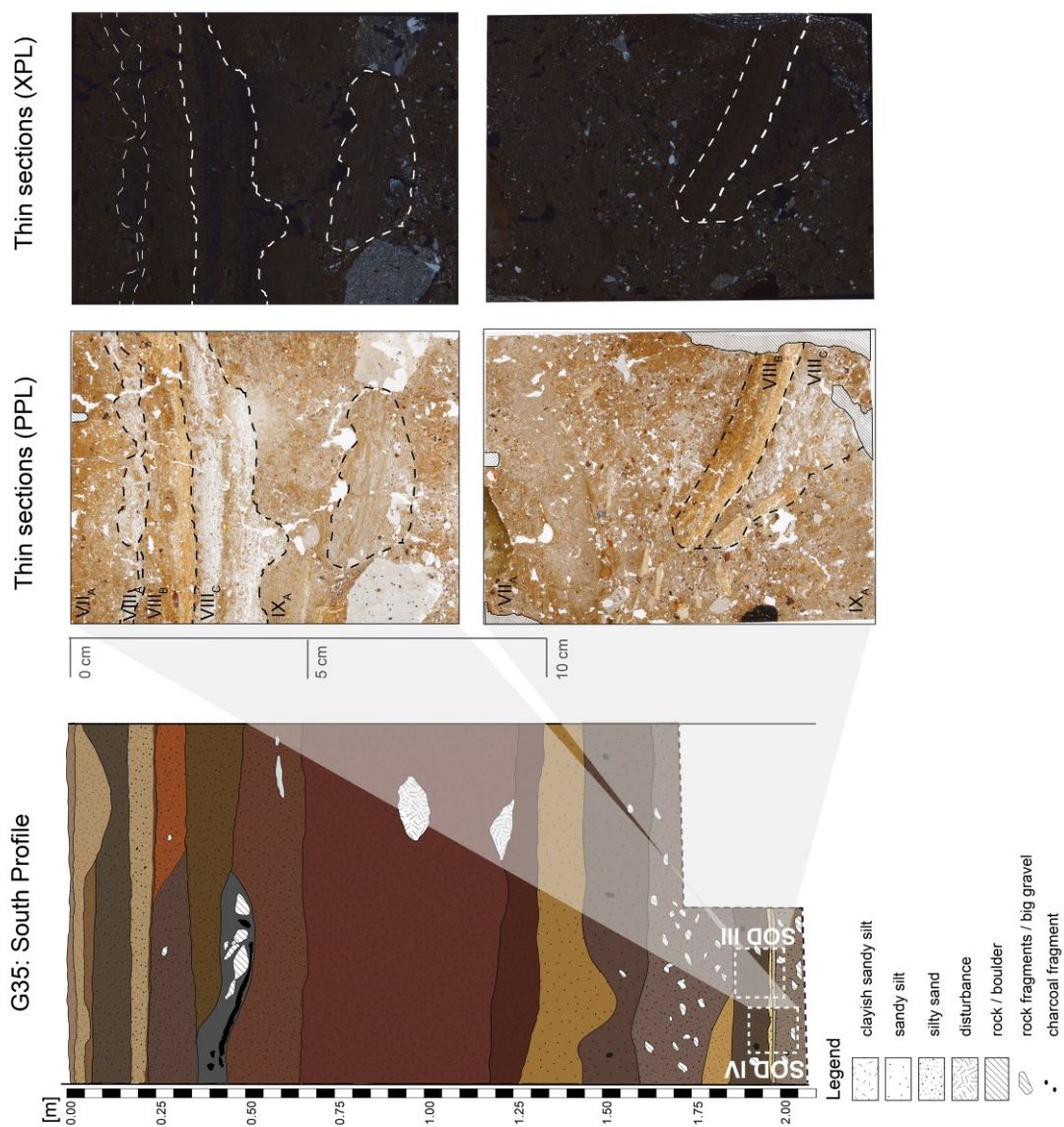


Figure A. 11 Schematic illustration of the micromorphological sample blocks SOD\_III and SOD\_IV, and the position of the thin sections (mod. from Hensel et al. 2022).

## Appendix C

### Database and supplementary material

The raw GIS data sets that support the findings of the article Hensel et al. (2019), are available to access online at the CRC 806 Database: <https://doi.org/10.5880/SFB806.49>.

The supplementary material that was published alongside the article Hensel et al. (2021), can be accessed online at:

<https://www.frontiersin.org/articles/10.3389/feart.2020.611700/full#supplementary-material>.

The geoarchaeological raw data that support the findings are available to access online at the CRC 806 Database: <https://doi.org/10.5880/SFB806.55>.

The supplementary material that was published alongside the article Hensel et al. (2022), can be accessed online at:

<https://www.mdpi.com/article/10.3390/geosciences12020092/s>.

## Chapter Contribution

Chapter II: **Hensel, E.A.**, Bödeker, O., Bubenzer, O., and Vogelsang, R. (2019). Combining geomorphological–hydrological analyses and the location of settlement and raw material sites – a case study on understanding prehistoric human settlement activity in the southwestern Ethiopia Highlands. *E&G Quaternary Science Journal* 68, 201–213. doi: <https://doi.org/10.5194/egqsj-68-201-2019>.

**[Contribution: 70 %]**

Fieldwork: 50 %

Gathering GIS data: 80 %

Evaluation and interpretation: 70 %

Authoring the publication: 80 %

Chapter III: **Hensel E.A.**, Vogelsang R., Noack, T. and Bubenzer, O. (2021). Stratigraphy and Chronology of Sodicho Rockshelter – A New Sedimentological Record of Past Environmental Changes and Human Settlement Phases in Southwestern Ethiopia. *Frontiers in Earth Science* 8. doi: <https://doi.org/10.3389/feart.2020.611700>.

**[Contribution: 77,5 %]**

Fieldwork: 80 %

Gathering data in the lab: 80 %

Evaluation and interpretation: 70 %

Authoring the publication: 80 %

Chapter IV: **Hensel, E.A.**, Kehl, M., Wöstehoff, L., Neumann, K., Vogelsang, R., and Bubenzer, O. (2022). A Multi-Method Approach for Deciphering Rockshelter Microstratigraphies – The Role of the Sodicho Rockshelter (SW Ethiopia) as a Geoarchaeological Archive. *Geosciences* 12(2), 92. doi: <https://doi.org/10.3390/geosciences12020092>.

**[Contribution: 70 %]**

Fieldwork: 90 %

Gathering data in the lab: 50 %

Evaluation and interpretation: 70 %

Authoring the publication: 70 %

## Curriculum vitae

Name	Elena Amelie Hensel
Geburtsdatum	08.10.1986 in Neustadt an der Weinstraße
Nationalität	deutsch
Familienstand	ledig

### Berufserfahrung und studienbegleitende Arbeiten

03/2022 - dato	Geoarchäologin bei ARCHAEOnet GbR, Bonn
01/2018 - 03/2021	Wissenschaftliche Mitarbeiterin, Geographisches Institut, (Sonderforschungsbereich 806), Universität zu Köln
	Lehre WS 2018/19, 2019/20, 2020/21, 2021/22: M.Sc. Seminar: Reconstructing Palaeoenvironments [gemeinsam mit Dr. Isabell Schmidt (2018-2022), Dr. Wei Chu (2019/20), Dr. Götz Ossendorf (2018/19)]
02/2017 - 12/2017	Wissenschaftliche Hilfskraft (WHK), Geographisches Institut, Universität zu Köln
04/2016 - 10/2016	Wissenschaftliche Hilfskraft (WHK), Institut für Ur- und Frühgeschichte, Universität zu Köln
04/2015 - 03/2016	Wissenschaftliche Hilfskraft (WHB), Institut für Ur- und Frühgeschichte, Forschungsstelle Afrika und Sonderforschungsbereich 806, Universität zu Köln
11/2014 - 01/2015	Studentische Hilfskraft (SHK), Geographisches Institut, Universität zu Köln

### Bildungsweg

01/2018 - dato	Promotionsstudium der Physischen Geographie, Department Geowissenschaften, Universität zu Köln
	Sonderforschungsbereich 806 „Our Way to Europe“, Teilprojekt A1: „Out of Africa – Late Pleistocene Rock Shelter Stratigraphies and Palaeoenvironments in Northeast Africa“
	Thema der Dissertation: Multiscale geoarchaeological investigation of rockshelter deposits using the example of Sodicho, Ethiopian Highlands

- 10/2013 - 02/2016 Studium der Quartärforschung und Geoarchäologie (M. Sc.),  
Department Geowissenschaften, Universität zu Köln  
  
Thema der Masterarbeit: Geoarchäologische Untersuchungen zur  
Genese der Sedimentabfolge des Middle & Early Later Stone Age  
im Pockenbank Rock Shelter, Südwest Namibia
- 10/2009 - 09/2013 Studium der Geowissenschaften (B. Sc.), Institut für  
Geowissenschaften, Johannes Gutenberg-Universität Mainz  
  
Thema der Bachelorarbeit: Isotopengeochemische  
Untersuchungen an mitteldevonischen Brachiopoden des  
Rheinischen Schiefergebirges
- 09/2005 - 03/2008 Kurfürst-Ruprecht-Gymnasium, Neustadt a. d. Weinstraße  
Abschluss Abitur

#### Förderungen und Programme

---

- 09/2019 Travel Grant, der Graduate School of Geosciences (GSGS),  
Universität zu Köln
- 09/2017 - 9/2018 Teilnehmerin des Cornelia Harte Mentoring MINT (CHM MINT)  
2017/2018, Universität zu Köln
- 2/2017 - 06/2017 Stipendium in Form eines "GSGS start-up honours grants" von der  
Graduate School of Geosciences (GSGS), Universität zu Köln

Brühl, den 21.08.2022



---

(Elena Amelie Hensel)

## Erklärung

„Hiermit versichere ich an Eides statt, dass ich die vorliegende Dissertation selbstständig und ohne die Benutzung anderer als der angegebenen Hilfsmittel und Literatur angefertigt habe. Alle Stellen, die wörtlich oder sinngemäß aus veröffentlichten und nicht veröffentlichten Werken dem Wortlaut oder dem Sinn nach entnommen wurden, sind als solche kenntlich gemacht. Ich versichere an Eides statt, dass diese Dissertation noch keiner anderen Fakultät oder Universität zur Prüfung vorgelegen hat; dass sie - abgesehen von unten angegebenen Teilpublikationen und eingebundenen Artikeln und Manuskripten - noch nicht veröffentlicht worden ist sowie, dass ich eine Veröffentlichung der Dissertation vor Abschluss der Promotion nicht ohne Genehmigung des Promotionsausschusses vornehmen werde. Die Bestimmungen dieser Ordnung sind mir bekannt. Darüber hinaus erkläre ich hiermit, dass ich die Ordnung zur Sicherung guter wissenschaftlicher Praxis und zum Umgang mit wissenschaftlichem Fehlverhalten der Universität zu Köln gelesen und sie bei der Durchführung der Dissertation zugrundeliegenden Arbeiten und der schriftlich verfassten Dissertation beachtet habe und verpflichte mich hiermit, die dort genannten Vorgaben bei allen wissenschaftlichen Tätigkeiten zu beachten und umzusetzen. Ich versichere, dass die eingereichte elektronische Fassung der eingereichten Druckfassung vollständig entspricht.“

Teilpublikationen:

1. **Hensel, E. A.**, Bödeker, O., Bubenzer, O., and Vogelsang, R. (2019). Combining geomorphological–hydrological analyses and the location of settlement and raw material sites – a case study on understanding prehistoric human settlement activity in the southwestern Ethiopia Highlands. *E&G Quaternary Science Journal* 68, 201–213. doi: <https://doi.org/10.5194/egqsj-68-201-2019>
2. **Hensel E. A.**, Vogelsang R., Noack, T., and Bubenzer, O. (2021). Stratigraphy and Chronology of Sodicho Rockshelter – A New Sedimentological Record of Past Environmental Changes and Human Settlement Phases in Southwestern Ethiopia. *Frontiers in Earth Science* 8. doi: <https://doi.org/10.3389/feart.2020.611700>
3. **Hensel, E. A.**, Kehl, M., Wöstehoff, L., Neumann, K., Vogelsang, R., and Bubenzer, O. (2022). A Multi-Method Approach for Deciphering Rockshelter Microstratigraphies – The Role of the Sodicho Rockshelter (SW Ethiopia) as a Geoarchaeological Archive. *Geosciences* 12(2), 92. doi: <https://doi.org/10.3390/geosciences12020092>

Brühl, den 21.08.2022



---

(Elena Amelie Hensel)